

To the Graduate Council:

I am submitting herewith a dissertation written by Edwin C. Jones entitled "*Electrical Transport Properties of Epitaxial and Granular Oriented $\text{YBa}_2\text{Cu}_3\text{O}_{7-\delta}$ Thin Films.*" I have examined the final copy of this dissertation for form and content and recommend that it be accepted in partial fulfillment of the requirements for the degree of Doctor of Philosophy, with a major in Physics.

James R. Thompson
James R. Thompson, Major Professor

We have read this dissertation
and recommend its acceptance:

Gerald D. Mohan

David K. Gupta

Philip W. Schaefer

T. A. Collins

H. R. Khan

Accepted for the Council:

Associate Vice Chancellor
and Dean of The Graduate School

**ELECTRICAL TRANSPORT PROPERTIES
OF EPITAXIAL AND GRANULAR ORIENTED
 $\text{YBa}_2\text{Cu}_3\text{O}_{7-\delta}$ THIN FILMS**

A Dissertation

Presented for the

Doctor of Philosophy

Degree

The University of Tennessee, Knoxville

EDWIN C. JONES

December 1992

To my wife Gita and my son Jonathan

ACKNOWLEDGEMENTS

My first gesture of thanks goes to my major professor Dr. James Thompson for giving me the opportunity to conduct research in the field of high- T_c superconductivity. I also wish to thank all of my advisors for their guidance and careful readings of the manuscripts. These advisors are (again) Prof. James Thompson, Dr. David Christen, Prof. Gerald Mahan, Prof. Ollie Thomson, and Prof. Philip Schaefer. Equal thanks goes to my parents Dale and Bernice, my wife Gita, and my son Jonathan, without whose support, this work would not have been possible. The educational and moral support offered by all of these individuals proved crucial in the completion of this degree.

Additional thanks goes to my colleagues who offered various other types of support. These are, first, Dr. Ron Feenstra who proved important in the development of the annealing furnace and annealing techniques. Second, my fellow graduate student Shen Zhu, Dr. David Norton, Prof. Douglas Lowndes, Dr. Julia Phillips, and Dr. Mike Siegal who supplied the many thin films needed for the transport measurements. Third, my fellow graduate student George Stejic supplied the Hall masks so that Pam Fleming could photolithographically pattern the Hall bridges. Fourth, Dr. John Budai and Dr. Bryan Chakoumakos performed the x-ray diffraction characterizations that proved useful in the final interpretations. Fifth, Charlie Klabunde helped in finding tools around the laboratory as well as developing some of the key ideas used in the logic of measuring J_c in the data acquisition programs. Sixth, Clay Wynn photographed the Hall cryostat and supplied several viewgraphs used in my

talks. Seventh, Prof. Stamatis Patapis carefully read and offered suggestions on the H_{c2} manuscript. Eighth, Dr. Philip Allen, Dr. Warren Pickett, and Dr. Jaejun Yu took the time to carefully discuss the band structure of $YBa_2Cu_3O_{7-\delta}$. Ninth, Jim Shoopman painstakingly machined several crucial parts necessary in the development of the Hall cryostat. Finally, I acknowledge useful suggestions offered by Prof. Bob Dynes, Dr. Richard Kerchner, Prof. Jorge Ossandon, Yangren Sun, Dr. Stuart Wolf, Prof. Guy Deutscher, Dr. Robby Beyers, Prof. Bob Markiewicz, and Dr. Jeffrey Clayhold.

ABSTRACT

Strong correlations between the Hall coefficient R_H , the transition temperature T_c , and the critical current density J_c were established in a series of epitaxial $\text{YBa}_2\text{Cu}_3\text{O}_{7-\delta}$ thin films as a function of oxygen deficiency δ . Steady increases in R_H with δ suggests that deoxygenation reduces the density of states which, according to BCS theory, should lead to corresponding decreases in T_c . In contrast, two well known plateaus occurring at 90K and 60K were observed in T_c vs. δ . Others have ascribed these plateaus to either electronic phenomena or oxygen clustering. We find that in the 90K plateau, the critical current density $J_c(\delta, H=0)$ decreases with δ and extrapolates toward zero at the edge of the plateau, while the relative field dependence of $J_c(\delta, H)$ is independent of δ . Furthermore, a fluctuation analysis of the resistive transitions indicates a constant upper critical field $B_{c2}(0) = 110\text{T}$ across this plateau. These observations suggest that the oxygen clustering/percolation scenario occurs on the 90K plateau.

Moreover, computer simulations showed this oxygen clustering/percolation picture to be a plausible explanation for the occasional observation of a sign reversal of R_H near T_c . For large oxygen deficiencies ($\delta > 0.5$) and for the granular oriented $\text{YBa}_2\text{Cu}_3\text{O}_{7-\delta}$ thin films, rapid decreases in J_c with applied field were observed which is reminiscent of the conventional granular alloys. In addition, the self-field critical current densities J_c behaved as SNS weak link systems in a Josephson mixed state. In sum, due to the short coherence length ξ in these materials, many properties formerly believed to be "*intrinsic*" in nature are apparently "*extrinsic*" in nature.

TABLE OF CONTENTS

I. INTRODUCTION	1
II. EXPERIMENTAL ASPECTS	12
A. Overview of the Most Important Procedures	12
B. Estimation of Oxygen Deficiency δ	15
C. The Hall Cryostat	21
D. The Data Acquisition System	27
III. THEORETICAL BACKGROUND	42
A. Anderson–Kim Flux Creep Model	42
B. The Hall Effect in Metals	47
1. Simple Metals: Single Parabolic Band	47
2. Multiband Effects	51
3. Bloch–Boltzmann Transport Theory	58
4. Geometric Interpretation of the Hall Conductivity	65
5. Unconventional Hall Effect Theories	69
C. H_{c2} Determined from Fluctuations	71

IV. CORRELATIONS BETWEEN R_H, T_c, AND J_c	73
A. Overview of Most Important Experimental Results . . .	73
B. Discussion of Results	74
1. Effect of Oxygen Deficiency δ on the Resistivity and Hall Coefficient	74
2. Temperature Dependence of the Hall Coefficient	80
3. Effect of Oxygen Deficiency δ on the Critical Current Density	84
4. Determination of the Pinning Energy	85
5. Constraints Imposed on Electronic Models	94
6. "Peaked" $T_c(\delta)$ Behavior	95
7. Brief Conclusion	99
V. UPPER CRITICAL FIELD H_{C2} ANALYSIS	100
A. Experimental Results	100
B. Phase Separation Effects	105
C. Implications for BCS Theory	109
VI. HALL EFFECT TRANSITIONS	112
A. Evidence for Percolation in the Transitions	112

B. Current Percolation Model	116
VII. GRANULAR ORIENTED THIN FILMS	123
VIII. SUMMARY	132
REFERENCES	135
A. Text References	136
B. Appendix References	143
C. Suggested Hall Effect Readings	144
APPENDICES	145
Appendix A. Hall (Resistivity) Acquisition Program	146
Appendix B. Critical Current Acquisition Program	158
Appendix C. I-V Acquisition Program	172
Appendix D. X-Y Plotter Emulator	184
Appendix E. Monte Carlo Computational Information	193
VITA	197

LIST OF TABLES

I.	Experimental data used in the determination of δ 's depicted in the figures pertaining to the coevaporated thin film	19
II.	Experimental data used in the determination of δ 's depicted in the figures pertaining to the laser ablated thin film	20
III.	Specifications of the custom designed 10 Tesla superconducting magnet built by Cryomagnetics for Martin Marietta Energy Systems	22

LIST OF FIGURES

1.	Accepted atomic structure of $\text{YBa}_2\text{Cu}_3\text{O}_7$ determined from neutron diffraction	3
2.	Band structure of $\text{YBa}_2\text{Cu}_3\text{O}_7$ in the $k_z = 0$ plane near the Fermi level ($E_F = 0$)	5
3.	Fermi surfaces for the four bands crossing the Fermi energy E_F	6
4.	Total and partial electronic densities of states (DOS) of $\text{YBa}_2\text{Cu}_3\text{O}_7$ near the Fermi energy E_F derived from the band structure results	7
5.	Typical current bridge pattern for the thin films used throughout this study	13
6.	Method of control of the residual oxygen deficiency δ	14
7.	Transverse-even coefficients R_{TE} observed in oxygen deficient $\text{YBa}_2\text{Cu}_3\text{O}_{7-\delta}$ (non-zero when $\delta > 0.5$)	16
8.	Example determination of the Hall coefficient R_H as described in the text	17

9.	Vacuum pump station and gas line diagram used with the Hall cryostat .	24
10.	Thermometer calibrations utilized by the data acquisition system	26
11.	Electronic block diagram of the computer controlled data acquisition system used in making Hall measurements	28
12.	Hardware Settings Menu for (a) DA-HALL.BAS and (b) DA-JCTH.BAS	30
13.	Set-Up Parameters Menu for (a) DA-HALL.BAS and (b) DA-JCTH.BAS	32
14.	Screen Graphics Parameters Menu for (a) DA-HALL.BAS and (b) DA-JCTH.BAS	39
15.	Periodic potential well of depth U_0 and spacing x used to depict the magnetic flux " <i>pinning</i> " centers for the cases of (a) no external driving forces and (b) an externally applied driving force	44
16.	Fermi sphere in the ground state of a free electron gas	48

17.	Contributions to the Hall effect from two bands of oppositely charged carriers	54
18.	Fits of the transport properties to the simple two band model described in the text	57
19.	Calculated electrical transport properties of $\text{YBa}_2\text{Cu}_3\text{O}_7$ assuming electron-phonon scattering mechanisms dominate	64
20.	Resistivity (a), Inverse Hall coefficient (b), and Inverse Hall angle (c) for a laser ablated film of $\text{YBa}_2\text{Cu}_3\text{O}_{7-\delta}$ as a function of temperature and oxygen deficiency δ	75
21.	The effect of room temperature annealing on the resistance in the "Ortho-II" phase $\text{YBa}_2\text{Cu}_3\text{O}_{\sim 6.5}$	77
22.	Magnetoresistance $\Delta\rho/\rho(0)$ observed in $\text{YBa}_2\text{Cu}_3\text{O}_{7-\delta}$ for oxygen deficiencies in excess of $\delta > 0.5$	81

23.	Transition temperature T_c , and critical current density J_c evaluated at fixed reduced temperatures, as a function of either the oxygen deficiency δ or the " <i>apparent carrier density</i> " from the Luttinger Liquid Theory described in the text	83
24.	Reduced critical current densities as a function of temperature (a), applied field for $H \parallel c$ (b), and applied field for $H \parallel ab$ (c) for various oxygen contents	86
25.	Superconducting Hall effect transitions obtained at 8 Tesla for various oxygen contents	88
26.	Pinning energy $U_{oo}(\delta) = U_o(\delta, T=0, B=1T)$ (open symbols) and $T_c(\delta)$ (solid circles) as a function of oxygen content $7-\delta$ for a film prepared by the BaF_2 process	91
27.	Normalized pinning force density F_p taken at 77K as a function of (a) B and (b) B/B^* as described in the text, both on and off the 90K plateau .	93
28.	High resolution x-ray diffraction scans of the (005) peak for (a) the laser ablated thin film at $7-\delta \approx 7.00$ and (b) the coevaporated thin film at $7-\delta \approx 6.90$	96

29.	Inverse Hall coefficients taken on two sets of films with identical precursors but post-annealed under different conditions	98
30.	Step by step determination of $-dH_{c2}/dT$ by utilization of the 3D scaling of the fluctuation theory	101
31.	Evidence of granular-like behavior at reduced oxygen contents in $YBa_2Cu_3O_{7-\delta}$	104
32.	Summary of the $H_{c2}(T)$ slopes as a function of oxygen deficiency δ in $YBa_2Cu_3O_{7-\delta}$ determined by the in-field fluctuation analysis of epitaxial thin films (filled circles)	106
33.	Predicted effect of phase separation on the "apparent" H_{c2} slopes as derived from the fluctuation analysis	108
34.	Example derivation of the Hall coefficient R_H by application of Equation (1) to the two opposing Hall "signals" R_{xy}	113
35.	Superconducting Hall effect transitions measured with $B = 8T$ for a single laser ablated film of $YBa_2Cu_3O_{7-\delta}$ at various estimated oxygen contents $7-\delta$	114

36.	Changes in the superconducting Hall effect transition due to the series of sequential anneals for the laser ablated film shown in Figure 35, both of which were obtained at full oxygenation and with $B = 8T$. . .	117
37.	Hall effect transitions predicted by the Monte Carlo simulations	120
38.	Example of a T_c distribution leading to a sign reversal of R_H near T_c .	122
39.	Critical current density hysteresis as a function of applied magnetic field history for a c -oriented granular $YBa_2Cu_3O_7$ thin film	125
40.	"Grain boundary" resistivities obtained by subtracting several polycrystalline c -oriented $YBa_2Cu_3O_7$ resistivity curves $\rho(T)$ from a single crystal resistivity curve grown under similar conditions	126
41.	Temperature dependence of the activation energy at an applied field of 1 Tesla for triaxial and c -oriented granular thin films of $YBa_2Cu_3O_7$.	128
42.	Reduced critical current density $J_c(T)/J_c(0)$ versus reduced temperature for the granular $YBa_2Cu_3O_7$ films	130

43.	In-field resistive transitions obtained from a highly crystalline, coevaporated, epitaxial thin film of $\text{YBa}_2\text{Cu}_3\text{O}_7$	196
-----	--	-----

LIST OF SYMBOLS AND ABBREVIATIONS

A. SYMBOLS

A_ℓ	"Stokes" area	Cu(2)	"plane" site copper
"a"	aged	Cu(3)	"plane" site copper
a, b, c	lattice dimensions	γ	anisotropy parameter
α	relative scaling factor	d	radius of a fluxoid
$\alpha_{tr}^2 F(\omega)$	electron-phonon spectral function	$\Delta(0)$	superconducting energy gap at T=0
B	magnetic induction	δ	oxygen deficiency
B_{c1}	lower critical field	$\delta(\epsilon - \epsilon_F)$	Dirac function
B_{c2}	upper critical field	∇	gradient operator
B_{irr}	irreversibility field	E	electric field
B_0	magnetic field constant	E_c	electric field
B^*	field at which the flux lattice melts		measurement criterion
$b_{c\Omega}, b_{s\Omega}$	bosonized charge/spin fluctuations	E_F	Fermi energy
		E_0	characteristic field (proportional to f_0)
$^\circ C$	degrees Centigrade	e	electron charge
c	speed of light	ϵ	energy
Cu(1)	"chain" site copper		

ϵ_{ijk}	totally antisymmetric tensor	H_c	thermodynamic critical field
ϵ_j	current direction " <i>effort</i> " factor	H_{c1}	lower critical field
		H_{c2}	upper critical field
\mathbf{F}	Lorentz force	Θ_D	Debye temperature
F_c	condensation energy	θ_H	Hall angle
$F(\mathbf{k})$	mean number of carriers in state \mathbf{k}	θ_k	angle between \mathbf{x} and $\ell(\mathbf{k})$
F_L	flux gradient driving force	I	applied current
		I_c	critical current
F_p	pinning force density	\mathbf{J}, \mathbf{j}	current density
F_{sc}	scattering force	J_c	critical current density
$F(\omega)$	electron-phonon matrix elements	J_{co}	critical current density in absence of flux creep
f_i	volume fraction of i -th phase	J_d	depairing critical current density
f_o	" <i>attempt</i> " frequency	K	Kelvin
$-\partial f / \partial \epsilon(\mathbf{k})$	Fermi-Dirac distribution	\mathbf{k}	\mathbf{k} -space momentum
$G(\omega)$	neutron-phonon matrix elements	k, k_B	Boltzmann constant
		k_F	Fermi momentum
\hbar	Planck's constant	κ	Ginzburg-Landau parameter
H	magnetic field strength		

$d\ell$	integration increment	ξ_N	normal metal coherence length
ℓ	average spacing between fluxoids	O(1)	"chain" site oxygen
ℓ	mean free path	O(2)	"plane" site oxygen
ℓ_B	magnetic length	O(3)	"plane" site oxygen
$\ell(\mathbf{k})$	"scattering path length"	O(4)	"chain" site oxygen
	vector	\mathbf{p}	linear momentum
$\Delta\ell/\ell_{av}$	"anisotropy" of $\ell(\mathbf{k})$		operator
λ	BCS coupling constant	ρ, ρ_{xx}	electrical resistivity
λ	flux penetration depth	ρ_{creep}	flux creep resistivity
m	mass	ρ_{flow}	flux flow resistivity
m_e	electron mass	ρ_o	flux creep resistivity
μ	carrier mobility		scaling constant
μ	chemical potential	ρ_{onset}	resistivity just above superconductivity
N	number of electrons		
$N(E_F)$	electronic DOS at Fermi surface	ρ_{xy}, ρ_{yx}	Hall resistivity
		$\Delta\rho/\rho_o$	magnetoresistance
n	charge carrier density	q	electric charge
$n_H, 1/R_H e$	Hall carrier density	" q "	quenched
ξ	superconducting coherence length	R	electrical resistance
		R_H	Hall coefficient

R_H, R_{xyz}^H	Hall tensor	U_o	flux pinning energy
R_N	normal state tunnelling resistance	U_{oo}	pinning energy at $T=0$ with $B=1T$
R_{TE}	Transverse-even field	u	pinning well depth
$\sigma, \sigma_{xx}; \sigma_{yy}$	electrical conductivity	V	electron-phonon matrix element
σ_f	fluctuation conductivity		
σ_{xyz}	Hall conductivity	V	flux bundle volume
T	temperature	V	Volt
T	Tesla	v	velocity
∇T	thermal gradient	v_F	Fermi velocity
T_c	superconducting transition temperature	$v(k)$	group velocity
		$ v ^{-1}$	density of states factor
$T_c(H)$	mean field transition temperature	ΔW	potential energy barrier height
ΔT_c	T_c distribution width	Φ_o, ϕ_o	flux quantum
T_D	Debye temperature	$x, 7-\delta$	oxygen stoichiometry
t	time	$x, y; z$	cartesian unit vectors
t_o	time scale	ω	frequency
τ	relaxation time	ω_c	cyclotron frequency
$1/\tau_{imp}$	impurity scattering rate	Ω	solid angle
τ_{tr}	"transport" relaxation time	Ω_o	normalization volume

B. ABBREVIATIONS

BCS	Bardeen, Cooper, and Schrieffer
CGR	Carbon glass thermometer
DOS	electronic density of states
DVM	digital voltmeter
FS	Fermi surface
I-V	current-voltage characteristics
LHe	liquid Helium
LN ₂	liquid Nitrogen
ORNL	Oak Ridge National Laboratory
SIS	superconductor-insulator-superconductor
SNS	superconductor-normal metal-superconductor
Y-123	YBa ₂ Cu ₃ O _{7-δ}
YBCO	YBa ₂ Cu ₃ O _{7-δ}
YSZ	Yttria-stabilized Zirconia

I. INTRODUCTION

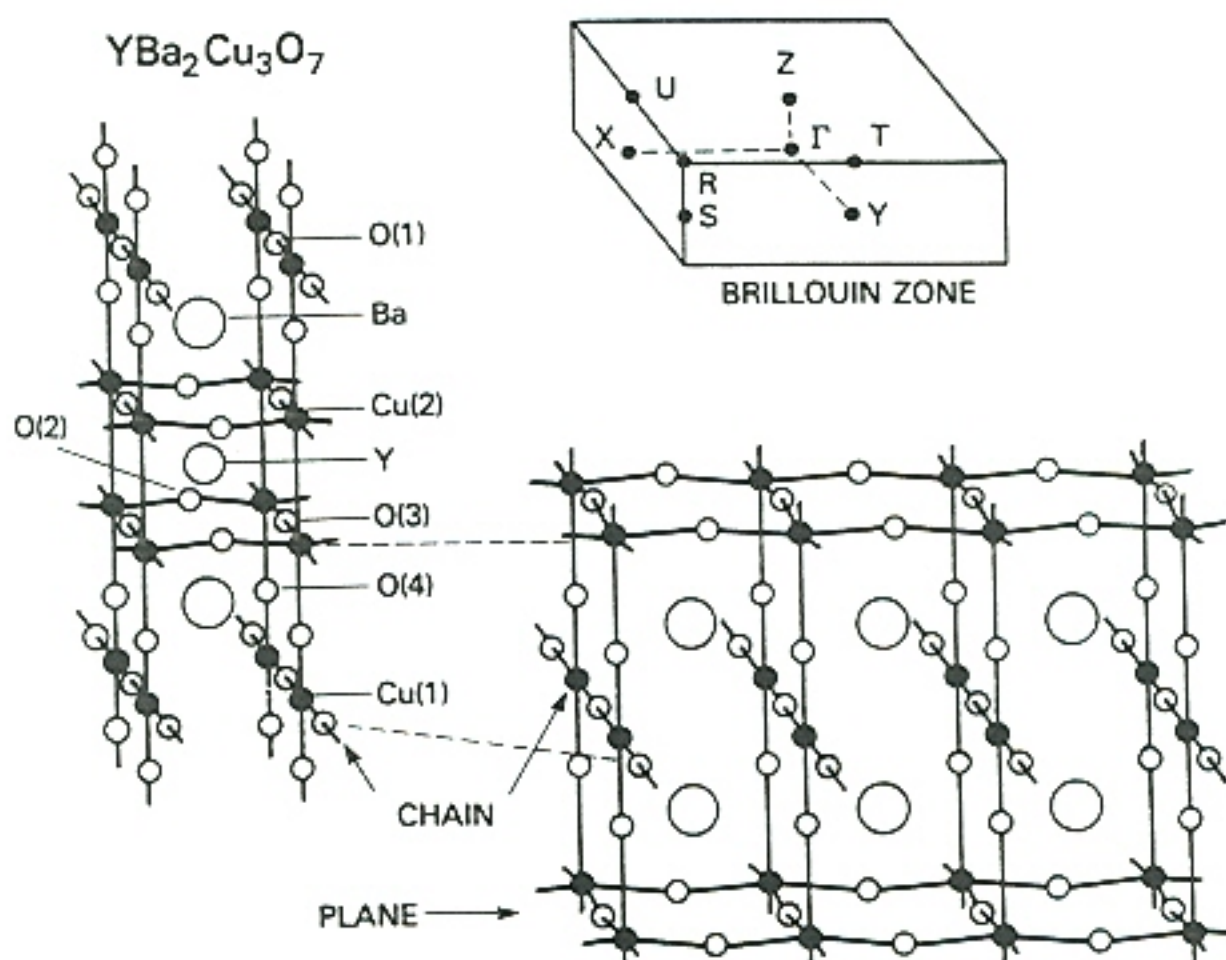
The electrical transport characteristics of a series of epitaxial and polycrystalline $\text{YBa}_2\text{Cu}_3\text{O}_{7-\delta}$ thin films were studied at the Oak Ridge National Laboratory's Solid State Division. This study was motivated by the desire to understand the mechanisms limiting the critical current density, J_c , in both the epitaxial and granular thin films. Since the recent discovery of this new class of high- T_c (transition temperature) superconductors,¹ researchers have continued to make improvements in these materials in the hopes that someday the important superconducting properties such as J_c will approach those of the earlier conventional superconductors,² but at liquid nitrogen temperatures instead of the more expensive liquid helium temperatures. Liquid helium currently costs about \$5.00 per liter as compared to \$0.18 per liter for liquid nitrogen.³ Each class of thin films could have many potential applications with only a few examples stated here. With the ease of growing long polycrystalline superconducting tapes,⁴ these materials may someday lead to the production of superconducting cables. However, the critical current densities occurring at the grain boundaries in these polycrystalline materials are limited to values well below those for high quality epitaxial films. Therefore, more immediate emphasis has been placed on the improvement of the epitaxial films. Potential uses for the epitaxial films include interconnects in integrated circuits and other devices such as bolometers. Future research magnets and motors could potentially be developed by either type of material, given a little luck with breakthroughs. This dissertation summarizes the findings for epitaxial and granular thin films, in the hope that these results may help others in

fulfilling such breakthroughs.

At present, $\text{YBa}_2\text{Cu}_3\text{O}_{7-\delta}$ is the most extensively studied high- T_c superconductor due to its early discovery and relative ease of processing. It was discovered in December 1986 by Chu *et al.*⁵ and has a transition temperature of about 92K near full oxygenation ($\delta \approx 0$). Like most other high- T_c superconductors, $\text{YBa}_2\text{Cu}_3\text{O}_{7-\delta}$ is a perovskite derived material having the structure shown in Figure 1. However, this material is more complicated than the other high- T_c materials since, $\text{YBa}_2\text{Cu}_3\text{O}_{7-\delta}$ has a "chain" copper-oxygen layer structure in addition to two "plane" layers. Both the "chains" and "planes" are believed to contribute to the normal state properties. Moreover, it is generally believed that the "planes" are responsible for the superconductivity, whereas the presence of the "chains" simply improves the superconducting performance by providing additional charge carriers to the "planes." Neutron diffraction data taken on oxygen deficient samples show that the oxygen loss primarily occurs in the "chain" sites, e.g., O(1) sites, whereas the "plane" sites are unaffected.⁶ However, the superconducting properties are known to change dramatically upon removal of oxygen, supporting the idea of charge transfer between the "chains" and "planes." Therefore, one approach to studying the effects of carrier density on the superconducting performance, i.e., critical current density J_c and transition temperature T_c , becomes possible in $\text{YBa}_2\text{Cu}_3\text{O}_{7-\delta}$. As a result, this project uses the Hall effect to detect relative changes in the carrier density while making comparisons to the superconducting performance.

Before proceeding, it is useful to present the theoretical electronic band structure

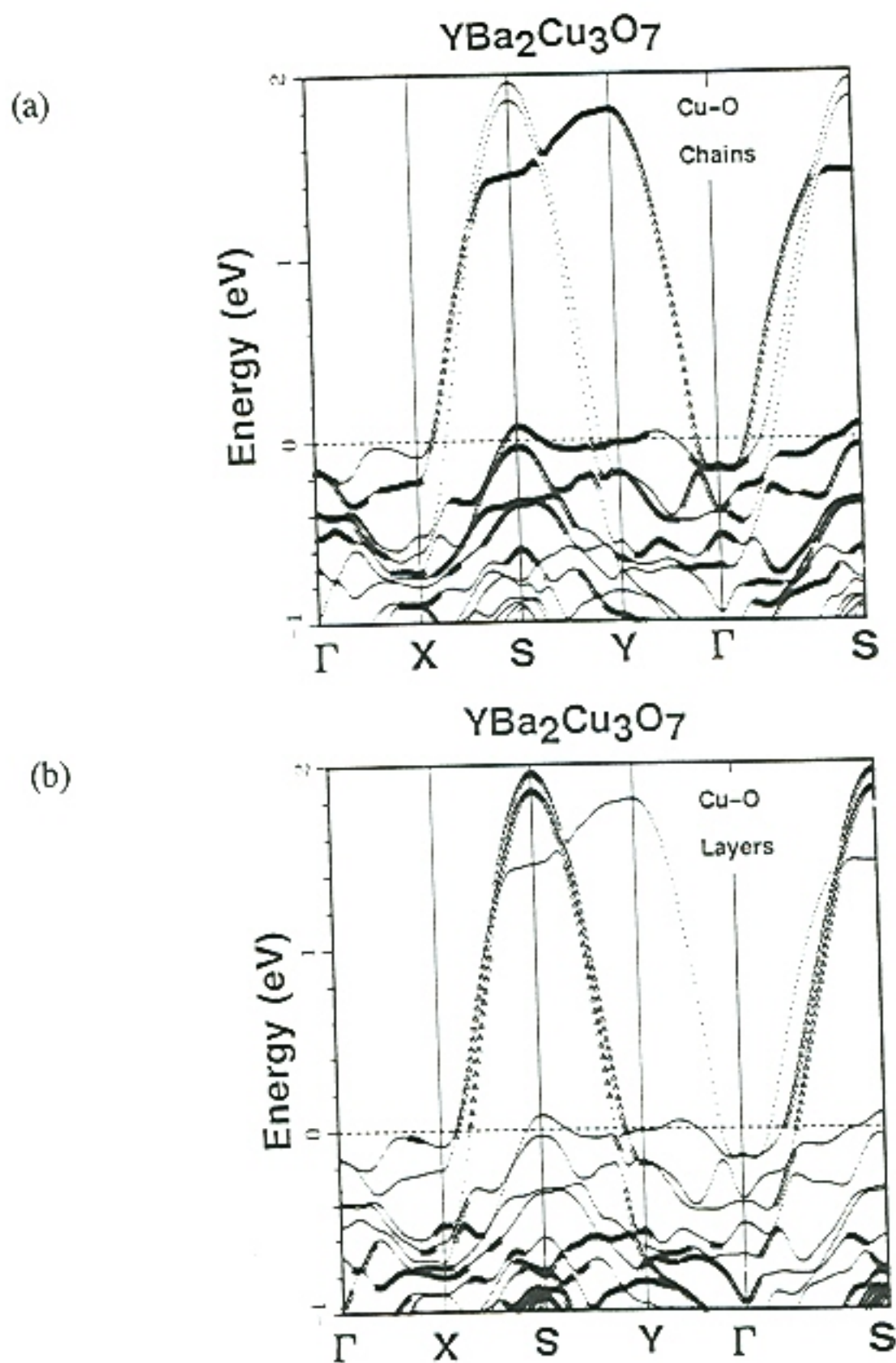
Figure 1



Accepted atomic structure of $\text{YBa}_2\text{Cu}_3\text{O}_7$ determined from neutron diffraction. The solid bars help to denote the Cu-O chains and the Cu-O_2 planes. This "orthorhombic" structure has the dimensions $3.822 \text{ \AA} \times 3.885 \text{ \AA} \times 11.680 \text{ \AA}$. The inset shows the corresponding Brillouin zone. *Source*: H. Krakauer, W. E. Pickett, and R. E. Cohen, J. Supercond. 1, 111 (1988).

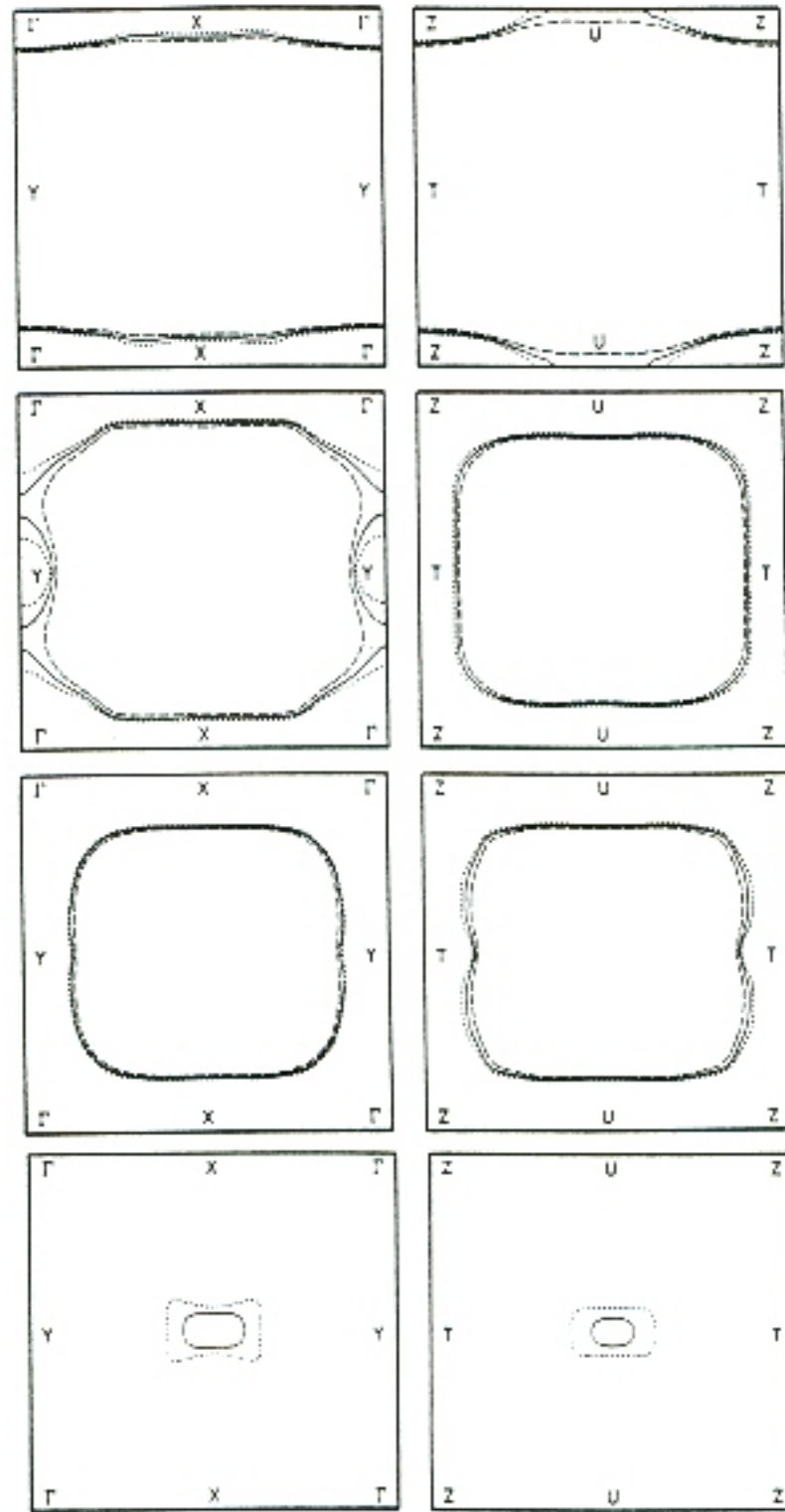
for $\text{YBa}_2\text{Cu}_3\text{O}_7$. These calculations were first performed by Krakauer *et al.*⁷ at the Naval Research Laboratory in Washington, D.C. using the linearized augmented plane wave (LAPW) method. The assumed lattice parameters used in this procedure were as follows: $a = 3.822 \text{ \AA}$, $b = 3.885 \text{ \AA}$, and $c = 11.680 \text{ \AA}$. The resulting band structure is shown in Figure 2. From this, it is apparent that four bands cross the Fermi level in $\text{YBa}_2\text{Cu}_3\text{O}_7$, and the corresponding Fermi surfaces are shown in Figure 3. Before the Santa Fe conference in 1991, few people believed these results due to the immense complexities involved in performing these calculations. However, recent experimental evidence from various types of measurements directly confirms the accuracy of these Fermi surfaces.⁸ Moreover, these band structures lead to interesting electronic DOS features. The calculated total and partial DOS [Figure 4] reveal two interesting features. First, the planar oxygen states, e.g., O(2) and O(3), have nearly identical DOS indicating that the orthorhombic distortion ($a \neq b$) has little effect on the chemical environment of the Cu-O₂ planes. Second, most of the states near and just below E_F are associated with the "chain" derived bands. Moreover, a striking peak associated with the "chain" related bands appears 0.085 eV below E_F . Krakauer *et al.*⁷ points out that this feature is associated with only the O(1) and O(4) atoms. In addition, this feature is probably not coincidental and Yu⁹ showed that it simply dropped farther below the Fermi energy E_F in the 60K phase of $\text{YBa}_2\text{Cu}_3\text{O}_{6.5}$. However, the physical significance of this DOS peak is not obvious at the present, but it is believed to be strongly associated with the normal state properties. As a result, a thorough study of the experimental data in the framework of these theoretical findings may shed some

Figure 2



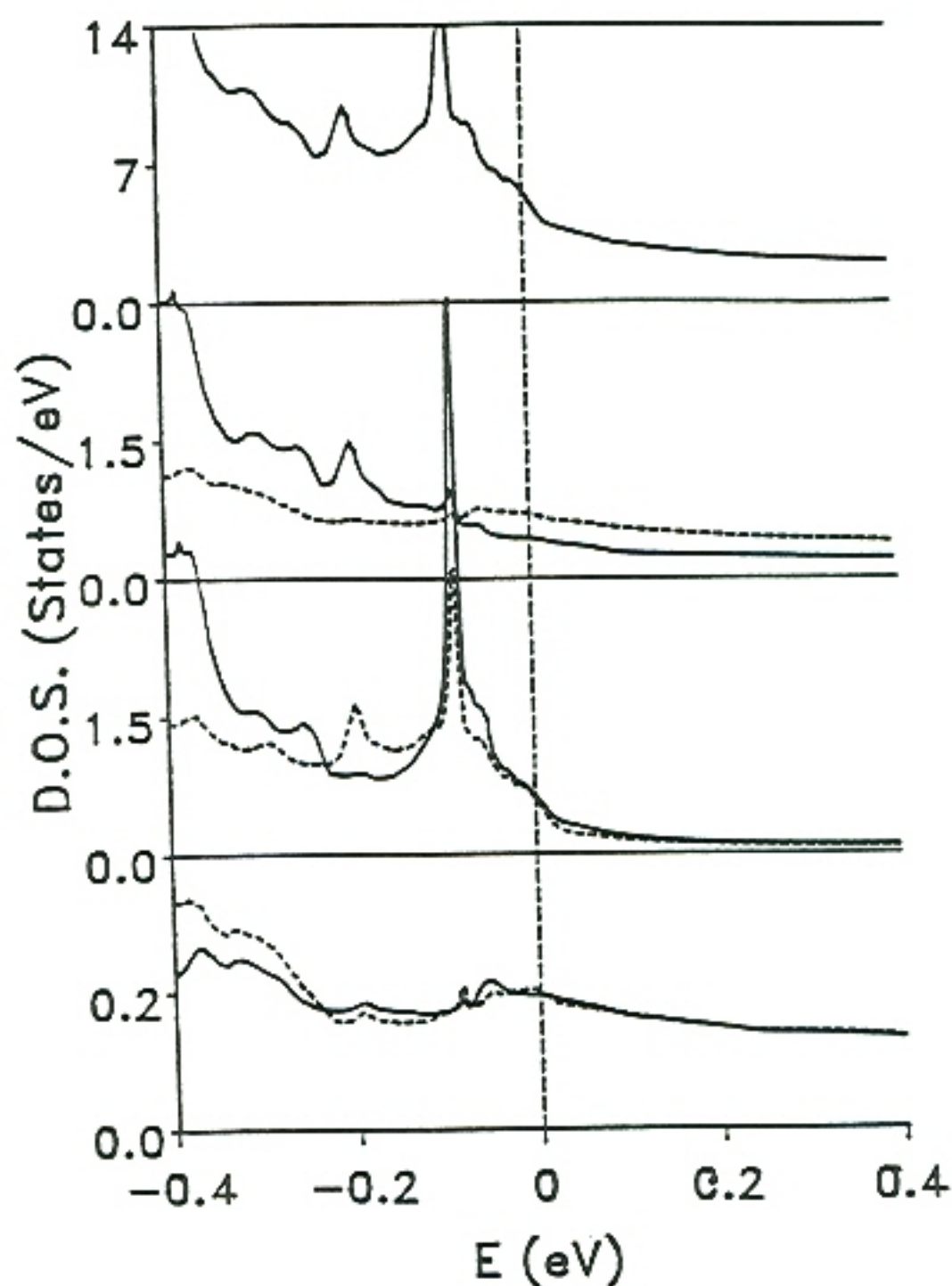
Band structure of $\text{YBa}_2\text{Cu}_3\text{O}_7$ in the $k_z = 0$ plane near the Fermi level ($E_F = 0$). (a) States derived mainly from the "chains" are emphasized by the large symbols, whereas in (b), states derived mainly from the "planes" are emphasized by the large symbols. Note that most of the states within 0.5 eV of the Fermi energy are "chain" derived states. Source: H. Krakauer, W. E. Pickett, and R. E. Cohen, J. Supercond. 1, 111 (1988).

Figure 3



Fermi surfaces for the four bands crossing the Fermi energy E_F . The left half represents the bands occurring at $k_z = 0$, whereas the right half represents the bands at $k_z = 0.5$. The top and bottom panels depict the "chain" derived bands which, show a quasi-one dimensional character, whereas the middle panels depict the "plane" derived bands which, are more two dimensional. The solid lines represent the calculated value of E_F , and the short (long) dashes represent the displacement due to 0.2 fewer (more) electrons. Hence, these differences reflect the band masses. *Source:* H. Krakauer, W. E. Pickett, and R. E. Cohen, *J. Supercond.* 1, 111 (1988).

Figure 4



Total and partial electronic densities of states (DOS) of $\text{YBa}_2\text{Cu}_3\text{O}_7$ near the Fermi energy E_F derived from the band structure results. Top panel, total DOS; second panel, Cu(1) [solid] and Cu(2) [dashed] DOS; third panel, O(1) [solid] and O(4) [dashed] DOS; bottom panel, O(2) [solid] and O(3) [dashed] DOS. Note the striking peak just below E_F involving only the "chain" related states. *Source*: H. Krakauer, W. E. Pickett, and R. E. Cohen, *J. Supercond.* **1**, 111 (1988).

light as to the actual significance of these features.

Early experimental work on oxygen deficient $\text{YBa}_2\text{Cu}_3\text{O}_{7-\delta}$ led to the discovery of two plateaus in $T_c(\delta)$ that are now well known.¹⁰ More recently, it was found that these plateaus are absent in samples prepared by rapid quenching from high temperatures.^{11,12} Although the origin of these features has proved difficult to elucidate, several elaborate electronic models have been proposed that rely either on a two-gap mechanism¹³, or on charge transfer from the Cu-O chains to the Cu-O₂ planes.^{14,15} However, magnetic hysteresis studies clearly show anomalous "fish tails" that have been attributed to defect clustering in oxygen deficient bulk samples.^{16,17} Electron diffraction studies^{18,19} and one neutron diffraction study²⁰ have suggested that a discrete series of ordered superstructures, with small differences in oxygen deficiency δ , are simultaneously present only in the δ -range of the plateaus. If the size of such domains exceeds that of the coherence length ξ ($\sim 20\text{\AA}$), then these domains should exist with distinct T_c values. A fundamental understanding of the plateaus requires knowledge of the nature of these domains. If regions of distinct T_c 's exist, experiments inducing finite electric fields would tend to generate normal currents, thereby averaging over the phase distribution. On the other hand, transport studies at the limit of relatively small electric fields ($1\text{ }\mu\text{V/cm}$) would greatly emphasize the phase(s) with the highest critical current densities J_c , providing insight into the validity of the phase-separation scenario.

In the epitaxial thin films studied here, correlations were examined between the Hall coefficient R_H , T_c , and J_c in a series of eleven epitaxial thin films that were

rendered oxygen deficient by thermal processing under controlled conditions. The results presented here are based on two samples representative of the highest quality thin films. Moreover, to better understand the origin of the $T_c(\delta)$ plateaus and to provide clues as to the possible pairing mechanism, systematic changes in the fluctuation regime of the resistive transitions $\rho(T,H)$ and the transition temperature T_c as a function of oxygen deficiency δ in two of these epitaxial thin films were also examined. This allowed the determination of the upper critical field H_{c2} as a function of oxygen deficiency δ by application of the high field fluctuation theory of Ullah and Dorsey²¹ to the experimental data. In these two films, a plateau in the slope of the upper critical field $dH_{c2}/dT = -1.7$ T/K, was found for $H \parallel c$. This result supports the applicability of the clean limit of BCS theory. On the contrary, the fluctuation theory did not accurately describe the transitions off the 90K plateau. This failure off the 90K plateau will be attributed to an extrinsic broadening of the transitions, arising from gross inhomogeneities in oxygen content for $\delta > 0.2$. Data will be presented to support the existence of such inhomogeneities off this T_c plateau, i.e., $\delta > 0.2$, which appears to occur in all of the epitaxial thin films.

The Hall effect has been of considerable interest in the high- T_c superconductors, due not only to the unusual temperature dependence,^{22,23} but also to the change in the sign of the Hall coefficient R_H sometimes observed near T_c .^{24,25} Several explanations have been offered to explain this sign reversal of the Hall coefficient,^{26,27,28} which appears mostly in impure^{29,30} and in polycrystalline samples.²⁴ In the eleven epitaxial films (two laser ablated and nine coevaporated) of

YBa₂Cu₃O_{7- δ} used throughout this work, the sign reversal was *not* universally observed. In fact, only the sample having the highest J_c [a laser ablated film with an irreversibility field $B_{irr}(H//c) = 4.5T$ at 77K and a critical current density $J_c(77K) = 5 \times 10^6$ A/cm²] showed a sign reversal of R_H near T_c . Moreover, the highly crystalline, coevaporated films with lower defect pinning *never* exhibited a sign reversal of R_H near T_c at any applied field.³¹ This is perplexing, as most intrinsic flux creep models describing this sign reversal predict that these effects should be observed only in the limit of *weak* pinning energies.²⁶ To pursue this issue, a study was initiated where the sample was annealed at various oxygen partial pressures at 550°C followed by slow cooling to vary the oxygen deficiency δ . After ten anneals, a final anneal at 1 atm O₂ returned the sample to full oxygenation. All of the starting properties, i.e., the resistivity ρ , R_H , J_c , and T_c , returned to their original values except for the superconducting Hall effect transition which no longer exhibited a sign reversal near T_c . Therefore, the random appearances of these sign reversals of R_H near T_c upon annealing prompted further investigation into the possibility of extrinsic mechanisms such as current percolation.

As for the granular thin films, a self-consistent critical current model in the Josephson mixed state is proposed for a series of *c*-oriented, polycrystalline and for a series of epitaxial triaxially-oriented YBa₂Cu₃O_{7- δ} thin films. The flux pinning activation energies were experimentally determined from electrical transport measurements over a wide range of temperatures and were found to behave quite differently for the two types of granular films. With the derived activation energies

applied to an SNS weak-link system, thermally activated flux motion is shown to reproduce the experimentally measured critical current densities.

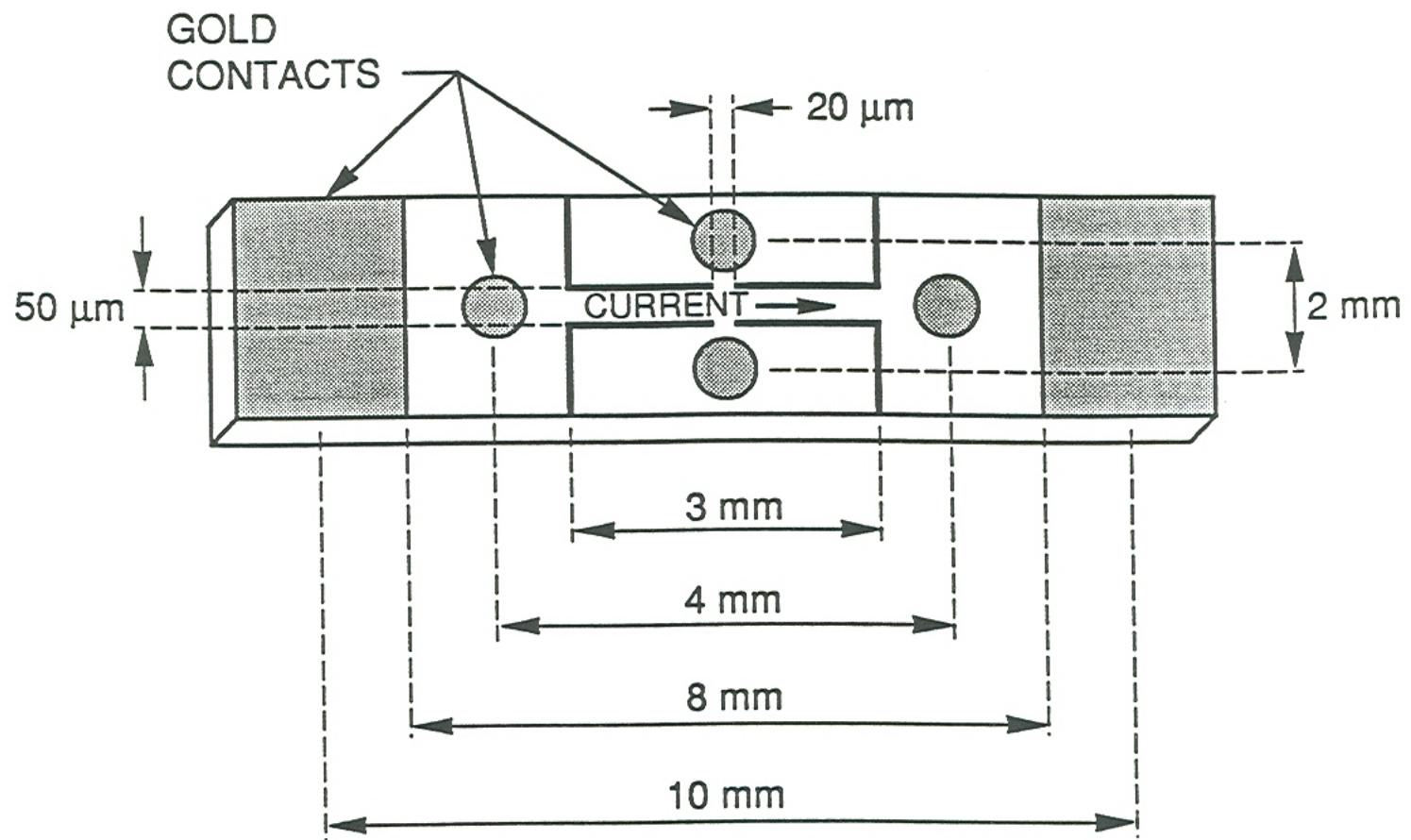
Overall, the present study answers many questions regarding the *intrinsic* or *extrinsic* nature of some properties of $\text{YBa}_2\text{Cu}_3\text{O}_{7-\delta}$. Many effects such as the sign reversals of R_H near T_c and the $T_c(\delta)$ plateaus appear to be *extrinsic* in origin, rather than *intrinsic* as previously thought. Earlier work on the I-V characteristics at the Naval Research Laboratory supports this argument.³² Like the fully oxygenated polycrystalline thin films, increasing the oxygen deficiency ($\delta > 0$) in the epitaxial films appears to create a weak link array of superconductor-normal metal-superconductor (SNS) junctions, probably due to clustering or inhomogeneous distributions of the oxygen atoms. Therefore, careful thought must be placed upon any new observations before deciding whether or not these observations are *intrinsic* properties in this new class of superconductors. Finally, the results of this dissertation were already made public in several oral talks^{33,34,35,36} and scientific articles,^{37,38,39,40} either published or as preprints awaiting clearance for publication.

II. EXPERIMENTAL ASPECTS

A. Overview of the Most Important Procedures

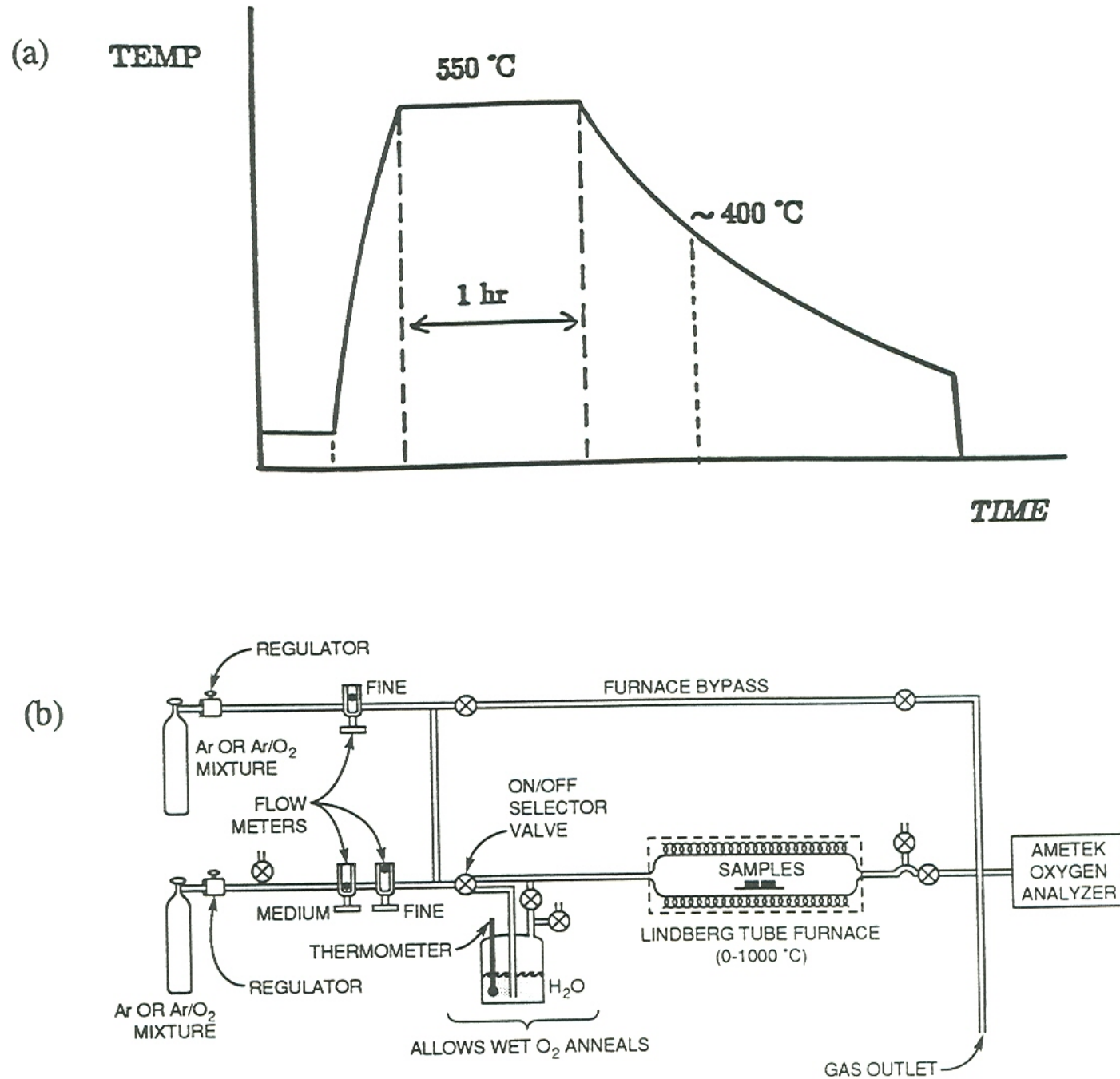
The epitaxial thin films used in this study were grown either by the BaF_2 process⁴¹ or by pulsed laser ablation⁴² onto LaAlO_3 substrates. For electrical transport measurements, the c -axis perpendicular films were photolithographically patterned with a 3 mm long by 50 μm wide bridge containing two opposing 20 μm wide Hall terminals. Six gold dots were then sputtered onto contact areas to allow simultaneous measurements of the resistive and Hall signals using standard dc techniques [see Figure 5]. Note that the use of inert gold contacts avoided the problems associated with sample contamination during the reannealing of these samples. Currents were systematically reversed to eliminate thermal emfs. Contact resistances were typically less than 0.1 m Ω after the first full oxygenation anneal at 550°C in 1 atm O_2 . This allowed easy, solder-free mounting and demounting with the use of Au-In-Au pressure pads and spring loaded "pogo" contacts. To control the oxygen deficiency δ , sequential isobaric anneals⁴³ at 550°C were conducted under reduced partial pressures of O_2 [see Figure 6(a) and Figure 6(b)]. Thus, small changes in T_c , J_c , and R_H as a function of δ could be obtained in a given sample of fixed bridge geometry, thereby eliminating the relative errors due to cross sectional differences which exist between samples. The effects of oxygen depletion were reversible, as demonstrated by a final anneal at 1 atm O_2 that reestablished the starting properties of the films even after eleven sequential anneals. To eliminate offset voltages due to the

Figure 5



Typical current bridge pattern for the thin films used throughout this study. The transport bridges were photolithographically defined as 3 mm x 50 μm ; these bridges contained two opposing 20 μm wide Hall terminals. Afterwards, six gold contacts (dark regions) were sputtered onto the samples. In general, resulting contacts had contact resistances of not more than 0.1 m Ω each.

Figure 6



Method of control of the residual oxygen deficiency δ . (a) The oxygen deficiencies were controlled by sequential anneals at 550°C, followed by the slow cooling shown. Flowing Ar+O₂ mixtures allowed easy control of the resulting oxygen content, since δ depended on the partial pressure of O₂ chosen. (b) This was accomplished with the furnace setup as shown. Note that the oxygen partial pressure was measured with an Ametek oxygen analyzer. Part (a) was adapted from R. Feenstra (unpublished).

physical Hall terminal mismatches and to the transverse-even field⁴⁴ R_{TE} [nonzero for $\delta > 0.5$, see Figure 7], the Hall coefficient in the limit of low-field was defined by the difference of the Hall resistivities taken in opposing fields,

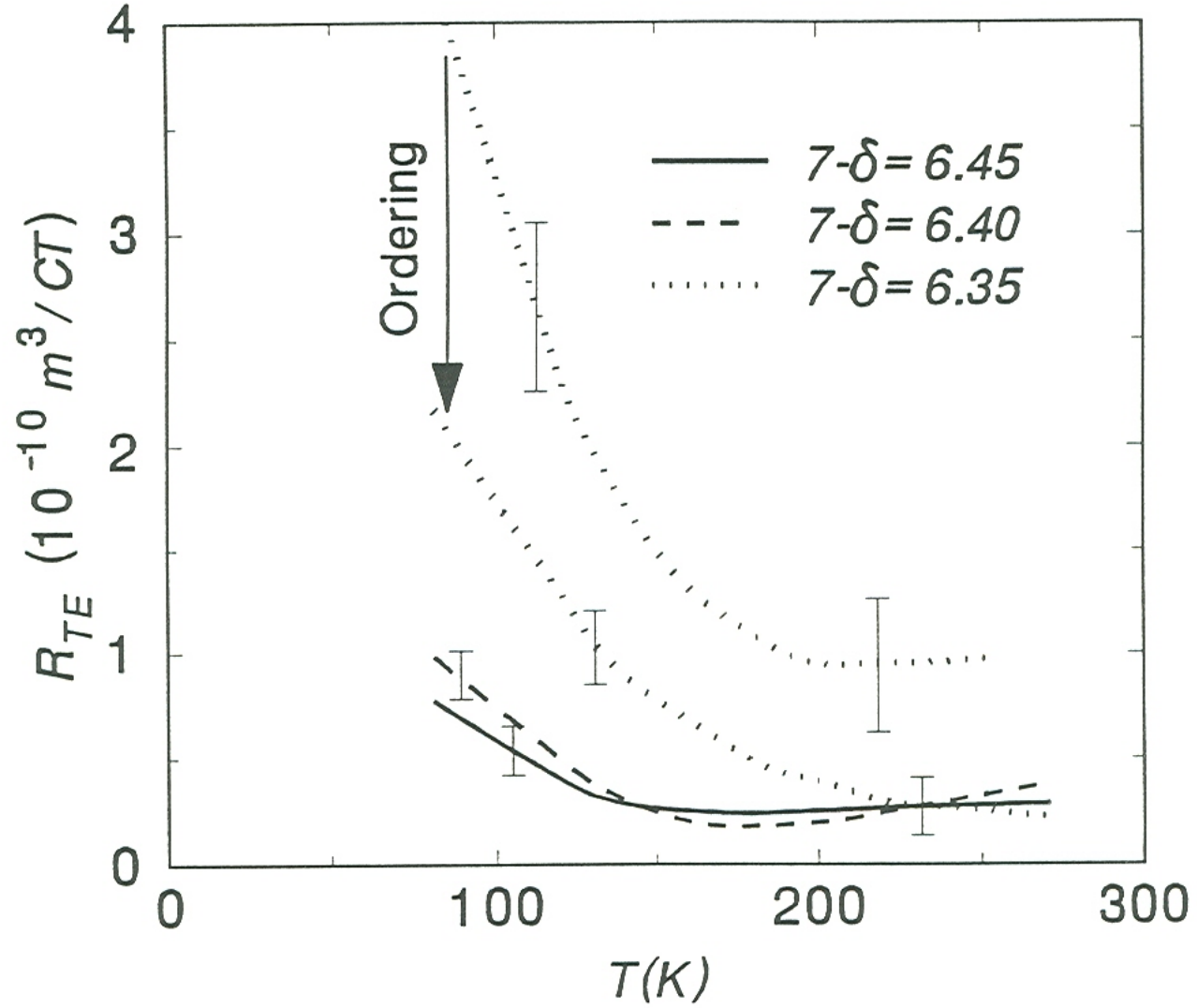
$$R_H = \frac{\rho_{yx}(H) - \rho_{yx}(-H)}{2H} . \quad (1)$$

Moreover, in order to perform this subtraction, each temperature sweep was interpolated at 0.5 Kelvin intervals using the Lagrange method. Thus, these subtractions were easily accomplished as a function of temperature [Figure 8] within a Lotus spreadsheet. In addition, magnetic fields of 8 Tesla were applied parallel to the c -axis, and were verified to be in the low-field regime, since no saturation was observed in the R_H vs. B behavior through 8 Tesla⁴⁴ while in the normal state at all oxygen deficiencies. More importantly, this "*subtraction*" procedure was utilized to determine the Hall coefficient in a copper test film patterned according to Figure 5. Fortunately, a temperature independent Hall coefficient $R_H = -5.9 \times 10^{-11} \text{ m}^3/\text{C}$ was obtained, which agrees with the accepted value for copper.⁴⁴ In sum, reliable values for the Hall coefficient in thin films can be obtained by utilizing the basic procedures outlined in this section.

B. Estimation of Oxygen Deficiency δ

From systematic x-ray diffraction studies of four films, the following correlation between the relative change in the c -axis lattice parameter c and the normal state electrical conductivity σ was obtained for oxygen contents in the regime of the 90K

Figure 7

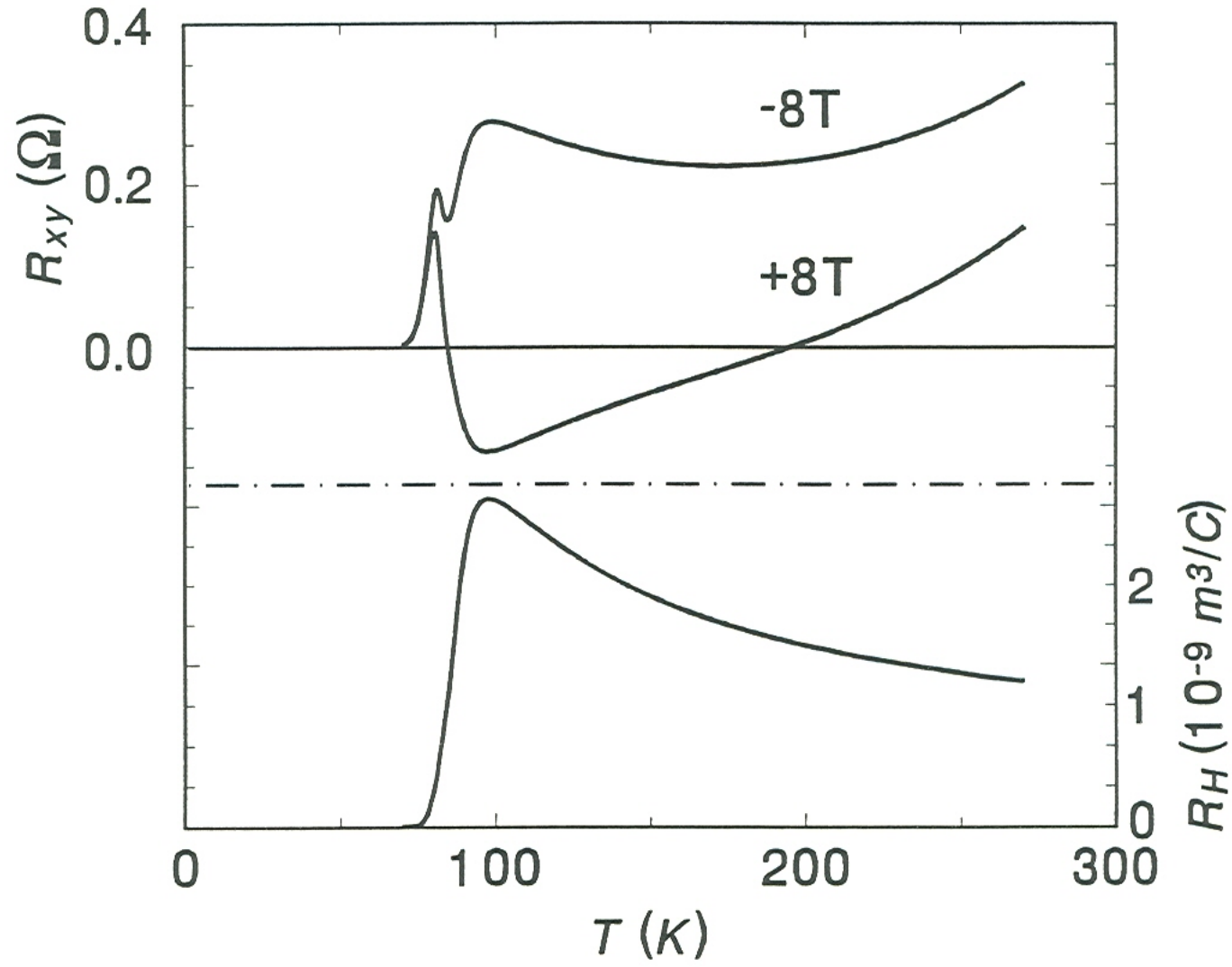


Transverse-even coefficients R_{TE} observed in oxygen deficient $\text{YBa}_2\text{Cu}_3\text{O}_{7-\delta}$ (non-zero when $\delta > 0.5$). These signals are defined by⁴⁴

$$R_{TE} = \frac{\rho_{yx}(H) + \rho_{yx}(-H) - 2\rho_{yx}(H=0)}{2H^2}, \quad (2)$$

where $\rho_{yx}(H)$ is the "apparent" Hall resistivity at an applied field $H \parallel c$. Note that $\rho_{yx}(H=0)$ must be inserted to eliminate the offset signals due to physical misalignments of the Hall probes. Moreover, the resulting signals are "extremely weak" and would not have been detected without the computerized data acquisition system described in Section D. In addition, aging effects (discussed in Chapter IV) were observed for the composition $7-\delta \approx 6.35$. However, *no* theory in the low-field limit exists at present to explain the significance of these signals. Unfortunately, such non-zero signals *require* the application of Equation (1) in defining the Hall coefficient.

Figure 8



Example determination of the Hall coefficient R_H as described in the text. The field reversal process (top half) followed by (1) a Lagrange interpolation of the data at 0.5K intervals and (2) the subtraction of these interpolated curves according to Equation (1) generates the defined Hall coefficient curve shown. Notice the complete disappearance of the "anomalous" bump in the superconducting transition.

plateau:

$$\frac{\Delta c}{c_o} = (4.8 \pm 0.5) \times 10^{-3} \frac{\Delta \sigma}{\sigma_o}, \quad (3)$$

where c_o and σ_o represent the fully oxygenated state.⁴⁵ In bulk $\text{YBa}_2\text{Cu}_3\text{O}_{7-\delta}$, the c -lattice expansion has been correlated with the oxygen deficiency δ in the orthorhombic state according to the average results of Cava *et al.* and Jorgensen *et al.*:^{46,47}

$$\frac{1}{c_o} \frac{\Delta c}{\Delta \delta} = +10.7 \times 10^{-3}. \quad (4)$$

Combining Equations (3) and (4) leads to the result

$$\delta \approx 0.45 \left| \frac{\Delta \sigma}{\sigma_o} \right|. \quad (5)$$

Values of δ obtained from Equation (5) must be regarded as provisional, since extrinsic factors such as substrate-induced strains may alter both the magnitude of the c -lattice parameter, as well as its response to δ . The values are quoted to provide a familiar and relative labeling of composition, but *none* of the following analyses in this dissertation depend quantitatively on the precision of the values. With this proviso, Tables I and II tabulate experimental information associated with the determination of the δ values for the two representative samples used in the figures throughout this work. Since Equation (5) generates a maximum value of only $\delta = 0.45$, e.g., $|\Delta \sigma / \sigma_o| \rightarrow 1$, this equation was utilized for the estimates of δ only in the range in which the x-ray data were obtained, i.e., $\delta \leq 0.3$. For larger oxygen deficiencies, δ was based entirely on

Table I. Experimental data used in the determination of δ 's depicted in the figures pertaining to the coevaporated thin film. The calculations of δ are described in the text and are rounded to the nearest 0.1. The letter "a" denotes "aged" at room temperature for 4 days before performing these measurements to avoid any "quenching" effects.

Estimated $7-\delta$	Anneal $\text{Log}(P_{O_2})$	$ \Delta\sigma/\sigma_0 $ (at 100K)	$J_c(1.2K)$ [A/cm ²]	T_c (at $0.01xR_N$)
7.0	1 atm	0	1.47×10^7	89.4K
6.9	-0.60	0.201	7.40×10^6	90.4K
6.8	-0.97	0.430	3.16×10^6	89.6K
6.7	-1.56	0.650	6.50×10^5	74.5K
6.6	-2.14	0.678	1.58×10^5	60.5K
6.5	-2.50	0.702	1.00×10^5	54.0K
6.4	-3.00	0.903 (a)	$\approx 1 \times 10^4$	29.0K (a)

Table II. Experimental data used in the determination of δ 's depicted in the figures pertaining to the laser ablated thin film. The calculations of δ are described in the text and are rounded to the nearest 0.05. The letters "q" and "a" denote "quenched" from 200°C and "aged" at room temperature for 4 days, respectively. Limited J_c measurements were conducted at 1.2K to avoid burning out this sample.

Estimated 7- δ	Anneal Log(P_{O_2})	$ \Delta\sigma/\sigma_0 $ (at 100K)	$J_c(1.2K)$ [A/cm ²]	T_c (at 0.01x R_N)
7.00	1 atm	0	2.50×10^7	88.3K
6.95	-0.60	0.110	N/A	88.9K
6.90	-1.00	0.210	N/A	89.4K
6.85	-1.48	0.355	N/A	88.8K
6.80	-1.78	0.460	N/A	87.0K
6.70	-2.09	0.645	N/A	76.0K
6.50	-2.53	0.719	N/A	56.2K
6.45	-3.05	0.835 (q); 0.824 (a)	N/A	38K (q); 42K (a)
6.40	-3.25	0.906 (q); 0.897 (a)	N/A	12K (q); 20K (a)
6.35	-3.55	0.967 (q); 0.963 (a)	N/A	Insulating

the comparisons of T_c to those published by Veal *et al.* and Jorgensen *et al.*^{15,47}

C. The Hall Cryostat

The electrical transport properties of the $\text{YBa}_2\text{Cu}_3\text{O}_{7-\delta}$ thin films were obtained using a custom designed cryostat built by Cryomagnetics in Oak Ridge, Tennessee. This cryostat contains a 10 Tesla superconducting magnet [Table III lists specifications] suspended in a vacuum insulated dewar. Moreover, this superconducting magnet was especially designed to operate in a "*persistent*" mode. This mode allows the magnet to operate without a power supply after the magnet is charged. This is accomplished by a superconducting "*short*" which is placed across the magnet leads near the magnet. Whenever the magnet is charged or discharged, a heater mounted against this "*short*" is activated causing the "*short*" to become normal. Thus, the charging (or discharging) current will not flow through this lead except when the heater is off. More importantly, such "*persistence*" modes allow very stable fields which are ideal for Hall effect studies. Moreover, the "*persistent*" mode minimizes liquid helium (LHe) boil-off due to the discontinued application of current to the magnet leads after the magnet is charged. In addition, other features minimizing liquid helium losses include (1) a liquid nitrogen (LN_2) jacket surrounding the liquid helium can and (2) a pair of vapor-cooled magnet leads. The liquid nitrogen jacket minimizes the thermal radiation load on the liquid helium bath whenever the magnet is cooled to 4.2 Kelvins. The helium vapor-cooled leads simply make the best use the helium boil-off gas by channeling this cold gas through the upper half of the current leads into the atmosphere. In sum, this

Table III. Specifications of the custom designed 10 Tesla superconducting magnet built by Cryomagnetics for Martin Marietta Energy Systems. The magnet consists of a coil of twisted multifilamentary NbTi wire in a copper matrix. The copper matrix used in the construction acts as a form of "*quench*" protection. Furthermore, the coil is completely epoxy impregnated to prevent any shifting of the wires during usage.

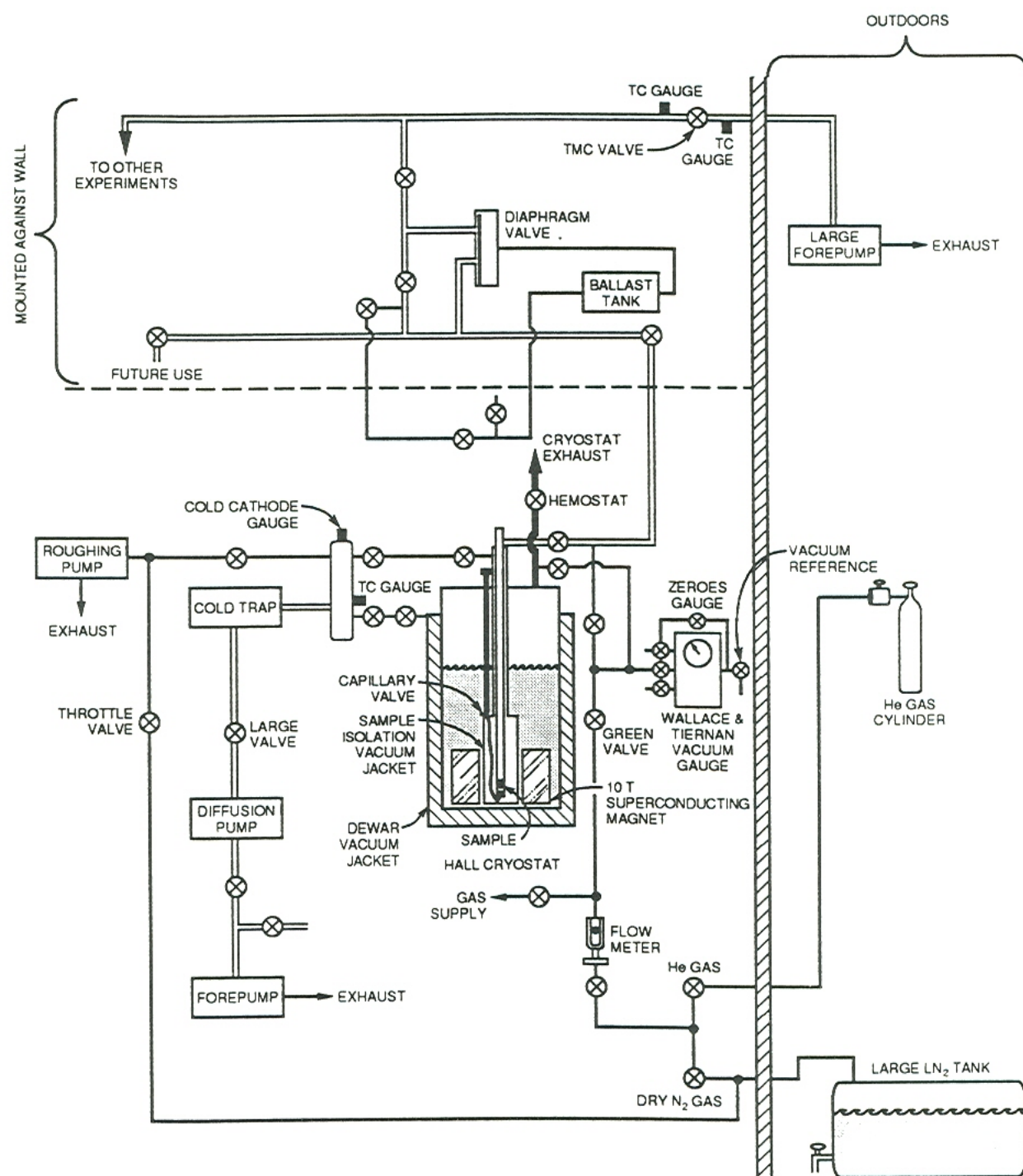
Superconducting Magnet Specifications Serial Number C182-M	
Rated Central Field	8 Tesla (4.2 K)
.....	10 Tesla (2.8 K)
Maximum Test Field	8.59 Tesla (4.2 K)
Rated Current	77.74 Amps (8 Tesla)
Inductance	3.45 Henries
Homogeneity (2.375 in. below top)	$\pm 0.5\%$ over 1 cm DSV
Field to Current Ratio	1029.1 Gauss / Ampere
Charging Voltage	2 Volts
Persistence Switch Current	45 mA

Source: Operating Instruction Manual for Superconducting Magnet System, for U. S. Department of Energy, Martin Marietta Energy Systems (Cryomagnetics, Oak Ridge, TN), p. 5.

superconducting magnet system was found to be very efficient in measuring both the Hall coefficient R_H and critical current density $J_c(H)$.

To control the sample temperature, this cryostat (called the *Hall cryostat*) can be operated in one of two modes. First, the sample can be submerged in either liquid nitrogen (LN_2) or liquid helium (LHe). The vacuum pump station shown in Figure 9 can then maintain a preset boiling point of either cryogen by controlling the vapor pressure. This is accomplished by placing a predetermined amount of gas in the ballast tank [Figure 9] which in turn controls the amount of suction placed by the diaphragm valve on the sample space. The advantages of this form of control include: (1) a high degree of temperature stability, and (2) minimization of sample heating at the resistive contacts by more efficient dissipation of generated heat into a liquid. However, the disadvantages include: (1) limited range over which the temperature can be controlled (e.g., 52K⁴⁸ – 78K using LN_2 and 1.2K – 4.2K using LHe), and (2) possible "plugging" of the capillary valve with nitrogen ice when the magnet is operating at liquid helium temperatures while the sample is submerged in liquid nitrogen. The second form of temperature control, however, is more versatile and was used for performing the Hall measurements. This type of control utilizes a capillary valve and transfer tube which transfers a small, controlled amount of cryogen, usually LHe, from the magnet can to the sample space [see Figure 9]. Moreover, just before this cryogen enters the sample space, it first passes through a copper block fitted with a heater coil. The setpoint temperature of this copper block is maintained by a DRC-91C Lake Shore temperature controller as well as the flow rate through the capillary valve. More

Figure 9

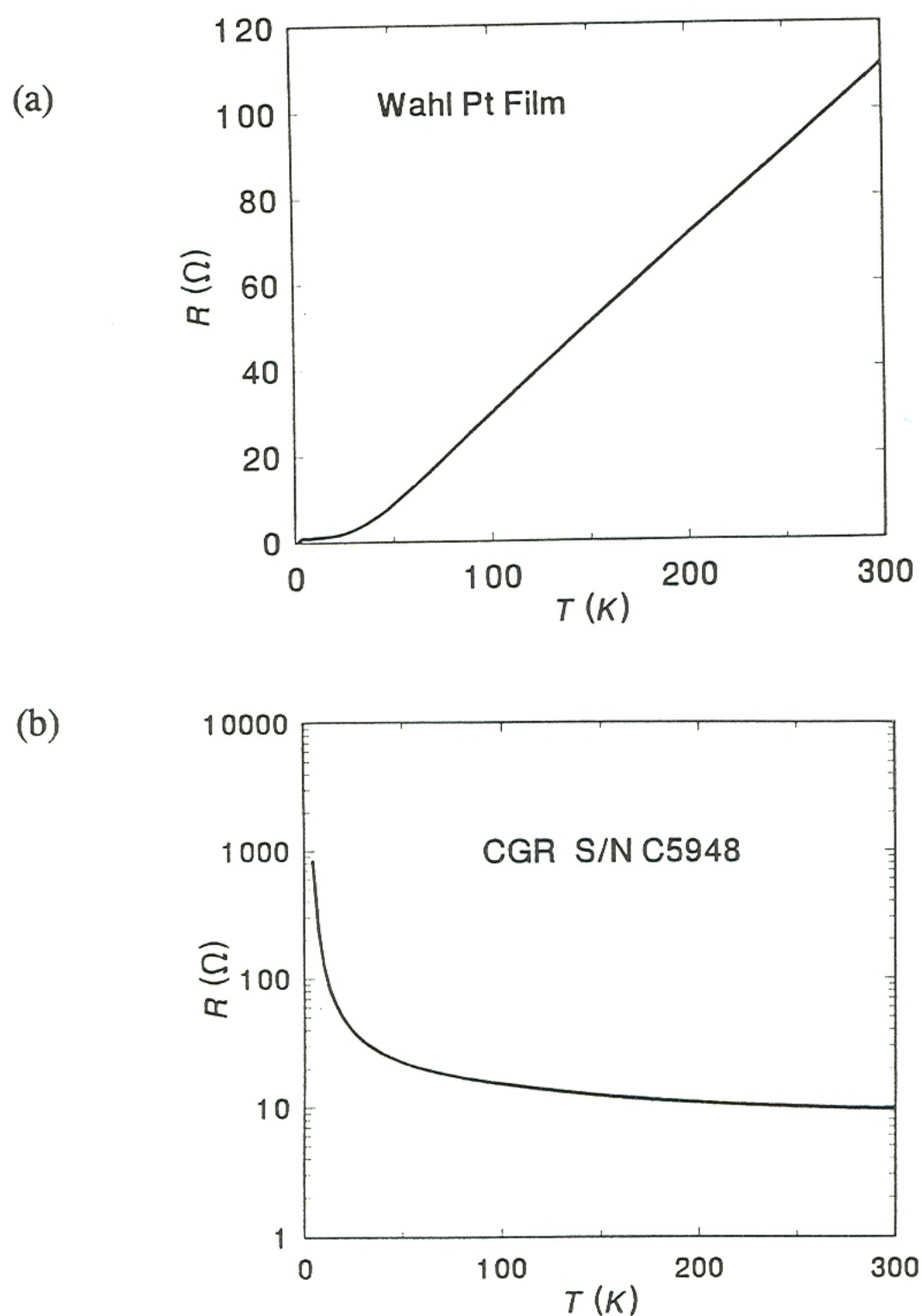


Vacuum pump station and gas line diagram used with the Hall cryostat. This system is located at the Solid State Division of the Oak Ridge National Laboratory. The main features include (1) the "house" vacuum (mounted against wall) which can be used to control the boiling point of either LN_2 or LHe using a diaphragm valve, and (2) the capillary valve which transfers controlled amounts of either cryogen from the magnet can to the sample space. Either feature can accurately control the sample temperature.

importantly, the temperature controller is connected to the computerized data acquisition system which is discussed in more detail in the next section. Therefore, the Hall cryostat was very versatile in performing the measurements used in this dissertation.

Finally and most importantly, the sample temperature must be known to a high degree of accuracy at all times while collecting data. Unfortunately, no single thermometer can give accurate readings while subjected to magnetic fields over the entire range of temperatures utilized (1.2K – 300K). Therefore, two thermometers were mounted onto a copper block along with the sample being studied. These thermometers were: (1) a Wahl Pt film, and (2) a Carbon Glass Thermometer (Lake Shore Serial Number C5948). The Pt film thermometer typically operates with 1 mA of current and is useful at all temperatures above ~ 40 K. Below this temperature, Pt film thermometers are affected by large magnetoresistances which lead to errors in the derived temperatures. Thus, for temperatures below ~ 40 K, a Carbon Glass thermometer was used. At low temperatures, Carbon Glass thermometers are almost unaffected by applied magnetic fields. However, currents on the order of $\sim 1 \mu\text{A}$ are required to prevent internal heating of these thermometers. The calibrated resistances of both thermometers are shown in Figure 10. In addition, both of these thermometer calibrations are loaded into two column ASCII files [resistance (ohms) vs. temperature (K)] for use by the data acquisition system. This allows the computerized data acquisition system to convert the thermometer readings into common units of Kelvins as the data is being collected. Thus, this process helps to avoid possible human mistakes involved in manually converting numerous readings required in these studies.

Figure 10



Thermometer calibrations utilized by the data acquisition system. (a) The Wahl Pt film calibration as a function of temperature. This thermometer is most useful above $\sim 40\text{K}$, since a significant magnetoresistance occurs in applied fields below this temperature. (b) The Carbon Glass thermometer calibration as a function of temperature. In contrast, this thermometer is most useful below $\sim 40\text{K}$, since the resistance changes rapidly with temperature in this regime. Fortunately, this thermometer has little magnetoresistance.

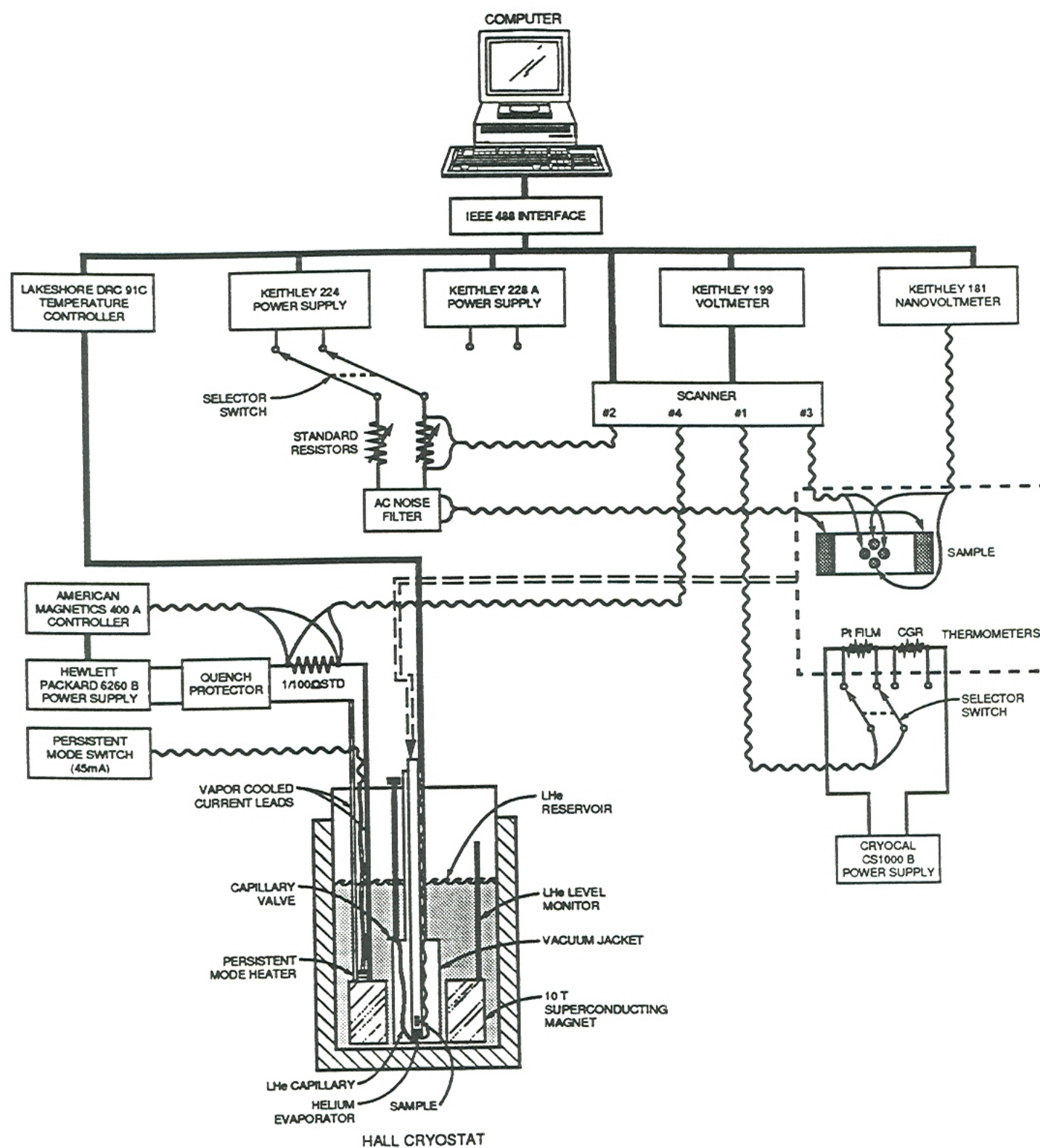
D. The Data Acquisition System

To obtain the high level of sensitivity required to accurately quantify the Hall coefficient, a computer controlled data acquisition system was developed over a period of 17 months. Interface of a computer to the instruments [Figure 11] made it possible to statistically average many sample readings taken over a short interval of time (e.g., ~ 4 readings per second), thereby eliminating most background noise sources. Moreover, the resulting computerized "*automation*" included an automatic current reversing procedure to eliminate the thermal emf's. In addition, rapid conversions from one set of units to another set of units was made possible during the actual data collection. Finally, an optional data interpolator using input temperature intervals was incorporated into the Hall acquisition program. More importantly, these tasks were accomplished with four separate (and user friendly) basic programs [listed in the Appendix] to cover every type of experiment conceived at the time of this work. These basic programs are

- (1) **DA-HALL.BAS** (to measure R_H and/or ρ versus T or H),
- (2) **DA-JCTH.BAS** (to measure J_c versus T or H),
- (3) **DA-IVT.BAS** (to obtain I-V curves), and
- (4) **DA-DRIFT.BAS** (to emulate a simple X-Y plotter).

Note that the fourth program simply records values from the "X" and "Y" voltmeters without actively controlling any instruments. This allows one to record data similar to X-Y plotters if new experiments are devised. Otherwise, one would have to wait until a new program was written in order to run the experiments with "*noise*" filtering.

Figure 11



Electronic block diagram of the computer controlled data acquisition system used in making Hall measurements. The actual software used by the computer is listed in the Appendix.

Finally, the operating principles of these programs are described below.

To activate the data acquisition system, type DA at the DOS prompt. (Note: user inputs will be denoted with bold characters throughout the rest of this section).

C:\> DA.

This automatically loads the GW-Basic software package as well as the IEEE interface commands into the computer memory. At the OK prompt, load the program (see the selections above) you intend to use by typing, for instance,

LOAD "DA-HALL.BAS"

followed by

RUN.

At this point, the program will display the first of several setup menus [e.g., Figure 12]. Here the program will prompt you to connect the Keithley 199 scanner channels to appropriate input signals (e.g., thermometer, sample voltage, standard resistor, ...). Keep in mind that Figure 11 serves as a relevant guide for such connections when performing Hall measurements. (Note: the *sample heat dissipation signal* is the smaller set of sample current leads and the *alt. signal* is intended for resistivity signals when performing Hall measurements). In addition, the Keithley 181 nanovoltmeter will be connected to either the Hall probes (for Hall measurements), or the sample voltage (for $\rho(T)$, J_c , or I-V measurements). After completing all of the connections, verify that the IEEE GPIB addresses (selected with pin settings on the back of the meters) agree with the settings shown in this setup menu. In case of a discrepancy, either change the pin settings on the back of the meters (see manuals) or

Figure 12

```

(a)      *** HARDWARE SETTINGS ***
1: X-INPUT: GPIB Address:  26      Meter ID: KEITHLEY 181/199/197
2: Y-INPUT: GPIB Address:  14      Meter ID: KEITHLEY 181/199/197

Set KEITHLEY 224 Power Supply GPIB Address to  19
and the Voltage Compliance to a Safe Value.

K-199 SETUP: Temp. signal <==> X-Channel # 1
              Curr. signal <==> X-Channel # 2
              Alt.  signal <==> X-Channel # 3
              Mag. current <==> X-Channel # 4
K-181 NANOVOLTMETER: Hall (or Rho) Signal

Reset LakeShore Temperature Controller & set GPIB address to  12

ENTER SELECTION # (<C/R> TO CONTINUE):


      *** HARDWARE SETTINGS ***
1: X-INPUT: GPIB Address:  26      Meter ID: KEITHLEY 181/199/197
2: Y-INPUT: GPIB Address:  14      Meter ID: KEITHLEY 181/199/197
3: P-INPUT: GPIB Address:  11      Pwr Supp ID: Keithley 228 Power Supply

(b)      Meter Setup:  X channel #1 <==> Thermometer Voltage Signal
                      X channel #2 <==> Sample Current Std. Resistor
                      X channel #3 <==> Sample Heat Dissipation Signal
                      X channel #4 <==> Magnet Curr. 1/100 Ohm Resistor
                      Y voltmeter <==> Sample Voltage

Reset DRC-91C & Set GPIB address to  12

ENTER SELECTION # (<C/R> TO CONTINUE):

```

Hardware Settings Menu for (a) DA-HALL.BAS and (b) DA-JCTH.BAS. This first program menu prompts the user to connect the various signals to the appropriate meter inputs. The menus for DA-IVT.BAS and DA-DRIFT.BAS are similar to these menus.

change the GPIB addresses in the program by typing 1, 2, or 3, followed by the **new GPIB setting** and a **RETURN**. Upon completion of this hardware setup menu, type **RETURN** to proceed.

At this point, the program will display a second menu entitled the SET-UP PARAMETERS menu. Examples of these menus are shown in Figure 13. Here, you can select an **option number** of a parameter that you intend to change (e.g., new thermometer calibration filename or a new scaling factor ...) followed by a **RETURN**. After all of the parameters meet your requirements, type a **RETURN** without a preceding option number to automatically begin the data acquisition sequence. Finally, a brief description of each set-up option is given below (note: the computer prompts are printed in upper case *ITALICS* for enhanced readability).

(1) *FILENAME OF SETUP AND GRAPHICS PARAMETERS*: This file contains the user parameters for all three menus saved from a previous run. Use of this feature is optional. Also, these files have the default directory C:\IEEE488\.

(2) *X1-VOLTAGE SCALE FACTOR*: Scaling factor necessary to convert the thermometer voltage reading to units of ohms, i.e., $1 / I_{\text{thermometer}}$.

(3) *X1-SIGNAL STEP SIZE*: Minimum change required in the thermometer resistance before storing the current sample readings to the specified file.

(4) *X2-SIGNAL SCALE FACTOR*: Scaling factor necessary to convert the voltage measured across the standard resistor to units of amps, i.e., $1 / R_{\text{std. ohms}}$.

Figure 13

(a)

```

*** SET-UP PARAMETERS ***
1:  FILENAME OF SETUP AND GRAPHICS PARAMETERS TO USE: HALL.PAR
2:  FILENAME OF SETUP AND GRAPHICS PARAMETERS TO SAVE TO: HALL.PAR
3:  X1-VOLTAGE SCALE FACTOR (Temp Signal/Vmeas): 1000
4:  X1-SIGNAL STEP SIZE: .2
5:  X2-SIGNAL SCALE FACTOR (1/STD Ohms) : .25
6:  X3-VOLTAGE SCALE FACTOR (Alt Signal/Vmeas) : 1000
7:  Y-VOLTAGE SCALE FACTOR (Nano Signal/Vmeas) : 1000
8:  Y-SIGNAL STEP SIZE : .005
9:  MAG. FIELD STEP SIZE (kOe) : 1
10: DATA FILENAME: Hall.dto
    TITLE: Hall Effect Measurement
11: THERM. CAL. TABLE FILENAME (for X1-signal conversion): HC2PT.CAL
    TITLE:
12: NO. OF SAMPLES IN DIGITAL FILTERING: 2
13: SCREEN GRAPHICS PARAMETERS SETUP: <ACTIVE>
14: TRANSPORT CURRENT [n.nnnE(sign)nn]: 1.000E-03
15: EXIT PROGRAM
16: TEMPERATURE CONTROLLER: <ACTIVE>
    Control Range = 83 - 300 K & Vap-Samp = -35 K @ RT
17: INTERPOLATE FILE GIVEN IN OPTION 10 ACCORDING TO TEMPERATURE

>ENTER SELECTION # (<C/R> TO EXECUTE):

```

(b)

```

*** SET-UP PARAMETERS for DA-JCTH.BAS ***
1:  FILENAME OF SETUP AND GRAPHICS PARAMETERS TO USE: JCTH.PAR
2:  FILENAME OF SETUP AND GRAPHICS PARAMETERS TO SAVE TO: JCTH.PAR
3:  X2-VOLTAGE SCALE FACTOR (Signal/Meas V or 1/STD ohms): 1
4:  X2-SIGNAL RANGE(Amps)/STEP SIZE fraction: .001 to 3 / .035
    X2-SIGNAL BACKSTEP (Fraction of Xminc): .05
5:  Y-VOLTAGE SCALE FACTOR (Signal/Meas V): 1000000
6:  Y-SIGNAL LIMIT: .3
7:  DATA FILENAME: JCTH.DTO
    TITLE: Ic(A) vs. T(K)
8:  THERM. CAL. TABLE FILENAME (for X1-signal conversion): HC2CGR.CAL
    TITLE:
9:  TEMPERATURE INTERVAL BETWEEN DATA: .3
10: NO. OF SAMPLES IN DIGITAL FILTERING: 5
11: SCREEN GRAPHICS PARAMETERS SETUP: <ACTIVE>
12: EXIT THE PROGRAM
13: Test circuit Resistance, or Sample Ic. Present Rcirc= 2
14: Ic Operating Range (H, >1mA; L, <10mA): H
15: TEMPERATURE CONTROLLER: <ACTIVE>
    Control Range = 0 - 115 K & Vap-Samp = 15 K @ RT
16: Maximum Heating Allowed (mW): 50

>ENTER SELECTION # (<C/R> TO EXECUTE):

```

Set-Up Parameters Menu for (a) DA-HALL.BAS and (b) DA-JCTH.BAS. This second program menu prompts the user to enter various scaling factors and various data filenames. Again, the menus for DA-IVT.BAS and DA-DRIFT.BAS are similar.

(5) *X3-VOLTAGE SCALE FACTOR*: Scaling factor for converting the channel #3 voltage into more useful units such as ohms. Only applies to DA-HALL.BAS.

(6) *Y-SIGNAL SCALE FACTOR*: Scaling factor for converting the nanovoltmeter readings into either units such as ohms, i.e., $1 / I_{\text{sample}}$, or units such as microvolts in case of J_c or I-V measurements.

(7) *Y-SIGNAL STEP SIZE*: Minimum change required in the scaled nanovoltmeter reading (usually in ohms) before saving the sample readings to the specified data file.

(8) *Y-SIGNAL LIMIT*: The criterion of the scaled nanovoltmeter reading for defining the presently applied current as the critical current I_c . Typically defined as $1 \mu\text{V} / \text{cm}$. This feature applies only to DA-JCTH.BAS.

(9) *MAG. FIELD STEP SIZE*: Minimum change required in the magnetic field before saving the present readings (note: the program automatically converts the reading from channel #4 into units of kOe). This feature only applies when performing field sweeps of the Hall coefficient R_H and/or the resistivity ρ .

(10) *X2-SIGNAL RANGE / STEP SIZE*: Three numbers (separated by commas when entered) defining the applied current sweeps in the DA-JCTH.BAS program. The first number represents the present applied current when attempting to measure I_c across the sample. The second number is the maximum current that is allowed which halts the program execution if it is ever reached. The third number is the current step size fraction (typically 0.035

meaning 3.5%) which increases the applied current by this fractional amount when attempting to reach the critical current I_c .

(11) *X2-SIGNAL BACKSTEP*: This number is the backup fraction (typically 0.05 meaning 5%) which decreases the applied current by this fractional amount whenever I_c is reached. Only applies to the DA-JCTH.BAS program.

(12) *DATA FILENAME*: The filename in which the final data points will be saved to the hard disk. The extensions .dt0, .dt1, .dt2, ..., will be added automatically and consecutively. Moreover, the default directory is C:\IEEE488\. Afterwards, you will be prompted to enter an optional title line which can consist of the date, sample ID, magnetic field orientation, etc.

(13) *THERM. CAL. TABLE FILENAME*: Optional filename of a two column wide ASCII table (ohms vs. T(K) listed with ascending ohms) containing the thermometer calibration. Current choices are **HC2PT** (for Pt Film) or **HC2CGR** (for CGR). The .CAL extension is automatically added. However, if this option is waived, thermometer resistances will be stored instead of Kelvins in the data file and the automatic temperature controller feature will be disabled.

(14) *TEMPERATURE INTERVAL BETWEEN DATA*: Minimum change required in the temperature reading (in Kelvins if a thermometer calibration file is specified) before the present I_c value is stored to the specified file. Nevertheless, every time I_c is reached, the computer will "beep" before starting the next current sweep. Note that this feature only applies to the

DA-JCTH.BAS program.

(15) *NO. OF SAMPLES IN DIGITAL FILTERING*: Number of readings to be averaged together in order to reduce the background noise. Typical values range from 1 to 5. Note that larger values should be avoided, since they tend to create shifts between the sample readings and the temperature readings. In the program DA-JCTH.BAS, values from 3 to 5 are preferred, since the calculated standard deviations of I_c are computed using these numbers and stored with the data.

(16) *SCREEN GRAPHICS PARAMETERS SETUP*: Activates the capability of plotting data on the screen at the time of the data acquisition. If this feature is activated, an *<ACTIVE>* will appear in the menu. Typing this option automatically activates this feature and temporarily places you in a third (graphics) parameters menu. This menu is discussed later.

(17) *TRANSPORT CURRENT*: Current chosen for making the transport measurements when running the DA-HALL.BAS program. Typical entries are 1.000E-03 for Hall measurements and 1.000E-06 for resistivity measurements. Enter the number using the format shown in the menu, i.e., n.nnnE(sign)nn .

(18) *EXIT PROGRAM*: Saves the current parameter settings to the file specified in this setup menu (optional) and ends program execution. To return to DOS, type **SYSTEM** after exiting the program. Unfortunately, the IEEE interface commands will remain in the computer memory causing a significant reduction in the available memory unless the computer is rebooted.

(19) *TEST CIRCUIT RESISTANCE*: Measures the total circuit resistance after prompting you to enter an estimated circuit resistance and a testing current. Warning: use this feature only when the sample is superconducting and use currents that are less than or equal to the expected I_c or the sample may be "*blown!*" This circuit resistance is used in the DA-JCTH.BAS program to compute ongoing safe voltage compliances for the Keithley 228 power supply in an attempt to prevent overshooting of the applied currents.

(20) *I_c OPERATING RANGE*: If "H" is specified, the Keithley 228 operates in a current limited mode. This mode is useful only for currents greater than ~ 1 mA. If "L" is specified, the Keithley 228 operates in a voltage limited mode which is useful for currents less than ~ 10 mA. When entering the latter mode, the program will prompt you to install a 1 k Ω resistor into the circuit.

(21) *TEMPERATURE CONTROLLER*: Toggles between *<ACTIVE>* and *<INACTIVE>* modes which enable or disable the computer control of the DRC-91C temperature controller, respectively. When this feature is activated, you will be prompted to enter three numbers separated by commas. The first and second numbers define the absolute limits allowed for the setpoints. For example, a lower limit of 83K is useful in preventing liquid nitrogen from flooding the sample space, if liquid nitrogen is being used as the cryogen. The third number represents the relative temperature of the cooling gas (either N₂ or He) with respect to the sample. In addition, this relative difference is automatically reduced by the program at lower temperatures, since the specific

heats are lower in this regime. More importantly, this feature must be utilized in order to obtain good temperature dependencies of the Hall coefficient. Typical numbers for the third parameter, called *Vap-Samp*, are $\pm 15\text{K}$, when using LN_2 as a cryogen, and $\pm 35\text{K}$, when using LHe as a cryogen.

(22) *INTERPOLATE FILE GIVEN IN OPTION 10...*: Interpolates the data file specified in Option #10 according to user input temperature specifications. To interpolate files not created by the DA-HALL.BAS program, make sure that these files contain 4 columns of ASCII numbers separated by either spaces or tabs where the first column is the temperature. Moreover, the first row is ignored, since it is considered to be a title; the second row must be a single number representing the total number of data rows, excluding the first two rows, contained in the array.

(23) *MAXIMUM HEATING ALLOWED*: This is a safety feature added to the DA-JCTH.BAS and DA-IVT.BAS programs which limits the amount of heating allowed at the sample contacts. To be useful, the second set of sample current leads, labelled I-I, must be plugged into scanner channel #3 as specified by the HARDWARE SETTINGS menu. A typical safety limit is not more than 50 mW. Even though the sample may not "blow" at low temperatures with this amount of contact heating, temperature errors will usually occur for heating in excess of ~ 3 mW below 20K. If the program detects excessive heating or excessive voltages across the sample (i.e., 100X the voltage criterion), the program displays a warning at the bottom of the screen and execution

temporarily halts. At this point you could either quit (by typing a **Q**), continue (by hitting a **RETURN**), or enter a **new heating limit** followed by a **RETURN**. This concludes the SET-UP PARAMETERS menu.

If the SCREEN GRAPHICS PARAMETERS SETUP option is chosen, a third menu screen is displayed. Examples are shown in Figure 14. This menu is very straightforward so that the excessive details can be left out here. However, in this setup, you will be given options to change the X and Y plotting limits, an option to add a graph title, and an option to plot a comparison graph (note: this file must be in the same format as produced by these programs as described under the interpolation option). Moreover, in DA-HALL.BAS, you are prompted with two additional options. First, the x-axis can be either the temperature reading (in case of R_H vs. temperature) or the applied field (in case of R_H vs. field). Second, the Keithley 199 channel #3 can be included (denoted as *alt data*) in these plots. This is usually the resistivity signal when obtaining Hall signals with the nanovoltmeter. Moreover, this signal is divided by the *Ratio* shown in Option #9 before being plotted. Note that obtaining simultaneous measurements of R_H and ρ are required in deriving accurate values of the Hall angle. In addition, if the value of the standard resistor does not agree with that given in the setup menu, the resulting error is more likely to be observed in the resistivity ρ signal rather than in the Hall coefficient R_H signal. After completion of this graphics menu, type a **RETURN** without an option number to return to the previous menu.

After all menu parameters are entered and the sample is ready to go, typing a **RETURN** without an option number automatically starts the data acquisition sequence.

Figure 14

(a)

```

*** SCREEN GRAPHICS PARAMETERS ***
1: PLOT TYPE (T=K-181 vs Temp.& H=K-181 vs Field):      T
2: X-axis Xmin, Xmax:          0          300
3: Y-AXIS YMIN, YMAX:         -.5          .5
4: X-axis label:              T(K)
5: Y-axis label:              RH (Ohms)
6: Graph Title:               Hall Effect
7: COMPARISON DATA SET FILENAME:
8: VIEW COMPARISON DATA SET:          <INACTIVE>
9: Ratio of E-alt/E-nano:          2000
10: Include alt data in plots? (Y=Yes; N=No):          Y

>ENTER SELECTION # (<C/R> TO CONTINUE):

```

(b)

```

*** SCREEN GRAPHICS PARAMETERS ***
1: T-axis Tmin, Tmax:          0          100
2: Jc-axis Jcmin, Jcmax:       0          3
3: T-axis label:              T(K)
4: Jc-axis label:              Ic(A)
5: Graph Title:               Ic vs. T
6: COMPARISON DATA SET FILENAME:
   TITLE:
7: VIEW COMPARISON DATA SET:          <INACTIVE>

>ENTER SELECTION # (<C/R> TO MAIN MENU):

```

Screen Graphics Parameters Menu for (a) DA-HALL.BAS and (b) DA-JCTH.BAS. This third program menu prompts the user to enter the plotting limits and a comparison graphics filename. The menus for DA-IVT.BAS and DA-DRIFT.BAS are again similar. These parameters allow the user to plot data while the data is being obtained.

At this time, data is collected and stored directly to the specified file on the hard disk. Moreover, each program monitors the keyboard for occasional interrupts from the user where these interruption options are summarized below.

(A) *RETURN*: In DA-HALL.BAS and DA-DRIFT.BAS, this stores the current readings even if the minimum step sizes have not been satisfied. In DA-JCTH.BAS and DA-IVT.BAS, this halts the program execution and prompts you for a new starting current. Note that a significant period of time can be avoided in obtaining the first I_c reading if this feature is utilized.

(B) *Q*: Ends the data acquisition sequence, restores the data array to the hard disk (now includes the total number of data points as the second row), and returns to the SET-UP PARAMETERS MENU. Note that the data file name is automatically incremented at this time, e.g., TEST.DT0 becomes TEST.DT1. In addition, in DA-HALL.BAS, you are asked whether or not to sort and/or interpolate the data according to temperature before restoring this data to the disk. Keep in mind that this step can be waived until a later time.

(C) *P*: Enters plot mode and plots the current data set on the computer screen.

(D) *L*: Enters list mode and lists the current data set on the computer screen.

(E) *G*: Redisplays the SCREEN GRAPHICS PARAMETERS MENU to allow you to change the plotting limits. However, adding a comparison set is not allowed at this time. Upon hitting a **RETURN**, the program execution continues in the plot mode. This feature is only available in DA-HALL.BAS.

Warning: do not spend too much time in this menu as the data collection is

temporarily suspended during this interruption.

(F) *A*: Toggles between "*automatic I_c mode*" and "*single I_c mode*." In the "*automatic I_c mode*," the program continuously scans for I_c values; this mode is used for obtaining I_c as a function of temperature. In the "*single I_c mode*," the program execution temporarily halts whenever I_c is reached followed by a user prompt to enter a new starting current. This mode is used when obtaining the field dependence of I_c . More importantly, the data acquisition starts out in "*single I_c mode*." In addition, this option only applies to DA-JCTH.BAS, and this interrupt feature is only possible when the program is currently executing.

(G) *C*: Toggles between high current mode ($I > 1$ mA) and low current mode ($I < 10$ mA). Prompts you to install a 1 k Ω resistor into the circuit as needed. This feature only applies to the DA-JCTH.BAS program.

(H) *T*: Halts program execution and prompts you to enter a new thermometer calibration file and a new scaling factor. As with the *A* and *C* interrupts, this feature only applies to the DA-JCTH.BAS program.

This concludes the operating principles of the data acquisition programs listed in the Appendix. For additional information, contact the author of this dissertation.

III. THEORETICAL BACKGROUND

A. Anderson–Kim Flux Creep Model

It is generally accepted that the critical current densities in the high- T_c superconductors are limited by flux creep in the Abrikosov flux lattice. Moreover, the Anderson–Kim flux creep model, discussed below, will be applied to the polycrystalline $\text{YBa}_2\text{Cu}_3\text{O}_{7-\delta}$ thin films discussed later in the results. Thus, it is appropriate to include a brief overview of the development of the Anderson–Kim model. Prior to the 1960's, Anderson did not take into account the interaction between the flux lines of the Abrikosov flux lattice; as a result, his first flux pinning theory predicted that the critical current density J_c was independent of the magnetic field H , with⁴⁹

$$J_c = \frac{c}{4\pi} \frac{H_{c1}}{\ell} \frac{\text{Ln}(d/\xi)}{\text{Ln}(\lambda/\xi)} . \quad (6)$$

Here d is the radius of the normal region of the fluxoid and ℓ is the average spacing of the fluxoids. The other symbols in this equation are commonly used in present theories. In addition, H_{c1} is the lower critical field at which the Abrikosov flux lattice penetrates the superconductor, ξ is the superconducting coherence length, and λ is the penetration depth. However, Kim soon observed that J_c had a large field dependence that could only be overcome by introducing a flux "*bundle*" concept.⁴⁹ In this revised theory, the critical current density was described by

$$J_c = \frac{c}{8\pi} \frac{\rho}{\ell} \frac{H_c(T)^2}{B} \frac{d^2}{\lambda^2} , \quad (7)$$

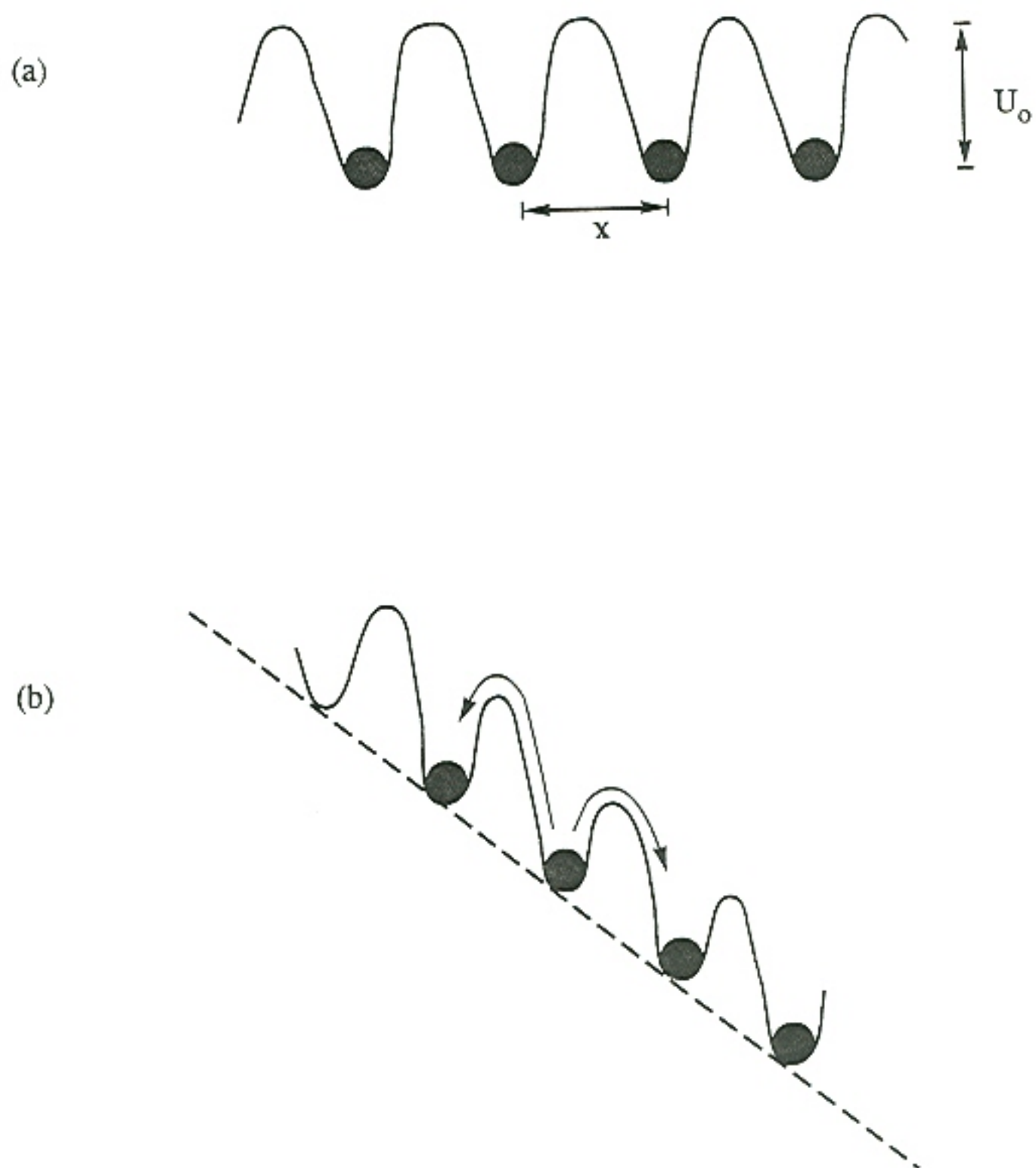
where ρ is the normal state resistivity extrapolated into the superconducting regime. Due to the weak temperature dependence of the thermodynamic critical field $H_c(T)$ below $T \approx 0.5 T_c$, J_c would be expected to be nearly independent of temperature at low temperatures, in contrast to the experimental observations. The key step in understanding the experimentally measured critical current densities occurred in 1962 when Anderson proposed that flux creep was initiated by a thermally activated process.⁴⁹ More explicitly, a flux creep hopping rate proportional to $e^{-\Delta W/kT}$ was proposed, where ΔW is the barrier height assuming no external driving forces are applied. This had been previously neglected, since superconductivity occurred only at extremely low temperatures ($T < 22K$) for which thermally activated processes were difficult to envision.

The familiar flux creep equations,⁵⁰ in the framework of the Anderson-Kim model, can be derived by considering a periodic potential well⁵¹ of depth U_0 and spacing x as shown in Figure 15(a). Let the flux bundles be trapped in these potential wells, hereafter called "*pinning*" centers. Also let x be the distance in which the bundles must be moved in order to be "*depinned*." The key equation⁴⁹ is the definition of the "*hop velocity*,"

$$v = x f_0 e^{-\Delta W/kT}, \quad (8)$$

where f_0 is the "*attempt*" frequency (phonon frequencies, $\sim 10^{11} - 10^{13} \text{ s}^{-1}$) and $\Delta W = U_0$ is the barrier height in the absence of external driving forces. An external flux gradient driving force (F_L) can be defined as a force density times a flux bundle volume.

Figure 15



Periodic potential well of depth U_0 and spacing x used to depict the magnetic flux "*pinning*" centers for the cases of (a) no external driving forces and (b) an externally applied driving force.

$$F_L = \frac{B(\partial B / \partial x)}{4\pi} V = \frac{J B}{c} V, \quad (9)$$

where V is the flux bundle volume. For simplicity, consider only forward and backward hopping of the fluxoids along a line parallel to F_L [Figure 15(b)]. Thus, the net flux velocity is given by

$$v = x f_o \left[e^{-(U_o - xF_L)/kT} - e^{-(U_o + xF_L)/kT} \right], \quad (10)$$

where the first term represents forward motion and the second term represents backward motion. Simple trigonometric relationships allow us to write this as

$$v = 2x f_o e^{-U_o/kT} \sinh \left(\frac{J B V x}{c k T} \right). \quad (11)$$

Moreover, the Lorentz equation allows us to write $E = v B / c$. Also define the critical current density in the absence of flux creep as $J_{co} = c U_o(T, B) / B V x$ and a prefactor $E_o = 2 x f_o B / c$ to obtain the familiar equations for the flux creep dissipative electric field at an applied current J :

$$E = E_o e^{-U_o/kT} \sinh \left(\frac{J}{J_{co}} \frac{U_o}{kT} \right), \quad (12)$$

where U_o is the "pinning" energy of the fluxoids, which depends on the applied magnetic field H , temperature T , and current density J . Simple algebra allows one to express this in terms of an observed critical current density J_c :

$$J_c = J_{co} \left(\frac{kT}{U_o} \right) \sinh^{-1} \left(\frac{E_c}{E_o} e^{U_o/kT} \right), \quad (13)$$

where E_c is a measurement criterion, usually chosen as $E_c \approx 1 \mu\text{V/cm}$. For

sufficiently strong pinning, the prefactor J_{co} is assumed to be proportional to the theoretical depairing critical current density⁵⁰

$$J_d = \frac{c H_c(T)}{3\sqrt{6} \pi \lambda(T)} . \quad (14)$$

For large applied fields (e.g., for $H > B^*$, where B^* is related to the field above which the flux lattice "melts"⁵²), we can define a flux creep "resistivity" in the limit $J \rightarrow 0$ as

$$\rho_{creep} = \frac{E}{J} = \frac{E_o}{J_{co}} \frac{U_o}{kT} e^{-U_o/kT} \propto e^{-U_o/kT} . \quad (15)$$

By obtaining a systematic set of I-V curves taken at several applied fields B and several temperatures T , this equation allows one to determine the functional form of the "pinning" energy. Zhu *et al.* performed this procedure on an epitaxial thin film of $YBa_2Cu_3O_7$ to obtain the following experimental expression for the "pinning" energy:⁵³

$$U_o(T, B, J) = U_{\infty} \frac{(1 - T/T_c)^{1.8}}{B} \left(1 - \frac{B}{B_{c2}} \right) e^{-J/J_{co}} . \quad (16)$$

Since this expression is not directly relevant to the measurements in this dissertation, readers interested in this expression are referred to Reference 53. Interestingly, a similar analysis was performed on two types of polycrystalline thin films of $YBa_2Cu_3O_7$ and these results are briefly discussed in Chapter VII.

B. The Hall Effect in Metals

1. Simple Metals: Single Parabolic Band

The Hall effect is defined as phenomenon that generate a potential difference between the edges of a strip of material carrying a longitudinal electric current when placed in an external magnetic field perpendicular to the direction of current. To better understand the significance of this effect, we must begin with the equation of motion for a particle of charge q in an applied electromagnetic field (SI units):

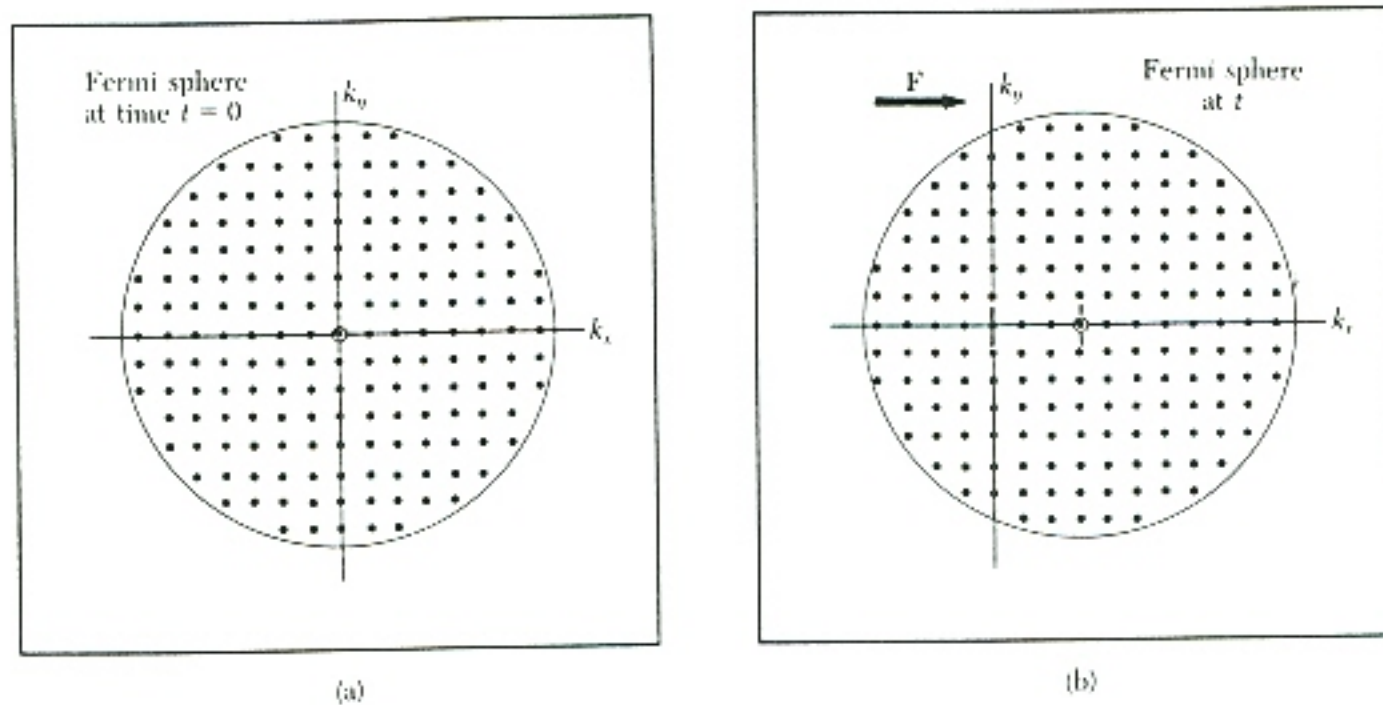
$$\mathbf{F} = q[\mathbf{E} + (\mathbf{v} \times \mathbf{B})] \quad , \quad (17)$$

where \mathbf{E} is the electric field, \mathbf{B} is the magnetic field, and **bold** characters denote vector quantities. Recall that a simple metal can be represented by an electron gas in which the Fermi sphere encloses the occupied electron orbitals in k -space.⁵⁴ If the external forces are balanced, the net momentum is zero so that for every occupied orbital \mathbf{k} there is a corresponding occupied orbital $-\mathbf{k}$. Moreover, upon the application of an external force, assumed constant, for a time interval t , every orbital has its \mathbf{k} vector increased by $\delta\mathbf{k} = \mathbf{F}t/\hbar$. This is equivalent to translating Fermi sphere by a displacement $\delta\mathbf{k}$ as shown in Figure 16. In actual metals, we cannot neglect the impulses due to scattering. Such collisions can be represented by $\mathbf{F}_{sc} = \hbar\delta\mathbf{k}/\tau$, where τ is the relaxation time. Thus, we can write

$$\hbar \left(\frac{d}{dt} + \frac{1}{\tau} \right) \delta\mathbf{k} = \mathbf{F} \quad . \quad (18)$$

If $m\mathbf{v} = \hbar\delta\mathbf{k}$ and $\mathbf{B} = B_z \mathbf{z}$, the equations of motion become

Figure 16



Fermi sphere in the ground state of a free electron gas. Left segment (a) represents the possible k -orbitals under no externally applied forces, whereas the right segment (b) represents the shifting of the average momentum upon application of a driving force: $N |\mathbf{F}| t$, where N is the number of electrons and t is the time. Source: C. Kittel, *Introduction to Solid State Physics* (Wiley, New York, 1986).

$$\begin{aligned}
m \left(\frac{d}{dt} + \frac{1}{\tau} \right) v_x &= q (E_x + B_z v_y) , \\
m \left(\frac{d}{dt} + \frac{1}{\tau} \right) v_y &= q (E_y - B_z v_x) ; \\
m \left(\frac{d}{dt} + \frac{1}{\tau} \right) v_z &= q E_z .
\end{aligned} \tag{19}$$

The steady state solution is obtained by setting the time derivatives equal to zero. For convenience, assume the charge carriers are electrons, i.e., $q = -e$, to obtain

$$\begin{aligned}
v_x &= -\frac{e\tau}{m} E_x - \omega_c \tau v_y ; \\
v_y &= -\frac{e\tau}{m} E_y + \omega_c \tau v_x ; \\
v_z &= -\frac{e\tau}{m} E_z .
\end{aligned} \tag{20}$$

These equations describe closed electron orbits having a **cyclotron frequency** of $\omega_c \equiv eB_z/m$. Moreover, taking $|e| = 1.6 \times 10^{-19}$ C, $m = m_e = 9.1 \times 10^{-31}$ kg, and B_z as our maximum attainable field of 8T, we see that the maximum cyclotron frequency that can be obtained with our cryostat is $1.4 \times 10^{12} \text{ s}^{-1}$. Using the band structure value for the Fermi velocity in $\text{YBa}_2\text{Cu}_3\text{O}_7$, i.e., $\langle v_F^2 \rangle^{1/2}_{ab} \approx 2.2 \times 10^7 \text{ cm/s}$,⁵⁵ the circumference of the cyclotron orbits can be calculated: $S = 2\pi \langle v_F^2 \rangle^{1/2}_{ab} / \omega_c \approx 10,000 \text{ \AA} \gg \text{mfp} (\sim 50 \text{ \AA})$. Thus, complete orbits are never attained before being scattered (defined as the **low-field limit**), which is the basis for all the remaining calculations in this chapter. Readers interested in the high-field limit are referred to Hurd.⁴⁴

The Hall field is the electric field developed perpendicular to both the current density \mathbf{j} and the externally applied magnetic field \mathbf{B} . Define a coordinate system so

that the current is constrained to move along the x-axis, the magnetic field is applied along the z-axis, and the resulting Hall field is measured along the y-axis. From Equation (20), the only solution is given by

$$E_y = -\omega_c \tau E_x = -\frac{eB_z \tau}{m} E_x . \quad (21)$$

The **Hall coefficient** is defined (in the low-field limit⁵⁶) by

$$R_H = \frac{E_y}{j_x B_z} . \quad (22)$$

The significance of this constant becomes apparent upon substitution of the electrical conductivity⁵⁴ $\sigma = j_x/E_x = n_H e^2 \tau/m$ into Equation (21):

$$R_H = -\frac{1}{n_H e} . \quad (23)$$

Inspection of this important result reveals that the Hall coefficient offers a means in which one can determine the sign and concentration n_H of carriers in a material. Moreover, using a free electron model with $N(E) \propto E^2$, Pickett shows that a more instructive expression for R_H can be written as⁵⁷

$$R_H = -\frac{3}{2e E_F N(E_F)} , \quad (24)$$

where E_F is the Fermi energy and $N(E_F)$ is the electronic density of states at the Fermi level. Also, the Hall coefficient R_H is negative for electrons and positive for holes. Note that the lower the Hall coefficient, the greater the carrier concentration. Although R_H is depicted in most experimental Hall plots, the **Hall resistivity** ρ_{xy} is

occasionally encountered. This quantity is simply defined by

$$\rho_{xy} = B_z R_H = \frac{E_y}{j_x} \quad (25)$$

In addition, another important quantity, known as the **Hall angle**, is defined as

$$\tan(\theta_H) = \frac{E_y}{E_x} = -\omega_c \tau = f(B, T) \quad (26)$$

The Hall angle above, which can be obtained from Equation (21), is a relative measure of the relaxation time τ . However, this quantity is field dependent due to the cyclotron frequency term and as a result, the field used to determine the Hall angle must be shown with the data. Unfortunately, the simple results [Equations (23)–(26)] derived in this section, although applicable to most simple metals, cannot be directly applied to $\text{YBa}_2\text{Cu}_3\text{O}_{7-\delta}$ materials, for at least three reasons. First, $\text{YBa}_2\text{Cu}_3\text{O}_7$ has four bands that cross the Fermi level requiring a more rigorous multi-band analysis of the Hall coefficient R_H . Second, the "*collision*" time τ changes across the various Fermi surfaces of this material. Finally, the simultaneous presence of both holes and electrons complicate the analysis. Therefore, the effects of multiple bands as well as the simultaneous presence of both electrons and holes on the Hall coefficient will be discussed in the succeeding sections.

2. Multiband Effects

Many metals have more than one band crossing the Fermi level; therefore, it is imperative to determine the effects of multiple bands on the observed Hall

coefficient R_H before attempting to interpret any Hall measurements. For simplicity, assume two isotropic bands cross the Fermi level so that we can take $R_{Hi} = -1/n_{Hi}e$ for each band and neglect scattering between the bands.⁵⁸ Later, the results will be generalized for any number of bands. The electric field for the first band is

$$\mathbf{E}_1 = \frac{\mathbf{j}_1}{\sigma_1} + \frac{q_1 \tau_1}{m_1 \sigma_1} (\mathbf{B} \times \mathbf{j}_1) , \quad (27)$$

where σ_1 is the conductivity of Band 1. Likewise, the electric field for the second band is

$$\mathbf{E}_2 = \frac{\mathbf{j}_2}{\sigma_2} + \frac{q_2 \tau_2}{m_2 \sigma_2} (\mathbf{B} \times \mathbf{j}_2) , \quad (28)$$

where σ_2 is the conductivity of Band 2. Since both bands occupy the same real space, *all* carriers experience the same electric field. Thus, the following two constraints are imposed:

$$\mathbf{E} = \mathbf{E}_1 = \mathbf{E}_2 , \text{ and} \quad (29)$$

$$\mathbf{j} = \mathbf{j}_1 + \mathbf{j}_2 \equiv \text{total current density} . \quad (30)$$

Ziman⁵⁹ solves these vector equations to obtain

$$\mathbf{j} = \left[\frac{\sigma_1}{1 + q_1^2 \tau_1^2 B^2 / m_1^2} + \frac{\sigma_2}{1 + q_2^2 \tau_2^2 B^2 / m_2^2} \right] \mathbf{E} - \left[\frac{\sigma_1 q_1 \tau_1 / m_1}{1 + q_1^2 \tau_1^2 B^2 / m_1^2} + \frac{\sigma_2 q_2 \tau_2 / m_2}{1 + q_2^2 \tau_2^2 B^2 / m_2^2} \right] (\mathbf{B} \times \mathbf{E}) . \quad (31)$$

Expressing this equation in terms of \mathbf{E} as a function of \mathbf{j} and $\mathbf{B} \times \mathbf{j}$ leads to

$$R_H = \frac{\sigma_1^2 R_{H1} + \sigma_2^2 R_{H2}}{(\sigma_1 + \sigma_2)^2} . \quad (32)$$

Furthermore, a more general result for the apparent Hall coefficient for any number of bands could be written as

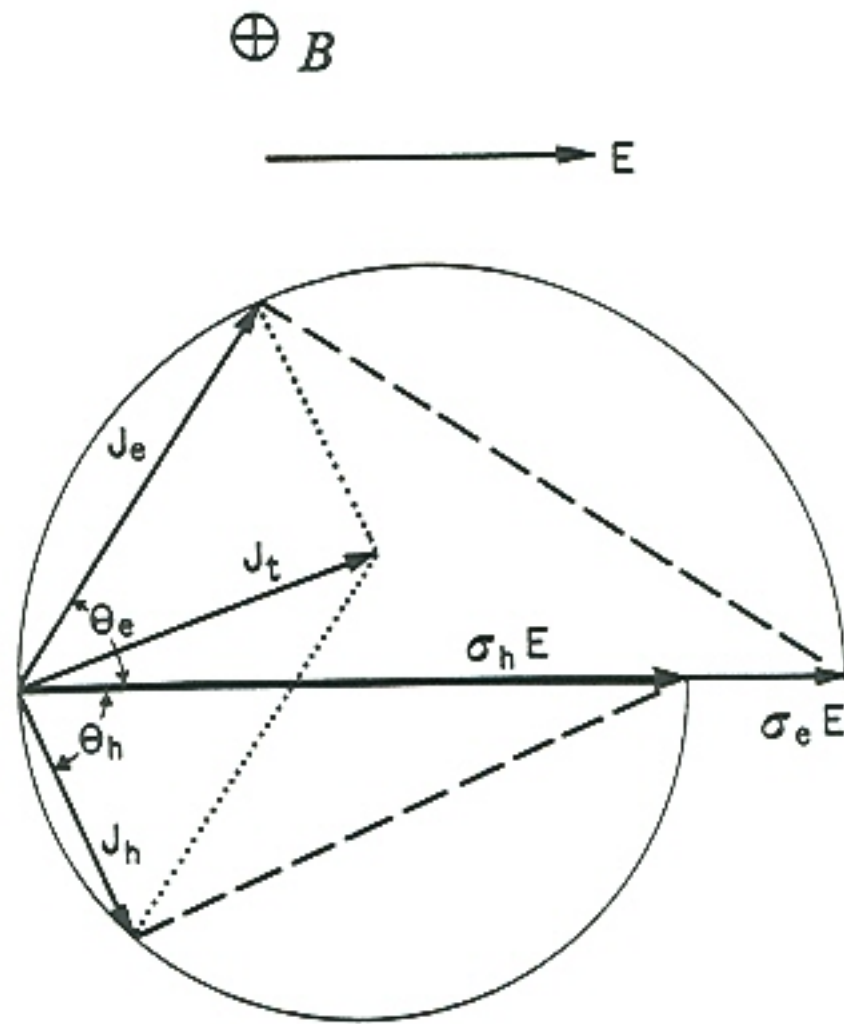
$$R_H = \sum_i R_{Hi} \left(\frac{\sigma_i}{\sigma} \right)^2 , \quad (33)$$

where R_{Hi} is the Hall coefficient of the i -th band, σ_i is the conductivity of the i -th band, and $\sigma = \sigma_1 + \sigma_2 + \dots$. Note that in a multiband system, with only one type of carrier, i.e., either electrons or holes, the minority carriers will usually not effect R_H noticeably. This follows since the observed Hall coefficient R_H is the average of the individual R_{Hi} 's associated with the separate bands, but weighted by the square of their conductivities. Thus, we are frequently justified in using the following equation for the dominant band:⁶⁰

$$n_H^* \approx -\frac{1}{R_H e} . \quad (34)$$

However, if both electrons and holes are present, n^* can become very large even if small carrier densities occur in all bands (termed compensated metals⁴⁴). For instance, in a two band scenario containing one electron band and one hole band, Equations (32) and (34) simplify [see Figure 17] to give

Figure 17



Contributions to the Hall effect from two bands of oppositely charged carriers. This vector diagram represents Equations (31)–(35). *Source*: C. M. Hurd, *The Hall Effect in Metals and Alloys* (Plenum, New York, 1972).

$$n_H^* = \frac{\sigma^2}{e^4} \left[\left| \frac{n_{el} \tau_{el}^2}{m_{el}^2} \right| - \left| \frac{n_{ho} \tau_{ho}^2}{m_{ho}^2} \right| \right]^{-1} . \quad (35)$$

Nevertheless, in any case, n_H^* tends to give an upper bound to the actual carrier density. Although not proven here, Ong generalized this statement to include any number of bands, in the 2D limit, where each Fermi surface could have any arbitrary shape.⁶¹

Like the multi-band Hall coefficient, the multi-band Hall angle is a function of the relaxation time of all bands. This can be shown by combining Equations (22) and (33), while utilizing $E_x = j_x/\sigma$:

$$\tan(\theta_H) = \frac{E_y}{E_x} = \frac{B_z}{\sigma} \sum_j R_{Hj} \sigma_j^2 . \quad (36)$$

Moreover, if each individual band is isotropic, e.g., can be described by $R_{Hj} = -1/n_{Hj}e$, this simplifies to a more instructive expression

$$\tan(\theta_H) = -\frac{1}{\sigma} \sum_j \omega_j \tau_j \sigma_j . \quad (37)$$

Therefore, the Hall angle is simply an average of the individual relaxation times weighted, not by the squares of the conductivities, but simply by the conductivities to the first power. The most important thing to note in a multi-band metal is that both the Hall coefficient and the Hall angle become functions of the carrier concentrations as well as the relaxation times.

Markiewicz⁶² first suggested that the anomalous temperature dependence of R_H observed in $\text{YBa}_2\text{Cu}_3\text{O}_{7-\delta}$,⁶³ e.g., $R_H \propto 1/T$, could be due to the collective

effects of a hole band associated with the planes and an electron band associated with the chains. Eagles⁶⁴ performed this analysis on the Hall data taken at full oxygenation ($\delta \sim 0$) in $\text{YBa}_2\text{Cu}_3\text{O}_{7-\delta}$. In order to obtain simultaneous fits to both the resistivity ρ and the Hall coefficient R_H as a function of temperature, it was determined that $n_{el}/n_{ho} \approx 1000$. In a similar fashion, the Hall data obtained for this dissertation were fit to this model at various oxygen contents across the 90K T_c vs. δ plateau. The electron and hole densities were assumed constant with temperature. The resulting fits [Figure 18] require

$$\mu_{el} = \frac{e^2 \tau_{el}}{m_{el}} \approx (9.4 \times 10^{-24}) T^{-0.77} + (3 \times 10^{-26}) ; \quad (38)$$

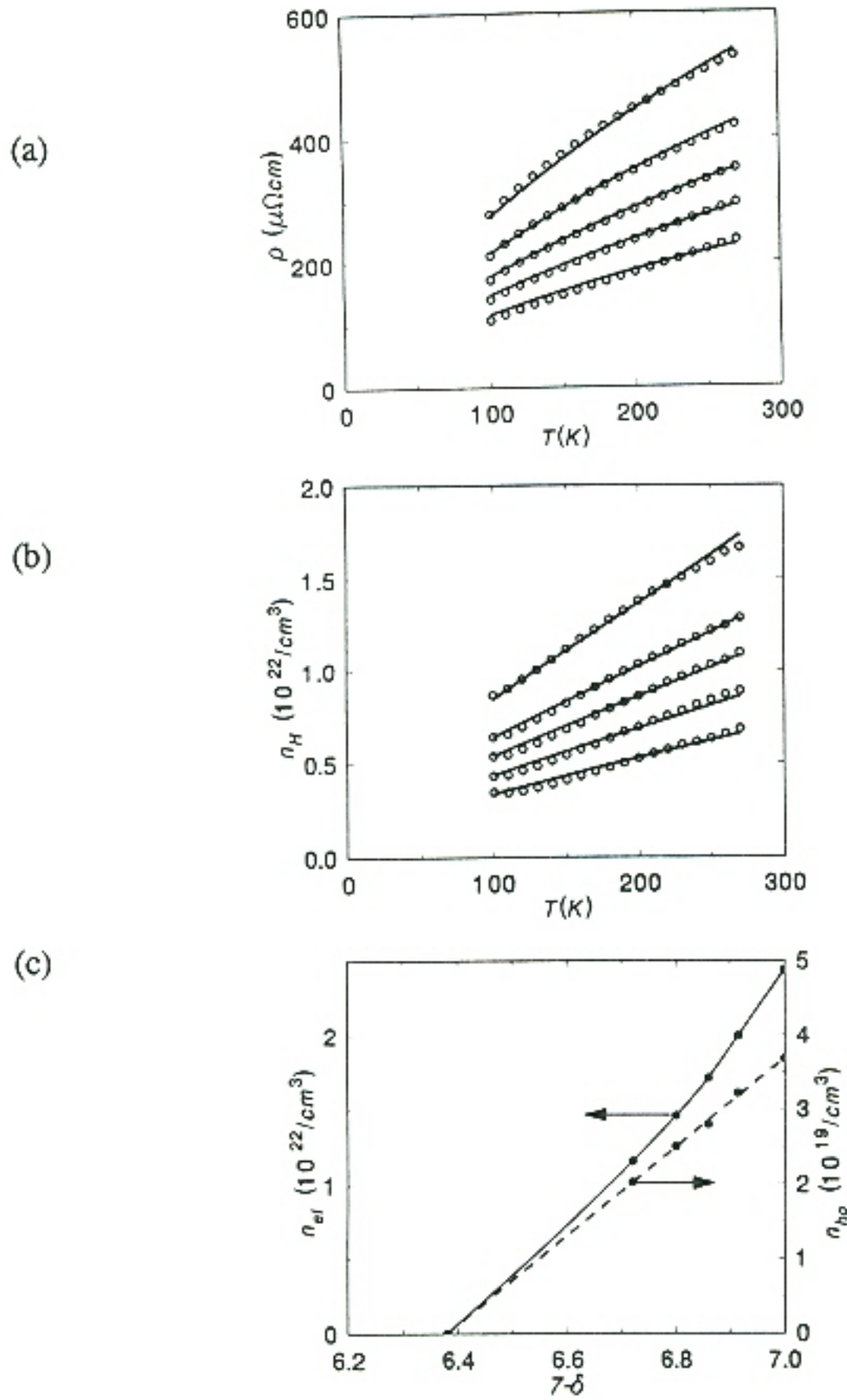
$$\mu_{ho} = \frac{e^2 \tau_{ho}}{m_{ho}} \approx (1.7 \times 10^{-21}) T^{-1} , \quad (39)$$

where T is the temperature in Kelvins and μ is defined as the **carrier mobility** (given in S.I. units). This analysis of R_H was restricted to oxygen deficiencies δ near the 90K plateau, since the carrier mobilities given above were assumed to be independent of δ . In actuality, the carrier mobilities probably decrease before reaching the semiconducting phase, e.g., $\delta \rightarrow 0.6$. Interestingly, it is important to point out that the observed Hall coefficient remains positive simply due to the relative mobility ratio

$$\frac{\mu_{ho}}{\mu_{el}} \approx 180 T^{-0.25} + 3 . \quad (40)$$

Therefore, the holes are more mobile than the electrons, and even though the electron

Figure 18



Fits of the transport properties to the simple two band model described in the text. (a) Resistivities taken across the 90K plateau (symbols) are fit to the model (curves). (b) Likewise, apparent Hall carrier densities fit to the same model. (c) The electron and hole density components as a function of oxygen deficiency δ required to obtain the fits above. Interestingly, each component carrier density extrapolate towards zero at the oxygen content for which T_c approaches zero.

carrier density is higher, the Hall coefficient remains positive as a result. Unfortunately, as interesting as this analysis seems, the results are probably "*fortuitous*", since $\text{YBa}_2\text{Cu}_3\text{O}_{7-\delta}$ actually has four bands crossing the Fermi level. Moreover, in a simple two band scenario in which each band has a different effective mass m_i or a different relaxation time τ_i , the application of a magnetic field would attempt to produce different deflections to each carrier, which is not allowed, since all carriers are subjected to the same electric fields. Resulting forces would undoubtedly lead to large magnetoresistances due the redistribution of the current between the two bands,⁵⁹ and such effects are not observed in $\text{YBa}_2\text{Cu}_3\text{O}_7$. In the band structure of $\text{YBa}_2\text{Cu}_3\text{O}_7$, two of the four bands are predominately "*hole like*" in character, whereas the remaining two are both "*hole like*" and "*electron like*" in character.⁵⁵ Finally, each band has a differing degree of dimensionality that complicates the meaning the Hall coefficient. As a result, a Bloch-Boltzmann approach must be utilized before we can understand the behavior of the Hall coefficient.

3. Bloch-Boltzmann Transport Theory

The Boltzmann equation governs the macroscopic transport properties of all materials.⁵⁹ Also known as the transport equation, this equation simply states that the local concentration of carriers in the state \mathbf{k} in the vicinity of a point \mathbf{r} in space does not change with time. Like most theories, in order to calculate the transport properties from this equation, careful approximations must be made. This is necessary, since a rigorous solution of this equation requires knowledge of the scattering operator, which

is difficult to calculate, especially for the layered cuprate perovskites that have complex structures.⁵⁵ Nevertheless, the variational principle⁶⁵ can be used to make reasonable approximations, and as it turns out, many of the transport properties, including the Hall coefficient, do not depend on the scattering mechanism to a first level of approximation. However, due to the excessive and tedious algebra involved in these derivations, which is described in more detail elsewhere,⁶⁶ only an outline of the derivation of the transport properties will be discussed, with an emphasis on the physics.

The first derivation of the transport coefficients, e.g., conductivity σ and Hall tensor \mathbf{R}_H , from the Boltzmann equation was performed by Jones *et al.*⁶⁷ This solution is now considered standard, and detailed accounts can be found in at least two common texts.^{44,65} Therefore, only an outline of this procedure is considered here. First, assume that an electronic relaxation time τ exists and it is a function of \mathbf{k} (this assumption is only valid in the low-field limit). Consider only the isothermal case so that the Boltzmann equation in the presence of both an electric field \mathbf{E} and a magnetic field \mathbf{B} can be written as⁶⁸

$$\frac{e}{\hbar} [\mathbf{E} + \mathbf{v} \times \mathbf{B}] \cdot \nabla_{\mathbf{k}} F(\mathbf{k}) = -\frac{F(\mathbf{k}) - f(\mathbf{k})}{\tau(\mathbf{k})} , \quad (41)$$

where $F(\mathbf{k})$ is the mean number of carriers in the state \mathbf{k} having an energy $\epsilon(\mathbf{k})$, and $f(\mathbf{k})$ is the mean number of carriers before the application of the fields. To solve this equation, set

$$F = f + g(\mathbf{v}) , \quad (42)$$

where $g(\mathbf{v})$ is the deviation from equilibrium upon applying the external fields. Placing

Equation (42) into Equation (41), while neglecting higher order terms having products of \mathbf{E} and $g(\mathbf{v})$, gives the result

$$\left[1 + \frac{e \tau(\mathbf{k})}{\hbar^2} (\nabla_{\mathbf{k}} \epsilon \times \mathbf{B} \cdot \nabla_{\mathbf{k}}) \right] g(\mathbf{v}) = -\frac{\tau(\mathbf{k})e \cdot \nabla_{\mathbf{k}} \epsilon}{\hbar} \left(\frac{\partial f}{\partial \epsilon(\mathbf{k})} \right), \quad (43)$$

where $-\partial f/\partial \epsilon(\mathbf{k})$ is the derivative of the Fermi-Dirac distribution with respect to energy ϵ . For small \mathbf{B} , this can be solved by a iterative procedure that gives

$$g(\mathbf{v}) = \sum_{n=0}^{\infty} \left(-\frac{\tau(\mathbf{k})e}{\hbar^2} \nabla_{\mathbf{k}} \epsilon \times \mathbf{B} \cdot \nabla_{\mathbf{k}} \right)^n \left(-\frac{\tau(\mathbf{k})e}{\hbar} \mathbf{E} \cdot \nabla_{\mathbf{k}} \epsilon \frac{\partial f}{\partial \epsilon(\mathbf{k})} \right). \quad (44)$$

Before establishing the physical meaning of each term in this series, we first need to calculate the net electric current density \mathbf{j} due to the perturbed distribution $F(\mathbf{k})$:

$$\mathbf{j} = -\frac{e}{\Omega_o} \sum_{\mathbf{k}} \mathbf{v}(\mathbf{k}) F(\mathbf{k}) = \frac{e}{\hbar \Omega_o} \sum_{\mathbf{k}} \nabla_{\mathbf{k}} \epsilon g(\mathbf{v}), \quad (45)$$

where Ω_o is a normalization volume, which is inversely proportional to the density of states in \mathbf{k} -space. Moreover, the equilibrium distribution has been omitted, since it makes no net contribution to the current density \mathbf{j} . Placing Equation (44) into Equation (45) leads to the following series expansion for \mathbf{j} , where each term represents a summation and a particular **galvanomagnetic coefficient**:

$$\mathbf{j} = -\left(\frac{e}{\Omega_o} \right) \sum_{\mathbf{k}} \mathbf{v} \tau(\mathbf{k}) e (\mathbf{E} \cdot \mathbf{v}) \left(\frac{\partial f}{\partial \epsilon(\mathbf{k})} \right) + \left(\frac{e}{\Omega_o} \right) \sum_{\mathbf{k}} \epsilon_{\gamma\delta\sigma} \mathbf{v} \frac{\tau(\mathbf{k})^2 e^2}{\hbar^2} \mathbf{v}_{\sigma} \mathbf{E} \cdot \left(\frac{\partial^2 \epsilon(\mathbf{k})}{\partial k_{\gamma} \partial k_{\delta}} \right) H_{\gamma} \left(\frac{\partial f}{\partial \epsilon(\mathbf{k})} \right) \dots, \quad (46)$$

where ϵ_{ijk} is the totally antisymmetric tensor (equal to +1 for even permutations of the

indices, -1 for odd permutations, and 0 if two indices are equal). To identify the physical meaning of each term in this series, we can compare the following Taylor expansion for the current density, valid for small \mathbf{B} , obtained from the theory of irreversible thermodynamics,⁶⁹ in a term by term manner to Equation (46):

$$j_{\alpha} = \sigma_{\alpha\beta} E_{\beta} + \sigma_{\alpha\beta\gamma} E_{\beta} B_{\gamma} + \sigma_{\alpha\beta\gamma\delta} E_{\beta} B_{\gamma} B_{\delta} + \dots = - \left(\frac{e}{\Omega_o} \right) \sum_{\mathbf{k}} v_{\alpha}(\mathbf{k}) F(\mathbf{k}) , \quad (47)$$

where the sums over repeated indices are understood. Direct comparisons allow us to now obtain explicit formulas for the standard transport coefficients:

$$\sigma_{\alpha\beta} = e^2 \left(\frac{\tau n}{m} \right)_{\alpha\beta} \equiv \left(\frac{e^2}{\Omega_o} \right) \sum_{\mathbf{k}} \tau(\mathbf{k}) v_{\alpha}(\mathbf{k}) v_{\beta}(\mathbf{k}) \left[-\frac{\partial f}{\partial \epsilon(\mathbf{k})} \right] ; \quad (48)$$

$$\sigma_{\alpha\beta\gamma} = -\frac{e^3}{\hbar \Omega_o} \sum_{\mathbf{k}} \tau(\mathbf{k}) v_{\alpha}(\mathbf{k}) \{ [v(\mathbf{k}) \times \nabla_{\mathbf{k}}]_{\gamma} \tau(\mathbf{k}) v_{\beta}(\mathbf{k}) \} \left[-\frac{\partial f}{\partial \epsilon(\mathbf{k})} \right]. \quad (49)$$

Moreover, the **Hall tensor** is defined as⁵⁷

$$R^H_{xyz} \equiv \frac{E_y}{j_x B_z} = \frac{\sigma_{xyz}}{\sigma_{xx} \sigma_{yy}} . \quad (50)$$

In these expressions, Ω_o is our normalization volume, whereas $-\partial f/\partial \epsilon$ is the Fermi-Dirac function. Unfortunately, most materials, including the high- T_c cuprates, require long and tedious calculations to obtain the transport coefficients from these equations. Thus, only the evaluated, three independent components of the Hall tensor and the temperature dependence of the resistivity, obtained elsewhere,⁵⁵ will be shown for $\text{YBa}_2\text{Cu}_3\text{O}_7$. For now, the only important thing to note from these equations is that the assumption of an isotropic scattering rate $1/\tau$ leads to a Hall tensor that is

independent of $1/\tau$. Such an assumption, along with the replacement of $-\partial f/\partial \epsilon$ by $\delta(\epsilon - \epsilon_F)$, leads to a temperature independent Hall coefficient R_H , since all other variables are independent of temperature.

Before further discussion of the anomalous temperature dependence observed in R_H , a brief diversion into the temperature dependence of the resistivity ρ will be presented in the framework of the isotropic scattering approximation. In a more general sense, the steady state distribution of electrons at an arbitrary point \mathbf{r} in the presence of an electric field \mathbf{E} , magnetic field \mathbf{B} , and thermal gradient ∇T is given by the functional form⁵⁵

$$F(\mathbf{k}, \mathbf{r}) = \frac{f \left[T - \tau \mathbf{v}(\mathbf{k}) \cdot \nabla T ; \epsilon(\mathbf{k} - \mathbf{F}_{ext} \tau / \hbar) \right]}{1 + \exp \left(\frac{\epsilon - \mu}{k_B T} \right)}, \quad (51)$$

where $\epsilon(\mathbf{k})$ is the energy, $\mathbf{v}(\mathbf{k})$ is the group velocity $\partial \epsilon / \partial (\hbar \mathbf{k})$ of an electron with quantum numbers (\mathbf{k} , band n , spin σ), and the denominator contains the Fermi-Dirac distribution. The physical meaning of Equation (51) can be stated more simply as the number of electrons in the state \mathbf{k} at point \mathbf{r} is the same as the number occurring at equilibrium, except that an external force shifts the momentum by an amount $\mathbf{F}_{ext} \tau$, since the previous collision, and the temperature shifts by the amount $-\tau \mathbf{v}_k \cdot \nabla T$. In addition, the external force can be written

$$\mathbf{F}_{ext} = -e\mathbf{E} - e\mathbf{v}(\mathbf{k} + e\mathbf{E}\tau/\hbar) \times \mathbf{B} . \quad (52)$$

Note that these equations are simply a more elaborate means of depicting the increase of the average momentum of the "*Fermi sphere*." The only free parameter in

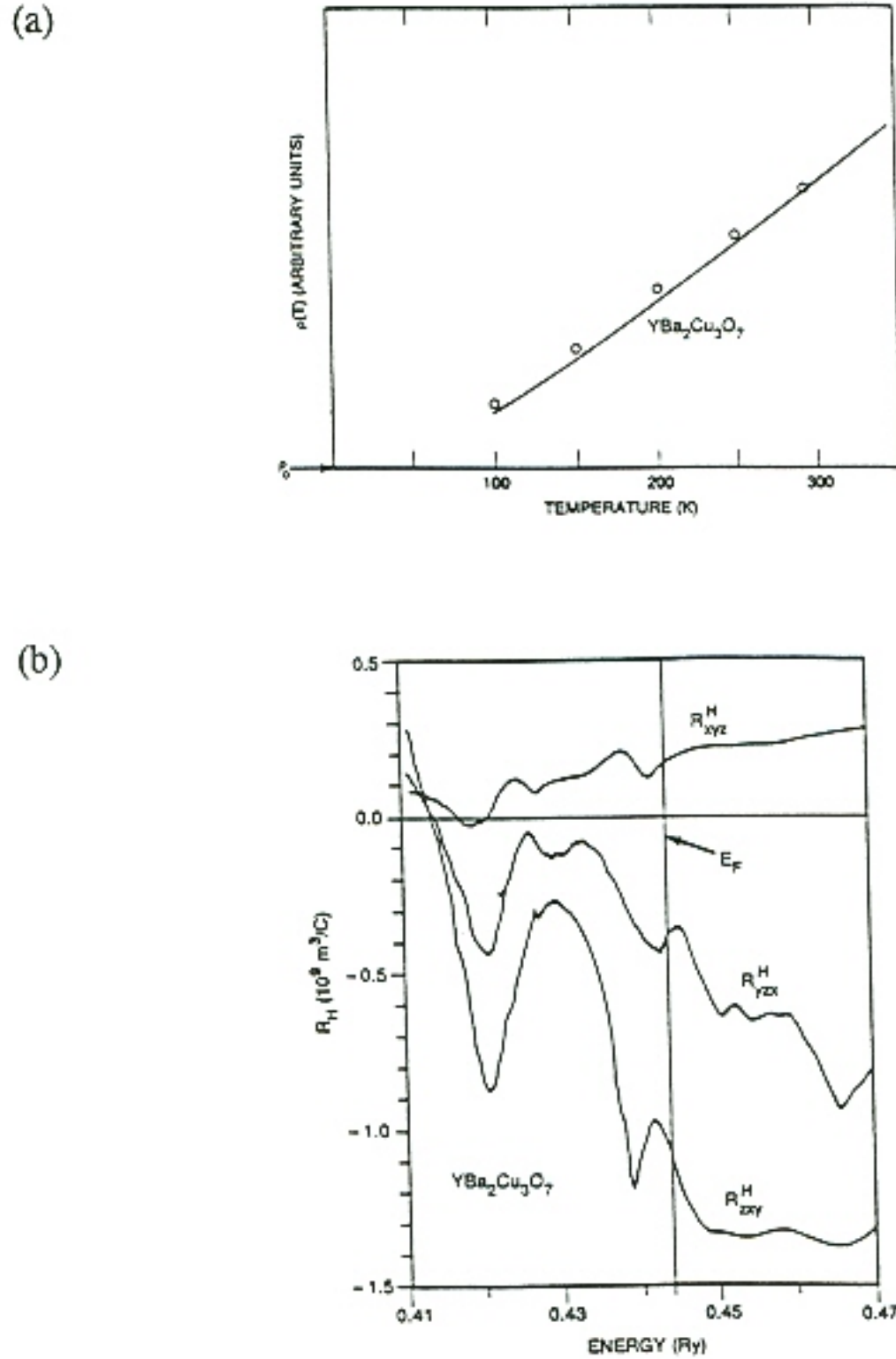
Equation (51) is the relaxation time τ ; it is argued in the variational approach⁶⁵ that τ should be chosen in a manner to maximize the current for a particular scattering operator. Assuming the only scattering mechanism is electron-phonon, then this approach applied to a metal in the limit $T < \Theta_D$, was shown by Allen⁶⁶ to yield a relaxation time

$$\frac{\hbar}{\tau_{el-ph}} = 4\pi k_B T \int_0^{\omega_{max}} \frac{d\omega}{\omega} \alpha_{tr}^2 F(\omega) \left[\frac{\hbar\omega/2k_B T}{\sinh(\hbar\omega/2k_B T)} \right]^2, \quad (53)$$

where $\alpha_{tr}^2 F(\omega)$ is the electron-phonon spectral function and ω_{max} is the maximum phonon frequency. Unfortunately, $\alpha_{tr}^2 F(\omega)$ is not known for any of the cuprates; however, inelastic neutron scattering was previously used to measure $G(\omega)$, which is $F(\omega)$ weighted by the neutron-phonon matrix elements rather than the electron-phonon matrix elements.⁵⁷ These spectral functions should be quite similar, since the electron-phonon interaction is expected to be dominated by the Cu and O atoms as with the neutron cross sections. Remarkably, Allen *et al.*⁵⁵ show that this relaxation time, calculated using the function $G(\omega)$, instead of $F(\omega)$, gives a resistivity curve of the form $\rho = \rho_0 + mT$ [Figure 19(a)], which agrees well with experimental findings. Therefore, the temperature dependence of the resistivity in $YBa_2Cu_3O_7$ appear to be consistent with an electron-phonon scattering mechanism.

Returning to the Hall effect discussions, Allen *et al.* calculated the three independent Hall tensor components for fully oxygenated $YBa_2Cu_3O_7$ [Figure 19(b)] utilizing the transport equations, their band structure results, and the Onsager relations $\sigma_{yxz} = -\sigma_{xyz}$...⁵⁵ As with the resistivity predictions, the magnitude of

Figure 19



Calculated electrical transport properties of $\text{YBa}_2\text{Cu}_3\text{O}_7$ assuming electron-phonon scattering mechanisms dominate. (a) Temperature dependence of the resistivity due to the Fermi-surface carriers. (b) The three elements of the Hall tensor calculated as a function of energy near E_F . These values agree with the experimental results for this dissertation. *Sources:* P. B. Allen, W. E. Pickett, and H. Krakauer, *Phys. Rev. B* **37**, 7482 (1988) and W. E. Pickett, *Rev. Mod. Phys.* **61**, 433 (1989).

the Hall tensor components agree very well with the experimental findings. However, the assumption of a constant scattering rate, as well as the replacement of the Fermi-Dirac function with the one occurring at absolute temperature, leads to a failure in explaining the source of the anomalous temperature dependence of R_H . This failure motivated Ong⁶¹ to develop an unique interpretation of the Boltzmann equation in terms of the basal plane anisotropy of the "*scattering path length*" vector $\Delta l/l_{av}$, in order to address the temperature dependence of R_H , which is discussed in the next section.

4. Geometric Interpretation of the Hall Conductivity

In the low-field limit, the Hall tensor components are known to be very sensitive to the local curvature of the Fermi surface (FS).⁷⁰ Moreover, many materials have very complex FS shapes making it difficult to explain the experimentally measured Hall data in context with the band structure predictions. On the other hand, Ong⁶¹ developed an unique interpretation of **Hall conductivity**, e.g., Equation (49), for the class of materials having two-dimensional Fermi surfaces. More explicitly, it is argued that the low-field limit Hall conductivity is proportional to the number of flux quanta ϕ_0 threading the I-curve, where the I-curve is defined as the "*scattering path length*" vector $l(\mathbf{k}) = \mathbf{v}_k \tau_k$, as \mathbf{k} traces out the FS. Furthermore, it will be shown that if the anisotropy of this "*scattering path length*" vector, denoted by $\Delta l/l_{av}$, changes with temperature, a temperature dependent Hall coefficient results.

This new interpretation of the Hall conductivity will be discussed starting with the standard transport coefficients. Taking the magnetic field $\mathbf{B} \parallel -\mathbf{z}$, and the electric

field $\mathbf{E} \parallel \mathbf{x}$, Equation (49) can be rewritten:⁶¹

$$\sigma_{xyz} = \frac{2e^3 B}{\hbar} \sum_{\mathbf{k}} \left(-\frac{\partial f}{\partial \epsilon(\mathbf{k})} \right) (v_y \tau_k) (\mathbf{v} \times \mathbf{B}) \cdot \nabla (v_x \tau_k) \quad . \quad (54)$$

For a 2D system, assuming $kT \ll \epsilon_F$, this can be written as an integral evaluated around the FS curve

$$\sigma_{xyz}^{2D} = \left(\frac{e^3}{2\pi^2 \hbar} \right) \oint \frac{dk_t}{|\mathbf{v}|} [v_y \tau_k (\mathbf{v} \times \mathbf{B}) \cdot \nabla (v_x \tau_k)] \quad , \quad (55)$$

where $|\mathbf{v}|^{-1}$ is the density of states factor, and k_t is the component of \mathbf{k} taken along \mathbf{t} (tangential unit vector to the FS curve). Furthermore, $\mathbf{v} \times \mathbf{B} / |\mathbf{v}| = B\mathbf{t}$, which allows the integral to be written as

$$B \oint dk_t (\mathbf{t} \cdot \nabla l_x) l_y = BA_l \quad , \text{ where} \quad (56)$$

$$A_l = \frac{B}{B} \cdot \oint d\mathbf{l} \times \frac{\mathbf{l}}{2} \quad . \quad (57)$$

A_l denotes the "Stokes" area swept out by the vector $\mathbf{l}(\mathbf{k})$ as \mathbf{k} moves around the FS.⁶¹

Substituting Equations (56) and (57) into Equation (55) leads to the important result

$$\sigma_{xyz}^{2D} = \frac{e^2}{h} \left(\frac{A_l}{\pi l_B^2} \right) = 2 \frac{e^2}{h} \left(\frac{\phi}{\phi_0} \right) \quad , \quad (58)$$

where $l_B = (\hbar/eB)^{1/2}$ is defined as a magnetic length, $\phi_0 = h/e$ is the flux quantum, and $\phi = BA_l$ is the magnetic flux threading the \mathbf{l} -curve. Recall that this is only the numerator of the Hall coefficient defined by Equation (50). In order to visualize how these findings might lead to a temperature dependent Hall coefficient, consider only

crystals having N-fold symmetries in the xy-plane. In this case, Ong argues⁶¹ that the in-plane conductivities can be written as scalars. More explicitly, for 2D systems, Ziman shows that the diagonal conductivities can be derived from Equation (48),⁶⁵

$$\sigma_{xx} = \left(\frac{e^2}{h\pi} \right) \oint ds l_k \cos^2 \theta_k, \quad (59)$$

where the integration is taken over the FS, and θ_k is the angle between the unit vector \mathbf{x} and $\mathbf{l}(\mathbf{k})$. Assuming N-fold symmetry exists ($N > 2$),⁷¹ the FS can be divided into N identical wedges, which may be mapped onto each other by rotations, where the angle θ_k is changed to $(\theta_k + 2\pi m/N)$ on the m -th wedge. Thus, Equation (59) can be written as

$$\frac{\sigma_{xx}}{(e^2/h)} = \frac{1}{\pi} \int_{\Delta S=S/N} ds l_k \sum_{m=1}^N \cos^2(\theta_k + 2\pi m/N). \quad (60)$$

Standard math handbooks equate the summation term to $N/2$, and furthermore, using the relationship⁶¹ $l_{av}S = N \oint ds l_k$, one obtains

$$\frac{\sigma_{xx}}{e^2/h} = \frac{\sigma_{yy}}{e^2/h} = \frac{l_{av}S}{2\pi}, \text{ where} \quad (61)$$

$$l_{av} = \oint ds \frac{l_k}{S}. \quad (62)$$

Again this integral is taken over the whole FS, where S is the FS circumference, and l_{av} is the average of l_k . Finally, upon placing Equations (58) and (61) into Equation (50), we obtain the simple relationship for the temperature dependence for the Hall coefficient:

$$R_H \propto \frac{\Delta l}{l_{av}}, \quad (63)$$

where $\Delta l/l_{av}$ is highly correlated to the "anisotropy" of the "scattering path length" vector in the xy-plane. Hence, $\Delta l/l_{av}$ is termed the anisotropy. Therefore, in the conventional Bloch-Boltzmann theory, the Hall coefficient R_H in 2D systems becomes temperature dependent only if $\Delta l/l_{av}$ changes with temperature. Furthermore, this result can be generalized, in a complicated fashion, to include 3D systems as well as multiband effects (readers interested in these cases are referred to Ref. 61), but, these cases are not discussed here because of the 2D nature of the layered cuprate perovskites.

However, if electron-phonon scattering dominates, the temperature dependence of $\Delta l/l_{av}$ should display three distinct regimes of differing behavior determined by Θ_D .⁶¹ At very low T , impurity scattering, which tends to have an isotropic- l , dominates the transport properties leading to a constant R_H with T . Unfortunately, this regime is out of reach in the high- T_c superconductors. At mid-range temperatures ($\sim 0.2T_D$), phonon scattering is highly anisotropic leading to a temperature dependent R_H in many materials. Third and most importantly, at high T ($\geq T_D$), the scattering by phonons tends to be isotropic, so that the isotropic τ assumption is valid.⁷² Furthermore, this should lead to a saturation of R_H above T_D (~ 440 K in $\text{YBa}_2\text{Cu}_3\text{O}_7$). Interestingly, Fiory *et al.* have measured R_H up to 600K ($\gg T_D$) in $\text{YBa}_2\text{Cu}_3\text{O}_7$, and find no evidence for such saturation.⁷³ Therefore, even though the resistivity vs. temperature follows the expected behavior for electron-phonon scattering,

the Hall coefficient is apparently dominated by a nonphononic mechanism, which is probably electronic in origin.

5. Unconventional Hall Effect Theories

Due to considerable regularities occurring in the normal state properties of $\text{YBa}_2\text{Cu}_3\text{O}_{7-\delta}$ (e.g., universal inverse Hall angles $\theta_H^{-1} = AT^2 + B$ upon doping with various impurities⁷⁴), led Anderson to suggest that $\text{YBa}_2\text{Cu}_3\text{O}_{7-\delta}$ behaved as a two-dimensional Luttinger liquid.⁷⁵ Although presently in an early stage of development and not generally accepted, Anderson argues that most transport properties, including the conductivity, can be represented by correlation functions derived in the framework of a bosonized form of a one-dimensional Hubbard model such as that given by Haldane:⁷⁶

$$\mathcal{H} = \sum_{\Omega} \sum_Q \hbar k_F(\Omega) \left[v_s(\Omega) Q b_{s\Omega}^* b_{s\Omega} + v_c(\Omega) Q b_{c\Omega}^* b_{c\Omega} \right], \quad (64)$$

where the b 's are bosonized representations of the charge and spin fluctuations. Moreover, it is argued that this Hamiltonian can be interpreted in terms of two kinds of solitons: **spinons**, which behave as electrons with spin and no charge with a momentum k_F located at an angle $+\Omega$; and **holons**, which carry the charge with a momentum $2k_F$ located at an angle $-\Omega$. In addition, the two are connected in the sense that when the holons move one way, the spinons moves in the opposite. Thus, in a Luttinger liquid, charge and spin separate.⁷⁵

Separation of charge and spin should lead to interesting behavior in the normal

state properties. For example, Anderson argues that upon application of an electric field, the holons are accelerated causing a backflow of the spinons, giving rise to a resistivity proportional to the number of thermally excited spinons, i.e., $\rho \propto kT$.⁷⁵ In contrast, an entirely different situation arises in the presence of a magnetic field. The equation of motion in a magnetic field is

$$\hbar \frac{\partial \mathbf{k}}{\partial t} = \frac{e}{\hbar} \left(\frac{\nabla e_{\mathbf{k}}}{\nabla \mathbf{k}} \times \mathbf{B} \right) - \frac{\hbar \partial \mathbf{k}}{\tau_{\perp}}, \quad (65)$$

where τ_{\perp} denotes the apparent relaxation time measured in the presence of a magnetic field. This equation of motion is argued to represent an acceleration of the spinons parallel to the Fermi surface, without disturbing the holon occupancies.⁷⁵ As a result, the spinons can only interact with other spinons or magnetic impurities. Being a fermion-fermion interaction, we are left with the well known T^2 behavior for the temperature dependence of the inverse Hall angle. Therefore, the different temperature dependencies for the resistivity and inverse Hall angle, e.g., T and T^2 , respectively, lead to the observed temperature dependence of the Hall coefficient $R_H \propto 1/T$.

Although the two-dimensional Luttinger liquid theory accurately describes the anomalous temperature dependent Hall coefficient R_H for $\text{YBa}_2\text{Cu}_3\text{O}_{7-\delta}$, this theory is far from being proved and generally accepted. On the other hand, Markiewicz recently provided an explanation for a weaker, but somewhat similar, temperature dependent Hall coefficient observed in $\text{La}_{2-x}\text{Sr}_x\text{CuO}_4$ (LSCO).⁷⁷ In this material, the 2D CuO_2 band is assumed to be nested while sitting near a peak in the 2D electronic density of states. In this model it is shown that the conductivity is given by

$$\sigma_{xx} = [P(T) + xQ(T)] \frac{ne^2\tau}{m}, \quad (66)$$

where P is the probability that the electrons are scattered into a particular CuO_2 branch and $Q = 1-P$ is the probability that the electrons are scattered into the remaining branches. Moreover, x is the hole doping away from half filling of the 2D CuO_2 band and n is the carrier density. Finally, this model predicts the following Hall coefficient:

$$R_H = \frac{x}{[P(T) + xQ(T)]^2 ne}. \quad (67)$$

Here the temperature dependence of R_H arises from the temperature dependence of the scattering probabilities P and Q . However, it is argued that the stronger temperature dependence of R_H in $\text{YBa}_2\text{Cu}_3\text{O}_{7-\delta}$ is probably due to another mechanism. Although possible, this proposed scattering mechanism is unlikely in $\text{YBa}_2\text{Cu}_3\text{O}_{7-\delta}$ since, P and Q are unlikely to be strongly temperature dependent. In addition, multiband effects probably occur in $\text{YBa}_2\text{Cu}_3\text{O}_{7-\delta}$ which are neglected in this model.

C. H_{c2} Determined from Fluctuations

The studies of fluctuation effects in superconductors have recently been revived due to the discovery of the high- T_c materials. In this dissertation research, the recent fluctuation theory of Ullah and Dorsey,²¹ in the limit of large magnetic fields, was utilized to deduce the H_{c2} slopes for $H \parallel c$. The fluctuation theory was developed in the framework of the Lawrence-Doniach model,⁷⁸ which accounts for the layered structure of the high- T_c materials. This theory gives the following set of equations for

the fluctuation conductivities for both the 3D and 2D scaling:

$$\left(\frac{H}{T}\right)^{1/2} \sigma_{yy}^{2D} = g \left[A \frac{T-T_c(H)}{(TH)^{1/2}} \right], \quad (68)$$

$$\left(\frac{H^{1/3}}{T^{2/3}}\right) \sigma_{yy}^{3D} = g \left[A \frac{T-T_c(H)}{(TH)^{2/3}} \right], \quad (69)$$

$$(TH)^{1/2} \sigma_{zz}^{2D} = f \left[A \frac{T-T_c(H)}{(TH)^{1/2}} \right]; \quad (70)$$

$$\sigma_{zz}^{3D} = f \left[A \frac{T-T_c(H)}{(TH)^{2/3}} \right]. \quad (71)$$

In these equations, σ_{ii} is the fluctuation conductivity along the i -th crystal axis (i.e., σ_{yy} denotes $\parallel ab$ -plane while σ_{zz} denotes $\perp ab$ -plane), H is the applied magnetic field along the c -axis, $T_c(H)$ is the mean field transition temperature, which is field dependent. The scaling functions g and f should be the same for all fields, and the constant A is independent of the temperature and field. The only free parameter is $T_c(H)$ which, selected carefully, leads to the H_{c2} slope. This is accomplished by simply plotting each side of the equation of interest, while neglecting the functions g , f , and A , along different axis, while selecting the $T_c(H)$ for each magnetic field transition to generate a universal curve. Interestingly, the best choices of $T_c(H)$ usually lead to linear H_{c2} slopes near T_c , as expected.⁷⁹ By inspection, Equations (68) and (69) apply to the c -oriented epitaxial films used in this dissertation, whereas Equations (70) and (71) could be applied to any untwinned a -oriented films, if ever developed.

IV. CORRELATIONS BETWEEN R_H , T_c , AND J_c

A. Overview of Most Important Experimental Results

Before discussing in detail each of the experimental results, a brief overview of the important principal findings will be presented. The electrical transport properties of $\text{YBa}_2\text{Cu}_3\text{O}_{7-\delta}$ vary systematically with increasing oxygen deficiency δ . Both the resistivity $\rho(\delta)$ and the Hall coefficient $R_H(\delta)$ increased with δ at similar rates, and consequently the Hall angle, given by $\tan(\theta_H) \equiv R_H B / \rho$, changes only slightly. In *all* films, the critical current densities $J_c(\delta, H=0)$ measured in self-field extrapolated towards zero for compositions near the edge of the 90K plateau, while the temperature and field dependencies of $J_c/J_c(H=0)$ remained fixed for $\delta < 0.15$, both of which are suggestive of geometrical effects. For larger oxygen deficiencies ($\delta > 0.3$), the field dependencies of $J_c(\delta, H)$ were similar to those observed in polycrystalline $\text{YBa}_2\text{Cu}_3\text{O}_7$ and the superconducting Hall effect transitions exhibited systematic "*noise*", indicative of granular-like behavior. Pinning energies determined both from the field dependence of $J_c/J_c(H=0)$ and from in-field resistive transitions show plateau-like behavior near full oxygenation even though J_c decreases rapidly in this region. On the 90K plateau, most films showed no broadening in the resistive transitions; however, *all* films showed some broadening in the transitions between the 90K and 60K plateaus. Films post-annealed at low- PO_2 usually showed "*peaked*" T_c behaviors with δ , unlike the high- PO_2 post-annealed films which typically show "*flat*" 90K plateaus.⁸⁰ However, the Hall coefficients were found not to rely on the processing conditions, suggesting that

differences in the measurable carrier densities are not responsible for these different $T_c(\delta)$ patterns.

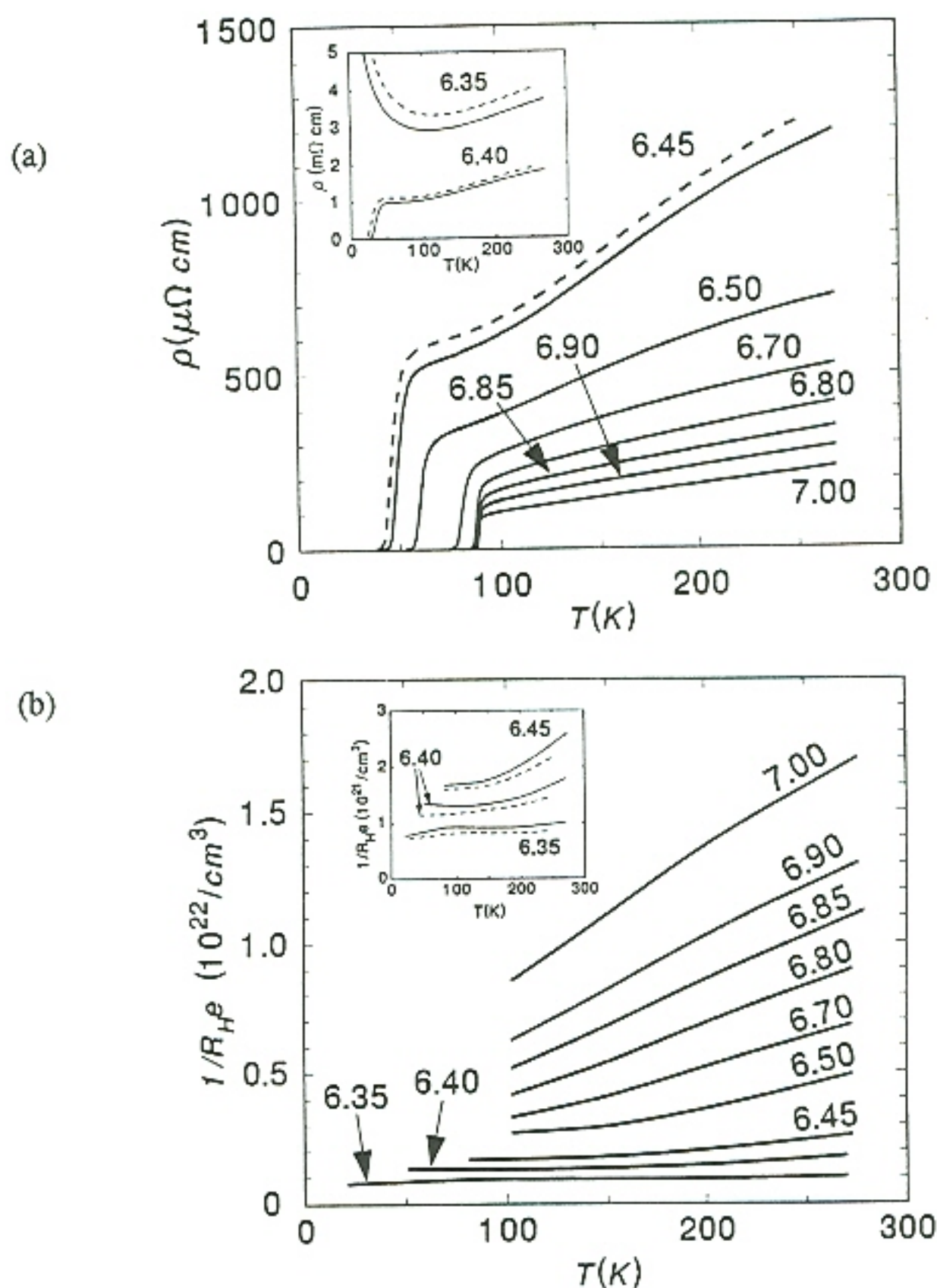
B. Discussion of Results

1. Effect of Oxygen Deficiency δ on the Resistivity and Hall Coefficient

The removal of oxygen from $\text{YBa}_2\text{Cu}_3\text{O}_{7-\delta}$ leads to a progressive increase in the resistivity [Figure 20(a)] as well as a decrease in Hall number [Figure 20(b)]. These observations suggest steady decreases in the density of states, which according to simple BCS theory should lead to steady decreases in T_c . In actuality, two plateaus are observed in T_c vs. δ which could be reconciled either by phase separation^{18,20} or by some complex electronic mechanism.^{13,14}

Interestingly, the insets of these figures show the effects of room temperature annealing which may be ascribed to the formation of oxygen-ordered "*Ortho-II*" phase at fixed $\delta \geq 0.4$.¹⁵ These room temperature ordering effects were studied at three estimated oxygen contents of 6.35, 6.40, and 6.45. For investigation at each of these fixed oxygen contents, the sample was quenched from 200°C, rapidly mounted, and cooled below 250K in about 30 minutes. No ordering effects were ever observed during measurements at $T < 250\text{K}$, and the final results are depicted by the dashed curves in Figure 20(a) and Figure 20(b). After completion of each data acquisition sequence, the sample was warmed to room temperature, and allowed to "*age*" until the resistivity reached a minimum saturation – approximately four days at each oxygen content [Figure 21]. These results are depicted by solid curves in the same figures.

Figure 20



Resistivity (a), Inverse Hall coefficient (b), and Inverse Hall angle (c) for a laser ablated film of $\text{YBa}_2\text{Cu}_3\text{O}_{7-\delta}$ as a function of temperature and oxygen deficiency δ . Insets show the apparent changes in the "Ortho-II" phase with room temperature annealing. The dashed curves in parts (a) and (b) represent the behavior immediately after quenching from 200°C, whereas the corresponding solid curves represent the behavior after aging for four days. The Inverse Hall angle is shown on a log-log plot to depict the relative insensitivity of the T^2 behavior to oxygen deficiency.

Figure 20 (continued)

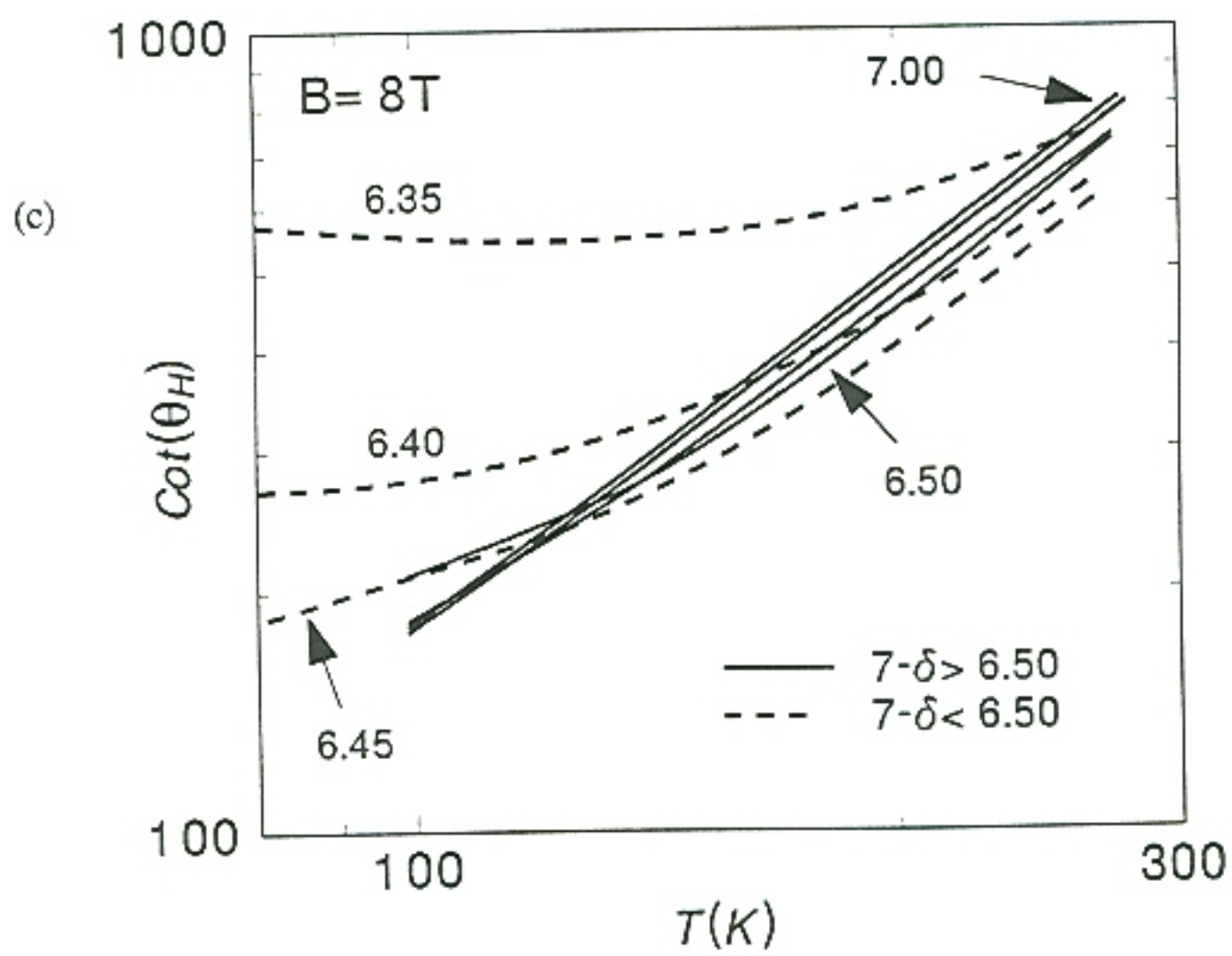
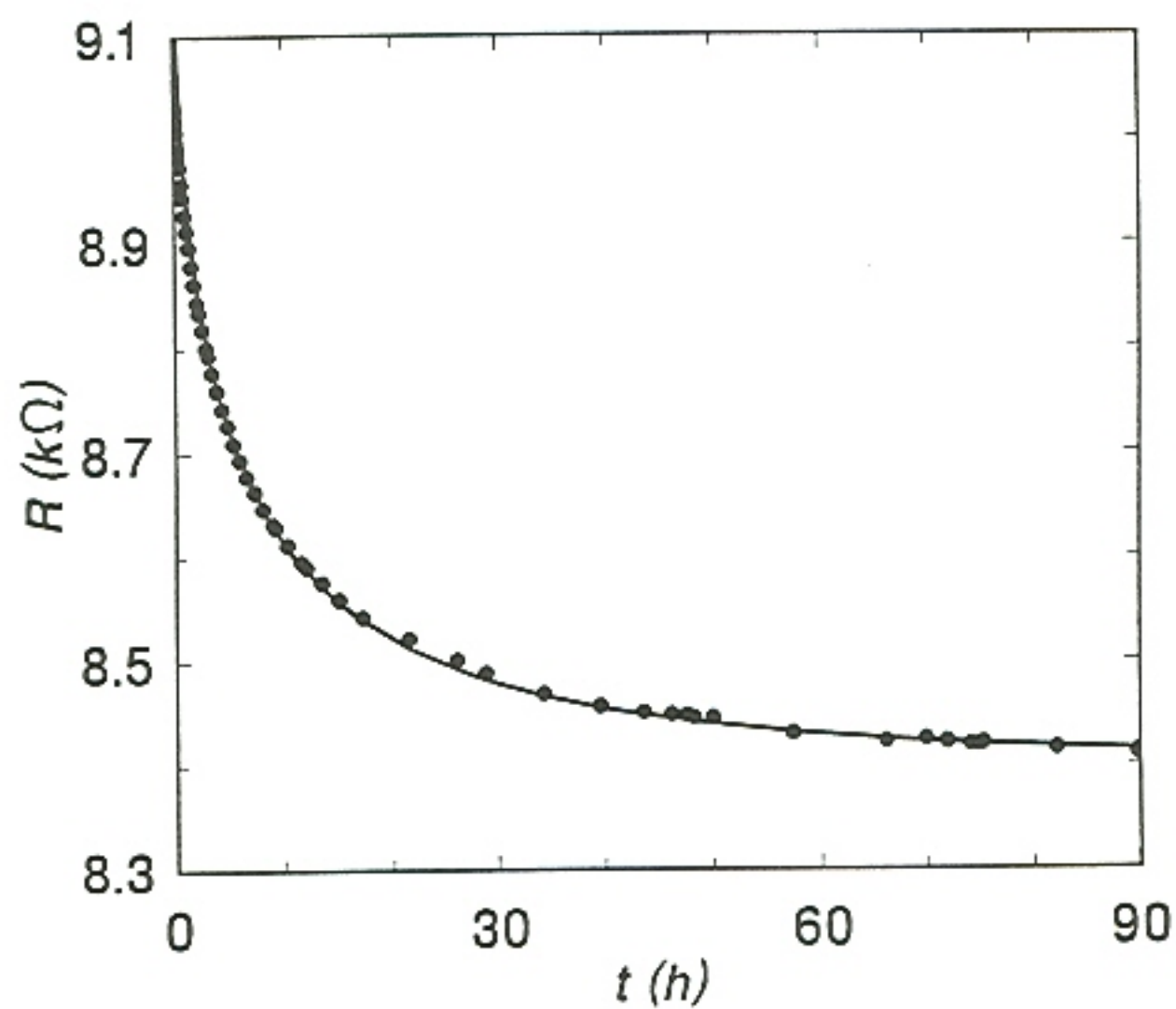


Figure 21



The effect of room temperature annealing on the resistance in the "Ortho-II" phase $YBa_2Cu_3O_{\sim 6.5}$. This data were obtained at a temperature of 297K and at an estimated oxygen content of $7-\delta \approx 6.40$. Note that four days were required to reach saturation. Similar plots were obtained at the oxygen contents 6.35 and 6.45. The solid curve is a guide to the eye.

In addition to an observed reduction in resistivity, this ordering-related annealing always led to an increase of the observed Hall number, which could be interpreted as an indication of additional charge carriers being transferred to the Cu-O₂ planes as suggested by the electronic model first proposed by Veal.¹⁵ However, this observation does not rule out a phase separation scenario, since a parallel configuration of two dissimilar conductors (denoted by indexes 1 and 2) will yield an observed Hall coefficient R_H given by,

$$R_H = \frac{R_2 R_{H1} + R_1 R_{H2}}{R_1 + R_2}, \quad (72)$$

where R_{Hi} and R_i refer to the Hall coefficient and the resistance contributed by the i -th conductor, respectively. It is clear from this equation that the phase contributing the least electrical resistance would average more heavily in the apparent Hall coefficient. Moreover, if phase separation leads to a larger proportion of the "better" phase, i.e., lesser resistivity and higher oxygen content, the apparent value of R_H would decrease with room temperature annealing. This would occur because the aging process would create a larger proportion (i.e., less resistance) of the phase having the smaller value of R_H [see Figure 20(b)]. Therefore, the normal state resistivity and normal state Hall coefficient results alone cannot determine whether or not phase separation occurs in oxygen deficient YBa₂Cu₃O_{7- δ} .

Another feature of Figure 20(a), which is observed in all samples, is a slight broadening of the resistive transitions off the 90K plateau. It is unlikely that this broadening results from the formation during cool down of layers with differing oxygen

contents, since no 90K onsets are observed for compositions off the 90K plateau [see Figure 20(a)]. Rather, this broadening off the 90K plateau is most likely due to a T_c distribution, with a series connection of domains with different T_c 's.

A potentially important finding is the relative constancy of the Hall angle $\text{Tan}(\theta_H) = E_y/E_x = R_H B / \rho$ for oxygen deficiencies δ when $\delta \leq 0.5$ [Figure 20(c)]. In a multiband system, the Hall angle can be derived from simple expressions for a multiband system⁵⁹

$$\text{Tan}(\theta_H) = \frac{E_y}{E_x} = \frac{B_z}{\sigma} \sum_i R_{Hi} \sigma_i^2 \quad . \quad (73)$$

Assuming each (parabolic) band can be described by the expressions $R_{Hi} = -1/n_i e$ and conductivity $\sigma_i = n_i e^2 \tau_i / m_i$, this becomes

$$\text{Tan}(\theta_H) = -\frac{1}{\sigma} \sum_i \omega_i \tau_i \sigma_i \quad . \quad (74)$$

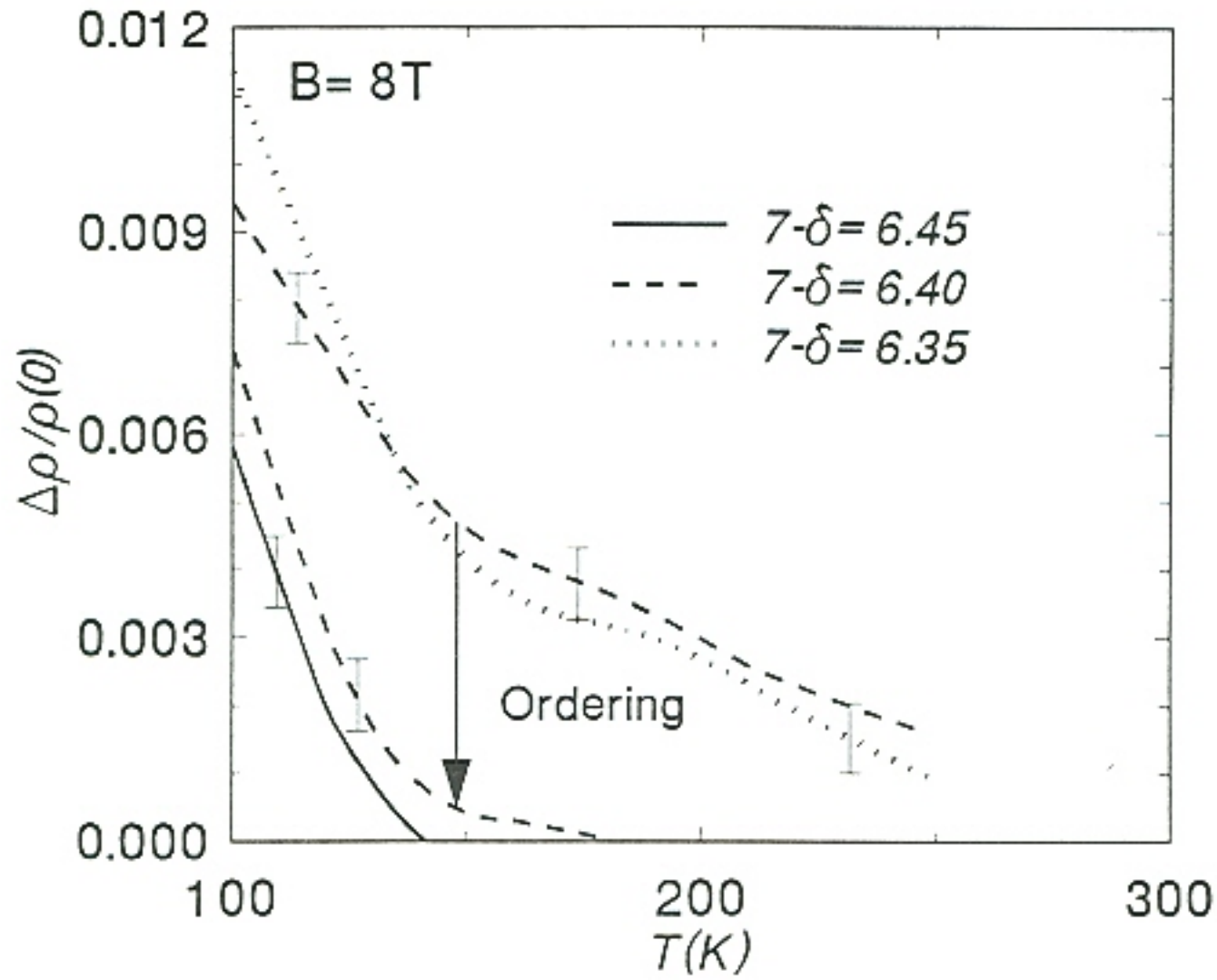
Here $\omega_i = eB/m_i$ and τ_i are the cyclotron frequencies and relaxation times for the i -th band, respectively. Moreover, the band structure calculations predict four bands crossing the Fermi level in $\text{YBa}_2\text{Cu}_3\text{O}_7$, and each of these bands is expected to have different effective masses.⁷ Therefore, it is plausible that upon oxygen depletion, the individual conductivities would change at different rates. Under these circumstances, Equation (74) suggests that significant deviations should occur in the observed magnitude and temperature dependence of the Hall angle with changing oxygen deficiency. On the contrary, the Hall angle changes only slightly over most of the oxygen content range [Figure 20(c)] and this suggests that one band dominates the

normal state properties with fields $H \parallel c$. On the other hand, for large oxygen deficiencies ($\delta > 0.5$), deviations occur in the temperature dependence of the Hall angle [Figure 20(c)]. In addition, these deviations correspond with onsets of magnetoresistance [Figure 22] supporting the existence of multiband effects only for the compositions of δ in excess of $\delta > 0.5$.⁵⁹

2. Temperature Dependence of the Hall Coefficient

To understand the temperature dependence of the Hall coefficient, one can use the proposal that $\text{YBa}_2\text{Cu}_3\text{O}_7$ behaves as a two-dimensional Luttinger liquid.⁷⁵ Use of this single band theory is justified by and consistent with the arguments just presented. In this formalism, the observed Hall angle $\tan(\theta_H)$ depends on a "*transverse*" relaxation rate τ as $\cot(\theta_H) = (\omega_c \tau)^{-1} = AT^2 + (\omega_c \tau_{\text{imp}})^{-1}$. Here ω_c is the field dependent cyclotron frequency and $1/\tau_{\text{imp}}$ is the scattering rate due to impurities. In a Luttinger liquid, separation occurs between the charge and spin quasiparticles. Furthermore, application of a magnetic field leads to the rotation of k space allowing the "*transverse*" relaxation rate to include only the effects of the spin-spin interactions. Being fermions, these interactions should lead to the well established T^2 scattering process in $\cot(\theta_H)$, whereas the impurity scattering term only includes the effects of magnetic scattering centers. Referring to the log-log plot [Figure 20(c)], the inverse Hall angle indeed varies as T^2 over a wide range of oxygen deficiencies ($\delta \leq 0.55$) in $\text{YBa}_2\text{Cu}_3\text{O}_{7-\delta}$. On the other hand, a "*transport*" relaxation rate τ_{tr} is measured in the resistivity and is proportional to the decay rate of the accelerated electrons into elementary excitations

Figure 22



Magnetoresistance $\Delta\rho/\rho(0)$ observed in $\text{YBa}_2\text{Cu}_3\text{O}_{7-\delta}$ for oxygen deficiencies in excess of $\delta > 0.5$. These data were obtained as a function of temperature and at an applied field of 8 Tesla. Note that "aging" effects associated with the ordering in the "Ortho-II" phase were observed at the composition $7-\delta \approx 6.40$. The onset of magnetoresistance corresponds with the same composition at which the inverse Hall angle deviates from its T^2 behavior. These observations are consistent with multiband effects when $\delta > 0.5$.⁵⁹

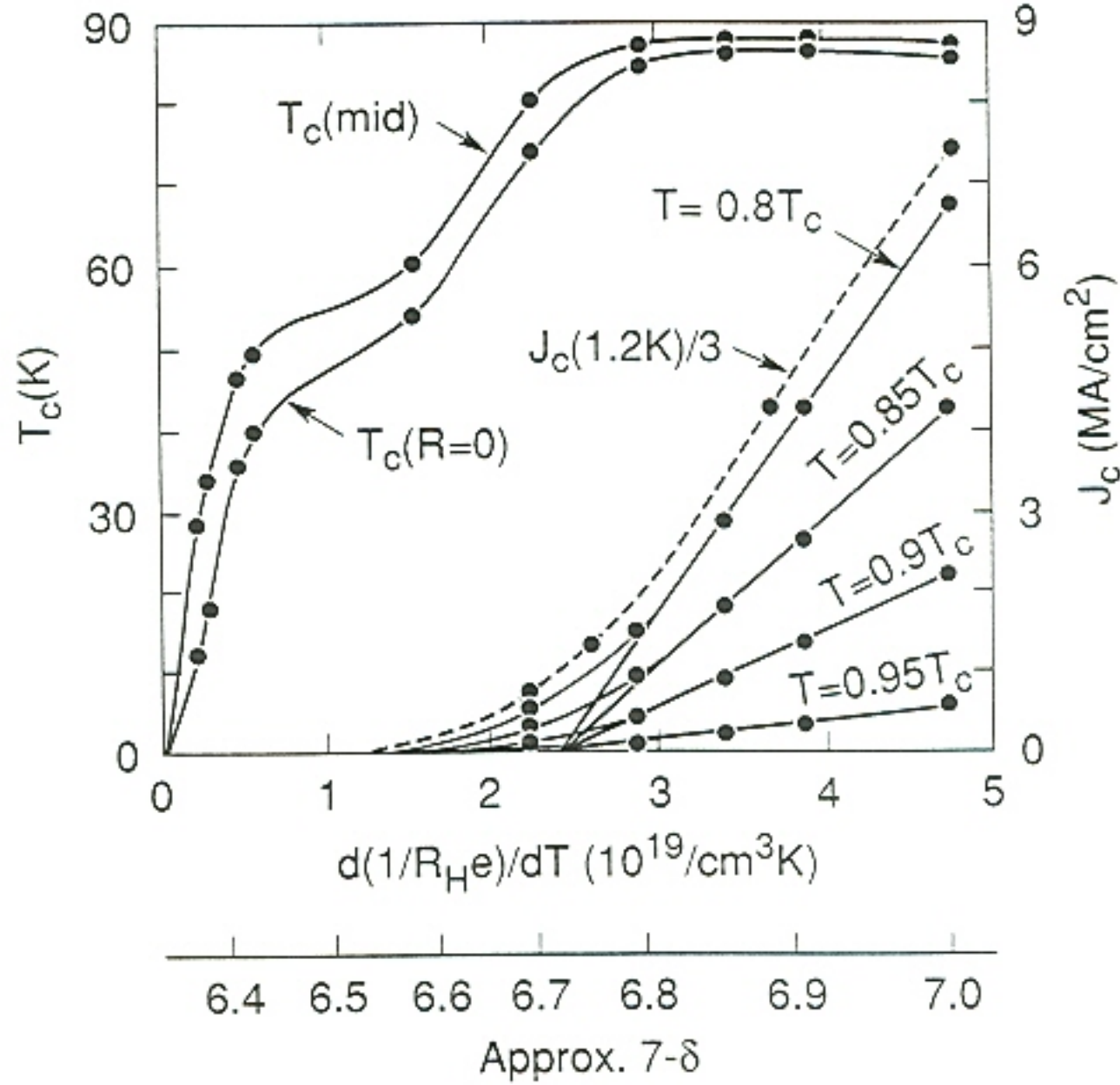
(holons and spinons), such that

$$\rho \propto \frac{m}{ne^2} \left(\frac{1}{\tau_{tr}} + \frac{1}{\tau_{imp}} \right) , \quad (75)$$

where⁷⁵ $\tau_{tr}^{-1} \propto T$. In relatively clean materials, the impurity scattering rate $1/\tau_{imp}$ may be neglected. Combining these results, one has $1/(R_H e) \propto \cot(\theta_H)/\rho \propto nT$, where n is the density of charge carriers and e is the electron charge. Thus, within the Luttinger liquid approach, the average slopes of the inverse Hall coefficient curves, which vary almost linearly with temperature [Figure 20(b)], serve as a relevant electronic parameter for displaying our data. In Figure 23 are plotted the transition temperatures $T_c(R=0)$ and $T_c(\text{mid})$ as well as the critical current densities in self-field $J_c(\delta, H=0)$, as a function of $d(1/R_H e)/dT$. Note that a simpler plot of superconducting properties, e.g., T_c and J_c , as a function of $1/(R_H e)$ would give qualitatively similar results [see Figure 20(b)]; however, the function $1/(R_H e)$ must be chosen at an arbitrarily fixed temperature when displaying data in this fashion. Overall, most superconducting properties improve with increasing $d(1/R_H e)/dT$.

Although this behavior is consistent with the Luttinger liquid model, alternate explanations for the temperature dependence of $1/(R_H e)$ may be found in a sharp peak in the electronic density of states (DOS) lying near the Fermi surface.^{77,81} The existence of such a van Hove singularity (vHs) is suggested in the band structure;^{7,82} however, band structure calculations place the DOS peak ~ 0.1 eV below the Fermi energy. According to Pickett,⁵⁷ this DOS peak is associated with the chain layer derived bands, which are more difficult to determine accurately than the plane related

Figure 23



Transition temperature T_c , and critical current density J_c evaluated at fixed reduced temperatures, as a function of either the oxygen deficiency δ or the "apparent carrier density" from the Luttinger Liquid Theory described in the text. Notice that J_c extrapolates toward zero at the edge of the 90K plateau, suggestive of phase separation. The solid (dashed) curves were obtained from a laser ablated (BaF_2 processed) film. Extrapolations do not occur at exactly the same point due to uncertainties in the film thickness.

bands. Interestingly, these same chain related bands in the 60K phase, $\text{YBa}_2\text{Cu}_3\text{O}_{6.5}$, lie farther below the Fermi surface, according to Yu.⁹ In this picture, the systematic decrease in the temperature dependence of R_H with δ merely reflects a steady displacement of the peaked DOS (vHs) from the Fermi energy. But, to be plausible, this scenario requires that the peak is actually nearer to the Fermi surface than calculated.

Yet another possible explanation comes from Bloch-Boltzmann theory. These calculations, however, are complicated and the Fermi-Dirac distribution $-\partial f/\partial \epsilon$ must often be approximated by $\delta(\epsilon - \epsilon_F)$. Moreover, the standard approximation of isotropic scattering leads⁵⁵ to a temperature-independent R_H . As described in Section III.4, Ong⁶¹ has shown that, in the framework of this conventional theory, a temperature dependent R_H can result from a changing anisotropy of the ab-plane "scattering path length" vector $\ell(\mathbf{k}) = \mathbf{v}_k \tau_k$ with temperature T . Nevertheless, these latter mechanisms may prove difficult in explaining the universal quadratic temperature dependence of the inverse Hall angle, $\cot(\theta_H) = AT^2 + B$ [Figure 20(c)]. Finally, this quadratic temperature dependence is also reported well above the Debye temperature⁷³ which tends to support a nonphononic scattering mechanism.

3. Effect of Oxygen Deficiency δ on the Critical Current Density

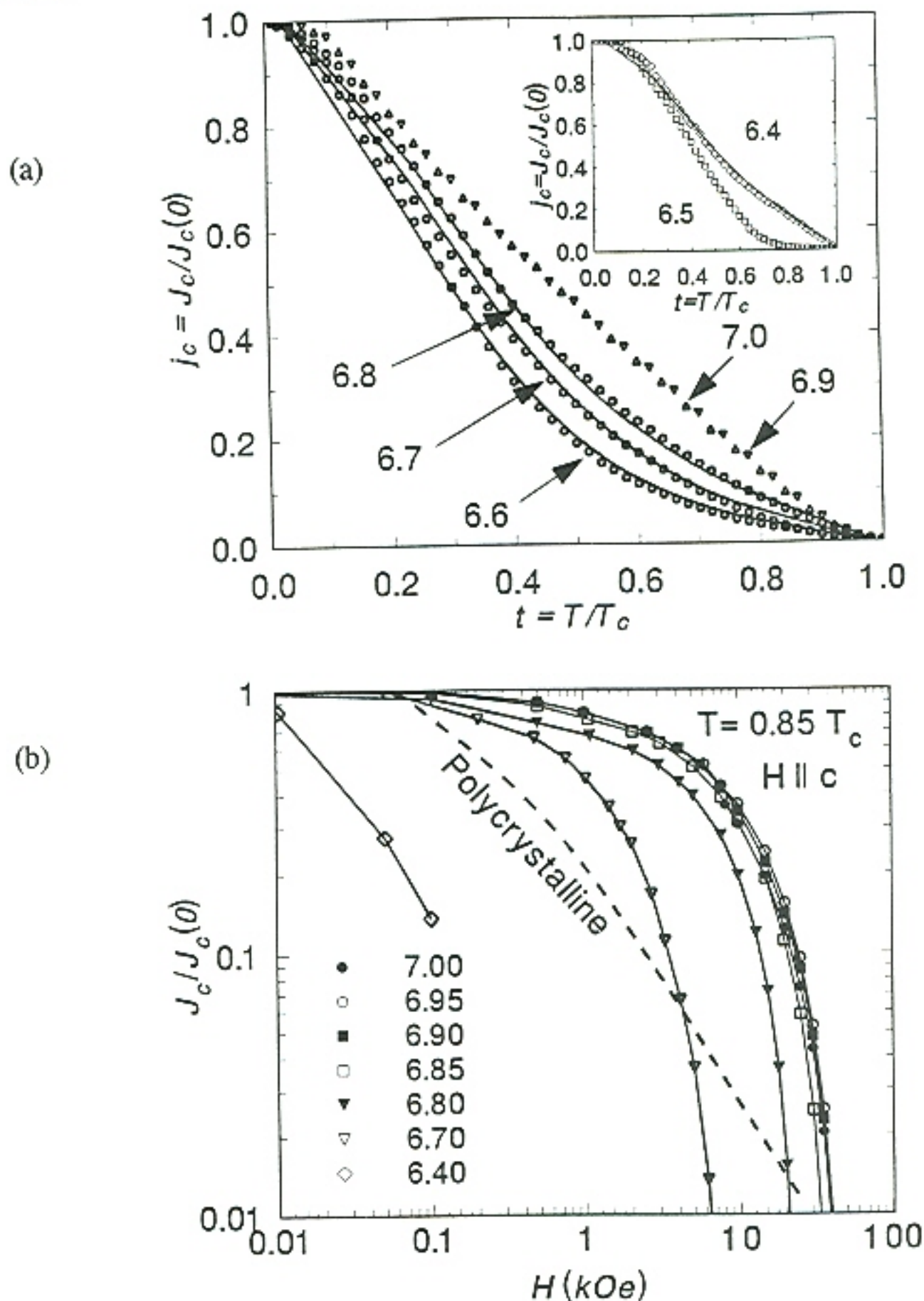
This section considers the transport critical current density J_c , measured in self-field. Examination of Figure 23 shows that J_c extrapolates toward zero at an oxygen deficiency near the edge of the 90K plateau. This feature was observed in *all* films,

and somewhat similar behavior was reported earlier by Ossandon *et al.*⁸³ in magnetic measurements of current density in bulk, aligned $\text{YBa}_2\text{Cu}_3\text{O}_{7-\delta}$. For $\delta \leq 0.15$, J_c varies linearly with δ . In this regime, the functional dependencies of J_c on temperature and field [Figure 24] are constant, which suggests a geometrical decrease in the amount of 90K phase. In this view, $J_c(\delta)$ deviates from its linear decrease with δ for compositions $\delta \geq 0.15$ because other, lower J_c phases then conduct appreciable portions of the supercurrent. This tapering occurs near the same oxygen content at which the field dependencies of J_c begin to degrade. This degradation implies reductions in the pinning energy, as discussed in the next section.

4. Determination of the Pinning Energy

Several methods provide means of determining the pinning energy. These include analyses of I-V curves, resistive transitions $\rho(T,H)$, or dependencies of critical currents $J_c(T,H)$ on field. Recently, self consistent values for the pinning energies were obtained in fully oxygenated $\text{YBa}_2\text{Cu}_3\text{O}_7$ epitaxial films determined from the I-V curves and from in-field resistive transitions.⁵³ However, if phase separation occurs in oxygen deficient $\text{YBa}_2\text{Cu}_3\text{O}_{7-\delta}$, the I-V curves would clearly be difficult to interpret, since the actual current path dimensions, which are required to calculate the flux creep resistivities, would be unknown. Similarly, Arrhenius plots of the resistive transitions would be expected to broaden (theoretically shown by others^{84,85}) as a result of inhomogeneities. For example, the apparent T_c distributions observed in the Hall transitions in Figure 25 would probably lead to errors in the derived pinning energies.

Figure 24



Reduced critical current densities as a function of temperature (a), applied field for $H \parallel c$ (b), and applied field for $H \parallel ab$ (c) for various oxygen contents. No apparent changes in pinning energy occur while on the 90K plateau even though $J_c(0)$ decreases rapidly [see Figure 23]. Interestingly, many of the curves in (a) behave as SNS proximity tunneling⁸⁶ (solid curves) off the 90K plateau. The dashed curve is a representative polycrystalline sample³⁷ which indicates the granular like behavior when $\delta > 0.2$.

Figure 24 (continued)

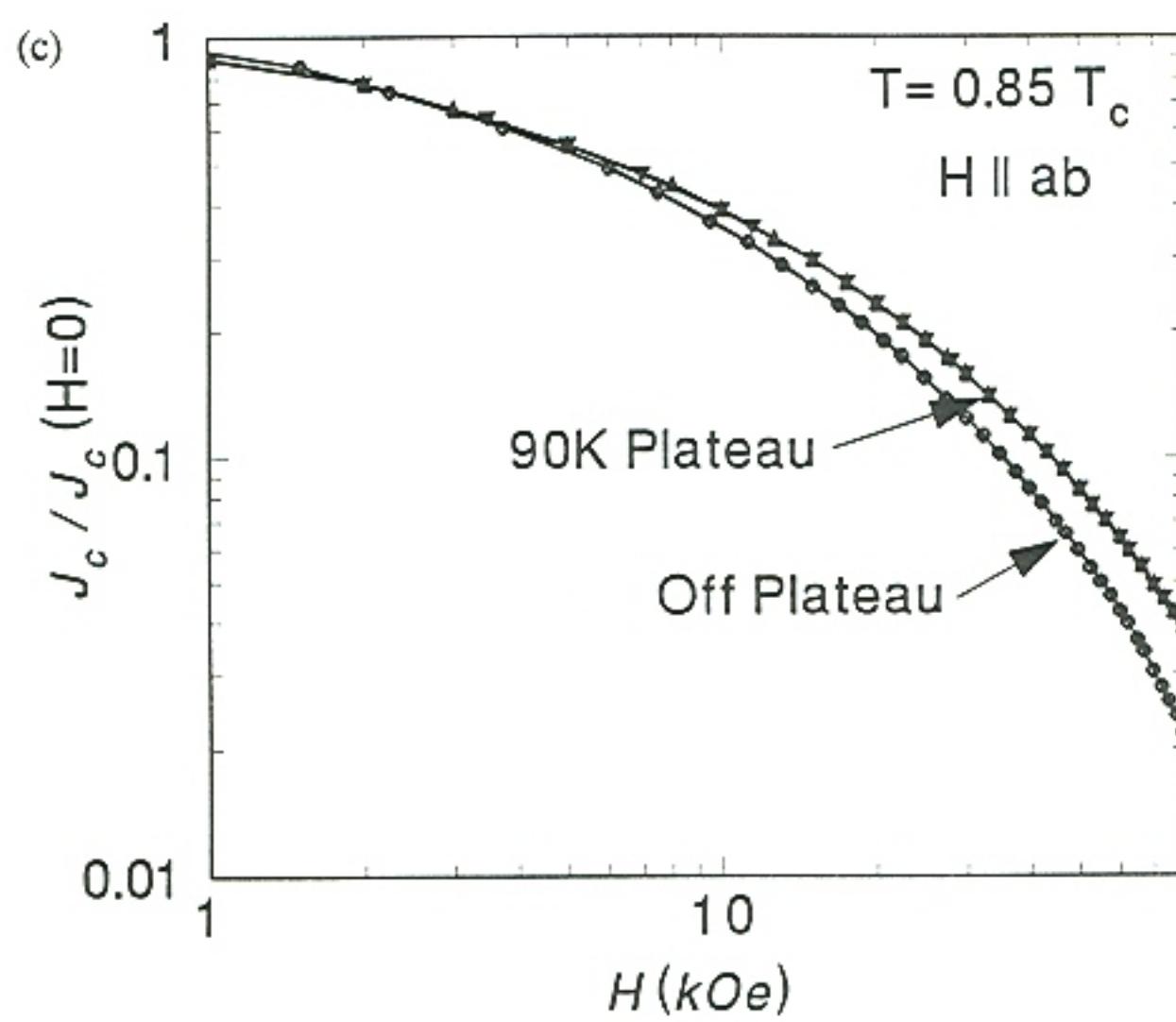
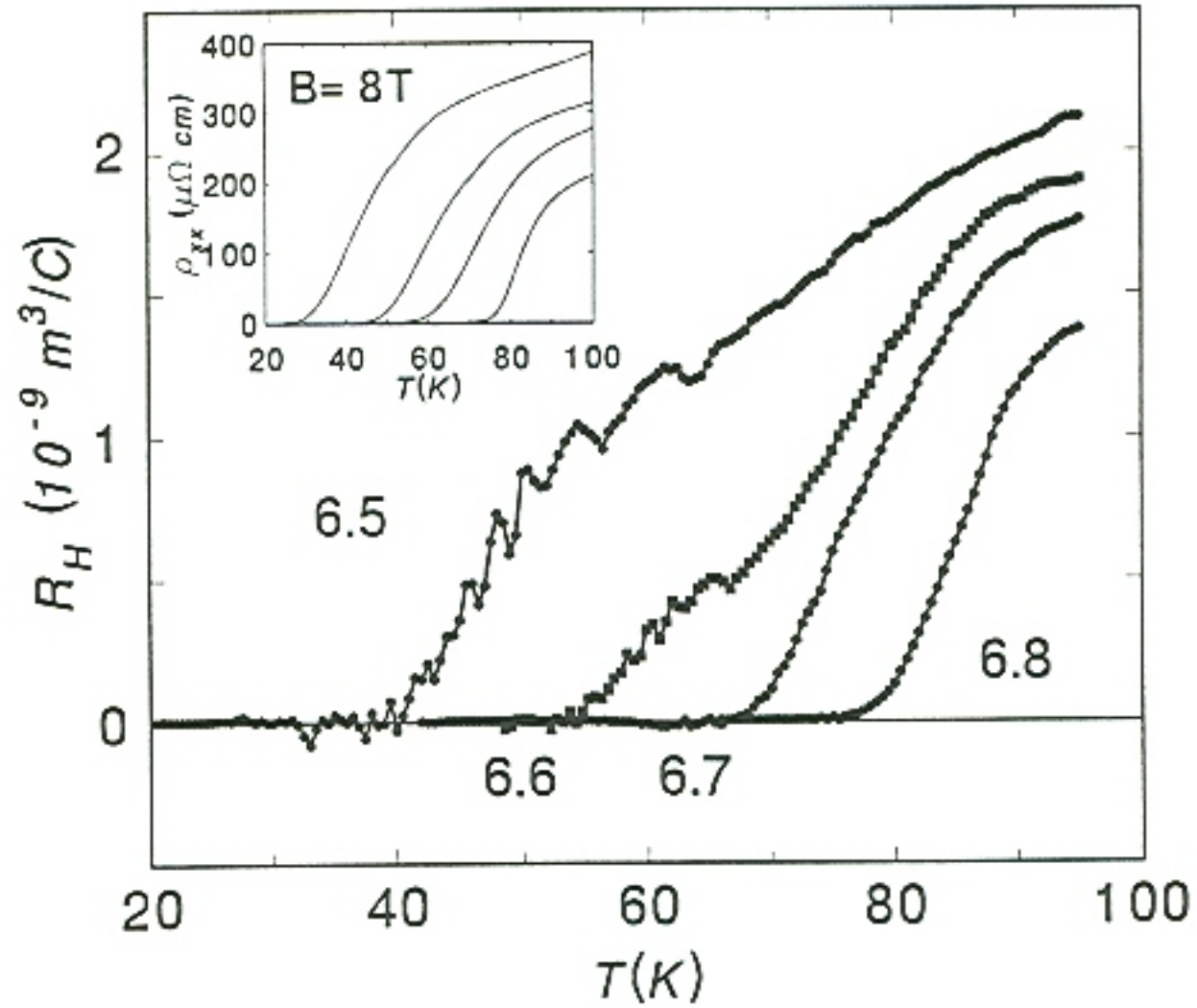


Figure 25



Superconducting Hall effect transitions obtained at 8 Tesla for various oxygen contents. All Hall transitions with $\delta \geq 0.3$ show reproducible "onsets" indicative of a distribution of T_c 's. However, these "onsets" were never observed on the 90K plateau nor in any resistive transition as shown in the inset.

Note also that, on the 90K plateau, J_c decreases by roughly an order of magnitude while the conductivity decreases by a factor of only 1.8. As a result, the derived pinning energies obtained under relatively high electric fields, i.e., resistive transitions, may be in error due to induced normal currents in the lower T_c phases which are forced normal by the applied magnetic fields.

To develop this more rigorously, consider the standard expression for the creep resistivity:⁵⁰

$$\rho = \frac{E_o}{J_{co}} \frac{U_o(T,B)}{kT} \exp \left(- \frac{U_o(T,B)}{kT} \right) , \quad (76)$$

which is valid in the limit of small current and thus is applicable to the resistive transition measurements. Here J_{co} is the critical current density in the absence of flux creep, E_o is proportional to the elementary "attempt" frequency, and U_o is the activation energy for flux creep. Due to the weak, logarithmic sensitivity of the analysis, the prefactor is generally approximated to be constant. It follows that the slopes of the Arrhenius plots of $\ln \rho$ vs. $1/T$ are equal to $-U_o(T,B)/k$. The situation becomes more complex in the phase separation scenario. Using the resistor combination equations

$$\rho^{\pm 1} = \sum_i^n f_i \rho_i^{\pm 1} , \quad (77)$$

where f_i denotes the volume fraction of the i -th phase, and $+/-$ specifies series/parallel combinations, respectively, the Arrhenius equation becomes

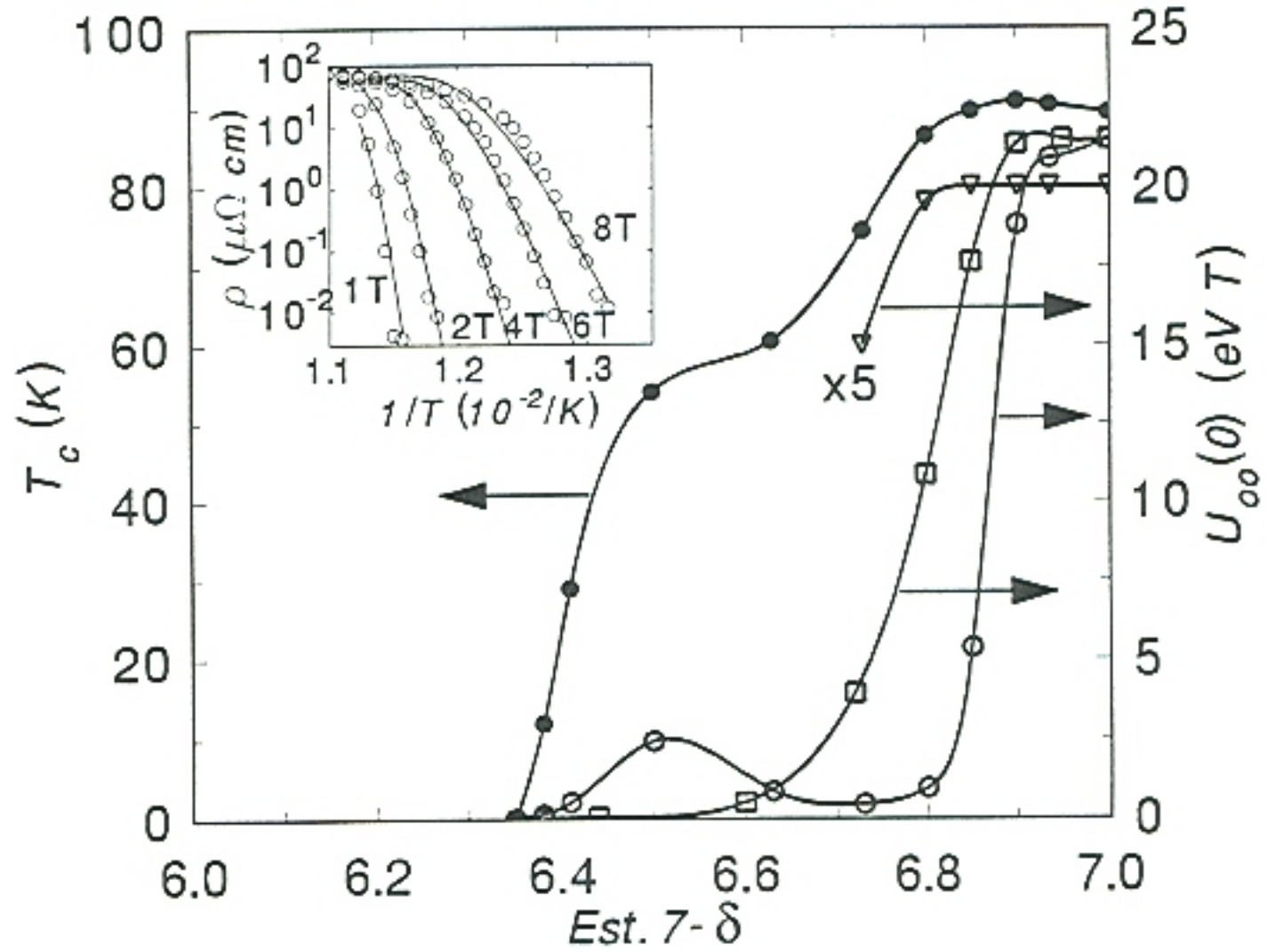
$$\ln \rho = \ln \left[\frac{E_o}{J_{co}} \frac{U_o(T,B)}{kT} \right] \pm \ln \left[\sum_s f_s \exp \left(\mp \frac{U_{os}(T,B)}{kT} \right) + \sum_n f_n (\alpha T)^{\pm 1} \right]. \quad (78)$$

The s/n indices represent superconducting/normal metal phases, respectively, and α represents the relative scaling between the flux creep and normal state resistivities, i.e.,

$$\alpha \propto \left[\frac{k J_{co}}{E_o U_o(T,B)} \right] \rho_{onset}. \quad (79)$$

In a percolative model, with parallel conduction channels dominating the resistive behavior, Equation (79) shows the factor α approaches zero as J_c extrapolates to zero near the edge of the 90K plateau. It follows that the normal metal term cannot be ignored in the determination of $U_o(T,B)$ from the Arrhenius plots. Otherwise, the pinning energies obtained from the analysis would be in error. Equation (78) was used to fit the resistive transitions of a film grown by the BaF_2 process⁴¹ [Figure 26 inset] at various oxygen deficiencies δ , assuming a parallel combination of one superconducting phase with one normal metal conduction channel. (Note that the normal metal term could be ascribed to the collection of lower T_c , oxygen deficient phases, which are forced normal in the temperature range of the resistive transitions). The ratio of the normal state resistivity to the flux creep resistivity at full oxygenation was assumed to be on the order of $\alpha \approx 10$ –100, and was allowed to decrease with increasing oxygen deficiency according to Equation (79). This analysis yields a plateau in the pinning energy U_o [Figure 26] as a function of δ near full oxygenation, even though J_c decreases in this region. In addition, a curious peak in U_o was obtained on the 60K plateau, possibly reflecting enhanced superconducting properties in the long

Figure 26



Pinning energy $U_{oo}(\delta) = U_o(\delta, T=0, B=1T)$ (open symbols) and $T_c(\delta)$ (solid circles) as a function of oxygen content $7-\delta$ for a film prepared by the BaF_2 process. The open circles represent $U_{oo}(\delta)$ as determined from fitting Equation (78) to the Arrhenius curves at various oxygen deficiencies. The inset depicts an actual fit at $\delta = 0$. The open squares (triangles) are $U_{oo} \propto B^*$ for $H \parallel c$ ($H \parallel ab$) as defined by Equation (80). The values of $U_{oo}(\delta)$ for $H \parallel ab$ are scaled by a factor of 1/5 for clarity.

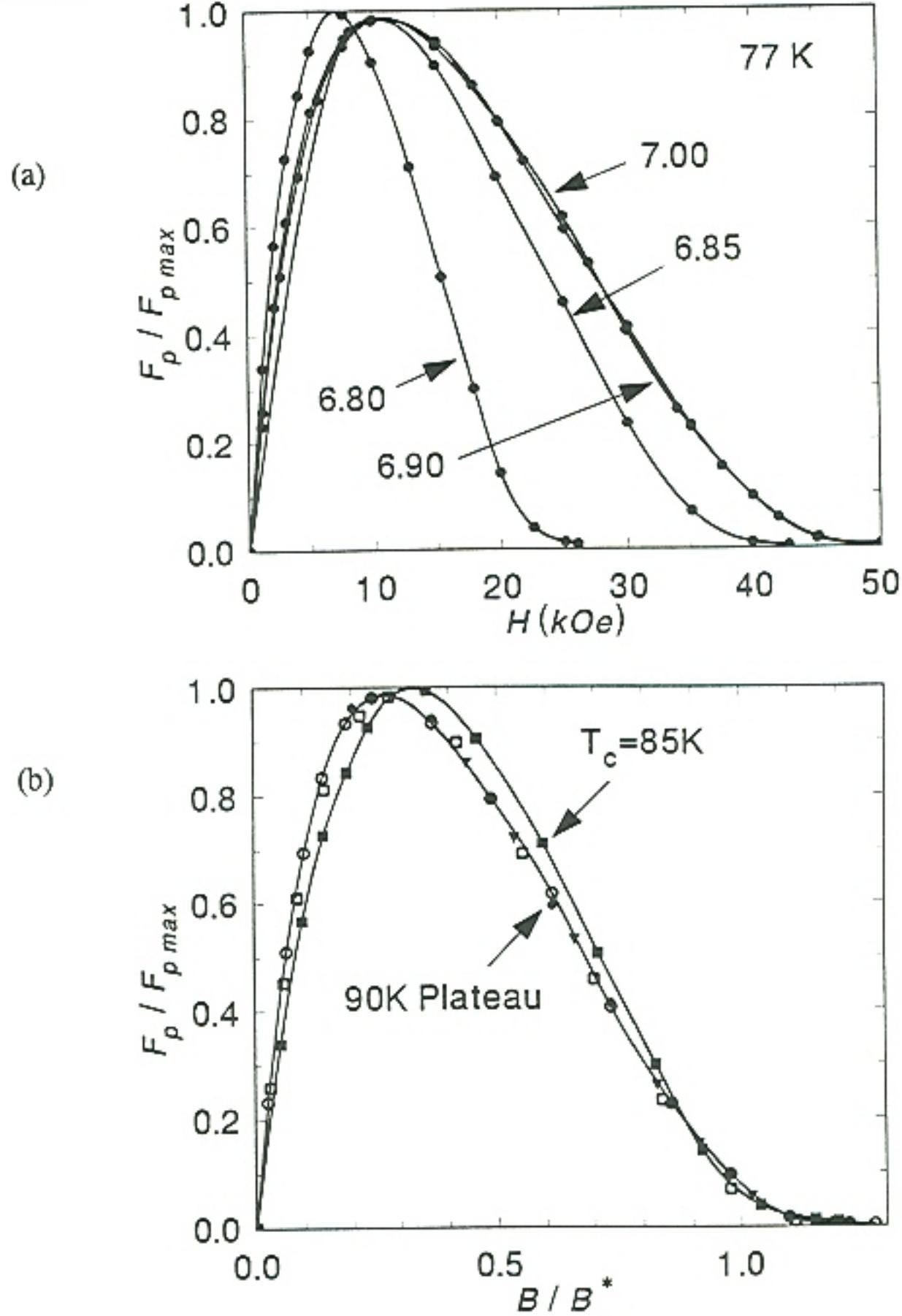
range ordered "Ortho-II" phase near $\delta = 0.5$. This peak also coincided with an increase in the critical current density J_c observed in this same film. Therefore, uncertainties still remain regarding the behavior of J_c and U_o in the region of the 60K plateau. Interestingly, the width of the $U_o(\delta)$ plateau varies depending upon the method used to determine U_o [Figure 26]. Hence, it is plausible that the resistive transition model above is oversimplified in assuming the presence of only two distinct phases. Thus, unlike the case of fully oxygenated $\text{YBa}_2\text{Cu}_3\text{O}_7$, these plots do not appear to be a reliable means of determining the subtle behavior of $U_o(T,B)$ in oxygen deficient $\text{YBa}_2\text{Cu}_3\text{O}_{7-\delta}$.

The most reliable method for determining the pinning energy is an analysis of the magnetic field dependencies of the critical current densities. This technique is unique in that knowledge of the bridge cross section is *not* required. Hettinger *et al.*⁸⁷ showed that the field dependence of $J_c/J_c(H=0)$ [see Figure 24(b)] could be described by the single parameter specifying the field at which the pinning force density extrapolates linearly to zero [Figure 27],

$$B^* = \frac{U_o B / kT}{\ln (E_o / 2E_c)} . \quad (80)$$

This analysis assumes that $U_o \propto 1/B$ as experimentally observed^{53,87} and that the denominator is roughly constant. The apparent degradation seen in $J_c(\delta, H//c)$ for $\delta \geq 0.15$, as well as in $J_c(\delta, H//ab)$ for $\delta \geq 0.20$, is clearly attributed to a decrease in U_o [Figure 26]. This probably leads to the progressive suppression of the $J_c(\delta, T)$ curves observed at higher temperatures [Figure 24(a)]. The normalized flux pinning

Figure 27



Normalized pinning force density F_p taken at 77K as a function of (a) B and (b) B/B^* as described in the text, both on and off the 90K plateau. The universal F_p curve observed on the 90K plateau suggests the field dependence of the pinning energy given by $U_0 \propto 1/B$ is fixed across the plateau. However, off the plateau, the relative B dependence may change, as in the polycrystalline films,³⁷ leading to the observed shift in $F_{p,max}$.

force density at various oxygen contents both on and off the 90K plateau are depicted in Figure 27. Off the 90K plateau, decreases in the relative strength of the B dependence in U_o , similar to that found in polycrystalline films,³⁷ e.g., $U_o \propto 1/B^{0.15}$, may occur as a result of the films developing a "granular" like $J_c(H)$ for large oxygen deficiencies.

5. Constraints Imposed on Electronic Models

If the phase separation scenario does not apply, the initial decreases of J_c ($\delta \leq 0.15$) could only be due to decreases in J_{co} since, the flux creep pinning energy U_o is constant in this regime. Recall that J_{co} is defined as the critical current density in the absence of flux creep and is often assumed to be proportional to the depairing critical current density. As a result, this assumption leads to the proportionality $J_{co} \propto H_c^2 \xi_{ab}$.⁸⁸ Moreover, others generally argue^{49,88,89,90} that U_o should scale as $H_c^2 \xi^3 / 8\pi$ in a point pinning model, where H_c is the thermodynamic critical field and ξ is the superconducting coherence length. In the highly anisotropic cuprates,⁹¹ one has $\xi^3 \approx \xi_{ab}^2 \xi_c$ so that the constraint imposed by a constant U_o becomes

$$H_c^2 \propto \frac{1}{\xi_{ab}^2 \xi_c} . \quad (81)$$

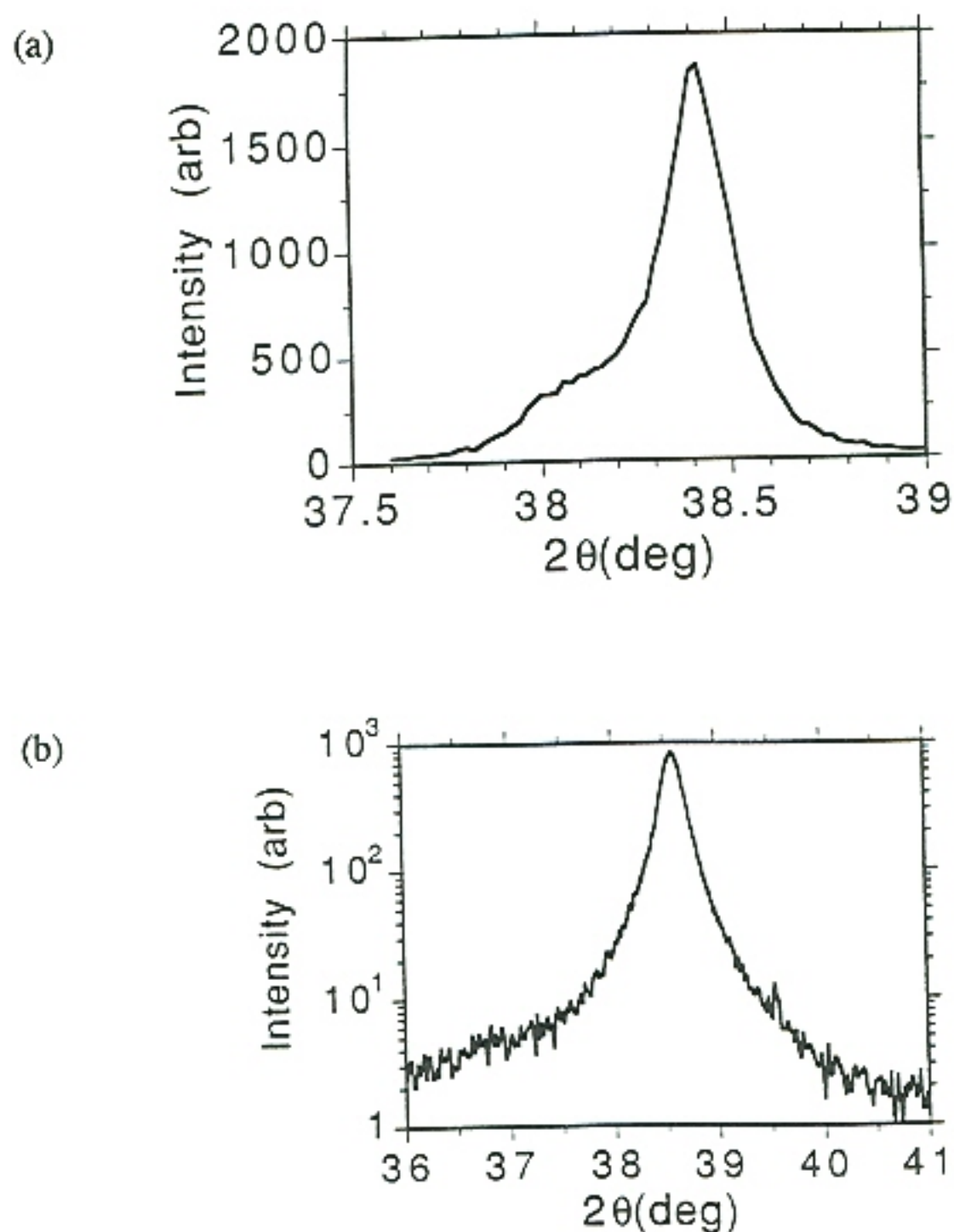
From magnetization studies, Ossandon *et al.*⁸³ concluded that the thermodynamic critical field H_c rapidly decreases with increasing oxygen deficiency. However, if the phase separation scenario applies, these apparent decreases in H_c could be due to a

decreasing volume fraction of the 90K phase with increasing δ . Equation (81) implies a significant increase in the coherence length ξ with increasing oxygen deficiency δ , which should be reflected as a decrease in the upper critical field, since $H_{c2} = \phi_0/2\pi\xi^2$. Unfortunately, conclusive systematics of H_{c2} vs. δ do not yet exist. The fluctuation analysis described in the next chapter indicates the existence of an H_{c2} plateau while a Hao-Clem⁹² analysis of magnetic measurements⁸³ show a steadily decreasing $H_{c2}(\delta)$. Thus, further information of the dependence of H_{c2} with δ would be very useful.

6. "Peaked" $T_c(\delta)$ Behavior

Until now, the "*peaked*" $T_c(\delta)$ behavior (i.e., a maximum in T_c at $\delta \neq 0$) has not been addressed, which is most apparent in epitaxial films initially grown under low oxygen partial pressures.^{80,93} This maximum in T_c is demonstrated midway on the 90K plateaus in T_c vs. δ depicted in Figure 23 and Figure 26. Feenstra⁹⁴ has shown that these T_c peaks occur with systematic values of oxygen deficiency δ depending on the initial growth conditions. This implies that the location of these peaks on the 90K plateau occur as a consequence of the level of cation "*doping*" introduced by the growth process. However, other mechanisms could be argued, including morphology differences or simply strains between the different phases, which are well established to have different c -lattice parameters. The latter argument appears possible since no significant splitting was observed in any of the x-ray diffraction peaks for the films studied [Figure 28(a) and Figure 28(b)]. However, keep in mind that one generally

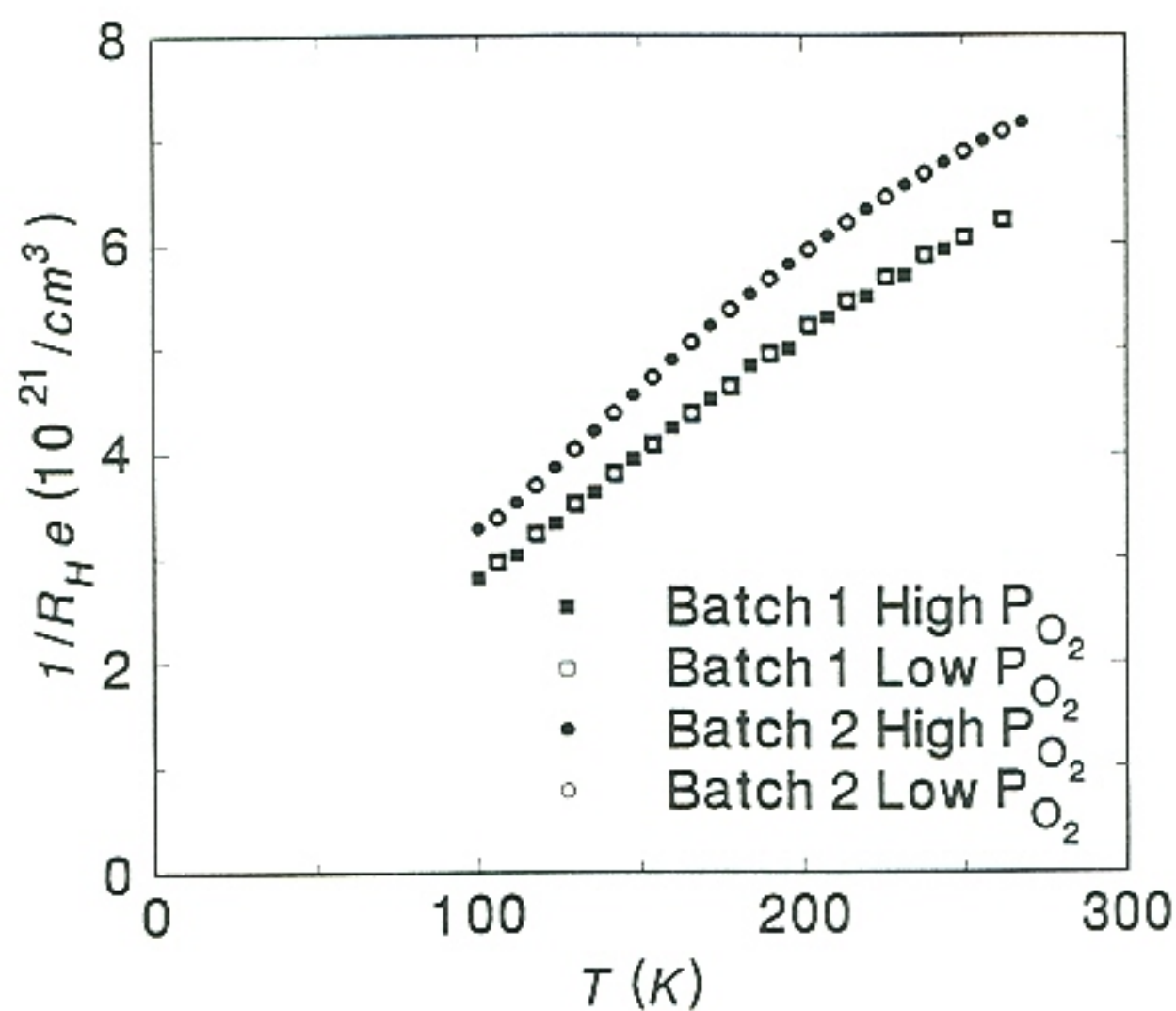
Figure 28



High resolution x-ray diffraction scans of the (005) peak for (a) the laser ablated thin film at $7-\delta \approx 7.00$ and (b) the coevaporated thin film at $7-\delta \approx 6.90$. The low angle tail occurring near full oxygenation in the laser ablated film supports the existence of oxygen deficient regions. However, such tails were not observed in the oxygen deficient coevaporated films, even though the $J_c(\delta)$ behavior with δ was identical. Adapted from J. D. Budai (unpublished).

speaks in terms of large "*doping*" levels for the high- T_c superconductors, i.e., involving tens of percent of the unit cells, which probably alter the phonon properties as well as the electronic properties. McMillan previously showed that the coupling constant is affected by the phonon frequency spectrum.⁵⁰ Thus, in the framework of an electron-phonon pairing mechanism,⁵⁰ a more intuitive argument for these $T_c(\delta)$ peaks could simply be stated as the "*optimization*" of the coupling constant $\lambda = VN(E_F)$. In the coupling constant, V represents the matrix element of the electron-phonon interaction, while $N(E_F)$ is the electronic density of states at the Fermi energy E_F . Since knowledge of the phonon properties and band structure are limited, no definite conclusions on the behavior of λ as a function of "*doping*" can be drawn at the present. However, Figure 29 illustrates the Hall coefficients for two sets of films, grown from identical precursor-batches, by the BaF_2 process,⁴¹ and post-annealed under different conditions. The data show that the apparent carrier densities do not depend upon the initial growth conditions. The differences between films of different precursors could stem either from slight compositional differences or simply from uncertainties in the film thickness. Overall, this result implies that the processing conditions have little or no effect on the electronic structure in the fully oxygenated state. Finally, recent evidence by others suggests that lattice instabilities, and not electronic mechanisms, are indeed responsible for the limiting transition temperature of $\sim 90K$ observed in $YBa_2Cu_3O_{7-\delta}$.⁹⁵

Figure 29



Inverse Hall coefficients taken on two sets of films with identical precursors but post-annealed under different conditions. The data suggest that growth conditions do not influence the overall carrier density. The slight differences between film batches may be attributed to small compositional differences in constituents or simply to errors in determining film thicknesses.

7. Brief Conclusion

In sum, the critical current densities J_c were observed to decrease linearly with δ , while extrapolating toward zero near the edge of the 90K $T_c(\delta)$ plateau. Over most of this regime, no changes were observed in the pinning energies U_0 and the upper critical fields H_{c2} (discussed in the next chapter). These findings support the "*extrinsic*" phase separation/percolation mechanism giving rise to these $T_c(\delta)$ plateaus. On the other hand, the strong correlation between the Hall coefficient R_H and the superconducting performance (i.e., T_c and J_c) is believed to be an "*intrinsic*" property which supports a charge transfer from the "*chains*" to the "*planes*." Finally, I believe that the width of the $T_c(\delta)$ plateaus reflect the domain sizes of these separated phases.

V. UPPER CRITICAL FIELD H_{c2} ANALYSIS

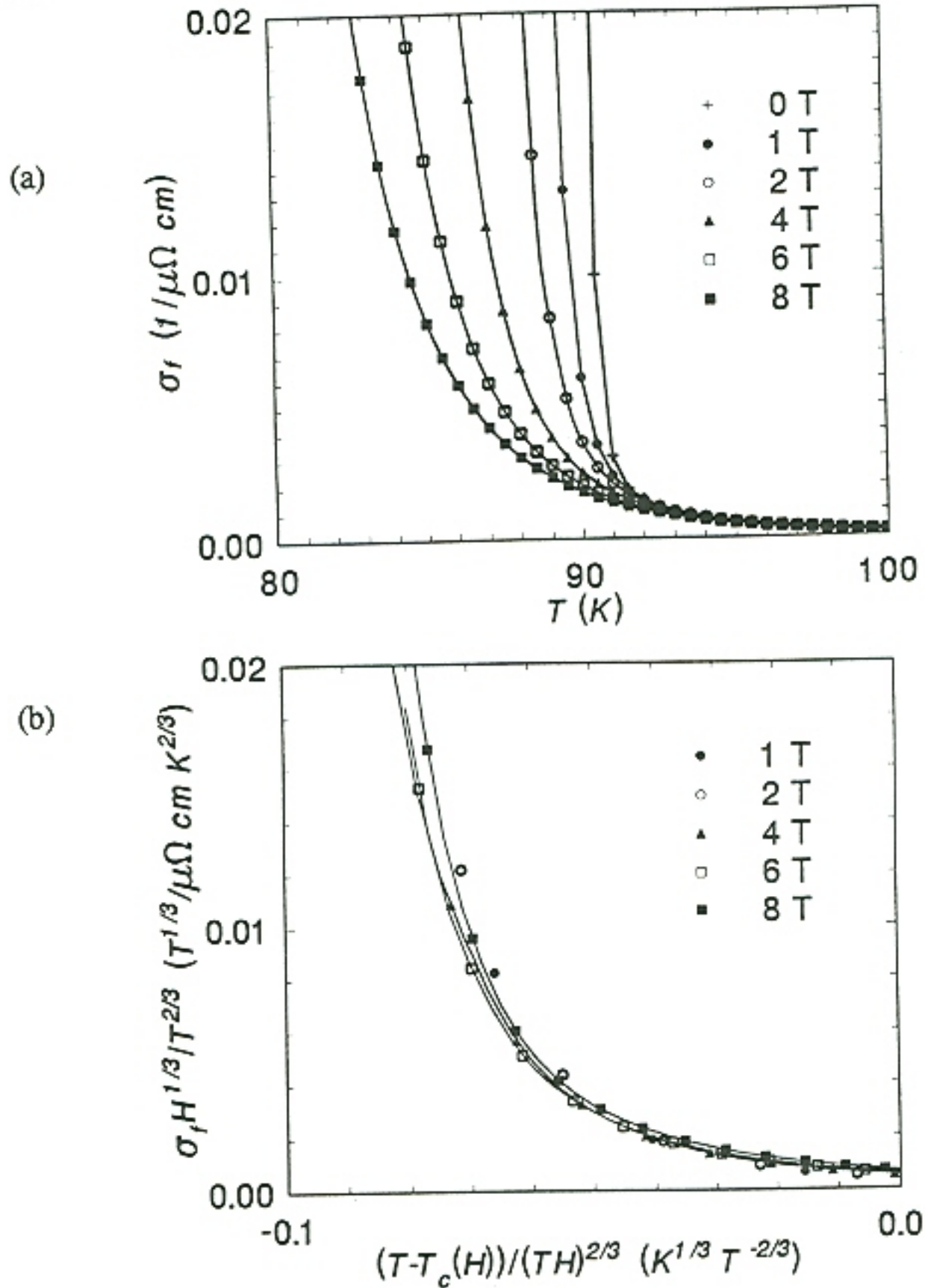
A. Experimental Results

In the previous chapter, it was argued that an " H_{c2} plateau" vs. oxygen deficiency δ supported a phase separation/percolation scenario occurring on the 90K $T_c(\delta)$ plateau. (The **upper critical field** H_{c2} is defined as the magnetic field required to destroy superconductivity). Thus, knowledge of this H_{c2} behavior with the oxygen deficiency δ was required. To determine this $H_{c2}(\delta)$ behavior, the Ullah-Dorsey fluctuation theory²¹ was applied to the experimental data on two epitaxial $\text{YBa}_2\text{Cu}_3\text{O}_{7-\delta}$ thin films grown by the BaF_2 process.⁴¹ The results (valid in the limit of large magnetic fields) support the existence of such a plateau in H_{c2} . More explicitly, an H_{c2} slope of -1.7 T/K near T_c was obtained for all oxygen stoichiometries in the range $6.8 \leq 7-\delta \leq 7.0$. In addition, this oxygen range corresponded to the complete range of the 90K plateau in both films. In Figure 30, the determination of the $H_{c2}(T)$ slope near T_c is depicted by a two step process based on Equation (69) [see Chapter III for details]. In order to obtain dH_{c2}/dT , the fluctuation conductivity $\sigma_f (= \sigma_{ii}^{3D,2D})$ must first be determined by extrapolating the normal state resistivity into the superconducting fluctuation regime followed by the application of

$$\sigma_f = \sigma_{total} - \frac{1}{\rho_o + mT} , \quad (82)$$

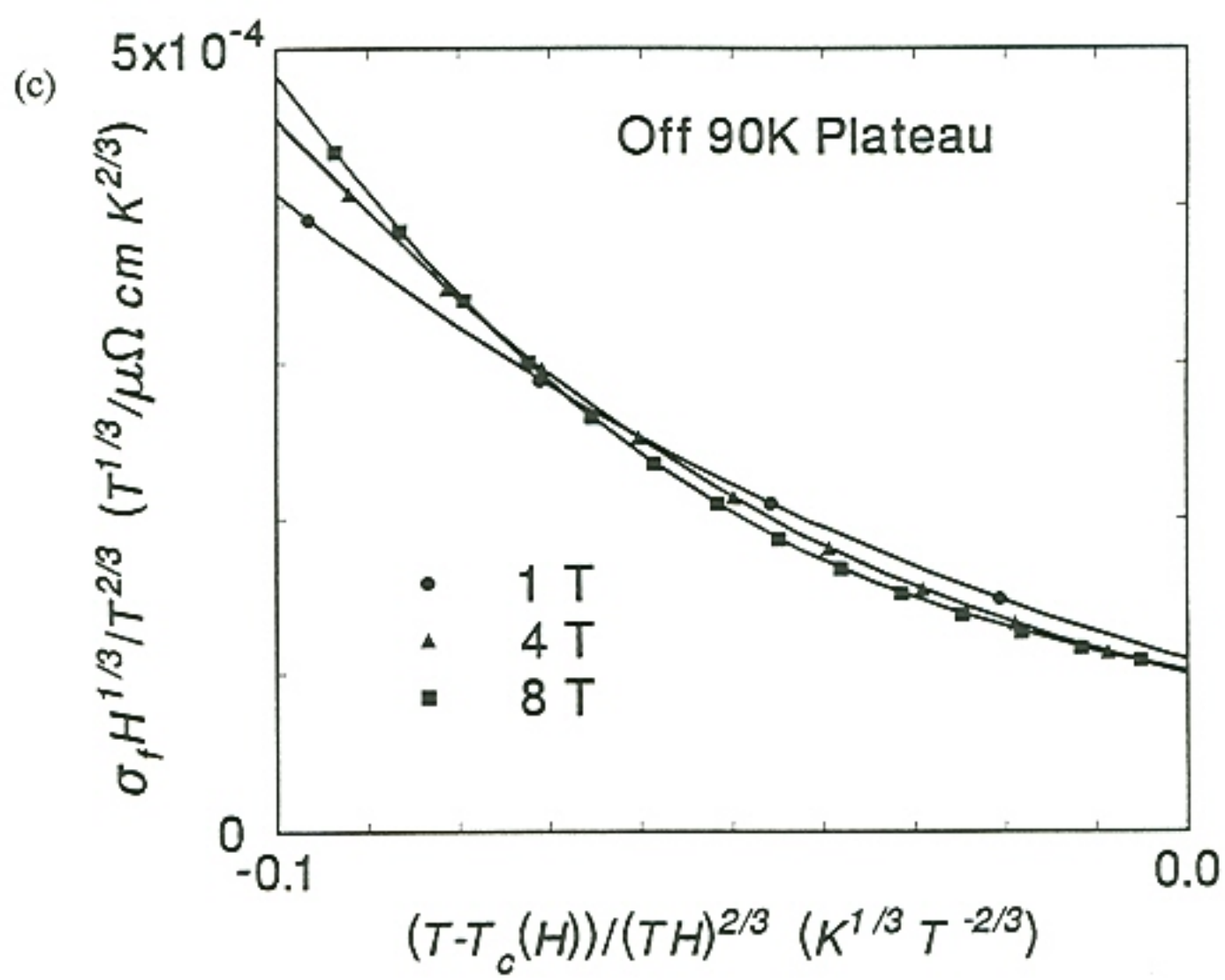
where σ_f is the fluctuation conductivity, σ_{total} is the observed conductivity, ρ_o and m are the constants describing the linear extrapolation of the normal state resistivity into

Figure 30



Step by step determination of $-dH_{c2}/dT$ by utilization of the 3D scaling of the fluctuation theory. (a) First, the fluctuation conductivity σ_f is determined as a function of temperature and applied field. These are plotted according to Equation (69) both on (b) and off (c) the 90K plateau. The only adjustable parameters are the mean field transition temperatures $T_c(H)$, which give T_c as a function of H_{c2} , and these are chosen in such a way as to generate the universal curve shown. The resistive transitions obtained off the 90K T_c vs. δ plateau are not adequately described by the fluctuation theory.

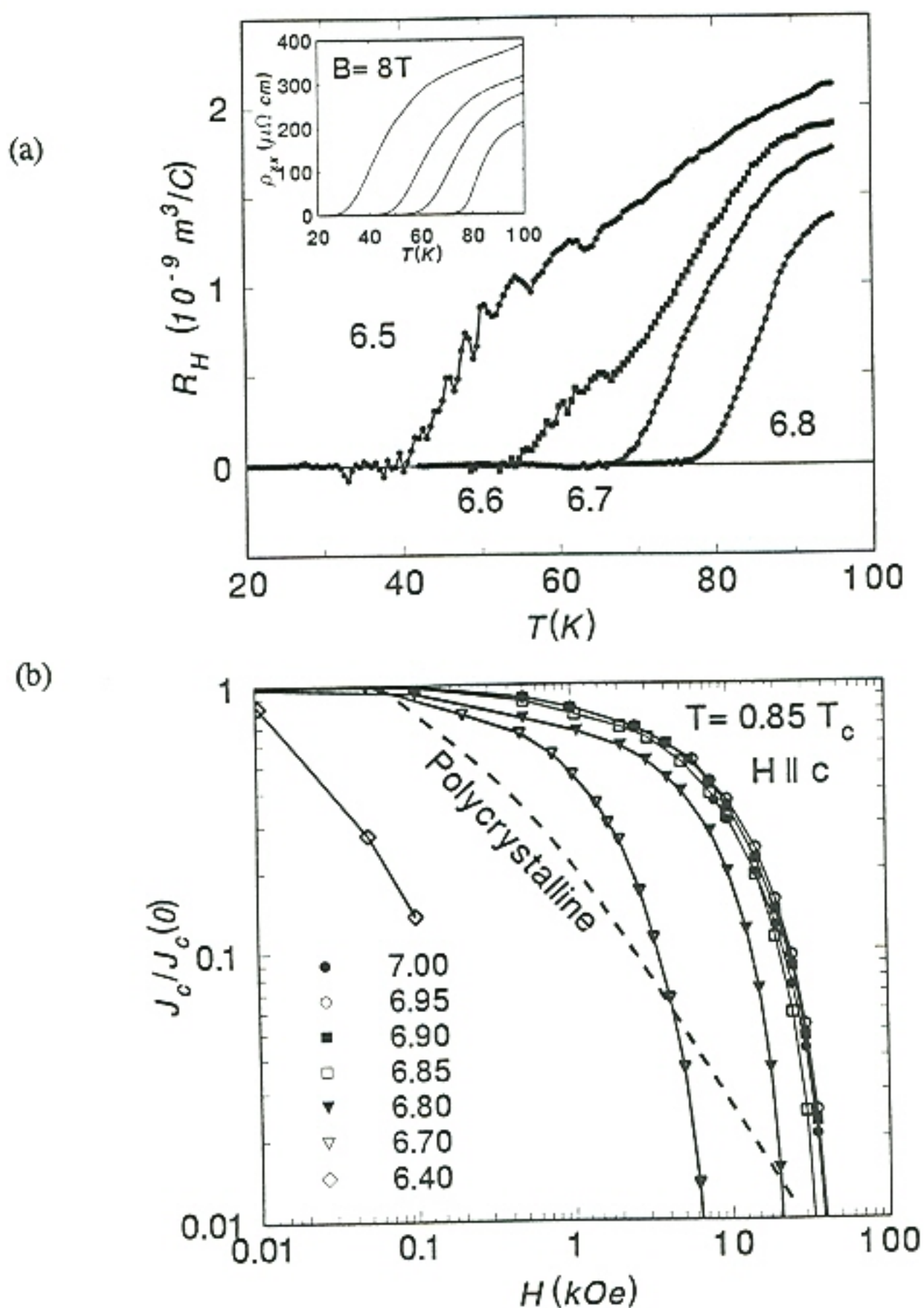
Figure 30 (continued)



the fluctuation regime. Due to the linearity of resistivity curves in temperature over a significant range of temperature in the normal state for both films, it was not necessary to obtain a quadratic fit. Second, these were in turn used in Figure 30(b) utilizing the 3D scaling behavior. The resulting H_{c2} curves were obtained by choosing $T_c(H)$ for each applied field in order to obtain a universal curve. For oxygen contents in the regime of the 90K plateau, the best convergence *always* occurred by application of the 3D scaling [Equation (69)] assuming a linear H_{c2} vs. T with a slope of -1.7 T/K near T_c . Interestingly, the temperature dependence of H_{c2} in both films extrapolated to zero at the mid point of the self-field resistive transitions. In contrast, the 2D scaling did not accurately describe the fluctuations; moreover, this scaling also suggested unacceptably low H_{c2} slopes, e.g., -1.2 T/K near T_c . Off the 90K plateau, however, neither the 3D nor the 2D fluctuation equations accurately described the fluctuation regime of the in-field resistive transitions. For instance, the best fit possible at an oxygen content of $7-\delta \approx 6.7$ was obtained by application of the 3D scaling and choosing an H_{c2} slope of about -2 T/K. These resulting curves [Figure 30(c)] clearly show differences in curvatures at each applied field. In addition, the convergence of these curves became worse as the oxygen content was further reduced.

For oxygen contents off the 90K plateau (typically $\delta \geq 0.2$), the resistive transitions taken in self-field for both samples were observed to be broadened. Figure 31 shows typical Hall transitions taken off the plateau as well as the field dependence of J_c taken with $H \parallel c$.³⁸ Both plots indicate granular-like behavior at reduced oxygen contents in the range $\delta \geq 0.3$. It is possible that this "*granularity*" is

Figure 31



Evidence of granular-like behavior at reduced oxygen contents in YBa₂Cu₃O_{7-δ}. (a) Systematic "peaks" always appear in the Hall effect transitions whenever $\delta \geq 0.3$. These "peaks" suggest a T_c distribution and never appear in the resistive transitions (see inset). (b) The field dependencies of the critical current density $J_c/J_c(H=0)$ behave more similarly to the polycrystalline materials (dashed curve) when $\delta \geq 0.3$.

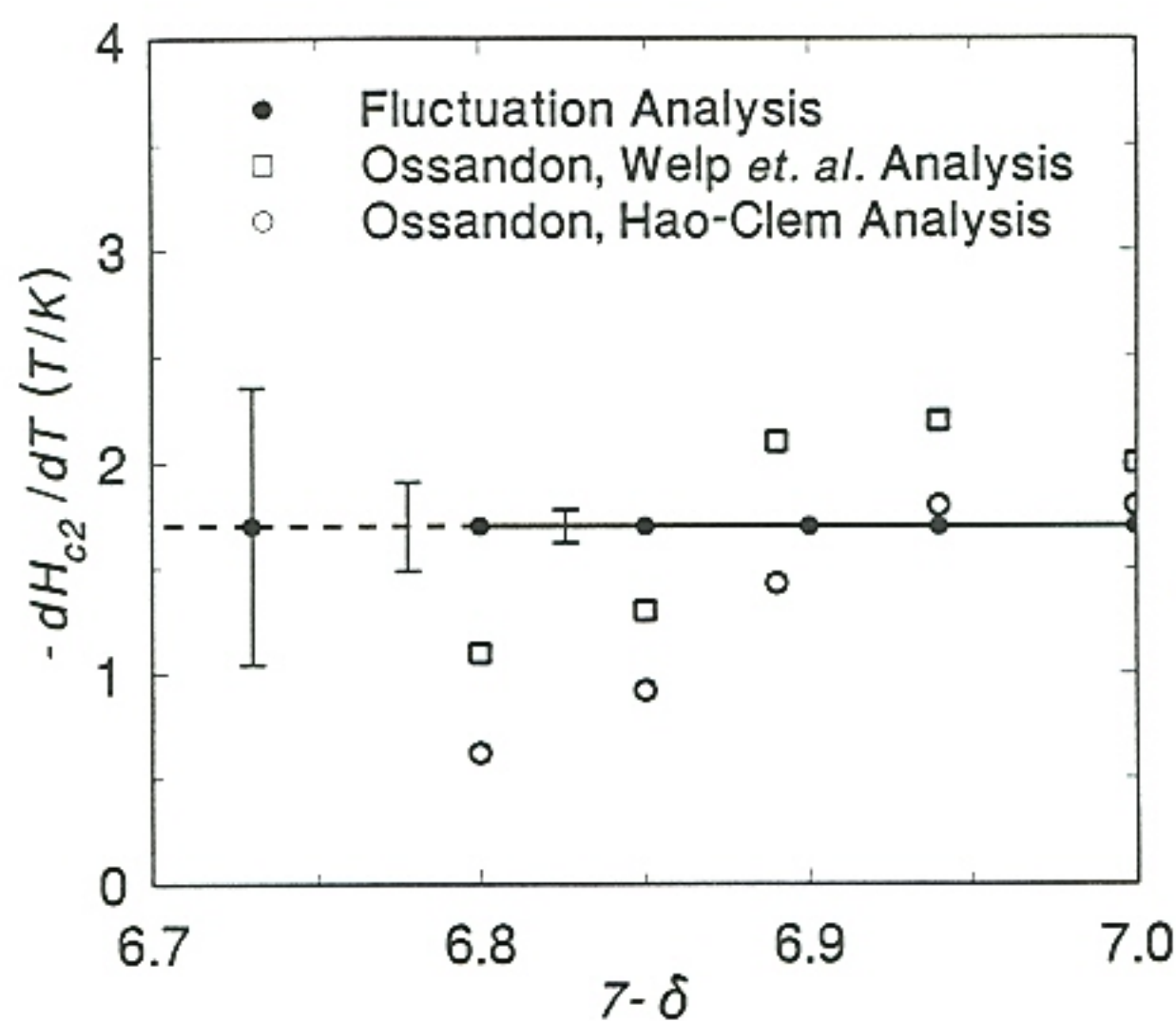
responsible for an extrinsic broadening of the resistive transitions taken off the 90K plateau. As a result, the fluctuation theory cannot be applied, since this broadening of the transitions is apparently the result of several mechanisms in addition to those of fluctuations.

The H_{c2} slopes determined by three different techniques are summarized in Figure 32. This figure compares the fluctuation results to the magnetization results of Ossandon *et al.*⁸³ In the magnetization measurements, application of the Welp *et al.*⁹⁶ analysis was found to give an initial H_{c2} plateau of about -2.1 T/K with increasing oxygen deficiency δ , whereas a recent Hao *et al.*⁹² analysis of the same data yielded a similar plateau, but with a smaller H_{c2} slope of -1.8 T/K. Interestingly, the Hao *et al.* analysis of the magnetization data agrees reasonably well with the fluctuation analysis with respect to the range of the 90K plateau. More explicitly, the magnetization studies yielded a 90K plateau that spanned over a smaller range of δ , e.g., $\sim 6.89 - 7.00$. This range suggests an H_{c2} plateau that occurs over most of the 90K plateau. Thus, an H_{c2} plateau probably occurs over part of the 90K plateau. Regardless of any conflicting results, a plateau in $H_{c2}(\delta)$ is expected over the entire 90K T_c vs. δ plateau and is discussed in the framework of BCS theory in Section C.

B. Phase Separation Effects

Evidence supportive of phase separation, i.e., chain site oxygen clustering, in oxygen deficient $YBa_2Cu_3O_{7-\delta}$ was presented in the previous chapter. In addition, others have also argued that this phenomenon occurs in these materials.^{16,17,18,20}

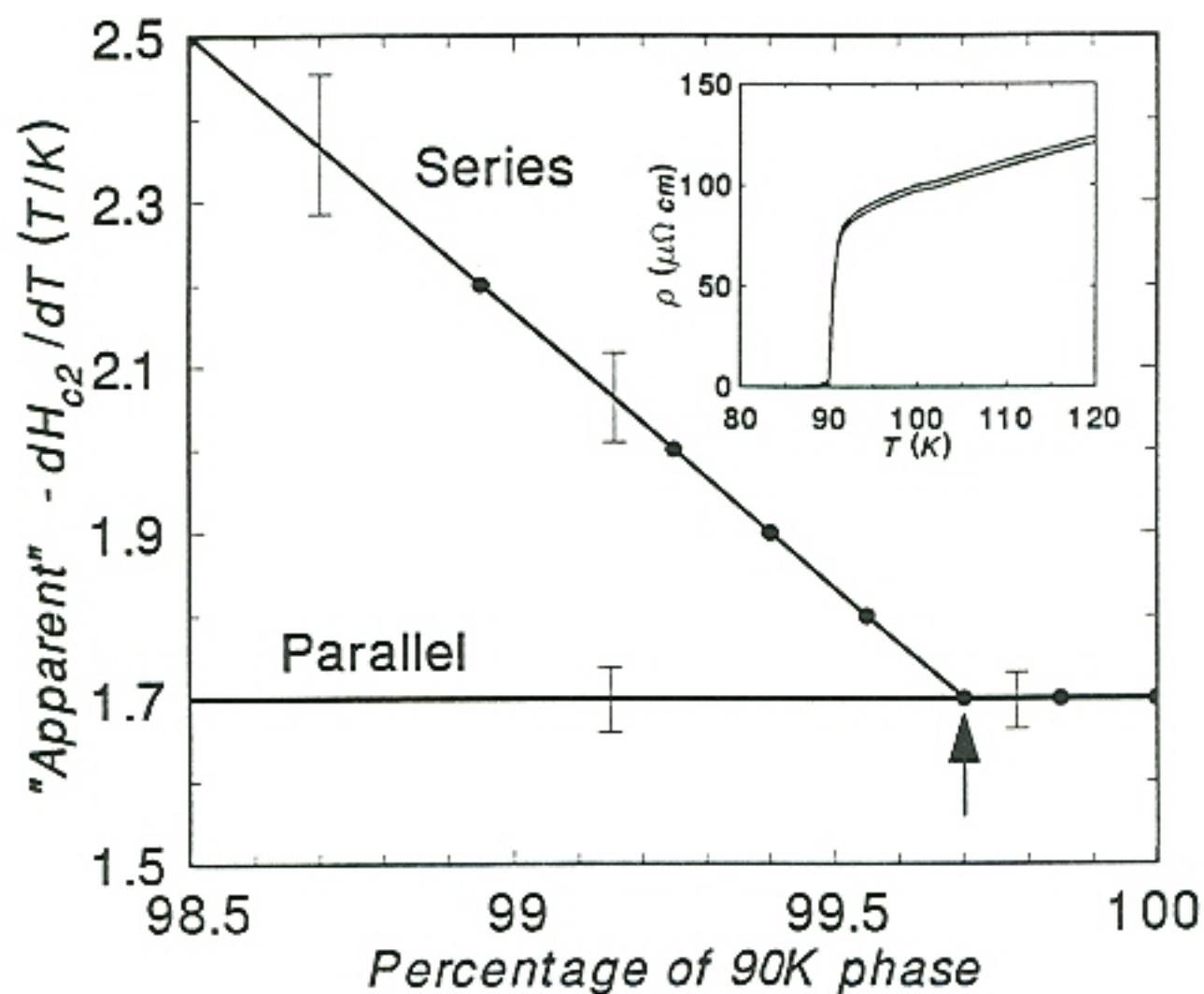
Figure 32



Summary of the $H_{c2}(T)$ slopes as a function of oxygen deficiency δ in $\text{YBa}_2\text{Cu}_3\text{O}_{7-\delta}$ determined by the in-field fluctuation analysis of epitaxial thin films (filled circles). These are compared to the magnetization results of bulk, aligned $\text{YBa}_2\text{Cu}_3\text{O}_{7-\delta}$ adapted from J. G. Ossandon *et al.*, Phys. Rev. B 45, 12534 (1992). (open symbols).

Furthermore, such occurrences of phase separation may be directly responsible for the 90K and 60K plateaus observed in T_c vs. δ via geometrical effects and the percolation of current as discussed earlier.³⁸ In the phase separation scenario, the actual current path dimensions are unknown except at full oxygenation; as a result, deviations probably occur between the observed H_{c2} slopes and the actual H_{c2} slopes due to cross sectional errors in the determination of the fluctuation conductivities. Testing this hypothesis, a rigorous analysis was conducted to determine the probable effects of phase separation on the "apparent" H_{c2} values as determined from the above fluctuation theory. In a simple model, it was assumed that oxygen deficient $YBa_2Cu_3O_{7-\delta}$ simply separated into regions of 90K and 85K "phases." Two sets of in-field resistive transitions were experimentally obtained—one at full oxygenation with $T_c = 90K$ and the other just off the 90K plateau with $T_c = 85K$. The former set had an apparent dH_{c2}/dT of -1.7 T/K near T_c , while the latter had an apparent dH_{c2}/dT of -2.0 T/K near T_c . Both parallel and series combinations of these two sets of resistive transitions were calculated as a function of temperature using $R = R_{90K} + R_{85K}$ for the series combinations and $1/R = 1/R_{90K} + 1/R_{85K}$ for the parallel combinations. The resulting resistive transitions were then analyzed in the framework of the fluctuation theory utilizing the 3D scaling. The resulting "apparent" $-dH_{c2}/dT$'s as a function of the volume percentage of the 90K phase [Figure 33] indicate that the fluctuation analysis is sensitive only to the presence of the 90K phase in a parallel conduction system. This important result indicates that errors in the bridge dimensions do not lead to errors in the H_{c2} values as determined from the fluctuation analysis. In contrast, series

Figure 33



Predicted effect of phase separation on the "apparent" H_{c2} slopes as derived from the fluctuation analysis. The model used to generate these results assumed that phase separation occurs between regions of $T_c = 90\text{K}$ and $T_c = 85\text{K}$. Parallel conduction phases should have little or no effect on the "apparent" H_{c2} , whereas series phases should lead to significant increases in the "apparent" H_{c2} values above a certain threshold amount of the minority phase (arrow). The inset indicates the appearance of the self-field resistive transitions for the left and right extremes of the main graph for series phases.

combinations of phases generate false increases in $-dH_{c2}/dT$. For instance, a mere 0.3% of the 85K phase in series with the 90K phase should lead to some error in the determined H_{c2} even though such series combinations would have little effect on the overall resistivity [see Figure 33 inset]. Moreover, in this analysis, if the 85K phase exceeds $\sim 2\%$ of the total volume fraction, the resistive transitions are found to be poorly described by the fluctuation theory, and such results are similar to the experimental results taken off the 90K plateau [Figure 30(c)]. In light of these results, the H_{c2} slopes of -1.7 T/K taken across the 90K plateau are believed to be unaffected by any phase separation effects, while the failure of the fluctuation theory off the 90K plateau is believed to reflect the presence of gross oxygen inhomogeneities.

C. Implications for BCS Theory

Unfortunately, universal results for H_{c2} ($H \parallel c$) as a function of oxygen deficiency δ in $YBa_2Cu_3O_{7-\delta}$ cannot be deduced from the various experimental determinations of H_{c2} summarized in Figure 32. However, a plateau in H_{c2} vs. δ probably exists over part of the 90K plateau in T_c vs. δ . Nevertheless, the importance of an H_{c2} plateau as a function of δ will be stressed here in the framework of simple BCS relationships. More explicitly, if H_{c2} changes with δ while on the 90K plateau, either changes must occur in the Fermi velocity or another pairing mechanism other than electron-phonon mediation would be responsible for superconductivity, assuming T_c is indeed limited by an electronic mechanism. Recall from the clean limit of BCS theory (Note: the latter equation is in the range of strong coupling and was adapted

from recent measurements of the energy gap⁹⁷⁾

$$H_{c2}(0) = \frac{\Phi_0 \pi \Delta^2(0)}{2 \hbar^2 v_F^2}, \text{ where} \quad (83)$$

$$\Delta(0) = \frac{(6-8)}{2} k T_c. \quad (84)$$

In the above equations, Φ_0 is the flux quantum 2.07×10^{-7} gauss-cm², $\Delta(0)$ is the superconducting energy gap at the Fermi surface at absolute zero, v_F is the Fermi velocity of the superconducting charge carriers, and T_c is the superconducting transition temperature. Combining Equations (83) and (84) leads to the simple proportionality

$$H_{c2}(0) \propto \frac{T_c^2}{v_F^2}. \quad (85)$$

Superconductivity is generally believed to be associated with the CuO₂ planes, and Yu⁹ has shown that the plane related pieces of the Fermi surface are virtually identical between the YBa₂Cu₃O₇ and YBa₂Cu₃O_{6.5} structures, suggesting that the Fermi velocity is relatively insensitive to changes in the oxygen deficiency δ . Finally, Equation (85) leads one to expect a plateau in the upper critical field H_{c2} as a direct consequence of the 90K T_c vs. δ plateau.

Finally, Allen *et al.* gives $\langle v_{x,y}^2 \rangle^{1/2} = 2.3 \times 10^7$ cm/s based on band structure calculations,⁵⁵ that implies $H_{c2} \approx 35$ kOe, which is over one order of magnitude below the accepted value of H_{c2} .⁹⁸ This discrepancy may be resolved by either an uncertainty in the prefactor of Equation (84) or by a non-BCS type pairing mechanism

that determines T_c . Moreover, recent evidence suggests that the maximum transition temperature of 92K in $\text{YBa}_2\text{Cu}_3\text{O}_{7-\delta}$ is limited by a phase instability,⁹⁵ which could explain this H_{c2} discrepancy in addition to the enhanced values for the prefactors in Equation (84) observed by others.⁹⁹ In sum, the "*apparent*" H_{c2} plateau in δ does not rule out a BCS type pairing mechanism in the $\text{YBa}_2\text{Cu}_3\text{O}_{7-\delta}$ system.

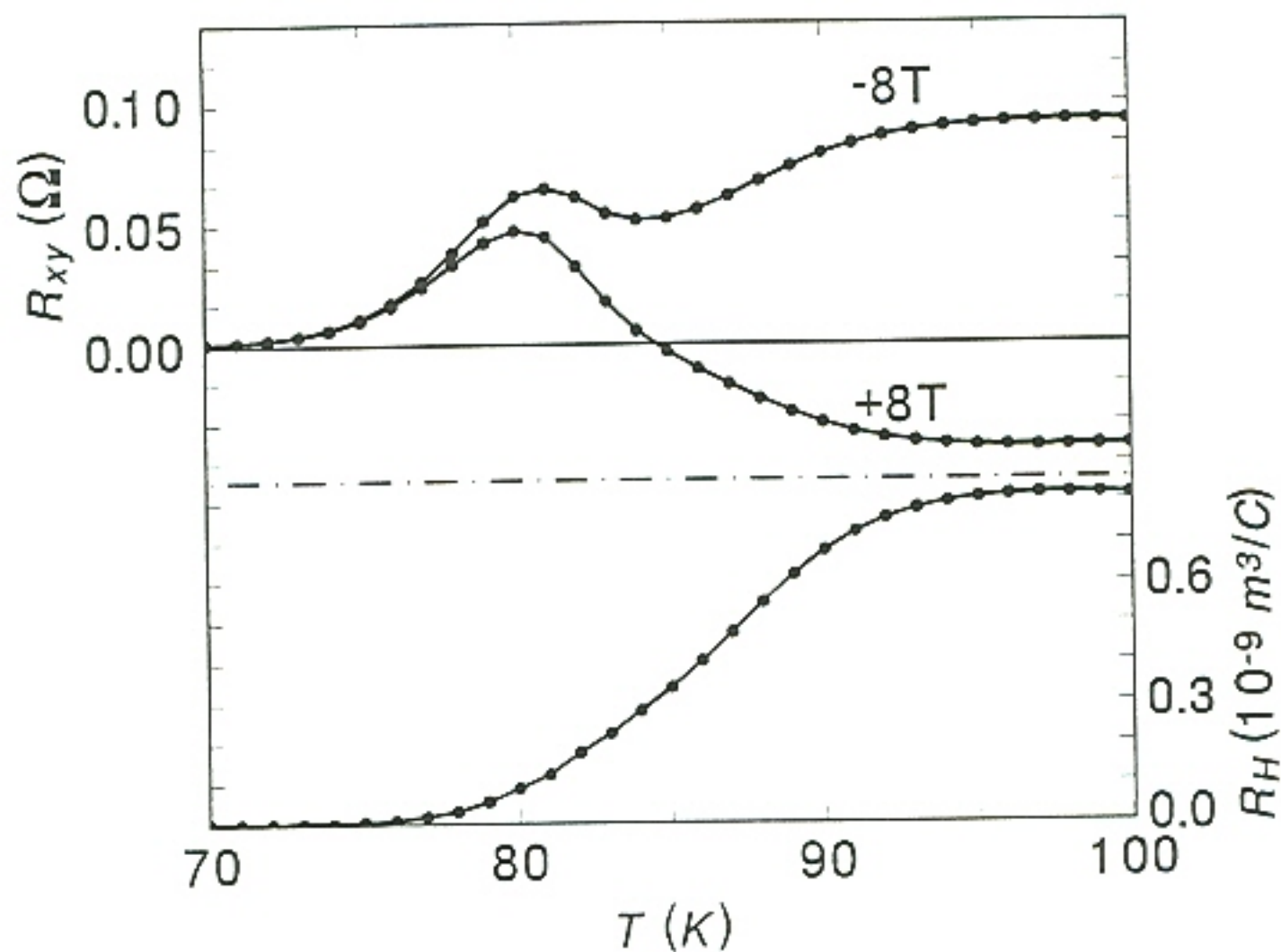
VI. HALL EFFECT TRANSITIONS

A. Evidence for Percolation in the Transitions

Further evidence for percolation in $\text{YBa}_2\text{Cu}_3\text{O}_{7-\delta}$ occurs in the superconducting Hall effect transitions. Indirect evidence for shifting current paths (i.e., percolation) with changing temperature is presented in Figure 34. This plot represents a typical derivation of the Hall coefficient for fully oxygenated $\text{YBa}_2\text{Cu}_3\text{O}_7$. In *all* of the thin films studied, the Hall "*offset*" (the average of the two opposing Hall "*signals*") never behaved as a simple scaled down resistivity versus temperature curve. Moreover, random peculiarities [see Figure 34] in these "*offsets*" existed in the superconducting transitions of each sample. If the current simply flowed longitudinally along the bridge without any percolation, these "*offsets*" should simply reflect the physical misalignment of the Hall probes. In contrast, no such behavior was ever observed, even at full oxygenation, indicating that the current paths probably change with temperature. Finally, such physical shifts with temperature can easily account for the unusual "*offsets*" of the Hall "*signals*."

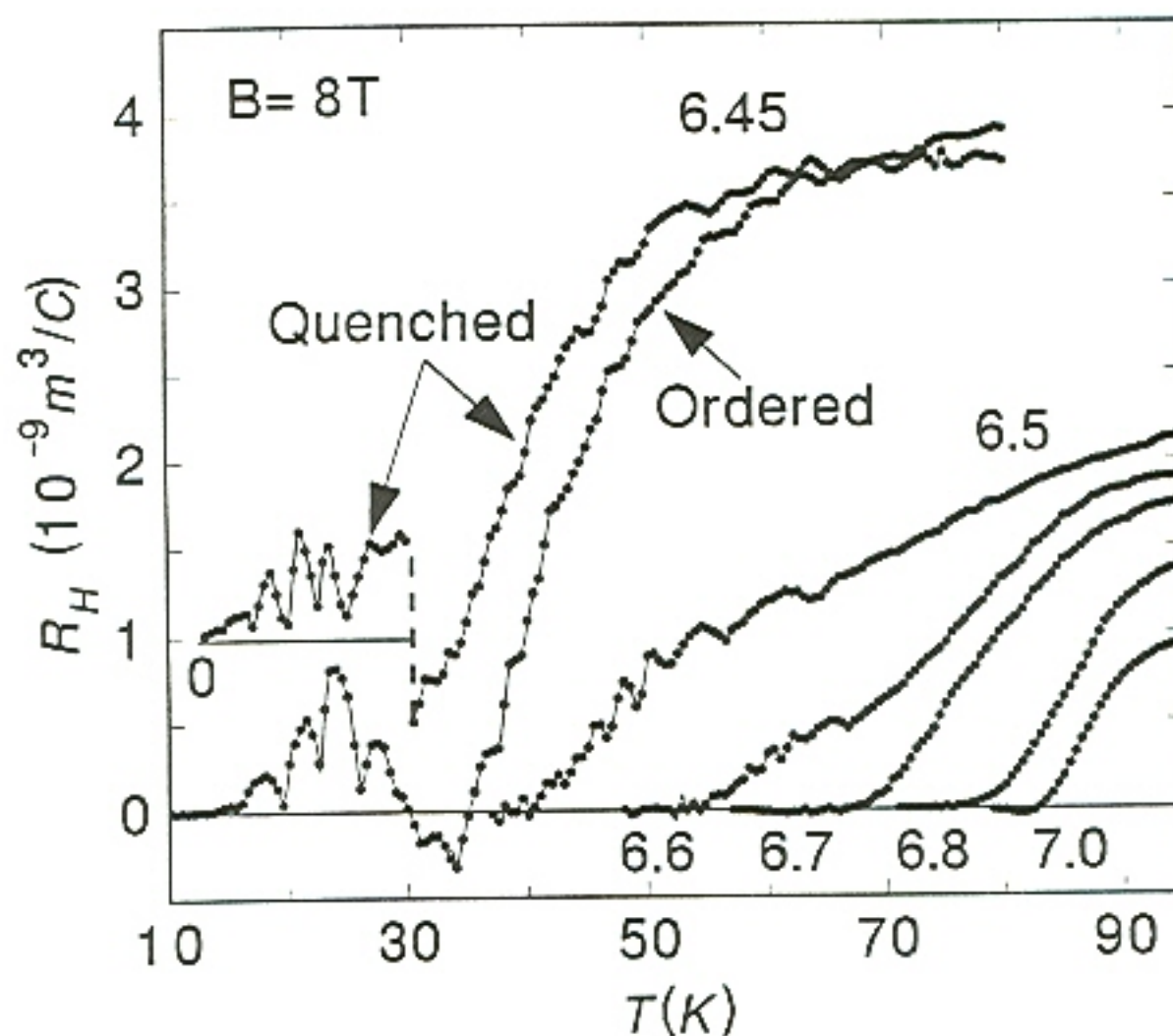
In addition, systematic changes were observed in the superconducting Hall effect transitions as the oxygen deficiency δ was sequentially increased. Figure 35 shows a monotonically increasing Hall coefficient R_H with δ , where δ is estimated from the c -lattice parameter. Details of the normal state Hall coefficient as well as the procedure used to estimate δ were presented in previous chapters. Equally important were the observations of reproducible, systematic "*noise*" [see Figure 35] that formed

Figure 34



Example derivation of the Hall coefficient R_H by application of Equation (1) to the two opposing Hall "signals" R_{xy} . This data set was obtained on a fully oxygenated, highly crystalline, coevaporated thin film of $\text{YBa}_2\text{Cu}_3\text{O}_7$.⁴¹ Notice the complete disappearance of the "peculiar" hump from the resulting Hall coefficient. The Hall "offset" (average of the opposing Hall "signals") was never observed to behave as a simple scaled down resistivity versus temperature curve. This suggests that the current paths do not travel exactly parallel to the patterned bridge. Moreover, these implied current paths probably vary with temperature.

Figure 35



Superconducting Hall effect transitions measured with $B = 8 \text{ T}$ for a single laser ablated film of $\text{YBa}_2\text{Cu}_3\text{O}_{7-\delta}$ at various estimated oxygen contents $7-\delta$. The reproducible, systematic "noise" observed below $7-\delta \approx 6.6$ was later found to occur in *all* thin films. These are currently believed to occur as a result of oxygen clustering. Reproducibility is well established by the similarities that occurred before and after oxygen vacancy ordering of the "Ortho-II" phase in $\text{YBa}_2\text{Cu}_3\text{O}_{6.45}$. Below 30 K, the "quenched" curve has been vertically displaced to avoid excessive overlap of data with the "ordered" curve. Note the small sign reversal of R_H that occurred at full oxygenation. Error bars are estimated to be on the order of the size of the symbols.

in *all* of the thin films studied as the oxygen deficiency exceeded roughly $\delta \geq 0.4$, whereas these were never observed in the resistive transitions. This systematic "*noise*" is currently believed to result from a clustering of the chain-site oxygen atoms¹⁶ which, in turn, causes unusually strong "*gyrations*" to occur in the current paths as the temperature is swept.

It is believed that oxygen vacancy ordering can occur at room temperature in the "*Ortho-II*" phase, i.e., $\text{YBa}_2\text{Cu}_3\text{O}_{\sim 6.5}$.¹⁰⁰ This effect was observed in the laser ablated film depicted in Figure 35 near a fixed, estimated oxygen content of $7-\delta \approx 6.45$. The overall similarities between the systematic Hall "*noise*" taken before and after four days of room temperature annealing support the notion that these features are generated by the samples and not by the measurement process. In preparation for this experiment, this sample was quenched from 200°C, rapidly mounted, then cooled to below 250K in less than 30 minutes. The resulting data are plotted in the curve labeled "*quenched*" in Figure 35. The systematic "*noise*" was originally believed to somehow result from the subtraction process of the two Hall "*signals*" taken in opposing fields described in Chapter II. However, upon aging the sample at 297K for four days, the sequence was repeated to determine if any changes had taken place. Interestingly, the "*ordered*" curve in Figure 35 shows that the same characteristic "*noise*" reappeared but at a slightly higher temperature, probably due to the 10K increase in T_c . This leads to the conclusion that these features are most probably due to inhomogeneities in the materials and not to the subtraction procedure, e.g., Equation (1), used to calculate the Hall coefficient R_H . Most importantly, it is

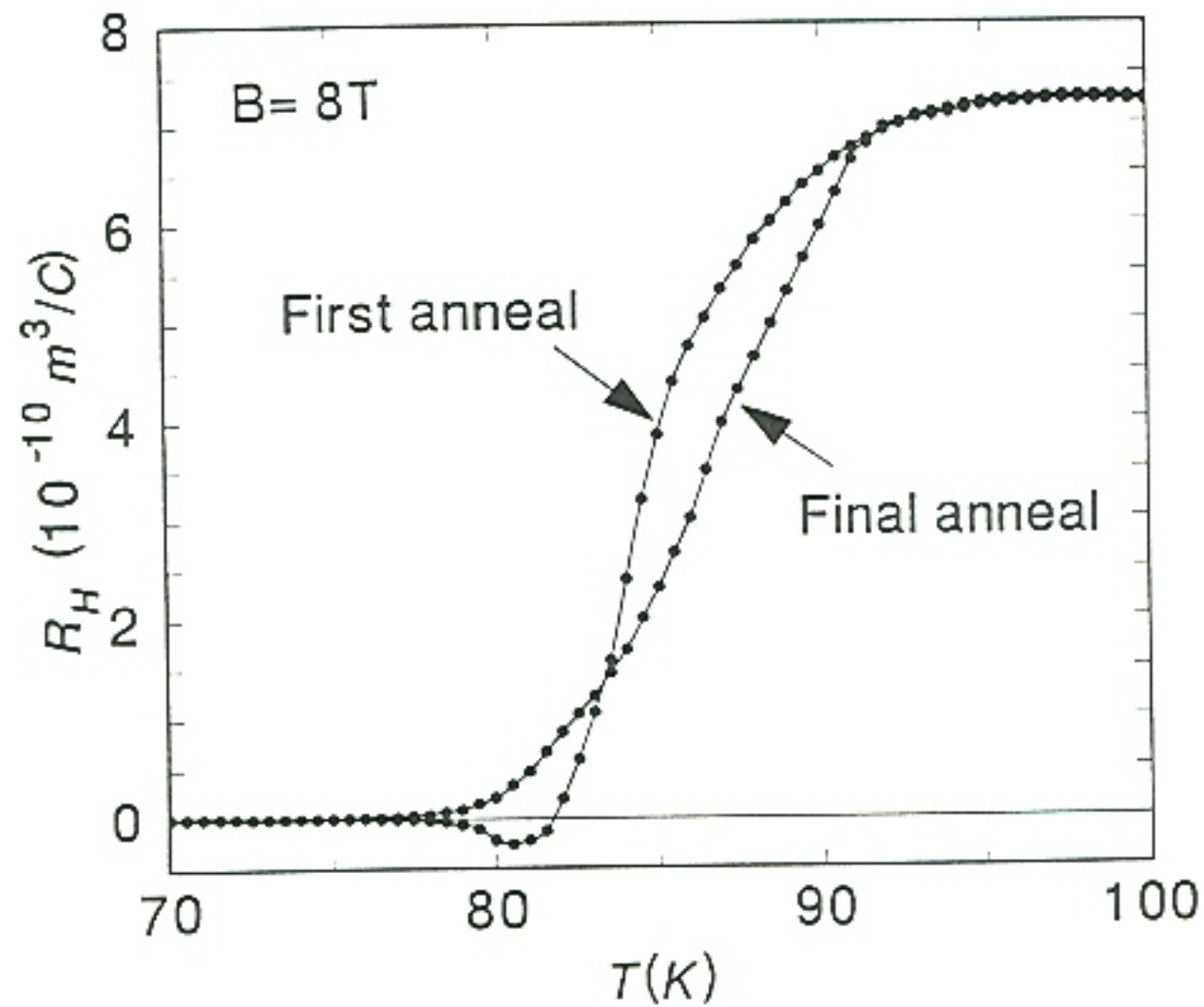
suspected that the sign reversal of R_H near 32K in the "*ordered*" curve results from current percolation due to an inhomogeneous distribution of resistivities. Finally, careful inspection of Figure 35 reveals that a sign reversal in the Hall coefficient occurred not only at $7-\delta \approx 6.45$, but at full oxygenation ($\delta \approx 0$), which suggests that both reversals have the same origin.

Final anneals at 550°C under 1 atm O_2 are usually conducted to determine whether or not any changes have occurred in the transport properties other than those due to variations in the oxygen content after a long series of sequential anneals. This procedure was performed on the laser ablated film for which a sign reversal occurred in R_H at full oxygenation ($\delta \approx 0$). Afterwards, all of the starting properties, i.e., resistivity ρ , critical current density J_c , and transition temperature T_c , were completely restored to their initial full oxygenation values with the exception of the sign reversal of R_H near T_c . Figure 36 shows that the superconducting Hall effect transition changed dramatically suggesting that these Hall transitions are highly sensitive to inhomogeneities in the oxygen content. Moreover, such dramatic effects prompted the series of computer simulations which are discussed in the next section.

B. Current Percolation Model

Contrary to the resistivity and critical current measurements which utilize large portions of the sample, the Hall effect demands smaller probes in order to minimize the "*flaring*" of the charge carriers into the Hall electrode region. Ideally, the Hall probes should be vanishingly small. These necessary small electrode dimensions (20 μm) lead

Figure 36



Changes in the superconducting Hall effect transition due to the series of sequential anneals for the laser ablated film shown in Figure 35, both of which were obtained at full oxygenation and with $B = 8 \text{ T}$. The curve labelled "*final anneal*" reveals the changes that resulted from these oxygen anneals, although T_c , J_c , and normal state resistivity returned to their original values. Notice the complete disappearance of the sign reversal of R_H near T_c .

to limited statistics which are probably responsible for at least some of the observations of the sign reversals of R_H . Therefore, a series of computer simulations of the superconducting Hall effect transitions was conducted utilizing Monte Carlo techniques to determine the percolative path of the current for various inhomogeneous mediums, while performing integrations to determine R_H . A total of 60 different spatial distributions with various Gaussian T_c widths ($\Delta T_c \leq 6K$) were tested. Interestingly, one-sixth of the total distributions were found to lead to an apparent sign reversal of R_H . The Hall coefficients resulting from the simulations were defined by¹⁰¹

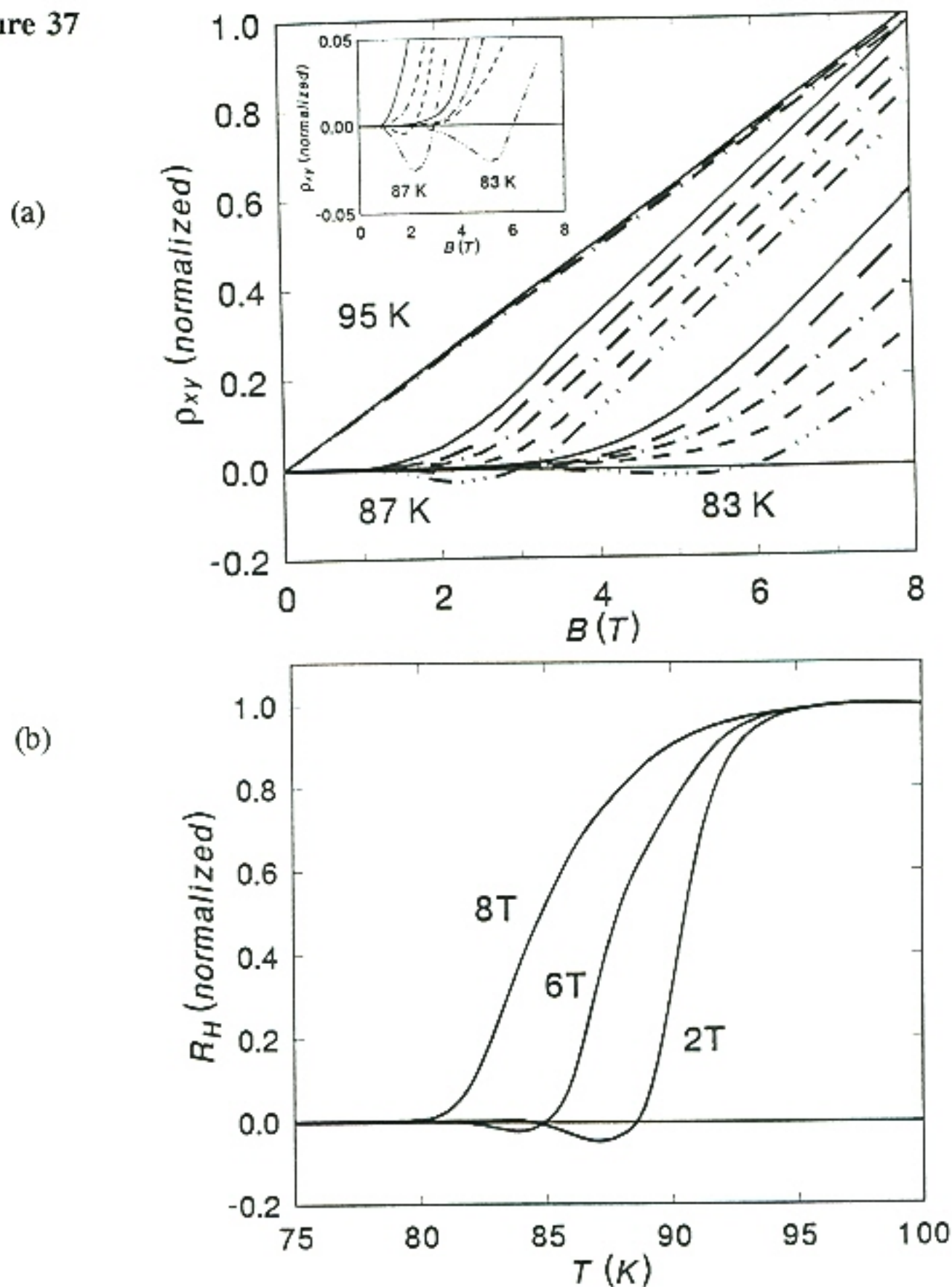
$$dR_H \propto \frac{\rho(T,H)}{T^2} \cos\theta \, dl \quad . \quad (86)$$

In this equation, the resistivity term $\rho(T,H)$ represents a typical set of resistive transitions [see Figure 43 in Appendix E]. In the actual computer simulations, the transitions were shifted up or down in temperature to represent the "local" T_c of the distribution being tested. The T^2 term was artificially inserted to give the observed $R_H \propto 1/T$ dependence observed in the normal state. Finally, the $\cos \theta$ term represents the direction of the local current increment with respect to the overall applied potential. However, this does not exactly fit the experimentally observed scaling, i.e., $|\rho_{xy}| \propto \rho_{xx}^{1.7}$, between the superconducting Hall effect transitions and resistive transitions.¹⁰² The interest here is to determine the overall impact of current percolation on the superconducting Hall effect transitions, especially R_H as a function of applied field. Monte Carlo methods, described in Appendix E, were utilized to determine the percolation paths of least resistance while integrating Equation (86). If

given a sufficiently large integration region, these effects become rather small. However, this is experimentally unfeasible since the electric currents would flare into the Hall probes, causing excessive offset signals and obscuring the real Hall signals.

The overall effect of current percolation on the Hall resistivities ρ_{xy} is evident in Figure 37(a). This family of curves summarizes the results obtained for the 60 different T_c distributions. Each random T_c distribution coupled to a limited integration region always led to an overall progressive reduction of ρ_{xy} . These relative reductions rely mainly on the spatial layout of the T_c contours in addition to the Gaussian T_c widths. In one-sixth of all the distributions tested, these parallel-like reductions were large enough to cause a sign reversal of ρ_{xy} , with one such distribution leading to the calculated Hall coefficient R_H as a function of temperature shown in Figure 37(b). Moreover, sign reversals occurred in some instances when the Gaussian T_c width was as little as 2K. Notice that these sign reversals usually occur at the lowest applied fields, disappearing as the fields are increased. These curves are remarkably similar to those published elsewhere by various authors.^{24,25} Another important feature is the relative insensitivity of ρ_{xy} to inhomogeneities while in the normal state. These features are simply explained by the argument that a T_c distribution in small applied fields leads to a larger distribution of resistivities than that produced by larger fields. As the fields are increased, the resistive transitions are broadened, causing an overlap in the transitions of the various regions which leads to a reduction in the total level of the current "gyration." The sign reversals result whenever the current momentarily reverses direction in order to seek out a path of lower resistance. If these reversals

Figure 37



Hall effect transitions predicted by the Monte Carlo simulations. (a) Hall resistivities as a function of applied field resulting from differing degrees of inhomogeneity. Increasing levels of current "gyration" lead to the parallel-like downward shifts in these curves. In about one-sixth of the total T_c distributions tested, these downward shifts were large enough to cause a sign reversal in R_H near T_c . Note that percolation has little effect on the normal state Hall coefficient. (b) The Hall coefficient plotted as a function of temperature at three different applied fields determined for a preselected T_c distribution that gives a sign reversal of R_H near T_c .

occur in resistive regions ($T > T_c$) while in proximity of the Hall probe, and if most of the other increments occur below T_c in this probe region, a sign reversal is likely. Thus, these reversals merely result from the limited statistics of the measurement due to the small probes. Finally, limited statistics are probably the cause for the sign reversal observed at full oxygenation in the laser ablated film depicted in Figure 36.

Nonuniform suppressions in the flux creep pinning energy¹⁰³ due to nonuniform current densities were neglected in these Monte Carlo simulations. These effects are rather important near T_c since, significant current densities are required to measure the weak Hall signals. Moreover, these effects tend to maintain some spatial separation of the current paths occurring within the superconducting regions near T_c , whereas these effects do not apply to the current paths occurring in the normal regions. As a result, current paths will not converge near any superconducting "*necks*." Such a case is illustrated in Figure 38 where these appear to be plausible current paths when the temperature is near 89K. Unfortunately, these current density dependencies on the flux creep dissipations are difficult to incorporate into the actual simulations. On the other hand, neglecting these dependencies do not alter the family of curves depicted in Figure 37(a), but rather, such neglects simply lead to underestimates in the total level of current "*gyration*" for a particular T_c distribution. Therefore, these simulations probably give too low of a reduction in ρ_{xy} for any given T_c distribution; as a result, the actual fraction of sign reversals of R_H is underestimated. Finally, it would be useful to study the "*statistics*" of Hall coefficient sign reversals in previous studies by others. If this picture is valid, it suggests that this effect is seen only part of the time.

VII. GRANULAR ORIENTED THIN FILMS

Oriented, deposited conductors hold potential for the fabrication of high- T_c superconducting tapes, thereby prompting the desire to understand the physical properties of such systems. This chapter investigates the mechanism limiting the transport critical current density J_c for two types of granular $\text{YBa}_2\text{Cu}_3\text{O}_{7-\delta}$ thin films: (1) c -oriented, but granular films grown on polycrystalline yttria-stabilized zirconia (YSZ) by pulsed laser ablation^{104,105} and (2) triaxial epitaxial films [composed of small grains having either the (110) or (103) orientation] grown on (110) SrTiO_3 by coevaporation and post-annealing.¹⁰⁶ Dimos *et al.* found relatively large J_c values ($\approx 4 \times 10^6$ MA/cm² at 4.2K) at low angle grain boundaries (less than 10°) of $\text{YBa}_2\text{Cu}_3\text{O}_{7-\delta}$ ¹⁰⁷ suggesting the possible existence of percolation paths of high J_c material in granular films. This implies a "scaled down", but otherwise similar $J_c(T,H)$ behavior as those seen in totally epitaxial films. On the contrary, the granular films presented in this chapter were found to behave as weak-link systems in the presence of giant Josephson vortices (described in some detail elsewhere¹⁰⁸). Typical values for zero resistance transition temperatures T_c were near 88K and 67K, respectively, and $J_c(T=0)$ values were near 130 kA/cm² and 245 kA/cm², respectively.

In this study, I - V curves were acquired for a set of temperatures and applied magnetic fields, and all curves displayed behavior indicative of flux-creep-limited superconductors ($E \propto J$ in fields $H \ll H_{c2}$). The temperature dependence of $J_c(H=0)$ for either type of thin film was found to fit neither the SIS (superconductor-insulator-superconductor) model,¹⁰⁹ nor any one of the SNS (superconductor-normal metal-

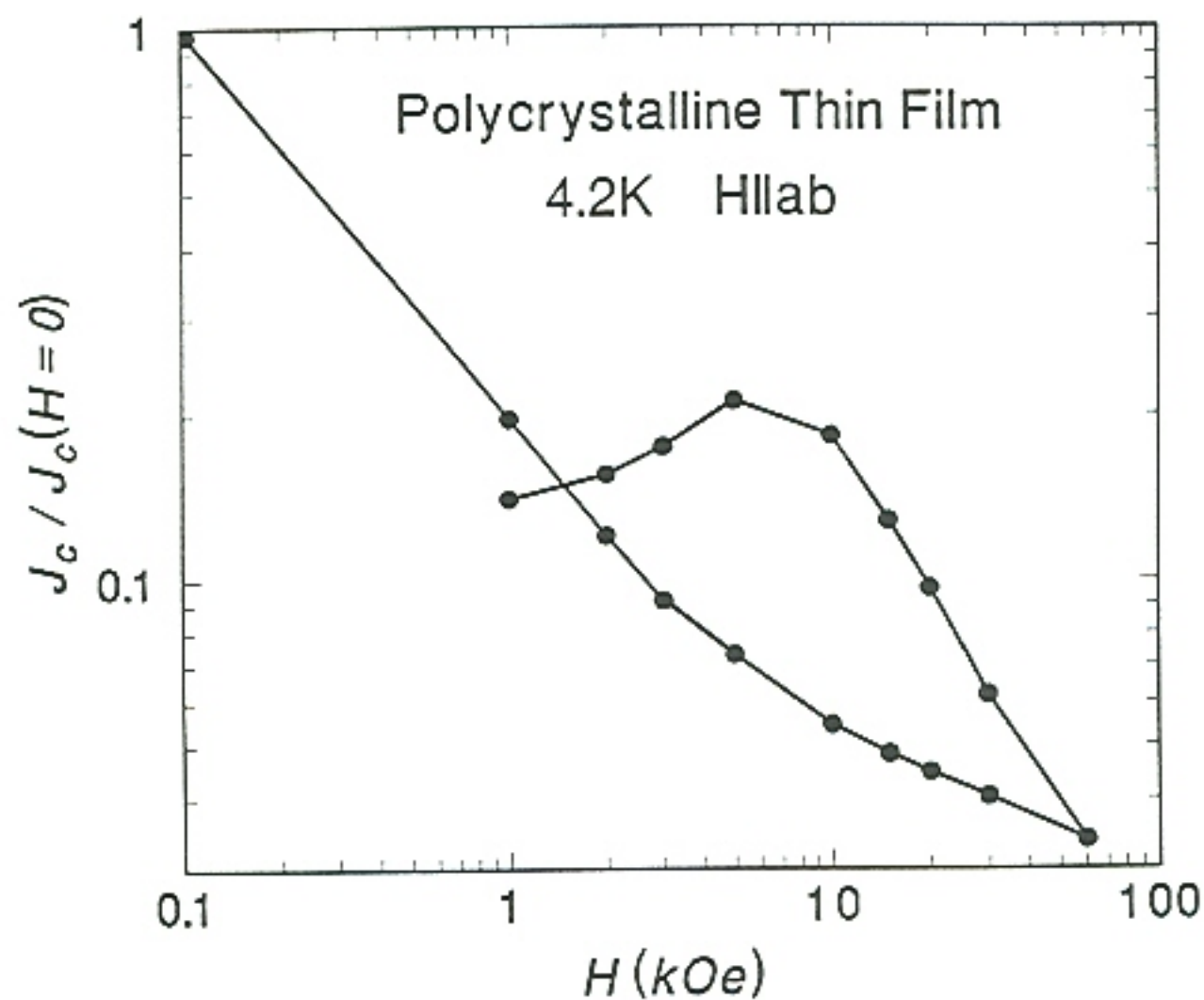
superconductor) family of curves, parametrized by the ratio of barrier thickness to normal state coherence length, $L/\xi_N(T_c)$.⁸⁶ However, critical current densities typically were two orders of magnitude below those of totally epitaxial films, and showed a strong dependence on the applied magnetic field history [Figure 39], indicative of a weak link system. For *c*-oriented films grown under the same conditions on both polycrystalline and single crystal YSZ (100) substrates, subtraction of the resulting polycrystal and single crystal resistivity curves $\rho(T)$, yield grain boundary resistivity curves which increase with temperature in a way consistent with dirty metals [see Figure 40]. In addition, using the measured grain size¹⁰⁵ (0.2 – 1.0 μm), $I_c R_N$ products were determined to fall between 0.3 mV and 2.1 mV, which are well below those expected for SIS barriers, i.e., approximately 20 mV at $T = 0$.¹¹⁰ Rather, it is shown in the following that these granular thin films behave as SNS systems for which the critical current densities are further limited by thermal activation of self-field created Josephson vortices at the grain boundaries.¹⁰⁸

From the Anderson-Kim thermally activated flux creep model,^{111,112} in the limit of weak pinning barriers (e.g., at large applied magnetic fields), one expects a thermally activated creep resistivity $\rho = (dE/dJ)$ at $J=0$ given by,¹¹³

$$\rho = \rho_o \exp \left(-\frac{U_o}{kT} \right), \quad (87)$$

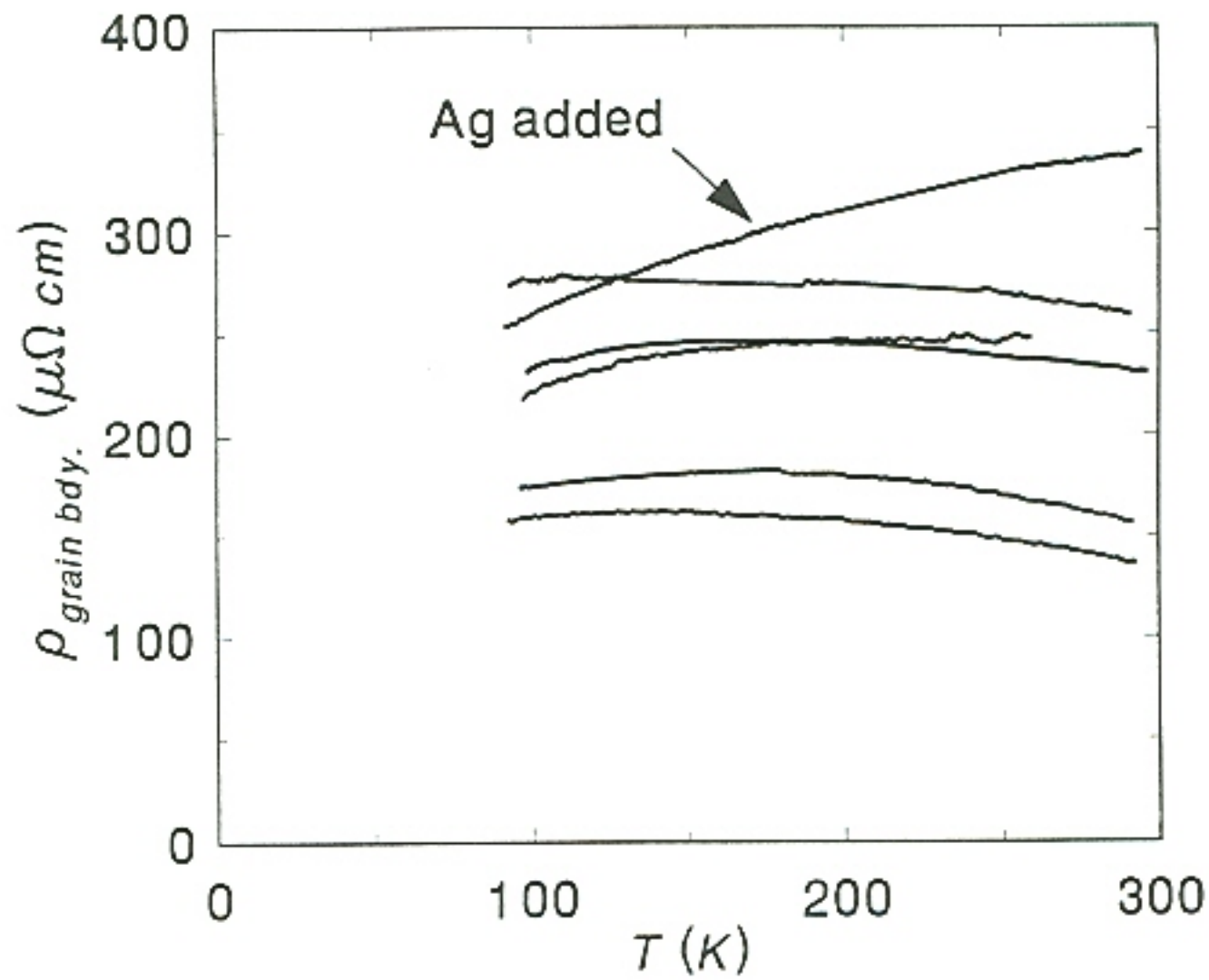
where U_o is the activation energy and ρ_o is at most a slowly varying function of T involving the flux lattice response. Thus, the systematic determinations of ρ as a function of field and temperature yield activation energies¹¹⁴ with the temperature

Figure 39



Critical current density hysteresis as a function of applied magnetic field history for a *c*-oriented granular $YBa_2Cu_3O_7$ thin film. These data were obtained at 4.2K with the field oriented parallel to the *ab*-plane. Similar effects were observed at other field orientations and at higher temperatures. These results are indicative of a Josephson mixed state.¹¹⁵

Figure 40



"Grain boundary" resistivities obtained by subtracting several polycrystalline c -oriented $\text{YBa}_2\text{Cu}_3\text{O}_7$ resistivity curves $\rho(T)$ from a single crystal resistivity curve grown under similar conditions. The temperature dependencies for these samples are consistent with dirty metals [i.e., maximum $\rho(T)$ at $T \gg 0\text{K}$ and $\rho(T=0) \gg 0$].

dependencies shown in Figure 41. The field dependencies of the activation energies could be described by

$$U_o(T,B) \propto \frac{1}{(B + B_o)^{0.15}}, \text{ for the c-oriented films ;} \quad (88)$$

$$U_o(T,B) \propto \frac{1}{(B + B_o)}, \text{ for the triaxial films.} \quad (89)$$

The constant B_o , taken to be approximately 10G, is included to prevent $U_o(T,B)$ from diverging under self-fields near T_c . The prefactor, ρ_o , is explicitly given by¹¹⁴

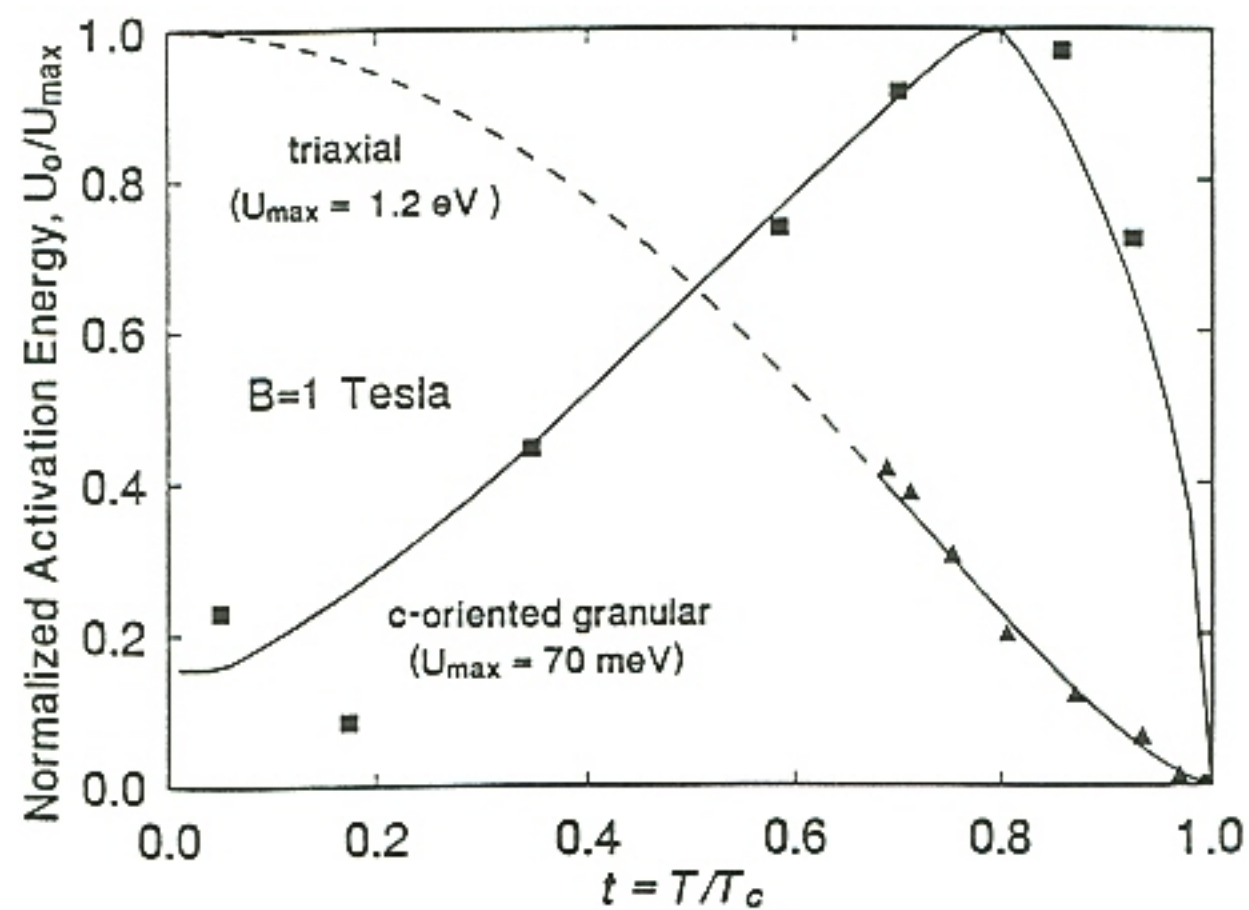
$$\rho_o = \left(\frac{E_o}{J_{co}} \right) \left(\frac{U_o}{kT} \right), \quad (90)$$

where in the present case J_{co} is taken as an SNS critical current density in the absence of flux creep. The parameter E_o , which is proportional to the elementary "attempt" frequency for flux hops, can be estimated by scaling the experimental I-V curves to the Anderson-Kim expression,^{111,112}

$$E = E_o \exp \left(-\frac{U_o}{kT} \right) \sinh \left[\left(\frac{J}{J_{co}} \right) \left(\frac{U_o}{kT} \right) \right]. \quad (91)$$

For the granular films studied, the E_o values were found to have temperature dependencies somewhat similar to the respective activation energies. Interestingly, these E_o dependencies are in qualitative agreement with the prediction of Feigel'man *et al.* for collective thermally activated processes in the vortex state:¹¹⁶

Figure 41



Temperature dependence of the activation energy at an applied field of 1 Tesla for triaxial and *c*-oriented granular thin films of $\text{YBa}_2\text{Cu}_3\text{O}_7$. The curves are empirical fits to the experimental data (symbols) for use in the flux creep models.

$$E_o \propto \rho_{flow} \frac{U_o}{T} . \quad (92)$$

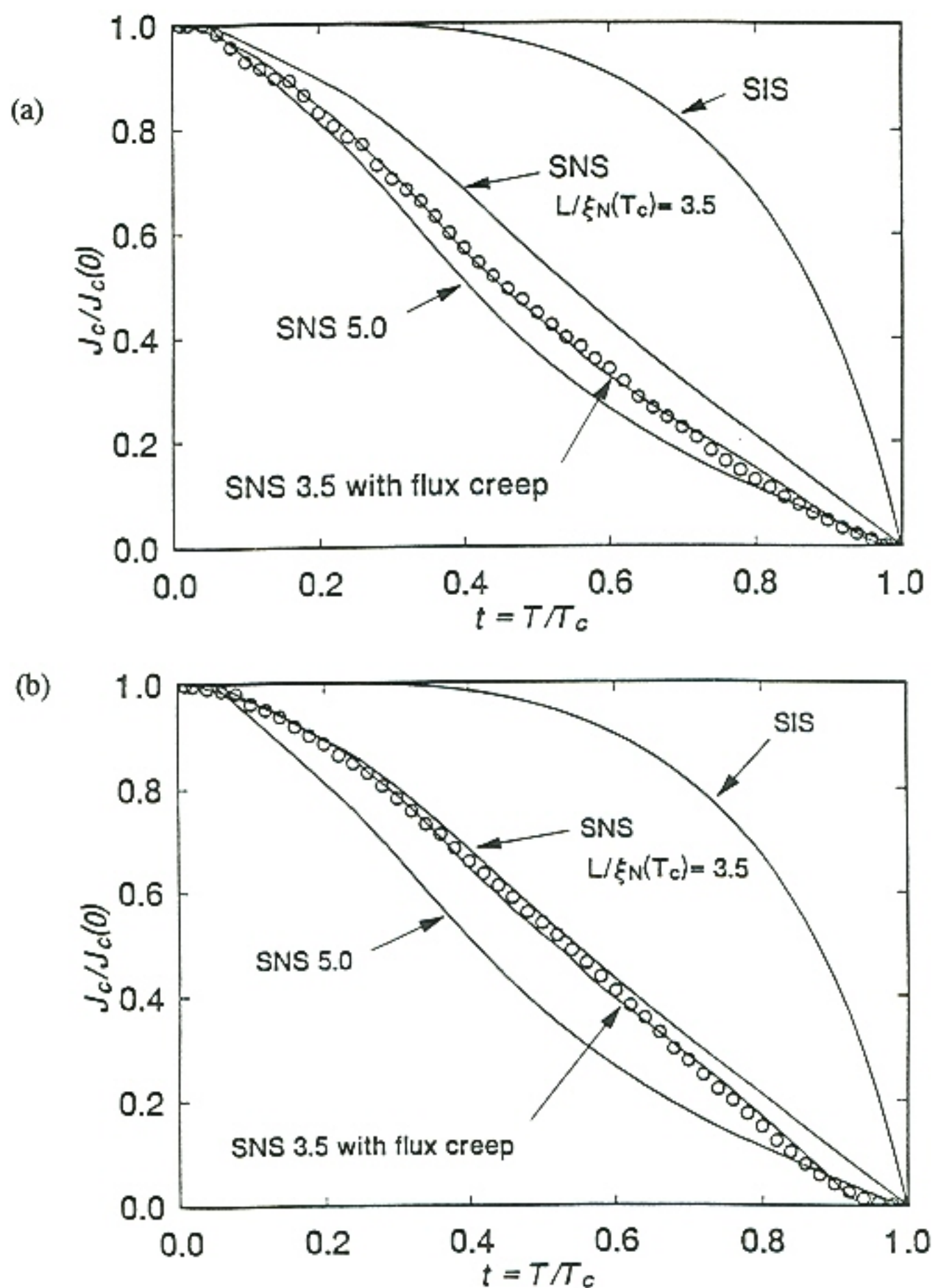
Self consistency of this model is shown for both types of granular films by substituting the U_o and E_o parameters, determined in the dissipative state, into the relationship for a creep-limited J_c :⁵⁰

$$J_c = J_{co} \left[\frac{kT}{U_o(T,B)} \right] \sinh^{-1} \left[\left(\frac{E_c}{E_o} \right) \exp \left(\frac{U_o(T,B)}{kT} \right) \right] , \quad (93)$$

where E_c is the electric field criterion of $1 \mu\text{V}/\text{cm}$. Here, the self fields, B , are assumed to be proportional to the current density¹¹⁷ and are on the order of 100G at 4.2K, estimated from the $J_c(H)$ data. In Figure 42(a) and Figure 42(b), best fits to the experimental data, for both types of film, are found by choosing the J_{co} function as the Likharev SNS curve⁸⁶ for which $L = 3.5 \xi_N(T_c)$. Even though the activation energies differ markedly, this model provides a good description of the experimental J_c data in both cases. The slight discrepancies which occur above $t \approx 0.7T_c$ could be ascribed to a number of effects, including high-temperature fluctuations, or simply errors in extrapolating high-field U_o values to the limit of self fields.

In conclusion, a self-consistent model for $J_c(T, H=0)$ was shown for two types of granular-oriented $\text{YBa}_2\text{Cu}_3\text{O}_{7-\delta}$ thin films. In both cases, the self field was found to penetrate along the grain boundaries producing a Josephson mixed state.¹¹⁸ The thermal activation energies of the resulting Josephson vortices, determined in the limit of large magnetic fields, were found in the triaxial films to behave as those seen in totally epitaxial films but scaled down by one order of magnitude. Unlike the triaxial

Figure 42



Reduced critical current density $J_c(T)/J_c(0)$ versus reduced temperature for the granular $\text{YBa}_2\text{Cu}_3\text{O}_7$ films. Symbols show experimental results for the (a) c-axis oriented and (b) triaxial thin films. In comparison, the solid curves show the conventional SIS and SNS weak link models and the SNS model with flux creep dissipation.

films which contain only special grain boundaries, the c -oriented granular films having random ab -plane grain boundaries were found to have even lower activation energies which exhibit maxima at temperatures near $0.8T_c$. Finally, thermally activated flux creep of the Josephson vortices applied to an SNS weak-link system⁸⁶ was shown to reproduce the experimentally measured critical current densities.

VIII. SUMMARY

The effects of oxygen deficiency on the resistivity, Hall coefficient, and critical current density were measured on a series of eleven epitaxial $\text{YBa}_2\text{Cu}_3\text{O}_{7-\delta}$ thin films. Solder free gold contacts and pressure pads facilitated the changing of the oxygen content by sequential anneals under carefully controlled conditions. All of the inverse Hall coefficients have linear temperature dependencies, as predicted by the Luttinger liquid theory,⁷⁵ and the implied carrier densities steadily diminish with increasing oxygen deficiency δ . Moreover, the relative insensitivity of the Hall angle to oxygen deficiency suggests that only one of the four predicted electronic bands crossing the Fermi level⁷ dominates the normal state properties with fields $H \parallel c$. Critical currents extrapolate to zero as the oxygen content nears the edge of the 90K plateau, suggestive of phase separation in which only the fully oxygenated phase has the high critical current density. Over much of the 90K plateau, no changes are seen in the pinning energies, further supporting this phase separation picture. However, electronic origins for the $T_c(\delta)$ plateaus were considered since pinning energies also depend on the coherence lengths ξ . Increases in ξ could account for the pinning energy plateau while allowing decreases of J_{c0} with δ to lead to the decreases of the critical current densities $J_c(\delta)$. Any increase in ξ should lead to a corresponding decrease in the H_{c2} slope near T_c . Therefore, the fluctuation theory of Ullah and Dorsey²¹ in the limit of large magnetic fields was applied to the in-field resistive transitions obtained from two of the epitaxial thin films of $\text{YBa}_2\text{Cu}_3\text{O}_{7-\delta}$ at various oxygen deficiencies δ . In both samples, an H_{c2} plateau corresponding to an H_{c2} slope of -1.7 T/K was observed for

oxygen deficiencies occurring on the 90K plateau, e.g., in the range $6.8 \leq 7-\delta \leq 7.0$. In contrast, the in-field resistive transitions taken off the 90K plateau, e.g., $\delta \geq 0.2$, were not adequately described by the fluctuation theory and may suggest the presence of such phase separation, whereas, evidence for granular-like behavior was observed in the Hall transitions and the field dependence of $J_c/J_c(H=0)$ when $\delta \geq 0.3$. Since an H_{c2} plateau was also observed in a recent Hao *et al.* analysis of the magnetization measurements⁸³ of bulk, aligned $\text{YBa}_2\text{Cu}_3\text{O}_{7-\delta}$, the plausible existence of an H_{c2} plateau as a function of oxygen deficiency δ supports the *extrinsic* origin of phase separation occurring on the 90K and 60K T_c vs. δ plateaus.

The non-universal observation of a sign reversal of R_H near T_c also suggests that the superconducting transitions are highly sensitive to the effects of *extrinsic* inhomogeneities. Therefore, Monte Carlo simulations of the superconducting Hall effect transitions were conducted assuming various random T_c distributions. The results clearly show that the occasional observation of a sign reversal of R_H can be attributed to inhomogeneities such as the oxygen content in $\text{YBa}_2\text{Cu}_3\text{O}_{7-\delta}$. Experimental results consistent with this picture were presented. Similar effects could also be ascribed to variations in the sample thickness that, near the observed T_c , would tend to smear the local T_c 's due to uneven depressions of the pinning energies resulting from current density variations. These results do not rule out the possibility of *intrinsic* flux motion effects in the limit of weak pinning energy; however, the non-universal observations of the sign reversals of R_H undoubtedly make such explanations very difficult. Therefore, it is most probable that most of the observed sign reversals in the high- T_c

materials are *extrinsic* in origin.

In the polycrystalline thin film studies, a self-consistent model for $J_c(T, H=0)$ was shown for two different types of granular-oriented $\text{YBa}_2\text{Cu}_3\text{O}_{7-\delta}$ thin films. In both cases, the self field was found to penetrate along the grain boundaries producing a Josephson mixed state.¹¹⁸ The thermal activation energies of the resulting Josephson vortices, determined in the limit of large magnetic fields, were found in the triaxial films to behave as those seen in totally epitaxial films but scaled down by one order of magnitude. Unlike the triaxial films that contain only special grain boundaries, the *c*-oriented granular films having random *ab*-plane grain boundaries were found to have even lower activation energies that exhibit maxima at temperatures near $0.8T_c$. Finally, thermally activated flux creep of the Josephson vortices applied to an SNS weak-link system⁸⁶ was shown to reproduce the experimentally measured critical current densities.

In sum, the most important findings from this work are as follows. First, only a small part of the band structure, i.e., perhaps a single band, appears to dominate the normal state properties. Second, *extrinsic* inhomogeneities of the oxygen content can account for the 90K and 60K plateaus in T_c vs. δ due to the short coherence length ξ . Third, the superconducting transitions are highly sensitive to the effects of inhomogeneities. Fourth, the grain boundaries behave as normal metal barriers instead of ideal Josephson junctions. Finally, it is recommended to use caution when deciding whether a particular property of these new high- T_c materials is *intrinsic* or *extrinsic*.

REFERENCES

A. Text References

1. J. G. Bednorz and K. A. Müller, *Z. Phys. B* **64**, 189 (1986).
2. M. Wilson, *Superconducting Magnets* (Oxford University Press, 1983).
3. Cost to ORNL as of 9/1992.
4. M. Okada, T. Yuasa, T. Matsumoto, K. Aihara, M. Seido, and S. Matsuda, *Advances in Superconductivity II* (Springer-Verlag, Tokyo, 1990), p. 296.
5. W. K. Wu, J. R. Ashburn, C. J. Torng, P. H. Hor, R. L. Meng, L. Gao, Z. J. Huang, Y. Q. Wang, and C. W. Chu, *Phys. Rev. Lett.* **58**, 908 (1987).
6. J. D. Jorgensen, M. A. Beno, D. G. Hinks, L. Soderholm, K. J. Volin, R. L. Hitterman, J. D. Grace, I. K. Schuller, C. U. Segre, K. Zhang, and M. S. Kleefisch, *Phys. Rev. B* **36**, 3608 (1987).
7. H. Krakauer, W. E. Pickett, and R. E. Cohen, *J. Supercond.* **1**, 111 (1988).
8. W. E. Pickett, H. Krakauer, R. E. Cohen, and D. J. Singh, *Science* **255**, 46 (1992).
9. J. Yu (private communication).
10. R. J. Cava, B. Batlogg, C. H. Chen, E. A. Rietman, S. M. Zahurak, and D. Werder, *Phys. Rev. B* **36**, 5719 (1987).
11. M. Däumling, L. E. Levine, and T. M. Shaw in *Adv. in Cryo. Eng. Mater.*, vol. 38, edited by F. R. Fickett and R. P. Reed (Plenum, New York, 1992), p. 949.
12. C. Namgung, J. T. S. Irvine, and A. R. West, *Physica C* **168**, 346 (1990).
13. V. Z. Kresin, S. A. Wolf, and G. Deutscher, *Physica C* **191**, 9 (1992).
14. R. McCormack, D. de Fontaine, and G. Ceder, *Phys. Rev. B* **45**, 12976 (1992).
15. B. W. Veal and A. P. Paulikas, *Physica C* **184**, 321 (1991).
16. M. S. Osofsky, J. L. Cohn, E. F. Skelton, M. M. Miller, R. J. Soulen, Jr., S. A. Wolf, and T. A. Vanderah, *Phys. Rev. B* **45**, 4916 (1992).
17. J. L. Vargas and D. C. Larbalestier, *Appl. Phys. Lett.* **60**, 1741 (1992).

18. R. Beyers, B. T. Ahn, G. Gorman, V. Y. Lee, S. S. P. Parkin, M. L. Ramirez, K. P. Roche, J. E. Vazquez, T. M. Gür, R. A. Huggins, *Nature* **340**, 619 (1989).
19. D. J. Werder, C. H. Chen, R. J. Cava, and B. Batlogg, *Phys. Rev. B* **38**, 5130 (1988).
20. T. Zeiske, R. Sonntag, D. Hohlwein, N. H. Andersen, and T. Wolf, *Nature* **353**, 542 (1991).
21. S. Ullah and A. T. Dorsey, *Phys. Rev. B* **44**, 262 (1991).
22. Z. Z. Wang, J. Clayhold, N. P. Ong, J. M. Tarascon, L. H. Greene, W. R. McKinnon, and G. W. Hull, *Phys. Rev. B* **36**, 7222 (1987).
23. H. L. Stormer, A. F. J. Levi, K. W. Baldwin, M. Anzlowar, and G. S. Boebinger, *Phys. Rev. B* **38**, 2472 (1988).
24. N. Thier and K. Winzer, *IEEE Transactions on Magnetism* **25**, 2293 (1989).
25. Y. Iye, S. Nakamura, and T. Tamegai, *Physica C* **159**, 616 (1989).
26. S. J. Hagen, C. J. Lobb, R. L. Greene, M. G. Forrester, and J. H. Kang, *Phys. Rev. B* **41**, 11630 (1990).
27. J. E. Hirsch and F. Marsiglio, *Phys. Rev. B* **43**, 424 (1991).
28. T. L. Francavilla and R. A. Hein, *IEEE Transactions on Magnetism* **27**, 1039 (1991).
29. A. K. Niessen, F. A. Staas, and C. H. Weijsenfeld, *Phys. Lett.* **25A**, 33 (1967).
30. N. Usui, T. Ogasawara, and K. Yasukōchi, *Phys. Lett.* **27A**, 139 (1968).
31. Sign reversals of R_H near T_c are often reported to occur at low fields ($B < 5T$), disappearing at higher fields. This is not the case with the coevaporated films.
32. M. M. Miller, M. S. Osofsky, R. J. Soulen, Jr, S. A. Wolf, J. L. Cohn, E. F. Skelton, and T. A. Vanderah, *Physica C* **185-189**, 2229 (1991).
33. E. C. Jones, D. K. Christen, C. E. Klabunde, J. R. Thompson, D. P. Norton, R. Feenstra, D. H. Lowndes, and J. D. Budai, *Transport Critical Currents in Granular-Oriented $Y_1Ba_2Cu_3O_{7-x}$ Thin Films*, March 1991 Meeting of the American Physical Society.

34. E. C. Jones, D. K. Christen, J. R. Thompson, R. Feenstra, J. M. Phillips, M. P. Siegal, and S. Zhu, *Effects of Carrier Density on the Electrical Transport Properties of Epitaxial $Y_1Ba_2Cu_3O_{7-\delta}$ Thin Films*, March 1992 Meeting of the American Physical Society.
35. E. C. Jones, *Origin of the T_c Plateaus in Oxygen-Deficient $YBa_2Cu_3O_{7-\delta}$* , High T_c Superconductivity Seminar at Oak Ridge National Laboratory, July 17, 1992.
36. E. C. Jones, D. K. Christen, J. R. Thompson, and S. Zhu, *Effect of Inhomogeneities on the Hall Effect near the Superconducting Transition*, November 1992 Meeting of the Southeastern Section of the American Physical Society.
37. E. C. Jones, D. K. Christen, C. E. Klabunde, J. R. Thompson, D. P. Norton, R. Feenstra, D. H. Lowndes, and J. D. Budai, *Flux Creep in the Josephson Mixed State of Granular-Oriented $YBa_2Cu_3O_{7-x}$ Thin Films*, Applied Physics Letters **59**, 3183-3185 (1991).
38. E. C. Jones, D. K. Christen, J. R. Thompson, R. Feenstra, S. Zhu, D. H. Lowndes, J. M. Phillips, M. P. Siegal, and J. D. Budai, *Correlations Between the Hall Coefficient and the Superconducting Transport Properties of Oxygen Deficient $YBa_2Cu_3O_{7-\delta}$ Epitaxial Thin Films*, (submitted to Physical Review B).
39. E. C. Jones, D. K. Christen, J. R. Thompson, R. C. Dynes, S. Zhu, Julia M. Phillips, and M. P. Siegal, *Effect of Current Percolation on the Superconducting Hall Transitions of Epitaxial Thin Films of $YBa_2Cu_3O_{7-\delta}$* , (submitted to Physical Review B).
40. E. C. Jones, D. K. Christen, J. R. Thompson, J. G. Ossandon, R. Feenstra, J. M. Phillips, and M. P. Siegal, *Upper Critical Fields in Oxygen Deficient $YBa_2Cu_3O_{7-\delta}$ Epitaxial Thin Films*, (awaiting internal review at ORNL for submission to the Physical Review B).
41. M. P. Siegal, J. M. Phillips, A. F. Hebard, R. B. van Dover, R. C. Farrow, T. H. Tiefel, J. H. Marshall, J. Appl. Phys. **70**, 4982 (1991).
42. Shen Zhu, Douglas H. Lowndes, X.-Y. Zheng, David P. Norton, and R. J. Warmack, Mater. Res. Soc. Symp. Proc. **237**, 541 (1991).
43. R. Feenstra, T. B. Lindemer, J. D. Budai, and M. D. Galloway, J. Appl. Phys. **69**, 6569 (1991).
44. C. M. Hurd, *The Hall Effect in Metals and Alloys* (Plenum, New York, 1972).

45. R. Feenstra has shown this to be a universal result in thin films. (unpublished).
46. R. J. Cava, A. W. Hewat, E. A. Hewat, B. Batlogg, M. Marezio, K. M. Rabe, J. J. Krajewski, W. F. Peck Jr., and L. W. Rupp Jr., *Physica C* **165**, 419 (1990).
47. J. D. Jorgensen, B. W. Veal, A. P. Paulikas, L. J. Nowicki, G. W. Crabtree, H. Claus, and W. K. Kwok, *Phys. Rev. B* **41**, 1863 (1990).
48. Note that the triple point of nitrogen is 63K. Thus, the 52K quoted here is obtained by subliming the nitrogen.
49. P. W. Anderson, *Phys. Rev. Lett.* **9**, 309 (1962).
50. M. Tinkham, *Introduction to Superconductivity* (McGraw-Hill, New York, 1975).
51. D. K. Christen (private communication).
52. H. R. Kerchner (private communication).
53. S. Zhu, D. K. Christen, C. E. Klabunde, J. R. Thompson, E. C. Jones, R. Feenstra, D. H. Lowndes, and D. P. Norton, *Phys. Rev. B* **46**, 5576 (1992).
54. C. Kittel, *Introduction to Solid State Physics* (Wiley, New York, 1986).
55. P. B. Allen, W. E. Pickett, and H. Krakauer, *Phys. Rev. B* **37**, 7482 (1988).
56. In the high-field limit, E_y saturates and no longer depends on the external field B . Since the field strengths required are currently inaccessible to most instruments (range of ~ 100 T), this regime is not considered in this dissertation.
57. W. E. Pickett, *Rev. Mod. Phys.* **61**, 433 (1989).
58. G. D. Mahan calculated $R_H(T)$ and $\rho(T)$ for the case of strong electron-electron scattering between two bands. (unpublished) In this case, every quantity is simply the average of the two bands. Unfortunately, the Hall coefficient remains independent of temperature in this scenario.
59. J. M. Ziman, *Principles of the Theory of Solids*, 2nd ed. (Cambridge, New York, 1972).
60. K. Schröder, *Electronic, Magnetic, and Thermal Properties of Solid Materials* (Dekker, New York, 1978).
61. N. P. Ong, *Phys. Rev. B* **43**, 193 (1991).

62. R. S. Markiewicz, Phys. Rev. B **38**, 5010 (1988).
63. T. Penney, M. W. Shafer, B. L. Olson, and T. S. Plaskett, Adv. Ceram. Mater. **2**, 577 (1987).
64. D. M. Eagles, Physica C **153-155**, 701 (1988).
65. J. M. Ziman, *Electrons and Phonons* (Oxford Univ. Press, New York, 1960).
66. P. B. Allen, Phys. Rev. B **17**, 3725 (1978).
67. H. Jones and C. Zener, Proc. R. Soc. A **145** (1934).
68. G. D. Mahan remarked that this equation is only valid for the case of elastic scattering of electrons from impurities; fortunately, the resulting transport coefficients predict accurate values for the conductivity and the Hall coefficient in most metals. Nevertheless, it would be desirable to develop a set of transport coefficients starting with the Boltzmann equation valid for electron-phonon scattering.
69. A. C. Smith, J. F. Janak, and R. B. Adler, *Electronic Conduction in Solids* (McGraw-Hill, New York, 1967).
70. M. Tsuji, J. Phys. Soc. Jpn. **13**, 979 (1958).
71. A similar procedure, for the case $N=2$, leads to the result $\sigma \equiv \text{scalar}$. For details, see Ref. 61.
72. J. S. Dugdale and L. D. Firth, J. Phys. C **2**, 1272 (1969).
73. A. T. Fiory and G. S. Grader, Phys. Rev. B **38**, 9198 (1988).
74. T. R. Chien, Z. Z. Wang, and N. P. Ong, Phys. Rev. Lett. **67**, 2088 (1991).
75. P. W. Anderson, Phys. Rev. Lett. **67**, 2092 (1991).
76. F. D. M. Haldane, Phys. Lett. **81A**, 153 (1981).
77. R. S. Markiewicz, Physica C **177**, 445 (1991).
78. W. E. Lawrence and S. Doniach, *Proc. 12th Intern. Conf. on Low Temp. Physics*, Kyoto, Japan, 1970 (Keigaku Publ. Co., 1971), p. 361.
79. Y. X. Jia, J. Z. Liu, M. D. Lan, P. Klavins, and R. N. Shelton (submitted to Physica C).

80. R. Feenstra, D. K. Christen, C. E. Klabunde, and J. D. Budai, *Phys. Rev. B* **45**, 7555 (1992).
81. C. C. Tsuei, C. C. Chi, D. M. Newns, P. C. Pattnaik, and M. Däumling (submitted for publication).
82. O. K. Andersen, A. I. Liechtenstein, O. Rodriguez, I. I. Mazin, O. Jepsen, V. P. Antropov, O. Gunnarsson, and S. Gopalan, *Physica C* **185-189**, 147 (1991).
83. J. G. Ossandon, J. R. Thompson, D. K. Christen, B. C. Sales, H. R. Kerchner, J. O. Thomson, Y. R. Sun, K. W. Lay, and J. E. Tkaczyk, *Phys. Rev. B* **45**, 12534 (1992).
84. Guy Deutscher, in *Percolation, Localization, and Superconductivity*, edited by Allen M. Goldman and Stuart A. Wolf (Plenum, New York, 1984), p. 95.
85. R. Wördenweber (submitted to *Phys. Rev. B*).
86. K. K. Likharev, *Rev. Mod. Phys.* **51**, 115 (1979).
87. J. D. Hettinger, A. G. Swanson, W. J. Skocpol, J. S. Brooks, J. M. Graybeal, P. M. Mankiewich, R. E. Howard, B. L. Straughn, and E. G. Burkhardt, *Phys. Rev. Lett.* **62**, 2044 (1989).
88. J. G. Ossandon, J. R. Thompson, D. K. Christen, B. C. Sales, Y. Sun, and K. W. Lay, *Phys. Rev. B* **46**, 3050 (1992).
89. Y. B. Kim, *Rev. Mod. Phys.* **36**, 39 (1964).
90. M. V. Feigel'man, V. B. Geshkenbein, and A. I. Larkin, *Physica C* **167**, 177 (1990).
91. Y. Yeshurun and A. P. Malozemoff, *Phys. Rev. Lett.* **60**, 2202 (1988).
92. Z. Hao, J. Clem, M. McElfresh, L. Civale, A. Malozemoff, and F. Holtzberg, *Phys. Rev. B* **43**, 2844 (1991).
93. V. Matijasevic, P. Rosenthal, K. Shinohara, A. F. Marshall, R. H. Hammond, and M. R. Beasley, *J. Mater. Res.* **6**, 682 (1991).
94. R. Feenstra (unpublished).
95. M. Lang, R. Kürsch, A. Grauel, C. Geibel, F. Steglich, H. Rietschel, T. Wolf, Y. Hidaka, K. Kumagai, Y. Maeno, and T. Fujita, *Phys. Rev. Lett.* **69**, 482 (1992).

96. U. Welp, W. K. Kwok, G. W. Crabtree, K. Vandervoort, A. Umezawa, and J. Z. Liu, Phys. Rev. Lett. **62**, 1908 (1989).
97. H. L. Edwards, J. T. Markert, and A. L. de Lozanne, Phys. Rev. Lett. **69**, 2967 (1992).
98. Accepted values for $H_{c2}(0)$ ($H \parallel c$) generally occur in the range 1000–1250 kOe as obtained from References 18 and 19.
99. S. A. Wolf and V. Z. Kresin, IEEE Transactions on Magnetism **27**, 852 (1991).
100. B. W. Veal, A. P. Paulikas, H. You, H. Shi, Y. Fang, and J. W. Downey, Phys. Rev. B **42**, 6305 (1990).
101. Electric fields parallel to the current paths are not considered here since, these are even functions of the magnetic field. Thus, these signals cancel from the defined Hall coefficients upon application of Equation (1).
102. J. Luo, T. P. Orlando, J. M. Graybeal, X. D. Wu, and R. Muenchausen, Phys. Rev. Lett. **68**, 690 (1992).
103. M. P. Maley, J. O. Willis, H. Lessure, and M. E. McHenry, Phys. Rev. B **42**, 2639 (1990).
104. D. P. Norton, D. H. Lowndes, J. D. Budai, D. K. Christen, E. C. Jones, K. W. Lay, and J. E. Tkaczyk, Appl. Phys. Lett. **57**, 1164 (1990).
105. D. P. Norton, D. H. Lowndes, J. D. Budai, D. K. Christen, E. C. Jones, J. W. McCamy, T. D. Ketcham, D. St. Julien, K. W. Lay, and J. E. Tkaczyk, J. Appl. Phys. **68**, 223 (1990).
106. R. Feenstra, J. D. Budai, D. K. Christen, M. F. Chisholm, L. A. Boatner, M. D. Galloway, and D. B. Poker, in *Science and Technology of Thin Film Superconductors*, edited by R. D. McConnell and S. A. Wolf (Plenum, New York, 1989), p. 327.
107. D. Dimos, P. Chaudhari, J. Mannhart, and F. K. LeGoves, Phys. Rev. Lett. **61**, 1653 (1988).
108. J. R. Clem, Physica C **153–155**, 50 (1988).
109. V. Ambegaokar and A. Baratoff, Phys. Rev. Lett. **10**, 486 (1963); **11**, 104(E) (1963).
110. J. Mannhart and P. Martinoli, Appl. Phys. Lett. **58**, 643 (1991).

111. P. W. Anderson and Y. B. Kim, *Rev. Mod. Phys.* **36**, 39 (1964).
112. A. M. Campbell and J. E. Evetts, *Adv. Phys.* **21**, 199 (1972).
113. D. K. Christen, C. E. Klabunde, R. Feenstra, D. H. Lowndes, D. Norton, H. R. Kerchner, J. R. Thompson, S. T. Sekula, J. D. Budai, L. A. Boatner, J. Narayan, and R. Singh, *Mater. Res. Soc. Symp. Proc.* **169**, 883 (1989).
114. R. C. Budhani, D. O. Welch, M. Suenaga, and R. L. Sabatini, *Phys. Rev. Lett.* **64**, 1666 (1990).
115. L. J. Campbell (unpublished).
116. M. V. Feigel'man, V. B. Geshkenbein, and V. M. Vinokur, *Phys. Rev. B* **43**, 6263 (1991).
117. Y. J. Zhao and W. K. Chu (unpublished).
118. M. Tinkham and C. J. Lobb in *Solid State Physics, Vol. 42*, edited by H. Ehrenreich and D. Turnbull (Academic Press, Boston, 1989), pp. 91-134.

B. Appendix References

1. P. Šmilauer, *Contemp. Phys.* **32**, 89 (1991).
2. J. Halbritter, *Inter. J. Mod. Phys. B* **3**, 719 (1989).

C. Suggested Hall Effect Readings

- [1] C. Kittel, *Introduction to Solid State Physics* (Wiley, New York, 1986).
- [2] J. M. Ziman, *Principles of the Theory of Solids*, 2nd ed. (Cambridge, New York, 1972).
- [3] J. M. Ziman, *Electrons and Phonons* (Oxford Univ. Press, New York, 1960).
- [4] K. Schröder, *Electronic, Magnetic, and Thermal Properties of Solid Materials* (Dekker, New York, 1978).
- [5] C. M. Hurd, *The Hall Effect in Metals and Alloys* (Plenum, New York, 1972).
- [6] J.-P. Jan, *Solid State Physics* 5, 1 (1957).
- [7] E. Fawcett, *Advanced Physics* 13, 139 (1964).

APPENDICES

Appendix A. Hall (Resistivity) Acquisition Program

```

10 DEFINT I-N
20 '
30 ' *** HALL.BAS ***
40 '*** KEITHLEY 570 SYSTEM ***
50 '*** Y-VOLTAGE VS X-VOLTAGES -- PERSONAL488 DATA ACQUISITION ***
100 ' DATA SAMPLED AFTER SPECIFIED X- & Y-ABS-VALUE-INTERVALS HAVE PASSED
110 ' OUTPUTS X1, X3, X4 AND Y DATA TO AN ASCII FILE
120 ' SPECIFIED BY THE USER. PLOTS AUXILIARY DATA FILE FOR COMPARISON
130 ' COMMAND P0 SENT TO Y-DVM (FOR K-181 TURNS OFF DIGITAL FILTERING)
135 ' SWITCHES K-224 POWER SUPPLY BETWEEN + & - OUTPUTS TO CANCEL THERMAL EMF'S
136 ' FROM THE NANOVOLTMETER SIGNAL. TEMP-signal & MAG-signals ARE NOT
137 ' CORRECTED FOR THERMALS SINCE TRANSPORT CURRENTS ARE RELATIVELY LARGE !
140 ' X1-channel is converted to a temperature (optional).
142 ' X2-channel verifies the K-224 output current and corrects the data ...
144 ' X3-channel meas. a 3rd signal such as rho(T) when K-181 is in use.
145 ' X4-channel meas. the magnet current (if not in persistent mode)
146 ' Y-voltmeter meas. the Hall signal which can be plotted .
148 ' Magnetic field determined assuming use of a 1/100 ohm std. resistor.
150 ' DATA OUTPUT: (1) If desired, will sort data according to X1-signal (temp)
151 '           when saving data to the disk in standard format.
152 '           (2) If X1-signal was converted to a temperature & after
153 '           sorting data, will prompt user to continue with a
154 '           temperature interpolation routine controlled by user
155 '           parameters Tmin, Tmax, & T-interval.
156 '           This new data is then saved to the disk.
160 ' Maintains Temperature Controller Set Point to values based on user
162 ' input and current sample temperature (optional).
190 '
200 '*** MAIN PROGRAM ***
210 '
220 GOSUB 400 '--- SET DEFAULT PARAMETER VALUES ---
225 GOSUB 4150 '--- READ IN FILE OF SETUP AND GRAPHICS PARAMETERS ---
230 GOSUB 700 '--- SIGN-ON & HARDWARE SETTINGS MENU ---
240 GOSUB 1000 '--- SETUP PARAMETERS MENU ---
245 GOSUB 4500 '--- STORE SETUP AND GRAPHICS PARAMS TO FILE ---
250 GOSUB 1600 '--- DATA ACQUISITION INITIALIZATION ---
260 GOSUB 1750 '--- TAKE ONE DATUM SAMPLE ---
270 GOSUB 3550 '--- CHECK FOR KEYBOARD INTERRUPT ---
280 GOSUB 1850 '--- TEST DATA FOR OUTPUT ---
290 GOSUB 3550 '--- CHECK FOR KEYBOARD INTERRUPT ---
300 GOSUB 3750 '--- CALC. TEMP. FROM THERM. CALIBRATION ---
305 IF TSET$=ACT$ THEN GOSUB 9000 '--- TEMPERATURE CONTROLLER SET POINTS ---
310 GOSUB 2000 '--- PRINT DATA TO DISK ---
320 GOSUB 2700 '--- PLOT OR PRINT DATA TO SCREEN ---
330 GOSUB 3550 '--- CHECK FOR KEYBOARD INTERRUPT ---
340 GOTO 260 '--- LOOP BACK FOR MORE DATA --
350 '
360 '*** END MAIN PROGRAM ***
370 '
380 '
400 '*** DEFINE DEFAULT PARAMETERS ***
410 CLS: KEY OFF: KEY 1,"LIST 200-400"+CHR$(13)
420 DEFINT I-N
425 JD=700 'JD=1400 for ~.25 sec delay to allow DVM triggering
430 DIM X(500),X2(500),X4(500),Y(500) 'DIM DATA FOR GRAPHICS REFRESH
440 DIM V(500),T(500) 'ARRAY FOR THERM. CALIBRATION TABLE(e.g. DIODE V,T)
445 DIM XG(500),XG4(500),YG(500) 'ARRAY OF COMPARISON DATA FOR GRAPHICS
450 ON ERROR GOTO 5400 '---ERROR TRAPPING
460 RESTORE 470
470 DATA 10,1,1,0,0,1,1,1,"1.000E-03",1
480 READ CUR,SCALEX,SCALEY,DEL,DELY,G0%,G1%,NFILT,CURRNT$,DELMAG 'Defaults
482 CURR$="+" +CURRNT$
483 CNEG$="-" +CURRNT$
485 SCALEX2=SCALEX: SCALEI=1: SCALEMAG=102.91 'Hall Cryostat & 1/100 Ohm Std.
490 DATA "<INACTIVE>","<ACTIVE>"

```



```

500 READ INACT$,ACT$: GSET$=INACT$: GCSET$=INACT$: TSET$=INACT$
504 '--- GPIB BUS ADDRESSES & METER PARAMS
505 DATA " 26"," 14","KEITHLEY 181/199/197","KEITHLEY 181/199/197",5,5," 19","KEITHLEY 224"
506 READ XADDR$,YADDR$,MX$,MY$,NXM,NYM,PADDR$,P$
508 TADDR$=" 12" 'Temp. Controller GPIB Address
510 '
520 'GRAPHICS DEFAULT PARAMETERS
525 PLOT$="T" : VUTT$="N"
527 RATIO=1000 'Typical E-rho/E-hall ratio
530 RESTORE 550
540 READ XMIN,XMAX,YMIN,YMAX
550 DATA 0,300,-0.5,0.5,0
560 READ X$,Y1$,Y2$,T$
570 RESTORE 590
580 READ X$,Y1$,Y2$,T$
590 DATA "X1-AXIS(UNITS)","Y-AXIS","(UNITS)","TITLEOF HALL GRAPH"
600 RESTORE 620
610 READ DXPIX,DYPIX, XPIX0,YPIX0 'AXIS CONTANTS IN PIXELS
620 DATA 550,300,80,15
630 RETURN 'TO MAIN PROGRAM
640 '
650 '
700 '*** SIGN-ON HARDWARE SETTINGS MESSAGE ***
710 CLS: PRINT CHR$(7)
720 PRINT:PRINT " *** HARDWARE SETTINGS ***"
730 PRINT " 1: X-INPUT: GPIB Address: ";XADDR$; " Meter ID: ";MX$
740 PRINT " 2: Y-INPUT: GPIB Address: ";YADDR$; " Meter ID: ";MY$
744 PRINT
745 PRINT " Set ";P$;" Power Supply GPIB Address to ";PADDR$
746 PRINT " and the Voltage Compliance to a Safe Value."
747 PRINT
748 PRINT " K-199 SETUP: Temp. signal < == > X-Channel # 1"
749 PRINT " Curr. signal < == > X-Channel # 2"
750 PRINT " Alt. signal < == > X-Channel # 3"
751 PRINT " Mag. current < == > X-Channel # 4"
752 PRINT " K-181 NANOVOLTMETER: Hall (or Rho) Signal":PRINT
754 PRINT " Reset LakeShore Temperature Controller & set GPIB address to ";TADDR$
756 PRINT
760 INPUT"ENTER SELECTION # (< C/R > TO CONTINUE): ",ICODE
770 ON ICODE GOTO 790,810
780 RETURN 'TO MAIN PROGRAM
790 INPUT"ENTER NEW GPIB ADDRESS FOR X-INPUT: ",XADDR
791 GOSUB 850 '--- METER ID CHOICES FOR READING STRING MASKING
792 INPUT"ENTER X-INPUT Meter ID CODE (DEFAULT = PREVIOUS): ",NMT
794 IF NMT < > 0 THEN NM=NMT ELSE 800
796 GOSUB 900: MX$=M$: NXM=NMSK '--- ASSIGN METER ID NAME & MASKING DATA
800 XADDR$=STR$(XADDR): GOTO 720
810 INPUT"ENTER NEW GPIB ADDRESS FOR Y-INPUT: ",YADDR
811 GOSUB 850 '--- METER ID CHOICES
812 INPUT"ENTER Y-INPUT Meter ID CODE (DEFAULT = PREVIOUS): ",NMT
814 IF NMT < > 0 THEN NM=NMT ELSE 820
816 GOSUB 900: MY$=M$: NYM=NMSK '--- ASSIGN METER ID NAME & MASKING DATA
820 YADDR$=STR$(YADDR): GOTO 720
830 '
840 '
850 ' *** ASSIGN STRING MASKING PARAMS FOR METERS ***
854 PRINT "**** Meter ID Codes ***"
855 PRINT" 1: KEITHLEY 181,197
856 PRINT" 2: FLUKE 8840A
860 RETURN
870 '
880 '
890 '
900 '*** ASSIGN METER ID NAME ***
910 ON NM GOTO 930,940
920 PRINT CHR$(7): PRINT " < < < WRONG METER ID > > ": RETURN 230
930 M$="KEITHLEY 181/197": NMSK=5: RETURN

```



```

940 M$="FLUKE 8840A": NMSK=1: RETURN
950 '
960 '
1000 SCREEN 0: CLS
1010 GOSUB 5500 '--- INCREMENT EXTENSION ON DATA FILENAME
1020 PRINT: PRINT: PRINT " *** SET-UP PARAMETERS *** "
1030 PRINT " 1: FILENAME OF SETUP AND GRAPHICS PARAMETERS TO USE: ";PUFL$
1040 PRINT " 2: FILENAME OF SETUP AND GRAPHICS PARAMETERS TO SAVE TO: ";PSFL$
1050 PRINT " 3: X1-VOLTAGE SCALE FACTOR (Temp Signal/Vmeas): ";SCALEX
1060 PRINT " 4: X1-SIGNAL STEP SIZE: ";DEL
1062 PRINT " 5: X2-SIGNAL SCALE FACTOR (1/STD Ohms): ";SCALEI
1065 PRINT " 6: X3-VOLTAGE SCALE FACTOR (Alt Signal/Vmeas): ";SCALEX2
1070 PRINT " 7: Y-VOLTAGE SCALE FACTOR (Nano Signal/Vmeas): ";SCALEY
1080 PRINT " 8: Y-SIGNAL STEP SIZE: ";DELY
1085 PRINT " 9: MAG. FIELD STEP SIZE (kOe): ";DELMAG
1090 PRINT "10: DATA FILENAME: ";DNM$
1095 IF DNM$="" GOTO 1110
1100 PRINT " TITLE: ";TITLE$
1110 PRINT "11: THERM. CAL. TABLE FILENAME (for X1-signal conversion): ";THNM$
1112 IF THNM$="" GOTO 1120
1115 PRINT " TITLE: ";THTTL$
1120 PRINT "12: NO. OF SAMPLES IN DIGITAL FILTERING: ";NFILT
1130 PRINT "13: SCREEN GRAPHICS PARAMETERS SETUP: ";GSET$
1132 PRINT "14: TRANSPORT CURRENT [n.nnnE(sign)nn]: ";CURRNT$
1135 PRINT "15: EXIT PROGRAM"
1137 PRINT "16: TEMPERATURE CONTROLLER: ";TSET$
1138 IF TSET$=ACT$ THEN PRINT " Control Range = " TC1"-TC2 "K & Vap-Samp = " TCDEL "K @ RT"
1140 PRINT "17: INTERPOLATE FILE GIVEN IN OPTION 10 ACCORDING TO TEMPERATURE"
1145 PRINT
1150 INPUT "> ENTER SELECTION # (<C/R> TO EXECUTE): ";ICODE
1160 ON ICODE GOTO 1400,1430,1290,1310,1467,1322,1180,1200,1212,1220,1350,1380,1330,1460,1335,1475,1482
1170 RETURN "TO MAIN PROGRAM
1180 INPUT " ENTER Y-VOLTAGE SCALE FACTOR (Nano Signal/Vmeas): ";SCALEY
1190 GOTO 1020
1200 INPUT " ENTER Y-SIGNAL STEP SIZE: ";DELY
1210 GOTO 1020
1212 INPUT " ENTER MAGNETIC FIELD STEP SIZE (kOe): ";DELMAG
1214 GOTO 1020
1220 INPUT " INPUT DATA FILENAME (EXT .DTn WILL BE ADDED IF NOT ENTERED): ";DNM$
1230 IF DNM$="" THEN 1280
1240 PRINT " ENTER 80 CHARACTER DATA SET TITLE(DEFAULT=PREVIOUS): ";INPUT"DUM$
1250 IF DUM$="" THEN 1270
1260 TITLE$=DUM$
1270 FOR J=1 TO LEN(DNM$): IF MID$(DNM$,J,1)<>"." THEN NEXT J ELSE 1280
1272 DNM$=DNM$+".DT0"
1280 GOTO 1020
1290 INPUT " ENTER X1-VOLTAGE SCALE FACTOR (Temp Signal/Vmeas): ";SCALEX
1300 GOTO 1020
1310 INPUT " ENTER X1-SIGNAL STEP SIZE: ";DEL
1320 GOTO 1020
1322 INPUT " ENTER X3-VOLTAGE SCALE FACTOR (Alt Signal/Vmeas): ";SCALEX2
1324 GOTO 1020
1330 GOSUB 2250 'Define Graphics Parameters
1332 GOTO 1020
1335 GOSUB 4500: END '--- STORE PARAMS TO FILE AND PREPARE TO EXIT
1336 PRINT#2,"OUTPUT";PADDR$;"R0FOX": END 'turn off current
1340 GOTO 1020
1350 INPUT " ENTER THERMOM. CALIB. TABLE FILENAME(EXT .CAL WILL BE ADDED): ";THNM$
1360 IF THNM$="" THEN 1370 ELSE THNM$=THNM$+".CAL"
1365 GOSUB 3900 '--- READ IN THERM. CALIB. DATA ---
1370 GOTO 1020
1380 INPUT " ENTER NO. SAMPLES IN DIGITAL FILTERING: ";NFILT
1390 GOTO 1020
1400 INPUT " ENTER FILENAME FOR SETUP PARAMS. TO USE(EXT .PAR WILL BE ADDED): ";PUFL$
1410 IF PUFL$="" THEN 1420 ELSE PUFL$=PUFL$+".PAR"
1420 GOSUB 4150: GOTO 230 '---READ IN SETUP AND GRAPHICS PARAMS
1430 INPUT " ENTER FILENAME FOR SETUP PARAMS TO SAVE TO (.PAR WILL BE ADDED): ";PSFL$

```



```

1440 IF PSFL$="" THEN 1450 ELSE PSFL$=PSFL$+".PAR"
1450 GOTO 1020
1460 INPUT " ENTER CURRENT IN AMPS [n.nnnE(sign)nn]: ",CURRNT$
1461 CURR$=" "+CURRNT$
1462 CNEG$="- "+CURRNT$
1465 GOTO 1020
1467 INPUT " ENTER CURRENT SIGNAL SCALE FACTOR (1/STD Ohms): ",SCALEI
1470 GOTO 1020
1475 IF THNM$="" THEN PRINT " Enter a temperature calibration file if you plan to use the controller !": GOTO 1020
1476 IF TSET$=ACT$ THEN TSET$=INACT$: GOTO 1020
1477 PRINT " Temperature Controller Settings": TSET$=ACT$
1478 INPUT " ENTER Tmin, Tmax & Vap-Samp Set Points: ",TC1,TC2,TCDEL
1479 IF TC1>TC2 OR TC2>320 OR TC1<0 THEN PRINT" Bad Entry !": GOTO 1478
1480 GOTO 1020
1482 INPUT "Are you sure ? <Y=Yes> ",R$
1484 IF R$="Y" OR R$="y" THEN GOTO 1485 ELSE GOTO 1020
1485 IF DNM$="" THEN PRINT "Must specify a data set to interpolate." : GOTO 1020
1486 CLOSE#1
1487 OPEN"1",#1, DNM$
1488 INPUT#1, TITLES "Title of data set
1489 INPUT#1, I "No. of data points
1490 FOR J=1 TO I
1491 INPUT#1, X(J),X2(J),Y(J),X4(J)
1492 NEXT J
1493 CLOSE#1
1494 IF THNMS$="" THEN THNMS$=" "
1495 GOSUB 6000
1496 IF THNMS$=" " THEN THNMS$=""
1497 GOTO 1020
1498 '
1500 '*** OPEN DATA FILE ***
1510 IF DNMS$="" THEN 1550
1520 OPEN "O",#1,DNMS$
1530 PRINT #1, TITLES$
1540 PRINT #1,"Temp-Signal Alt-Signal Nano-Signal H(kOe) "
1550 RETURN
1560 '
1570 '
1600 ' *** INITIALIZATION FOR DATA ACQU. ***
1604 CURR$=" "+CURRNT$
1605 CNEG$="- "+CURRNT$ '--- NEG CURRENT STRING
1610 GOSUB 4050 '---PRINT MESSAGE AT SCREEN BOTTOM
1620 I=0 'INITIALIZE DATA ARRAY INDEX
1630 GOSUB 4850 '--- ESTABLISH COMMUNICATION W/PERSONAL488
1640 GOSUB 4950 '--- SIGNON MESSAGE
1650 GOSUB 5050 '---ASSIGN REMOTE MODE ADDRESSES
1660 FLG$="L" 'INITIALIZE FOR DATA SCREEN PRINTOUT
1680 GOSUB 1500 '--- OPEN DATA FILE
1690 IVXFLG=0 '--- FLAG FOR FIRST TIME THRU
1700 PRINT "****Beginning Data Acquisition ****"
1710 RETURN 'TO MAIN PROGRAM
1720 '
1730 '
1750 ' *** TAKE DATA SAMPLE ***
1760 '--- GPIB INPUT ---
1770 GOSUB 5200 '--- FIND AVG OF NFILT GPIB READINGS
1780 VX=SUMX*SCALEX: VX2=SUMX2*SCALEX2: VY=SUMY*SCALEY: VMAG=SUMX4*SCALEMAG
1781 VERC=VERI*SCALEI 'Actual K-224 current output
1787 VY=VY*VAL(CURR$)/VERC 'Correction for K-224 current drift
1788 VX2=VX2*VAL(CURR$)/VERC 'Correction for K-224 current drift
1790 RETURN 'TO MAIN PROGRAM
1800 '
1810 '
1850 '*** DATA TEST FOR OUTPUT ***
1860 IF IVXFLG=0 THEN IVXFLG=1: VXT=VX: VYT=VY: VMAGT=VMAG: RETURN '1st Pass
1870 DELVX=VX-VXT: DELVY=VY-VYT: DELVM=VMAG-VMAGT
1880 IF IDATFLG=0 THEN 1920

```



```

1890 IF INK$ < > "P" AND INK$ < > "p" THEN PRINT "MANUAL STORE"
1900 PRINT CHR$(7); "— BELL TO INDICATE MANUAL DATA STORAGE"
1910 IDATFLG=0: GOTO 1970 "MANUAL DATA STORAGE"
1920 IF DEL=0 THEN 1970
1925 IF DELMAG=0 THEN 1970
1930 IF DELY=0 THEN 1970
1940 IF ABS(DELVY) > =DELY THEN 1970 "STORE DATA"
1945 IF ABS(DELVM) > =DELMAG THEN 1970 "STORE DATA"
1950 IF ABS(DELVX) > =DEL THEN 1970 ELSE RETURN 260 "TAKE MORE DATA"
1970 VXT=VX: VYT=VY: VMAGT=VMAG: RETURN "TO MAIN PROGRAM"
1980 '
1990 '
2000 ' *** PRINT VALUES ON DISK ***
2010 I=I+1: X2(I)=VX2: Y(I)=VY: X4(I)=VMAG "INCREMENT INDEX"
2020 IF THNMS="" THEN X(I)=VX: GOTO 2040
2030 X(I)=T
2040 IF DNM$="" THEN 2060
2050 PRINT #1,X(I);X2(I);Y(I);X4(I)
2060 RETURN "TO MAIN PROGRAM"
2070 '
2080 '
2100 ' *** TEST TO REDEFINE GLOBAL GAIN ***
2110 IF VTST > =5 THEN G% =1: GOTO 2150
2120 IF VTST > =2 THEN G% =2: GOTO 2150
2130 IF VTST > =1 THEN G% =5: GOTO 2150
2140 G% =10
2150 RETURN
2160 IF VTST$="VX" THEN GT%=G%: GOSUB 1790: RETURN "CHANGE TO NEW X-GAIN"
2170 GS%=G%: GOSUB 1790 "CHANGE TO NEW Y-GAIN"
2180 RETURN
2190 '
2200 '
2250 ' *** GRAPHICS PARAMETERS ***
2255 SCREEN 0: CLS
2260 GSET$=ACT$ "SCREEN GRAPHICS ACTIVE"
2270 PRINT: PRINT: PRINT " *** SCREEN GRAPHICS PARAMETERS ***"
2275 PRINT* 1: PLOT TYPE (T=K-181 vs Temp.& H=K-181 vs Field): ",PLOT$
2280 PRINT* 2: X-axis Xmin, Xmax: ",XMIN,XMAX
2290 PRINT* 3: Y-axis Ymin, Ymax: ",YMIN,YMAX
2300 PRINT* 4: X-axis label: ",X$
2310 PRINT* 5: Y-axis label: ",Y1$;Y2$
2320 PRINT* 6: Graph Title: ",T$
2325 PRINT* 7: COMPARISON DATA SET FILENAME: ",GCOMFL$
2326 IF GCOMFL$="" THEN GOTO 2327 ELSE PRINT " TITLE: ";GTTL$
2327 PRINT* 8: VIEW COMPARISON DATA SET: ",GCSET$
2328 PRINT* 9: Ratio of E-alt/E-nano: ",RATIO
2329 PRINT*10: Include alt data in plots? (Y=Yes; N=No): ",VUIT$
2330 PRINT
2340 INPUT* > ENTER SELECTION # (<C/R> TO CONTINUE): ",ICODE
2350 ON ICODE GOTO 2362,2370,2390,2410,2430,2470,2481,2483,2462,2366
2355 CLS
2360 GOTO 2490
2362 INPUT* ENTER PLOT TYPE (T=K-181 vs Temp.& H=K-181 vs Field): ",PLOT$
2363 IF PLOT$="H" GOTO 2270
2364 IF PLOT$="T" GOTO 2270
2365 PRINT "Error": BEEP: GOTO 2362
2366 INPUT* INCLUDE ALT DATA IN PLOTS? (Y=Yes; N=No): ",VUIT$
2367 IF VUIT$="Y" GOTO 2270
2368 IF VUIT$="N" GOTO 2270
2369 PRINT "Error": BEEP: GOTO 2366
2370 INPUT* ENTER X-axis Xmin, Xmax: ",XMIN,XMAX
2380 GOTO 2270
2390 INPUT* ENTER Y-axis Ymin, Ymax: ",YMIN,YMAX
2400 GOTO 2270
2410 INPUT* ENTER X-axis label: ",X$
2420 GOTO 2270
2430 INPUT* ENTER Y-axis label: ",Y$

```

```

2440 FOR J=1 TO LEN(Y$): IF MID$(Y$,J,1) <> "(" THEN NEXT J
2450 Y1$=LEFT$(Y$,J-1): J=LEN(Y$)-J+1: Y2$=RIGHT$(Y$,J)
2460 GOTO 2270
2462 INPUT" ENTER Typical E-rho/E-hall Value: ",RATIO
2464 GOTO 2270
2470 INPUT" ENTER Graph Title: ",T$
2480 GOTO 2270
2481 IF FIXIT$="NO" THEN GOTO 2270 ELSE INPUT" ENTER COMPARISON FILE: ",GCOMFL$
2482 GOSUB 5800: GOTO 2270 'READ IN DATA SET FROM FILE
2483 IF FIXIT$="NO" THEN GOTO 2270 ELSE INPUT" VIEW PLOT OF DATA SET (Y=YES)?: ",ANS$
2484 IF ANS$="Y" OR ANS$="y" THEN GCSET$=ACT$ ELSE GCSET$=INACT$:GOTO 2270
2485 GOSUB 2490 'DEFINE GRAPH AXES RANGES
2486 GOSUB 5900 'PLOT DATA SET
2487 GOSUB 4111 'PRINT MESSAGE AT SCREEN BOTTOM
2488 IF INKEY$="" THEN 2488 ELSE SCREEN 0: GOTO 2270
2489 '
2490 XRNG=XMAX-XMIN: YRNG=YMAX-YMIN
2500 XMIN$=STR$(XMIN): XMAX$=STR$(XMAX)
2510 YMIN$=STR$(YMIN): YMAX$=STR$(YMAX)
2520 GOSUB 2610: GOSUB 2660 'DEFINE FUNCTION TO CALC COORD IN PIXELS
2530 RETURN
2540 '
2550 '
2600 '*** FN TO CALCULATE Y IN SCREEN PIXELS ***
2610 DEF FNYPIX(YVAR,YMIN,YRNG,DYPIX,YPIX0)=-(YVAR-YMIN)*DYPIX/YRNG+YPIX0+DYPIX
2620 RETURN
2630 '
2640 '
2650 '*** FN TO CALCULATE X IN SCREEN PIXELS ***
2660 DEF FNXPIX(XVAR,XMIN,XRNG,DXPIX,XPIX0)=(XVAR-XMIN)*DXPIX/XRNG+XPIX0
2670 RETURN
2680 '
2690 '
2700 ' *** PLOT OR PRINT DATA ***
2710 IF INK$ <> "L" THEN IF INK$ <> "I" THEN 2740
2720 IF FLG$="L" THEN 2780
2730 FLG$="L": GOSUB 3050: GOSUB 4050: RETURN 'LIST DATA TO CURRENT I
2740 IF GSET$=INACT$ THEN 2780
2750 IF INK$ <> "P" THEN IF INK$ <> "p" THEN 2780
2760 IF FLG$="P" THEN 2800
2770 FLG$="P": GOSUB 2900: GOSUB 4050: RETURN 'PLOT DATA TO CURRENT I
2780 IF FLG$="L" THEN PRINT I;X(I);X2(I);Y(I);X4(I): RETURN 'TO MAIN PROGRAM
2790 IF GSET$=INACT$ THEN 2840
2800 IF PLOT$="T" THEN XP=FNXPPIX(X(I),XMIN,XRNG,DXPIX,XPIX0)
2802 IF PLOT$="H" THEN XP=FNXPPIX(X4(I),XMIN,XRNG,DXPIX,XPIX0)
2805 IF ABS(XP)>10000 THEN 2840 '---OUT OF RANGE
2810 YP=FNYPIX(Y(I),YMIN,YRNG,DYPIX,YPIX0)
2812 IF VUIT$="Y" THEN YPR=X2(I)/RATIO
2813 IF VUIT$="Y" THEN YPR=FNYPIX(YPR,YMIN,YRNG,DYPIX,YPIX0)
2815 IF ABS(YP)>10000 THEN 2840
2820 PSET (XP,YP) 'PLOTS POINT
2825 IF VUIT$="Y" THEN PSET(XP,YPR) 'PLOTS RHO POINT
2830 IF THNMS="" GOTO 2840
2833 LOCATE 1,67: PRINT "T= " INT(T) " K ";
2836 LOCATE 24,1
2840 RETURN 'TO MAIN PROGRAM
2850 '
2860 '
2900 ' *** REFRESH PLOT OF DATA UP TO CURRENT POINT ***
2910 CLS: GOSUB 3150: GOSUB 3300 'DRAW AND LABEL AXES
2920 FOR J=1 TO I
2930 IF PLOT$="T" THEN XP=FNXPPIX(X(J),XMIN,XRNG,DXPIX,XPIX0)
2932 IF PLOT$="H" THEN XP=FNXPPIX(X4(J),XMIN,XRNG,DXPIX,XPIX0)
2935 IF ABS(XP)>10000 THEN 2970 '---OUT OF RANGE
2940 YP=FNYPIX(Y(J),YMIN,YRNG,DYPIX,YPIX0)
2942 IF VUIT$="Y" THEN YPR=X2(J)/RATIO
2943 IF VUIT$="Y" THEN YPR=FNYPIX(YPR,YMIN,YRNG,DYPIX,YPIX0)

```



```

2945 IF ABS(YP) > 10000 THEN 2970
2950 'CIRCLE (XP,YP),3
2960 PSET (XP,YP)
2965 IF VUIT$="Y" THEN PSET (XP,YPR)
2970 NEXT J
2975 IF GCOMPL$="" THEN RETURN
2976 IF GCSET$=ACT$ THEN GOSUB 5920 ' PLOT COMPARISON DATA
2980 RETURN
3000 '
3010 '
3050 '*** PRINT DATA ON SCREEN ***
3060 SCREEN 0: CLS
3070 J1=I-20: IF J1 < 0 THEN J1=1
3080 FOR J=J1 TO I
3090 PRINT J;X(J);X2(J);Y(J);X4(J)
3100 NEXT J
3110 RETURN
3120 '
3130 '
3150 '*** SUB TO DRAW GRAPH AXES ***
3160 SCREEN 9 'HI RES GRAPHICS SCREEN
3170 CLS
3180 PSET (80,15)
3190 DWN=300: RGT=550: TICKU=30: TICKR=55: ZERO=0
3200 FOR J=1 TO 10: DRAW"D=TICKU;NM+550,0;": NEXT J '---LEFT VERT AXIS
3210 FOR J=1 TO 10: DRAW"R=TICKR;NM+0,-300;": NEXT J '---BOTTOM HORIZ AXIS
3220 DRAW"U=DWN;L=RGT;":
3230 RETURN
3240 '
3250 '
3300 '*** SUB TO LABEL AXES ***
3310 IF LEN(X$) > 60 THEN X$=LEFT$(X$,60) 'TRUNCATE IF TOO LONG
3320 XAX=44-.5*LEN(X$)
3330 LOCATE 24,XAX: PRINT X$;
3340 IF LEN(Y1$) > 9 THEN Y1$=LEFT$(Y1$,9) 'TRUNCATE IF TOO LONG
3350 TAX=5-.5*LEN(Y1$)
3360 LOCATE 12,TAX: PRINT Y1$;
3370 IF LEN(Y2$) > 9 THEN Y2$=LEFT$(Y2$,9)
3380 TAX=5-.5*LEN(Y2$)
3390 LOCATE 13,TAX: PRINT Y2$;
3400 IF LEN(T$) > 70 THEN T$=LEFT$(T$,70) 'TRUNCATE IF TOO LONG
3410 TAX=44-.5*LEN(T$)
3420 LOCATE 1,TAX: PRINT T$;
3430 LOCATE 24,12-LEN(XMIN$): PRINT XMIN$;
3440 IF XMAX$="" THEN 3460
3450 LOCATE 24,81-LEN(XMAX$): PRINT XMAX$;
3460 LOCATE 23,10-LEN(YMIN$): PRINT YMIN$;
3470 LOCATE 2,10-LEN(YMAX$): PRINT YMAX$;
3480 RETURN
3490 '
3500 '
3550 ' *** SUB TO CHECK KEYBOARD STATUS ***
3560 IN$=INKEY$
3570 IF IN$="" THEN RETURN
3580 IF IN$=CHR$(13) THEN IDATFLG=1: GOTO 3710 'MANUAL DATA STORAGE
3590 INK$=IN$
3600 IF INK$ < > "Q" AND INK$ < > "q" THEN 3675
3610 IF DNMS$="" THEN 3625 'DATA FILENAME
3620 CLOSE #1: SCREEN 0: GOSUB 6000 '---REWRITE DATA TO FILE IN STD FORMAT
3625 PRINT#2,"OUTPUT";PADDR$;";FOX" 'turn off current
3630 SCREEN 0: INPUT "ANOTHER DATA SET? (Y/N):",ANS2$
3640 IF ANS2$="y" OR ANS2$="Y" THEN 3670
3650 ON ERROR GOTO 0 'DISABLE ERROR TRAPPING
3655 PRINT#2,"LOCAL";TADDR$
3660 CLS: END
3670 CLOSE: RETURN 240 'TO MAIN PROGRAM AT MENU
3675 IF INK$="G" OR INK$="g" THEN FLG$="L": FEXIT$="NO": GOSUB 2250

```

```

3677 IF INK$="G" OR INK$="g" THEN INK$="P" : FIXIT$="" : GOSUB 4120
3680 IF INK$ <> "P" THEN IF INK$ <> "p" THEN RETURN
3690 IF INK$ <> "I" THEN IF INK$ <> "L" THEN RETURN
3700 RETURN 320 'TO MAIN PROGRAM AT PLT OR PRNT DATA
3710 RETURN 260 'TO MAIN PROGRAM AT TAKE ONE DATUM
3720 '
3730 '
3750 '*** SUB TO INTERPOLATE TEMPERATURES FROM DIODE T,V TABLE ***
3760 IF THNMS="" THEN RETURN 'TO MAIN PROGRAM
3770 VXC=VX
3780 NLO=1: NHI=NDATA 'LOW AND HI INDICES OF TABLE DATA
3790 N=(NHI+NLO)/2 'INTEGER DIVIDE 'TABLE INDEX TO BE COMPARED TO DATUM
3800 IF VX < V(N) THEN NHI=N: GOTO 3820
3810 NLO=N
3820 IF NHI <> NLO+1 THEN GOTO 3790
3830 T=T(NHI)+(VX-V(NHI))*(T(NHI)-T(NLO))/(V(NHI)-V(NLO))
3840 RETURN
3850 '
3860 '
3900 '*** SUB TO READ IN THERM. CALIB DATA ***
3910 IF THNMS="" THEN RETURN
3930 THNMT$=THNMS
3940 PRINT"*** Reading in therm. calibration table ***"
3950 OPEN "I",#1,THNMS
3952 INPUT#1, THTTLS '---TITLE OF DATA SET
3960 INPUT #1,NDATA
3970 FOR J=1 TO NDATA
3980 INPUT #1,V(J),T(J)
3990 NEXT J
4000 CLOSE #1
4010 RETURN
4020 '
4030 '
4050 '*** PRINT MESSAGE AT BOTTOM OF SCREEN ***
4060 IF GSET$=ACT$ THEN 4090
4070 CLS: LOCATE 25,1: PRINT"PRESS: <C/R> STORE PT. <Q> QUIT <G> GRAPHICS";
4080 LOCATE 1,1: GOTO 4110
4090 LOCATE 25,1: PRINT"PRESS: <C/R> STORE PT. <Q> QUIT <P> PLOT RESTORE <L> LIST <G>
GRAPHICS";
4100 LOCATE 24,1
4110 RETURN
4111 LOCATE 25,1: PRINT" PRESS <C/R> TO CONTINUE";
4112 LOCATE 24,1
4113 RETURN
4120 LOCATE 25,1: PRINT" PLEASE STANDBY";
4122 LOCATE 24,1
4125 RETURN
4128 '
4130 '
4150 '*** READ IN SETUP AND GRAPHICS PARAMETERS ***
4160 IF PUFL$="" THEN RETURN
4170 OPEN "I",#1, PUFL$
4180 PRINT"*** RETRIEVING PARAMETERS FROM: ";PUFL$;" ***"
4190 '---SETUP PARAMETERS
4195 INPUT#1,PSFL$
4200 INPUT #1,SCALEX
4205 INPUT #1,SCALEX2
4207 INPUT #1,SCALEI
4210 INPUT #1,DEL
4220 INPUT #1,SCALEY
4230 INPUT #1,DELY
4235 INPUT #1,DELMAG
4240 INPUT #1,DNMS
4250 INPUT #1,TITLE$
4260 DUM$=TITLE$
4270 INPUT #1,THNMS
4280 INPUT #1,NFILT

```



```

4290 INPUT #1,GSET$
4300 '---GRAPHICS PARAMETERS
4305 INPUT #1,PLOTS
4306 INPUT #1,RATIO
4307 INPUT #1,VUTTS
4310 INPUT #1,XMIN,XMAX
4320 INPUT #1,YMIN,YMAX
4330 INPUT #1,X$
4340 INPUT #1,Y1$
4350 INPUT #1,Y2$
4360 INPUT #1,T$
4370 '---GPIB & METER PARAMS
4380 INPUT#1,XADDR$
4390 INPUT#1,YADDR$
4400 INPUT#1,MXS
4410 INPUT#1,MYS
4420 INPUT#1,NXM,NYM
4422 '--- COMPARISON GRAPHICS DATA FILE INFO
4424 INPUT#1,GCOMFL$ 'DATA FILENAME
4426 INPUT#1,GCSET$ 'FLAG FOR GRAPHICS COMPARISON
4428 INPUT#1,CURRNT$ 'TRANSPORT CURRENT
4430 CLOSE #1
4440 IF GSET$=ACT$ THEN GOSUB 5800: GOSUB 2490 '---READ IN COMP DATA SET
4445 GOSUB 3900 '---READ IN THERM CALIB. DATA
4450 RETURN
4460 '
4470 '
4500 '*** SAVE SETUP AND GRAPHICS PARAMETERS TO FILE ***
4510 IF PSFL$="" THEN RETURN
4520 OPEN "O",#1, PSFL$
4530 PRINT"*** STORING PARAMETERS TO: ";PSFL$;" ****"
4540 '---SETUP PARAMETERS
4545 PRINT#1,PSFL$
4550 PRINT#1,SCALEX
4555 PRINT#1,SCALEX2
4557 PRINT#1,SCALEI
4560 PRINT#1,DEL
4570 PRINT#1,SCALEY
4580 PRINT#1,DELY
4585 PRINT#1,DELMAG
4590 PRINT#1,DNM$
4600 PRINT#1,TITLE$
4610 PRINT#1,THNMS
4620 PRINT#1,NFILT
4630 PRINT#1,GSET$
4640 '---GRAPHICS PARAMETERS
4645 PRINT#1,PLOTS
4646 PRINT#1,RATIO
4647 PRINT#1,VUTTS
4650 PRINT#1,XMIN,XMAX
4660 PRINT#1,YMIN,YMAX
4670 PRINT#1,X$
4680 PRINT#1,Y1$
4690 PRINT#1,Y2$
4700 PRINT#1,T$
4710 '---GPIB & METER PARAMS
4720 PRINT#1,XADDR$
4730 PRINT#1,YADDR$
4740 PRINT#1,MXS
4750 PRINT#1,MYS
4760 PRINT#1,NXM,NYM
4762 '---COMPARISON GRAPHICS DATA FILE INFO
4764 PRINT#1,GCOMFL$ 'FILENAME OF COMPARISON DATA SET
4766 PRINT#1,GCSET$ 'FLAG FOR ACTIVE GRAPICS COMPARISON
4768 PRINT#1,CURRNT$ 'TRANSPORT CURRENT
4770 CLOSE #1
4780 RETURN

```

```

4790 '
4800 '
4850 ' *** Establish communications with Personal488 ***
4860 OPEN "\DEV\IEEEOUT" FOR OUTPUT AS #2
4870 'Reset Personal488
4880 IOCTL#2,"BREAK"
4885 PRINT#2,"RESET"
4890 'Open file to read responses from Personal488
4900 OPEN "\DEV\IEEEIN" FOR INPUT AS #3
4904 'Enable SEQUENCE error detection by Personal488
4905 PRINT#2,"FILL ERROR"
4906 PRINT#2,"TIME OUT 5"
4910 RETURN
4920 '
4930 '
4950 ' *** Read the signon and revision message ***
4960 PRINT#2,"HELLO"
4970 INPUT#3,A$
4980 PRINT AS
4990 RETURN
5000 '
5010 '
5050 '*** Put the 197's into REMOTE ***
5060 PRINT#2,"REMOTE";YADDR$
5070 PRINT#2,"REMOTE";XADDR$
5075 PRINT#2,"REMOTE";PADDR$
5090 'R0: Auto range X: Execute PO: Disable filter T1: Trigger @ read
5100 PRINT#2,"OUTPUT";XADDR$;"R0FOX"
5110 PRINT#2,"OUTPUT";YADDR$;"P0T1X"
5115 PRINT#2,"OUTPUT";PADDR$;"D0R0G1FOX"
5116 PRINT#2,"OUTPUT";PADDR$;"I";CURR$;"FIX" 'turn on current
5130 RETURN
5140 '
5150 '
5200 ' *** Find the average of Navg readings ***
5210 SUMX=0: SUMX2=0: SUMY=0: VERI=0: SUMX4=0
5212 FOR I1=1 TO 2
5214 IF I1=1 THEN PRINT#2,"OUTPUT";PADDR$;"I";CNEG$;"FIX" '- curr
5216 IF I1=2 THEN PRINT#2,"OUTPUT";PADDR$;"I";CURR$;"FIX" '+ curr
5218 FOR J1=1 TO 10 : NEXT J1 'time delay
5220 FOR J=1 TO NFILT
5225 PRINT#2,"OUTPUT";YADDR$;"FOX" 'Uses front panel range
5227 FOR J1=1 TO JD : NEXT J1 'time delay
5230 PRINT#2,"ENTER";YADDR$
5235 INPUT#3,R$: VALY=VAL(MID$(R$,NYM))
5240 IF ABS(VALY)>100 THEN GOSUB 5350: GOTO 5210 '---START OVER
5245 IF I1=1 THEN SUMY=SUMY-VALY ELSE SUMY=SUMY+VALY
5246 NEXT J
5247 NEXT I1
5248 SUMX=0: SUMX2=0: VERI=0: SUMX4=0
5250 PRINT#2,"OUTPUT";XADDR$;"R0N1X" '---Uses X-scanner channel # 1
5252 FOR J1=1 TO JD : NEXT J1 'time delay
5255 PRINT#2,"ENTER";XADDR$
5260 INPUT#3,R$: VALX=VAL(MID$(R$,NXM))
5265 IF ABS(VALX)>100 THEN GOSUB 5350: GOTO 5248 '---PARTIAL RESTART
5269 SUMX=ABS(VALX) 'DOES NOT filter the thermometer readings !
5270 FOR I2=1 TO 2
5271 IF I2=1 THEN PRINT#2,"OUTPUT";PADDR$;"I";CNEG$;"FIX" '- curr
5272 IF I2=2 THEN PRINT#2,"OUTPUT";PADDR$;"I";CURR$;"FIX" '+ curr
5273 FOR J1=1 TO 10 : NEXT J1 'time delay
5274 FOR J=1 TO NFILT
5275 PRINT#2,"OUTPUT";XADDR$;"R0N3X" '---Uses X-scanner channel # 3
5277 FOR J1=1 TO JD : NEXT J1 'Time Delay for Auto Range Chng.
5280 PRINT#2,"ENTER";XADDR$
5285 INPUT#3,R$: VALX2=VAL(MID$(R$,NXM))
5287 PRINT#2,"OUTPUT";XADDR$;"R0N4X" '---Uses X-scanner channel # 4
5288 FOR J1=1 TO JD : NEXT J1 'time delay

```



```

5290 PRINT#2,"ENTER";XADDR$
5293 INPUT#3,R$: VALX4=VAL(MID$(R$,NXM))
5295 IF I2=1 THEN SUMX2=SUMX2-VALX2 ELSE SUMX2=SUMX2+VALX2
5300 SUMX4=SUMX4+ABS(VALX4)
5302 PRINT#2,"OUTPUT";XADDR$;"R0N2X" '---Uses X-scanner channel # 2
5303 FOR J1=1 TO JD : NEXT J1      'time delay
5304 PRINT#2,"ENTER";XADDR$
5306 INPUT#3,R$: VERIF=VAL(MID$(R$,NXM))
5307 IF ABS(VERIF)>100 THEN GOSUB 5350: GOTO 5248 '---PARTIAL RESTART
5308 IF I2=1 THEN VERI=VERI-VERIF ELSE VERI=VERI+VERIF
5310 NEXT J
5312 NEXT I2
5320 SUMX2=ABS(SUMX2/(2*NFLT)): SUMY=SUMY/NFLT: VERI=ABS(VERI/(2*NFLT))
5325 SUMX4=SUMX4/(2*NFLT): SUMY=SUMY/2      'correct for + & - data sets
5330 RETURN
5340 '
5350 '*** PRINTOUT MESSAGE FOR BAD READING ***
5360 PRINT CHR$(7);
5365 IF FLG$="L" OR FLG$="I" THEN PRINT ">>> BAD READING <<<";R$
5370 RETURN
5380 '
5390 '
5400 '*** ERROR TRAPPING ***
5410 PRINT CHR$(7); '---BELL TO INDICATE ERROR
5420 IF ERR <> 53 THEN RESUME 260 '---TRY TO TAKE MORE DATA
5425 PRINT">> BAD FILENAME <<": FOR J=1 TO 1000: NEXT J: RESUME 240
5440 '
5450 '
5500 ' *** INCREMENT EXTENSION ON DATA FILENAME ***
5510 PRINT CHR$(7)
5520 IF DNM$="" THEN RETURN
5530 FOR J=1 TO LEN(DNM$): IF MID$(DNM$,J,1) <> "." THEN NEXT J
5540 J1=LEN(DNM$)-J+1
5550 EXT$=RIGHT$(DNM$,J1): DNM$=LEFT$(DNM$,J-1)
5560 IEXT=VAL(RIGHT$(EXT$,1)): IEXT=IEXT+1
5570 IEXT$=RIGHT$(STR$(IEXT),1)
5580 EXT$=LEFT$(EXT$,3)+IEXT$
5590 DNM$=DNM$+EXT$
5600 RETURN
5610 '
5620 '
5800 '*** READ IN DATA SET FOR GRAPHICS COMPARISON ***
5805 PRINT"*** RETRIEVING COMPARISON DATA SET *****"
5810 IF GCOMFL$="" THEN RETURN
5820 OPEN"1",#1, GCOMFL$
5822 INPUT#1, GTTL$ '---TITLE OF FILE DATA
5830 INPUT#1, NDATG
5835 XMX=XG(1): XMN=XG(1): YMX=YG(1): YMN=YG(1)
5840 FOR J=1 TO NDATG
5850 INPUT#1, XG(J),X2G,YG(J),XG4(J)
5852 IF PLOT$="H" GOTO 5882
5855 IF XG(J)>XMX THEN XMX=XG(J): GOTO 5857
5856 IF XG(J)<XMN THEN XMN=XG(J)
5857 IF YG(J)>YMX THEN YMX=YG(J): GOTO 5860
5858 IF YG(J)<YMN THEN YMN=YG(J)
5860 NEXT J
5870 CLOSE #1
5875 PRINT" XMIN: ";XMN,"XMAX: ";XMX
5876 PRINT" YMIN: ";YMN,"YMAX: ";YMX
5880 RETURN
5882 IF XG4(J)>XMX THEN XMX=XG4(J): GOTO 5857
5884 IF XG4(J)<XMN THEN XMN=XG4(J)
5886 GOTO 5857
5890 '
5900 ' *** PLOT OF COMPARISON DATA ***
5910 CLS: GOSUB 3150: GOSUB 3300 'DRAW AND LABEL AXES
5920 FOR J=1 TO NDATG

```

```

5930 IF PLOT$="T" THEN XP=FNXP(XG(J),XMIN,XRNG,DXPIX,XPIX0)
5932 IF PLOT$="H" THEN XP=FNXP(XG4(J),XMIN,XRNG,DXPIX,XPIX0)
5935 IF ABS(XP)>10000 THEN 5970 '—OUT OF RANGE
5940 YP=FNYP(YG(J),YMIN,YRNG,DYPIX,YPIX0)
5945 IF ABS(YP)>10000 THEN 5970
5950 CIRCLE (XP,YP),1
5960 'PSET (XP,YP)
5970 NEXT J
5980 RETURN
5990 '
6000 '*** REWRITE DATA TO FILE AFTER INTERPOLATING TO USER SPECIFICATIONS ***
6002 LOCATE 24,1
6005 IF DNMS="" THEN RETURN
6010 NP=1 'NO. OF DATA POINTS IN SET
6015 OPEN"O",#1, DNMS
6020 PRINT#1, TITLE$
6025 PRINT#1,NP '—No. data points in set
6030 INPUT "Do you wish to sort data according to temperature <Y=Yes> ? ";RR$
6035 IF RR$="Y" THEN PRINT "**** STORING SORTED DATA TO FILE ****" : GOTO 6075
6040 IF RR$="y" THEN PRINT "**** STORING SORTED DATA TO FILE ****" : GOTO 6075
6045 PRINT "**** STORING DATA ARRAY DIRECTLY TO FILE ****"
6050 FOR J=1 TO NP
6055 PRINT#1, X(J);X2(J);Y(J);X4(J)
6060 NEXT J
6065 CLOSE#1
6070 RETURN
6075 PRINT: LOCATE 24,1: PRINT "Percentage Completed: ";
6076 FOR I=1 TO NP
6077 COMPL=INT(100*(I/NP)+.5)
6079 LOCATE 24,23: PRINT COMPL;
6080 TMP=X(1) : JP=1
6085 FOR J=1 TO NP
6090 IF TMP>X(J) THEN TMP=X(J) : JP=J
6095 NEXT J
6100 PRINT#1, X(JP);X2(JP);Y(JP);X4(JP)
6105 IF I=1 THEN TMIN=X(JP)
6110 IF I=NP THEN TMAX=X(JP)
6115 X(JP)=999999!
6120 NEXT I
6125 CLOSE#1
6130 FOR I=1 TO 500
6135 X(I)=0 : X2(I)=0 : Y(I)=0 : X4(I)=0
6140 NEXT I
6145 IF THNMS="" THEN RETURN
6150 PRINT : PRINT "Tmin = " TMIN " & Tmax = " TMAX : PRINT
6155 INPUT"Do you wish to interpolate temperatures <Y=Yes> ? ";RR$
6160 IF RR$="Y" GOTO 6170
6165 IF RR$="y" THEN 6170 ELSE RETURN
6170 INPUT"ENTER Tmin, Tmax & T-interval for data interpolation: ";TMIN,TMAX,DLT
6175 NN=INT(1+(TMAX-TMIN)/DLT) 'No. of data points to interpolate
6180 IF NN>500 THEN PRINT "Too Many Data Points !" : BEEP : GOTO 6170
6185 IF TMIN>TMAX THEN PRINT "Try Again !" : BEEP : GOTO 6170
6190 PRINT "Interpolating Data for Output ..." : PRINT
6192 LOCATE 24,1: PRINT "Percentage Completed: ";
6195 FOR J=1 TO NN
6196 COMPL=INT(100*(J/NN)+.5)
6198 LOCATE 24,23: PRINT COMPL;
6200 TMP=TMIN+DLT*(J-1)
6205 OPEN"I",#1, DNMS
6210 INPUT#1, TITLE$
6215 INPUT#1, NP
6220 T2=0 : HALL2=0 : RHO2=0 : RMAG2=0
6225 K=1 'Do-Loop to find values nearest temp=TMP
6230 T1=T2 : HALL1=HALL2 : RHO1=RHO2 : RMAG1=RMAG2
6235 INPUT#1, T2,RHO2,HALL2,RMAG2
6240 IF T2<TMP THEN IF K<NP THEN K=K+1 : GOTO 6230
6245 CLOSE#1

```



```

6250 X(J)=TMP                                'Interpolation Temperature
6255 X2(J)=(TMP-T1)*(RHO2-RHO1)/(T2-T1)+RHO1  'Interpolated RHO value
6260 Y(J)=(TMP-T1)*(HALL2-HALL1)/(T2-T1)+HALL1 'Interpolated HALL value
6265 X4(J)=(TMP-T1)*(RMAG2-RMAG1)/(T2-T1)+RMAG1 'Interpolated H(kOe) value
6270 NEXT J
6272 PRINT: PRINT "Interpolation of data complete ...": BEEP: BEEP
6275 PRINT "*** STORING INTERPOLATED DATA TO FILE ***"
6280 OPEN "O", #1, DNMS$
6285 PRINT #1, TTLES$
6290 PRINT #1, NN      'No. Interpolated Data Points in the Set.
6295 FOR I=1 TO NN
6300 PRINT #1, X(I);X2(I);Y(I);X4(I)
6305 NEXT I
6310 CLOSE #1
6320 RETURN
6330 '
9000 ' *** LAKESHORE TEMPERATURE CONTROLLER PARAMETERS ***
9010 PRINT #2, "REMOTE"; TADDR$
9020 PRINT #2, "OUTPUT"; TADDR$; ";F0KF1AKF2A0"      'Display Units
9030 IF T >= 45 THEN PRINT #2, "OUTPUT"; TADDR$; ";R5I15D0.0W0" 'Control Settings
9035 IF T < 45 AND T >= 19 THEN PRINT #2, "OUTPUT"; TADDR$; ";R4I10D0.5W0" 'Med. heat
9037 IF T < 19 THEN PRINT #2, "OUTPUT"; TADDR$; ";R3I10D1.0W0"      'Low heat
9040 IF T >= 130 THEN PRINT #2, "OUTPUT"; TADDR$; ";P10"      'Gain Setting = 10
9050 IF T >= 65 AND T < 130 THEN PRINT #2, "OUTPUT"; TADDR$; ";P6.0" 'Gain = 6
9060 IF T >= 25 AND T < 65 THEN PRINT #2, "OUTPUT"; TADDR$; ";P3.0" 'Gain = 3
9070 IF T < 25 THEN PRINT #2, "OUTPUT"; TADDR$; ";P0.5"      'Gain = 0.5
9080 TC=T+SQR(ABS(T)/300)*TCDEL      'Calculate the Set Point
9083 IF ABS(T)>40 THEN TC=TC+.00897*ABS(T)+1.309      'CGR Correction Factor
9086 IF ABS(T)<=40 THEN TC=TC+.0417*ABS(T)      'CGR Correction Factor
9090 IF TC<TC1 THEN TC=TC1      'Minimum Set Point Allowed
9100 IF TC>TC2 THEN TC=TC2      'Maximum Set Point Allowed
9110 TC$=";"&STR$(INT(10*TC)/10)
9120 PRINT #2, "OUTPUT"; TADDR$; TC$      'Set Point Temperature
9130 RETURN
10000 END

```

Appendix B. Critical Current Acquisition Program

```

10 DEFINT I-N
20 '
30 ' *** JcTH.BAS *** "Smart" Jc determination, using K-228 Pwr Suppl
31 ' - - - with steps up & back defined as Fractions of Xminc.
40 '*** KEITHLEY 570 SYSTEM ***
50 '*** PERSONAL488 DATA AQUISITION ***
100 ' X-VOLTAGE (J) IS STEPPED, AS CONTROLLED BY K-228 Power Supply
105 ' Program operates digital Pwr Suppl in Curr-limited mode with 10% spare V
106 ' K-228 mini step is 1/1000 of any Full-Range V: 1, 10; I: 0.1, 1, 10
107 ' There is provision (Menu step 13) for manual search for -Ic
110 ' ACQUIRED X1, X2, X4 AND Y DATA UPON SPECIFIED Y-VOLTAGE CRITERION.
111 ' X's @ #1, 2 & 4 rear inputs of X-meter. #2=Sam-curr stdR, #4=Mag curr;
112 ' #1 = Thermometer: This gets converted to T(K); Mag curr=plot-X
120 ' DATA STORED TO ASCII FILE. PLOTS AUXILIARY DATA FILE FOR COMPARISON
130 ' COMMAND P0 SENT TO Y-DVM (FOR K-181 TURNS OFF DIGITAL FILTERING)
132 ' JcH = Meas Jc[Ic] vs H (Imag*Scalemag); with No cooling pauses [jp]
133 ' # Ic is interpolated between last below-Vc & 1st above-Vc reads of I.
134 ' *** Waits after ca recorded pt for Input new Xminc or use prgm value.
135 ' ** AUTO mode available: Set AUTODATA=1 for continuous recording per prgm
136 ' >>> * * Now uses + & - curr, with minimum switching of K-228
137 ' * note that Like old JcZ, this has delx as fraction of x.
138 ' # * Saves avgStd Dev of Ic calc'd from extrapolated Hi&Lo err limits.
139 ' # *when V>Vc on 1st pass then stores I,Vy,I,T; not Ic,asdV,csdI,T
140 'TWO RANGES: Now has a low current output mode (MODE$="L") allowing
145 ' 1 uA < I < 10 mA operating range. This is achieved by

```



```

150 '      use of a 1000 ohm std. resistor and utilization of the
155 '      voltage limit mode of the K-228...
160 ' Maintains Temperature Controller Set Point to values based on user
162 ' input and current sample temperature (optional).
190 '
200 '*** MAIN PROGRAM ***
210 '
220 GOSUB 400 '--- SET DEFAULT PARAMETER VALUES ---
225 GOSUB 4150 '--- READ IN FILE OF SETUP AND GRAPHICS PARAMETERS ---
230 GOSUB 700 '--- SIGN-ON & HARDWARE SETTINGS MENU ---
240 GOSUB 1000 '--- SETUP PARAMETERS MENU ---
245 GOSUB 4500 '--- STORE SETUP AND GRAPHICS PARAMS TO FILE ---
246 AUTODATA=0 '---for Manual Initiation of data. Set AUTO=1 for auto.
250 GOSUB 1600 '--- DATA ACQUISITION INITIALIZATION ---
251 VXL=0 '--- preset for initial pass
252 DELXC=DELX*XMINC 'initial step size
253 IF MODE$="H" THEN IF DELXC < .0001 THEN DELXC = .0001
254 IF MODE$="L" THEN IF DELXC < .000001 THEN DELXC = .000001
255 FOR XC=XMINC TO XMAXC STEP DELXC '---STEP SCAN X-PARAMETER
256 GOSUB 7500 ' Get Pwr Supp control params spos$, sneg$ from XC, RCIRC
260 GOSUB 1750 '--- TAKE ONE FILTERED DATUM-THERMAL EMP ---
270 GOSUB 3550 '--- CHECK FOR KEYBOARD INTERRUPT ---
280 GOSUB 1850 '--- TEST DATA FOR OUTPUT ---
290 GOSUB 3550 '--- CHECK FOR KEYBOARD INTERRUPT ---
295 NEXT XC '--- LOOP BACK FOR MORE DATA --
297 GOTO 346
300 GOSUB 3750 '--- CALC. TEMP. FROM THERM. CALIBRATION ---
301 IF TSET$=ACT$ THEN GOSUB 9000 '---TEMPERATURE CONTROLLER SET POINTS---
302 GOSUB 6200 '--- Test TEMP. for designated interval---
310 GOSUB 2000 '--- PRINT DATA TO DISK ---
320 GOSUB 2700 '--- PLOT OR PRINT DATA TO SCREEN ---
330 GOSUB 3550 '--- CHECK FOR KEYBOARD INTERRUPT ---
338 IF AUTODATA=1 GOTO 341
340 INPUT " ",XCC: IF XCC < > 0 THEN XMINC=XCC: DELXC=XCC*DELX: GOTO 342
341 XMINC=XCC*(1-XOFFC): DELXC=XCC*DELX '--- Rerefine DELXC & Take more data .
342 IF MODE$="H" THEN IF DELXC < .0003 THEN DELXC = .0003 : GOTO 255
343 IF MODE$="L" THEN IF DELXC < .000005 THEN DELXC = .000005 : GOTO 255
344 GOTO 255
346 LOCATE 24,1: PRINT"--- SCAN FINISHED ---";
347 GOSUB 3550 '--- CHECK FOR KEYBOARD INTERRUPT ---
348 GOTO 347
349 GOTO 240
350 '
360 '*** END MAIN PROGRAM ***
370 '
380 '
400 '*** DEFINE DEFAULT PARAMETERS ***
410 CLS: KEY OFF: KEY 1,"LIST 200-400"+CHR$(13)
420 DEFINT I-N
425 JD=30 'JD=1400 for ~.25 sec delay after curr-switching
427 EMSTOP=.00003 'allowed safety limit for sample voltage
428 HLIMIT=50 'allowed safety limit for sample heating (mW)
430 DIM X(500),Y(500),ZT(500),XM(500),Q(500),YD(20) 'DIM DATA
440 DIM V(200),T(200) 'ARRAY FOR THERM. CALIBRATION TABLE(e.g. DIODE V,T)
445 DIM XG(500),YG(500),ZG(500),XMG(500),QG(500) 'COMPARISON DATA FOR GRAPHICS
450 ON ERROR GOTO 5400 '---ERROR TRAPPING
460 RESTORE 470
470 DATA 10,1,2,1,0,0,1,1,1,1
480 READ CUR,SCALEX,RCIRC,SCALEY,DEL,DELY,G0%,G1%,NFILT,SCALEZ 'Defaults
490 DATA "<INACTIVE>","<ACTIVE>"
500 READ INACT$,ACT$: GSET$=INACT$: GCSET$=INACT$: TSET$=INACT$
504 '--- GPIB BUS ADDRESSES & METER PARAMS
505 K$="KEITHLEY 181/199/197" '--- GPIB BUS ADDRESSES & METER PARAMS
506 KP$="Keithley 228 Power Supply"
507 DATA " 26"," 14"," 11"," 5,5,1","H"," 12"
508 READ XADDR$,YADDR$,PADDR$,NXM,NYM,NPM,MODE$,TADDR$
509 MX$=K$: MY$=K$: MP$=KP$

```



```

510 '
520 'GRAPHICS DEFAULT PARAMETERS
530 RESTORE 550
540 READ XMIN,XMAX,YMIN,YMAX
550 DATA 0,100,0,1,0
560 READ X$,Y1$,Y2$,T$
570 RESTORE 590
580 READ X$,Y1$,Y2$,T$
590 DATA "X-AXIS(UNITS)", "Y-AXIS", "(UNITS)", "TITLE OF GRAPH"
600 RESTORE 620
610 READ DXPIX,DYPIX, XPIX0,YPIX0 'AXIS CONTANTS IN PIXELS
620 DATA 550,300,80,15
630 RETURN 'TO MAIN PROGRAM
640 '
650 '
700 '*** SIGN-ON HARDWARE SETTINGS MESSAGE ***
710 CLS: PRINT CHR$(7)
720 PRINT:PRINT " *** HARDWARE SETTINGS ***"
730 PRINT " 1: X-INPUT: GPIB Address: ";XADDR$; " Meter ID: ";MX$
740 PRINT " 2: Y-INPUT: GPIB Address: ";YADDR$; " Meter ID: ";MY$
747 PRINT " 3: P-INPUT: GPIB Address: ";PADDR$; " Pwr Supp ID: ";MP$
750 PRINT:PRINT
752 PRINT " Meter Setup: X channel #1 <===> Thermometer Voltage Signal"
754 PRINT " X channel #2 <===> Sample Current Std. Resistor"
755 PRINT " X channel #3 <===> Sample Heat Dissipation Signal"
756 PRINT " X channel #4 <===> Magnet Curr. 1/100 Ohm Resistor"
758 PRINT " Y voltmeter <===> Sample Voltage ":PRINT
759 PRINT " Reset DRC-91C & Set GPIB address to ";TADDR$: PRINT
760 INPUT"ENTER SELECTION # (<C/R> TO CONTINUE): ",ICODE
770 ON ICODE GOTO 790,810,840
780 RETURN 'TO MAIN PROGRAM
790 INPUT"ENTER NEW GPIB ADDRESS FOR X-INPUT: ",XADDR
791 GOSUB 850 '--- METER ID CHOICES FOR READING STRING MASKING
792 INPUT"ENTER X-INPUT Meter ID CODE (DEFAULT = PREVIOUS): ",NMT
794 IF NMT < > 0 THEN NM=NMT ELSE 800
796 GOSUB 900: MX$=M$: NXM=NMSK '--- ASSIGN METER ID NAME & MASKING DATA
800 XADDR$=STR$(XADDR): GOTO 720
810 INPUT"ENTER NEW GPIB ADDRESS FOR Y-INPUT: ",YADDR
811 GOSUB 850 '--- METER ID CHOICES
812 INPUT"ENTER Y-INPUT Meter ID CODE (DEFAULT = PREVIOUS): ",NMT
814 IF NMT < > 0 THEN NM=NMT ELSE 820
816 GOSUB 900: MY$=M$: NYM=NMSK '--- ASSIGN METER ID NAME & MASKING DATA
820 YADDR$=STR$(YADDR): GOTO 720
840 INPUT"ENTER NEW GPIB ADDRESS FOR P-INPUT: ",PADDR
841 GOSUB 850 '--- METER ID CHOICES
842 INPUT"ENTER P-INPUT Meter ID CODE (DEFAULT = PREVIOUS): ",NMT
843 IF NMT < > 0 THEN NM=NMT ELSE 848
844 GOSUB 900: MP$=M$: NPM=NMSK '--- ASSIGN METER ID NAME & MASKING DATA
848 PADDR$=STR$(PADDR): GOTO 720
849 '
850 ' *** ASSIGN STRING MASKING PARAMS FOR METERS ***
854 PRINT "*** Meter ID Codes ***"
855 PRINT" 1: KEITHLEY 181,199,197
856 PRINT" 2: FLUKE 8840A
857 PRINT" 3: Keithley 228 Pwr Supp
860 RETURN
870 '
880 '
890 '
900 '*** ASSIGN METER ID NAME ***
910 ON NM GOTO 930,940,950
920 PRINT CHR$(7): PRINT "<<<WRONG METER ID>>": RETURN 230
930 M$="KEITHLEY 181/199/197": NMSK=5: RETURN
940 M$="FLUKE 8840A": NMSK=1: RETURN
950 M$="KEITHLEY 228 Pwr Supp": NMSK=1: RETURN
960 '
1000 SCREEN 0: CLS: EMS$=""

```



```

1010 GOSUB 5500 '--- INCREMENT EXTENSION ON DATA FILENAME
1020 PRINT: PRINT " *** SET-UP PARAMETERS for DA-JcTH.BAS *** "
1030 PRINT " 1: FILENAME OF SETUP AND GRAPHICS PARAMETERS TO USE: ";PUFL$
1040 PRINT " 2: FILENAME OF SETUP AND GRAPHICS PARAMETERS TO SAVE TO: ";PSFL$
1050 PRINT " 3: X2-VOLTAGE SCALE FACTOR (Signal/Meas V or 1/STD ohms): ";SCALEX
1060 PRINT " 4: X2-SIGNAL RANGE(Amps)/STEP SIZE fraction: ";XMINC;"to";XMAXC;" / ";DELX
1062 PRINT " X2-SIGNAL BACKSTEP (Fraction of Xminc): ";XOFFC
1070 PRINT " 5: Y-VOLTAGE SCALE FACTOR (Signal/Meas V): ";SCALEY
1075 PRINT " 6: Y-SIGNAL LIMIT: ";DELY
1080 PRINT " 6: Y-SIGNAL STEP SIZE: ";DELY
1090 PRINT " 7: DATA FILENAME: ";DNM$
1095 IF DNM$="" GOTO 1110
1100 PRINT " TITLE: ";TTITLE$
1110 PRINT " 8: THERM. CAL. TABLE FILENAME (for X1-signal conversion): ";THNM$
1112 IF THNM$="" GOTO 1120
1115 PRINT " TITLE: ";THTITLE$
1120 PRINT " 9: TEMPERATURE INTERVAL BETWEEN DATA: ";DELT
1125 PRINT "10: NO. OF SAMPLES IN DIGITAL FILTERING: ";NFILT
1130 PRINT "11: SCREEN GRAPHICS PARAMETERS SETUP: ";GSET$
1135 PRINT "12: EXIT THE PROGRAM
1137 PRINT "13: Test circuit Resistance, or Sample Ic. Present Rcirc = ";RCIRC
1140 PRINT "14: Ic Operating Range (H, > 1mA; L, < 10mA): ";MODE$
1142 PRINT "15: TEMPERATURE CONTROLLER: ";TSET$
1143 IF TSET$=ACT$ THEN PRINT " Control Range = " TC1"-TC2 "K & Vap-Samp = " TCDEL "K @ RT"
1145 PRINT "16: Maximum Heating Allowed (mW): ";HLIMIT
1147 PRINT
1150 INPUT " > ENTER SELECTION # (< C/R > TO EXECUTE): ";ICODE
1160 ON ICODE GOTO 1400,1430,1290,1310,1180,1200,1220,1350,1460,1380,1330,1335 ,1480,1491,1472,1325
1170 RETURN 'TO MAIN PROGRAM
1180 INPUT " ENTER Y-VOLTAGE SCALE FACTOR (Signal/Vmeas): ";SCALEY
1190 GOTO 1020
1200 INPUT " ENTER Y-SIGNAL LIMIT: ";DELY
1210 GOTO 1020
1220 INPUT " INPUT DATA FILENAME (EXT .DTn WILL BE ADDED IF NOT ENTERED): ";DNM$
1230 IF DNM$="" THEN 1280
1240 PRINT " ENTER 80 CHARACTER DATA SET TITLE(DEFAULT=PREVIOUS): ";INPUT$,DUM$
1250 IF DUM$="" THEN 1270
1260 TTITLE$=DUM$
1270 FOR J=1 TO LEN(DNM$): IF MID$(DNM$,J,1) < > "." THEN NEXT J ELSE 1280
1272 DNM$=DNM$+" .DT0"
1280 GOTO 1020
1290 INPUT " ENTER X-VOLTAGE SCALE FACTOR (Signal/Vmeas or 1/STD ohms): ";SCALEX
1300 GOTO 1020
1310 INPUT " ENTER X-SIGNAL RANGE & STEP SIZE(XMIN,XMAX,STEP(Fraction)): ";XMINC,XMAXC,DELX
1315 INPUT " ENTER X-SIGNAL BACKSTEP (Backstep (fraction of Xminc)): ";XOFFC
1320 GOTO 1020
1325 INPUT " ENTER MAXIMUM HEATING ALLOWED (mW): ";HLIMIT
1326 GOTO 1020
1330 GOSUB 2250 'Define Graphics Parameters
1332 GOTO 1020
1335 GOSUB 4500: END '--- STORE PARAMS TO FILE AND EXIT
1340 GOTO 1020
1350 INPUT " ENTER THERM. CALIB. TABLE FILENAME(EXT .CAL WILL BE ADDED): ";THNM$
1360 IF THNM$="" THEN 1370 ELSE THNM$=THNM$+".CAL"
1365 GOSUB 3900 '--- READ IN THERM. CALIB. DATA ---
1366 INPUT " ENTER VOLTAGE SCALE FACTOR (signal/voltage): ";SCALEZ
1370 GOTO 1020
1380 INPUT " ENTER NO. SAMPLES IN DIGITAL FILTERING: ";NFILT
1390 GOTO 1020
1400 INPUT " ENTER FILENAME FOR SETUP PARAMS. TO USE(EXT .PAR WILL BE ADDED): ";PUFL$
1410 IF PUFL$="" THEN 1420 ELSE PUFL$=PUFL$+".PAR"
1420 GOSUB 4150: GOTO 230 '---READ IN SETUP AND GRAPHICS PARAMS
1430 INPUT " ENTER FILENAME FOR SETUP PARAMS TO SAVE TO (.PAR WILL BE ADDED): ";PSFL$
1440 IF PSFL$="" THEN 1450 ELSE PSFL$=PSFL$+".PAR"
1450 GOTO 1020
1460 INPUT " ENTER TEMPERATURE INTERVAL BETWEEN DATA: ";DELT
1470 GOTO 1020

```



```

1472 IF THNMS="" THEN PRINT " Enter a temperature calibration file if you plan to use the controller!": GOTO 1020
1473 IF TSET$=ACT$ THEN TSET$=INACT$: GOTO 1020
1474 PRINT " Temperature Controller Settings": TSET$=ACT$
1475 INPUT " ENTER Tmin, Tmax & Vap-Samp Set Points: ",TC1,TC2,TCDEL
1476 IF TC1>TC2 OR TC2>320 OR TC1<0 THEN PRINT" Bad Entry !": GOTO 1475
1477 GOTO 1020
1480 GOSUB 7000      'Check out circuit resist with new STDR
1490 GOTO 1020
1491 INPUT " ENTER OPERATING RANGE (H, >1mA; L, <10mA): ",MODE$
1492 IF MODE$ = "H" THEN GOSUB 1800 : GOTO 1020
1493 IF MODE$ = "L" THEN GOSUB 1810 : GOTO 1020
1494 PRINT "Error" : BEEP : GOTO 1491
1495 '
1496 '
1500 '*** OPEN DATA FILE ***
1510 IF DNMS="" THEN 1550
1520 OPEN "O",#1,DNMS
1530 PRINT #1, TITLE$
1540 PRINT #1," T(K)    Ic(A)    H(kOe) Heating(mW) EstDev(Ic) "
1550 RETURN
1560 '
1570 '
1600 ' *** INITIALIZATION FOR DATA ACQU. ***
1605 CLOSE      '—close any open files
1610 GOSUB 4050 '—PRINT MESSAGE AT SCREEN BOTTOM
1620 I=0 'INITIALIZE DATA ARRAY INDEX
1630 GOSUB 4850 '— ESTABLISH COMMUNICATION W/PERSONAL488
1640 GOSUB 4950 '— SIGNON MESSAGE
1650 GOSUB 5050 '—ASSIGN REMOTE MODE ADDRESSES
1657 'GOSUB 5700 '— INITIALIZE FOR ANALOG OUTPUT --not used here
1660 FLG$="L" 'INITIALIZE FOR DATA SCREEN PRINTOUT
1680 GOSUB 1500 '— OPEN DATA FILE
1685 ADAT=1 ' Key switch for AUTODATA control via KBD
1690 IVXFLG=0 '— FLAG FOR FIRST TIME THRU
1700 PRINT " ***Beginning Data Acquisition ***"
1705 PRINT " #    T(K)    Ic(A)    H(kOe) Heating(mW)    DevIc    next I"
1710 RETURN 'TO MAIN PROGRAM
1720 '
1730 '
1750 ' *** TAKE DATA SAMPLE ***
1760 '— GPIB INPUT —
1770 EMSTOP=100*(DELY/SCALEY) 'allowed safety limit for sample voltage
1775 GOSUB 6400 '— FIND AVG OF NFILT READINGS using K-228 +/- & min switching
1780 VX=ABS(SUMX*SCALEX): VY=ABS(SUMY*SCALEY): VZ=ABS(SUMZ*SCALEZ): DVY=QY*SCALEY
1781 SCALEMAG=102.91 '— to convert Mag Curr (Hall cryostat) with .01 std
1782 VM=ABS(SUMM*SCALEMAG) '— Mag field in kG
1785 IF HEAT>HLIMIT GOTO 8100 'Excessive Heating Detected
1790 RETURN 'TO MAIN PROGRAM
1800 SOUND 880, 15
1801 INPUT " REMOVE 1 kOhm Std. Resistor at K-228 Output then Press RTN",DUM$
1803 IF DELXC < .0001 THEN DELXC = .0001
1805 RETURN
1810 SOUND 880, 15
1815 INPUT " INSTALL 1 kOhm Std. Resistor at K-228 Output then Press RTN",DUM$
1817 IF DELXC < .000001 THEN DELXC = .000001
1820 RETURN
1830 '
1840 '
1850 '*** DATA TEST FOR OUTPUT ***
1880 IF IDATFLG=0 THEN 1920
1890 IF INK$<>"P" AND INK$<>"p" THEN PRINT "MANUAL STORE"
1900 PRINT CHR$(7); '— BELL TO INDICATE MANUAL DATA STORAGE
1910 IDATFLG=0: GOTO 1970 'MANUAL DATA STORAGE
1920 IF VY<DELY THEN VYL=VY: VXL=VX: DVYL=DVY: RETURN 295 'for MORE DATA
1930 BEEP: IF VXL=0 THEN XIC=VX: DA=1: RETURN 300 'store data as is: vx,vy,I,T
1940 DX=VX-VXL: DY=VY-VYL 'now calc interpolated Xc & hi, lo err limits
1945 XIC=(DELY-VYL)*DX/DY+VXL 'Xic is Ic    DELY is Yc

```

163


```

2500 XMIN$=STR$(XMIN): XMAX$=STR$(XMAX)
2510 YMIN$=STR$(YMIN): YMAX$=STR$(YMAX)
2520 GOSUB 2610: GOSUB 2660 'DEFINE FUNCTION TO CALC COORD IN PIXELS
2530 RETURN
2540 '
2550 '
2600 '*** FN TO CALCULATE Y IN SCREEN PIXELS ***
2610 DEF FNYPIX(YVAR,YMIN,YRNG,DYPIX,YPIX0)=-(YVAR-YMIN)*DYPIX/YRNG+YPIX0+DYPIX
2620 RETURN
2630 '
2640 '
2650 '*** FN TO CALCULATE X IN SCREEN PIXELS ***
2660 DEF FNXPIX(XVAR,XMIN,XRNG,DXPIX,XPIX0)=(XVAR-XMIN)*DXPIX/XRNG+XPIX0
2670 RETURN
2680 '
2690 '
2700 ' *** PLOT OR PRINT DATA ***
2710 IF INK$ < > "L" THEN IF INK$ < > "I" THEN 2740
2720 IF FLG$="L" THEN 2780
2730 FLG$="L": GOSUB 3050: GOSUB 4050: RETURN 'LIST DATA TO CURRENT I
2740 IF GSET$=INACT$ THEN 2780
2750 IF INK$ < > "P" THEN IF INK$ < > "p" THEN 2780
2760 IF FLG$="P" THEN 2800
2763 PRINT USING " ###.#### ";ZT(I);
2770 FLG$="P": GOSUB 2900: GOSUB 4050: RETURN 'PLOT DATA TO CURRENT I
2780 IF AUTODATA=1 THEN PRINT
2781 IF FLG$ < > "L" THEN GOTO 2790
2782 PRINT USING " ### ";I;
2783 PRINT USING " ###.#### ";ZT(I);
2784 PRINT USING " +##.##### ";X(I);
2785 PRINT USING " +##.#### ";XM(I);
2786 PRINT USING " +#.####^";Y(I);Q(I);
2787 RETURN ' to MAIN program
2790 IF GSET$=INACT$ THEN 2840
2800 XP=FNXPPIX(ZT(I),XMIN,XRNG,DXPIX,XPIX0)
2805 IF XP>10000 THEN 2840
2810 YP=FNYPIX(X(I),YMIN,YRNG,DYPIX,YPIX0)
2815 IF ABS(YP)>10000 THEN 2840
2820 PSET (XP,YP) 'PLOTS POINT
2830 IF THNM$="" GOTO 2840
2833 LOCATE 1,67: PRINT "T= " INT(T) " K ";
2836 LOCATE 24,1
2840 RETURN 'TO MAIN PROGRAM
2850 '
2860 '
2900 ' *** REFRESH PLOT OF DATA UP TO CURRENT POINT ***
2910 CLS: GOSUB 3150: GOSUB 3300 'DRAW AND LABEL AXES
2920 FOR J=1 TO I
2930 XP=FNXPPIX(ZT(J),XMIN,XRNG,DXPIX,XPIX0)
2935 IF ABS(XP)>10000 THEN 2970 '— PT OUT OF RANGE
2940 YP=FNYPIX(X(J),YMIN,YRNG,DYPIX,YPIX0)
2945 IF ABS(YP)>10000 THEN 2970
2950 'CIRCLE (XP,YP),3
2960 PSET (XP,YP)
2970 NEXT J
2975 IF GCOMFL$="" THEN RETURN
2976 IF GCSET$=ACT$ THEN GOSUB 5920 ' PLOT COMPARISON DATA
2980 RETURN
3000 '
3010 '
3050 '*** PRINT DATA ON SCREEN ***
3060 SCREEN 0: CLS: LOCATE 23,1,0
3065 PRINT " # T(K) Ic(A) H(kOe) Heating(mW) DevIc next I"
3070 J1=I-20: IF J1<0 THEN J1=1
3080 FOR J=J1 TO I
3092 PRINT USING " ### ";J;
3093 PRINT USING " ###.#### ";ZT(J);

```

```

3094 PRINT USING " ##.##### ";X(J);
3095 PRINT USING " ##.#### ";XM(J);
3096 PRINT USING " ##.####^ ^ ^ ^ ";Y(J);Q(J)
3100 NEXT J
3110 RETURN
3120 '
3130 '
3150 '*** SUB TO DRAW GRAPH AXES ***
3160 SCREEN 9 'HI RES GRAPHICS SCREEN
3170 CLS
3180 PSET (80,15)
3190 DWN=300: RGT=550: TICKU=30: TICKR=55: ZERO=0
3200 FOR J=1 TO 10: DRAW"D=TICKU;NM+550,0;":NEXT J '---LEFT VERT AXIS
3210 FOR J=1 TO 10: DRAW"R=TICKR;NM+0,-300;":NEXT J '---BOTTOM HORIZ AXIS
3220 DRAW"U=DWN;L=RGT;";
3230 RETURN
3240 '
3250 '
3300 '*** SUB TO LABEL AXES ***
3310 IF LEN(X$)>60 THEN X$=LEFT$(X$,60) 'TRUNCATE IF TOO LONG
3320 XAX=44-.5*LEN(X$)
3330 LOCATE 24,XAX: PRINT X$;
3340 IF LEN(Y1$)>9 THEN Y1$=LEFT$(Y1$,9) 'TRUNCATE IF TOO LONG
3350 TAX=5-.5*LEN(Y1$)
3360 LOCATE 12,TAX: PRINT Y1$;
3370 IF LEN(Y2$)>9 THEN Y2$=LEFT$(Y2$,9)
3380 TAX=5-.5*LEN(Y2$)
3390 LOCATE 13,TAX: PRINT Y2$;
3400 IF LEN(T$)>70 THEN T$=LEFT$(T$,70) 'TRUNCATE IF TOO LONG
3410 TAX=44-.5*LEN(T$)
3420 LOCATE 1,TAX: PRINT T$;
3430 LOCATE 24,12-LEN(XMIN$): PRINT XMIN$;
3440 IF XMAX$="" THEN 3460
3450 LOCATE 24,81-LEN(XMAX$): PRINT XMAX$;
3460 LOCATE 23,10-LEN(YMIN$): PRINT YMIN$;
3470 LOCATE 2,10-LEN(YMAX$): PRINT YMAX$;
3480 RETURN
3490 '
3500 '
3550 ' *** SUB TO CHECK KEYBOARD STATUS ***
3560 IN$=INKEY$ 'Read Keyboard Buffer...
3565 IF EMS$="Q" THEN IN$="Q" 'Emergency Stop
3570 IF IN$="" THEN RETURN
3572 IF IN$<>"A" AND IN$<>"a" THEN 3580
3574 ADAT=-ADAT ' switch status
3576 IF ADAT<0 THEN AUTODATA=1
3578 IF ADAT>0 THEN AUTODATA=0
3580 IF IN$=CHR$(13) GOTO 3710 'MANUAL DATA interrupt (to revise Xmin)
3590 INK$=IN$
3600 IF INK$<>"Q" AND INK$<>"q" THEN 3680
3610 IF DNMS="" THEN 3630 'DATA FILENAME
3620 CLOSE #1: GOSUB 6000 '---REWRITE DATA TO FILE IN STD FORMAT
3630 SCREEN 0: INPUT "ANOTHER DATA SET (Y=YES)?:"ANS2$
3640 IF ANS2$="y" OR ANS2$="Y" THEN 3670
3650 ON ERROR GOTO 0 'DISABLE ERROR TRAPPING
3655 PRINT#2,"LOCAL";TADDR$
3660 CLS: END
3670 CLOSE: RETURN 240 'TO MAIN PROGRAM AT MENU
3680 IF INK$="A" THEN AUTODATA=1: RETURN
3682 IF INK$="a" THEN AUTODATA=1: RETURN
3684 IF INK$="C" GOTO 3720
3685 IF INK$="c" GOTO 3720
3687 IF INK$="T" GOTO 3730
3688 IF INK$="t" GOTO 3730
3690 IF INK$<>"P" THEN IF INK$<>"p" THEN RETURN
3695 IF INK$<>"I" THEN IF INK$<>"L" THEN RETURN
3700 RETURN 320 'TO MAIN PROGRAM AT PLT OR PRNT DATA

```



```

3710 PRINT " Start Current ? ";
3715 RETURN 340 ' to Main Progr at input next XCC
3720 INPUT " ENTER OPERATING RANGE (H, > 1mA; L, < 10mA): ",MODE$
3721 XC=XMINC 'Set XC to a safe value.
3722 IF MODE$ = "H" THEN GOSUB 1800: INK$="L": RETURN 320
3724 IF MODE$ = "L" THEN GOSUB 1810: INK$="L": RETURN 320
3726 PRINT "Error": BEEP: GOTO 3720
3730 PRINT:INPUT " ENTER NEW THERM. CAL. TABLE (EXT .CAL WILL BE ADDED): ",THNMS
3732 IF THNMS="" THEN 3690 ELSE THNMS=THNMS+".CAL"
3733 CLOSE #1 '---TEMPORARILY CLOSE DATA OUTPUT FILE
3734 GOSUB 3900 '---READ IN THERM. CAL. TABLE
3735 OPEN DNM$ FOR APPEND AS #1 '---REOPEN THE DATA OUTPUT FILE
3736 INPUT " ENTER NEW SCALE FACTOR (Signal/Voltage): ",SCALEZ
3738 INK$="L": RETURN 320
3740 '
3745 '
3750 '*** SUB TO INTERPOLATE TEMPERATURES FROM DIODE T,V TABLE ***
3760 IF THNMS="" THEN RETURN 'TO MAIN PROGRAM
3770 VZC=VZ
3780 NLO=1: NHI=NDATA 'LOW AND HI INDICES OF TABLE DATA
3790 N=(NHI+NLO)/2 'INTEGER DIVIDE 'TABLE INDEX TO BE COMPARED TO DATUM
3800 IF VZ<V(N) THEN NHI=N: GOTO 3820
3810 NLO=N
3820 IF NHI<>NLO+1 THEN GOTO 3790
3830 T=T(NHI)+(VZ-V(NHI))*(T(NHI)-T(NLO))/(V(NHI)-V(NLO))
3840 RETURN
3850 '
3860 '
3900 '*** SUB TO READ IN THERM. CALIB DATA ***
3910 IF THNMS="" THEN RETURN
3930 THNMT$=THNMS
3940 PRINT"*** Reading in therm. calibration table ****"
3950 OPEN "I",#1,THNMS
3952 INPUT #1, THTTLS '---TITLE OF DATA SET
3960 INPUT #1,NDATA
3970 FOR J=1 TO NDATA
3980 INPUT #1,V(J),T(J)
3990 NEXT J
4000 CLOSE #1
4010 RETURN
4020 '
4030 '
4050 '*** PRINT MESSAGE AT BOTTOM OF SCREEN ***
4060 IF GSET$=ACT$ THEN 4090
4070 CLS: LOCATE 25,1: PRINT"PRESS: RTN=>RESET_I Q=>QUIT C=>POWER RANGE A=>AUTO on/off
T=>THERM ";
4080 LOCATE 1,1: GOTO 4110
4090 LOCATE 25,1: PRINT"PRESS: RTN=>SET_I Q=>QUIT P=>PLOT L=>LIST A=>AUTO C=>POWER RANGE
T=>THERM ";
4100 LOCATE 24,1
4110 RETURN
4111 LOCATE 25,1: PRINT" PRESS <C/R> TO CONTINUE ";
4112 LOCATE 24,1
4113 RETURN
4120 '
4130 '
4150 '*** READ IN SETUP AND GRAPHICS PARAMETERS ***
4160 IF PUFL$="" THEN RETURN
4170 OPEN "I",#1, PUFL$
4180 PRINT"*** RETRIEVING PARAMETERS FROM: ";PUFL$;" ****"
4190 '---SETUP PARAMETERS
4195 INPUT #1,PSFL$
4200 INPUT #1,SCALEX
4205 INPUT #1,RCIRC
4207 INPUT #1,XMINC,XMAXC,DELX
4210 INPUT #1,XOFFC
4220 INPUT #1,SCALEY

```

```

4230 INPUT #1,DELY
4240 INPUT #1,DNMS$
4250 INPUT #1,TITLE$
4260 DUM$=TITLE$
4270 INPUT #1,THNMS$
4272 INPUT #1,SCALEZ
4275 INPUT #1,DELT
4280 INPUT #1,NFILT
4290 INPUT #1,GSET$
4300 '---GRAPHICS PARAMETERS
4310 INPUT #1,XMIN,XMAX
4320 INPUT #1,YMIN,YMAX
4330 INPUT #1,X$
4340 INPUT #1,Y1$
4350 INPUT #1,Y2$
4360 INPUT #1,T$
4370 '---GPIB & METER PARAMS
4380 INPUT#1,XADDR$
4390 INPUT#1,YADDR$
4397 INPUT#1,PADDR$
4400 INPUT#1,MX$
4410 INPUT#1,MY$
4417 INPUT#1,MP$
4420 INPUT#1,NXM,NYM,NPM
4422 '--- COMPARISON GRAPHICS DATA FILE INFO
4424 INPUT#1,GCOMFL$ 'DATA FILENAME
4426 INPUT#1,GCSET$ 'FLAG FOR GRAPHICS COMPARISON
4428 'DO NOT INCLUDE MODE$
4430 CLOSE #1
4435 GOSUB 3900 '---READ IN THERM CALIB. DATA
4440 IF GSET$=ACT$ THEN GOSUB 5800: GOSUB 2490 '---READ IN COMP DATA SET
4450 RETURN
4460 '
4470 '
4500 '*** SAVE SETUP AND GRAPHICS PARAMETERS TO FILE ***
4510 IF PSFL$="" THEN RETURN
4520 OPEN "O",#1, PSFL$
4530 PRINT*** STORING PARAMETERS TO: ";PSFL$;" ****
4540 '---SETUP PARAMETERS
4545 PRINT#1,PSFL$
4550 PRINT#1,SCALEX
4555 PRINT#1,RCIRC
4557 PRINT#1,XMINC,XMAXC,DELT
4560 PRINT#1,XOFFC
4570 PRINT#1,SCALEY
4580 PRINT#1,DELY
4590 PRINT#1,DNMS$
4600 PRINT#1,TITLE$
4610 PRINT#1,THNMS$
4612 PRINT#1,SCALEZ
4615 PRINT#1,DELT
4620 PRINT#1,NFILT
4630 PRINT#1,GSET$
4640 '---GRAPHICS PARAMETERS
4650 PRINT#1,XMIN,XMAX
4660 PRINT#1,YMIN,YMAX
4670 PRINT#1,X$
4680 PRINT#1,Y1$
4690 PRINT#1,Y2$
4700 PRINT#1,T$
4710 '---GPIB & METER PARAMS
4720 PRINT#1,XADDR$
4730 PRINT#1,YADDR$
4737 PRINT#1,PADDR$
4740 PRINT#1,MX$
4750 PRINT#1,MY$
4757 PRINT#1,MP$

```



```

4760 PRINT#1,NXM,NYM,NPM
4762 '—COMPARISON GRAPHICS DATA FILE INFO
4764 PRINT#1,GCOMFL$ 'FILENAME OF COMPARISON DATA SET
4766 PRINT#1,GCSET$ 'FLAG FOR ACTIVE GRAPICS COMPARISON
4768 'DO NOT INCLUDE MODE$
4770 CLOSE #1
4780 RETURN
4790 '
4800 '
4850 ' *** Establish communications with Personal488 ***
4860 OPEN "DEV\IEEEOUT" FOR OUTPUT AS #2
4870 'Reset Personal488
4880 IOCTL#2,"BREAK"
4885 PRINT#2,"RESET"
4890 'Open file to read responses from Personal488
4900 OPEN "DEV\IEEEIN" FOR INPUT AS #3
4904 'Enable SEQUENCE error detection by Personal488
4905 PRINT#2,"FILL ERROR"
4906 PRINT#2,"TIME OUT 10"
4910 RETURN
4920 '
4930 '
4950 ' *** Read the signon and revision message ***
4960 PRINT#2,"HELLO"
4970 INPUT#3,AS
4980 PRINT A$
4990 RETURN
5000 '
5010 '
5050 '*** Put the METERS into REMOTE ***
5060 PRINT#2,"REMOTE";XADDR$
5065 PRINT#2,"REMOTE";YADDR$
5075 PRINT#2,"REMOTE";PADDR$ 'K-228 Pwr Supp
5080 'RETURN
5090 'R0: Auto range X: Execute
5100 PRINT#2,"OUTPUT";XADDR$;"POH8X"
5102 PRINT#2,"OUTPUT";XADDR$;"H4X" 'put X-meter (K199) on #4 rear input H
5110 PRINT#2,"OUTPUT";YADDR$;"POT1X" 'K-181: P0=FILT OFF,T1=FRESH BUF @ TALK
5117 PRINT#2,"OUTPUT";PADDR$;"COA0K0G5X" 'K0=await finish; G5=v,i val read
5120 RETURN
5130 '
5140 '
5150 '
5350 '*** PRINTOUT MESSAGE FOR BAD READING ***
5360 PRINT CHR$(7); IF FLG$="L" OR FLG$="I" THEN PRINT ">>> BAD READING<<<";RS
5370 RETURN
5380 '
5390 '
5400 '*** ERROR TRAPPING ***
5410 PRINT CHR$(7); '—BELL TO INDICATE ERROR
5415 IF ERR<>53 THEN PRINT ERR: END '—STOP AFTER ERROR
5420 'IF ERR<>53 THEN RESUME 260 '—TRY TO TAKE MORE DATA
5425 PRINT">> BAD FILENAME<<"; FOR J=1 TO 1000: NEXT J: RESUME 240
5440 '
5450 '
5500 ' *** INCREMENT EXTENSION ON DATA FILENAME ***
5510 PRINT CHR$(7)
5520 IF DNMS="" THEN RETURN
5530 FOR J=1 TO LEN(DNMS): IF MID$(DNMS,J,1)<> "." THEN NEXT J
5540 J1=LEN(DNMS)-J+1
5550 EXT$=RIGHT$(DNMS,J1): DNMS=LEFT$(DNMS,J1)
5560 IEXT=VAL(RIGHT$(EXT$,1)): IEXT=IEXT+1
5570 IEXT$=RIGHT$(STR$(IEXT),1)
5580 EXT$=LEFT$(EXT$,3)+IEXT$
5590 DNMS=DNMS+EXT$
5600 RETURN
5610 '

```

```

5620 '
5700 '*** ANALOG OUTPUT INITIALIZATION ***
5705 '---SLOT 3, CHANNEL 1
5710 'CALL IONAME("ANOUT1",3,1) 'NOT USED HERE !
5720 RETURN
5730 '
5740 '
5800 '*** READ IN DATA SET FOR GRAPHICS COMPARISION ***
5805 PRINT"*** RETRIEVING COMPARISON DATA SET *****"
5810 IF GCOMFL$="" THEN RETURN
5820 OPEN"1",#1, GCOMFL$
5822 INPUT#1, GTTL$ '---TITLE OF FILE DATA
5830 INPUT#1, NDATG
5833 INPUT#1,ZG(1),XG(1),XMG(1),YG(1),QG(1)
5835 XMX=ZG(1): XMN=ZG(1): YMX=XG(1): YMN=XG(1)
5840 FOR J=2 TO NDATG
5850 INPUT#1, ZG(J),XG(J),XMG(J),YG(J),QG(J)
5855 IF ZG(J)>XMX THEN XMX=ZG(J): GOTO 5857
5856 IF ZG(J)<XMN THEN XMN=ZG(J)
5857 IF XG(J)>YMX THEN YMX=XG(J): GOTO 5860
5858 IF XG(J)<YMN THEN YMN=XG(J)
5860 NEXT J
5870 CLOSE #1
5875 PRINT" TMIN: ";XMN,"TMAX: ";XMX 'Note that x-axis is "T", y-ax is X (lc)
5876 PRINT" YMIN: ";YMN,"YMAX: ";YMX
5880 RETURN
5890 '
5900 ' *** PLOT OF COMPARISON DATA ***
5910 CLS: GOSUB 3150: GOSUB 3300 'DRAW AND LABEL AXES
5920 FOR J=1 TO NDATG
5930 XP=FNXP(XG(J),XMN,XRNG,DXPIX,XPIX0)
5935 IF ABS(XP)>10000 THEN 5970 '--- PT OUT OF RANGE
5940 YP=FNYP(XG(J),YMN,YRNG,DYPIX,YPIX0)
5945 IF ABS(YP)>10000 THEN 5970
5950 CIRCLE (XP,YP),1
5960 'PSET (XP,YP)
5970 NEXT J
5980 RETURN
5990 '
6000 '*** REWRITE DATA TO FILE ***
6010 IF DNMS$="" THEN RETURN
6020 OPEN"O",#1, DNMS$
6030 PRINT"*** STORING DATA ARRAY TO FILE ****"
6040 PRINT#1, TTTL$
6050 PRINT#1,I '---NO. OF DATA IN SET
6060 FOR J=1 TO I
6070 PRINT#1, ZT(J);X(J);XM(J);Y(J);Q(J)
6080 NEXT J
6090 CLOSE#1
6100 RETURN
6110 '
6200 '*** Test Temperature for designated interval ***
6205 IF THNMS$="" THEN RETURN '---NO THERM CALIBRATION
6210 IF IVXFLG=0 THEN IVXFLG=1: TTMP=T: RETURN 'FIRST TIME THROUGH
6220 DELTT=T-TTMP
6230 IF ABS(DELT) < DELT THEN RETURN 341 'LOOP BACK FOR MORE DATA
6250 TTMP=T: RETURN 'TO MAIN PROGRAM, STORE DATA
6260 '
6270 '
6400 ' *** Find the average of Navg readings ***
6410 ' ** using +&- curr: read +/-Sam:V(y), +/-Sam:I(x2), Mag:I(x4), T:V(x1)
6420 SUMX=0: SUMY=0: SUMZ=0: SUMM=0
6430 PRINT#2,"output";PADDR$;"R0X" 'auto-range
6440 PRINT#2,"output";PADDR$;SPOS$ 'v,i control string
6450 PRINT#2,"output";PADDR$;"F1X" 'turn on curr
6460 FOR J= 1 TO NFILT
6470 FOR J1=1 TO JD: NEXT J1 ' ~ .25 sec delay

```



```

6490 PRINT#2,"output";XADDR$;"R0N2X" 'channel #2 for std R, sam-curr
6500 FOR J1=1 TO JD: NEXT J1 ' ~ .25 sec delay
6510 PRINT#2,"ENTER";XADDR$
6520 INPUT#3,RX$: VALX=VAL(MID$(RX$,NXM))
6530 IF ABS(VALX)>100 THEN GOSUB 5350: GOTO 6420 '---START OVER -- BAD READING
6540 PRINT#2,"OUTPUT";YADDR$;"P0X" 'K-181: P0=FILTER OFF
6550 PRINT#2,"ENTER";YADDR$
6560 INPUT#3,RY$: VALY=VAL(MID$(RY$,NYM))
6570 PRINT#2,"output";PADDR$;SNEG$ 'v,i control string for Neg Curr
6580 FOR J1=1 TO JD: NEXT J1 ' ~ .25 sec delay
6590 PRINT#2,"OUTPUT";YADDR$;"P0X" 'K-181: P0=FILTER OFF
6600 PRINT#2,"ENTER";YADDR$
6610 INPUT#3,RS: VALY=.5*(VALY-VAL(MID$(RS$,NYM))) 'avg + & - readings
6615 IF VALY>EMSTOP GOTO 8000 'EMERGENCY Current Stop !
6620 SUMY=SUMY+VALY: YD(J)=VALY
6625 PRINT#2,"OUTPUT";XADDR$;"R0N2X" 'channel #2 for std R, sam-curr
6630 PRINT#2,"ENTER";XADDR$
6640 INPUT#3,RX$: VALX=.5*(VALX-VAL(MID$(RX$,NXM)))
6650 SUMX=SUMX+VALX
6660 'thermometer signal reading
6664 PRINT#2,"OUTPUT";XADDR$;"R0N1X" 'channel #1 for thermometer
6666 FOR J1=1 TO JD: NEXT J1 ' ~ .25 sec delay
6670 PRINT#2,"ENTER";XADDR$
6680 INPUT#3,RZ$: VALZ=VAL(MID$(RZ$,NXM))
6690 SUMZ=SUMZ+VALZ
6710 PRINT#2,"output";XADDR$;"R0N4X" 'channel #4 for Mag curr
6720 FOR J1=1 TO JD: NEXT J1 ' ~ .25 sec delay
6730 PRINT#2,"ENTER";XADDR$
6740 INPUT#3,RM$: VALM=VAL(MID$(RM$,NXM))
6750 SUMM=SUMM+VALM
6760 PRINT#2,"output";PADDR$;SPOS$ 'v,i control string for Pos Curr
6770 NEXT J
6772 PRINT#2,"OUTPUT";XADDR$;"R0N3X" 'channel #3: heat dissipation
6774 FOR J1=1 TO JD: NEXT J1 ' ~ .25 sec delay
6776 PRINT#2,"ENTER";XADDR$
6778 INPUT#3,RM$: HEAT=ABS(1000*XC*VAL(MID$(RM$,NXM))) 'total mW heating
6779 PRINT#2,"OUTPUT";XADDR$;"R0N4X" 'exit SUB in chann. #4
6780 PRINT#2,"output";PADDR$;"V.0011.0001W1X" 'set a very low curr
6785 IF AUTODATA=0 THEN PRINT#2,"output";PADDR$;"F0X" 'turn off curr
6790 SUMX=SUMX/NFILT: SUMY=SUMY/NFILT: SUMZ=SUMZ/NFILT: SUMM=SUMM/NFILT
6800 SUMDEV=0 'Now calc Std Dev of YD from SUMY
6810 FOR J=1 TO NFILT
6820 SUMDEV=SUMDEV+(SUMY-YD(J))^2
6830 NEXT J
6840 NDEV=NFILT-1: IF NDEV=0 THEN NDEV=1
6850 QY=SQR(SUMDEV/NDEV) ' "Quality of Y" defined as Std Dev(Y)
6860 RETURN
6870 '
6880 '
7000 '*** MEASURE CIRCUIT RESISTANCE (HIGH CURRENT MODE) ***
7002 IF MODE$="L" THEN INPUT "Remove 1 kOhm resistor and press RTN",DUM$
7005 CLOSE 'close any open files
7010 GOSUB 4850 '--- establish communication with Personal488
7020 GOSUB 5050 '--- put instruments in REMOTE mode & give addresses
7030 '--- for K-228: K0=await instruc complete, G5=readout:v,i
7040 PRINT#2,"OUTPUT";PADDR$;"R0X" 'R0=auto-range
7045 PRINT#2,"OUTPUT";XADDR$;"R0N3X" 'display heating @ contacts
7050 INPUT "What is EST RESISTANCE of circuit (ohms) ? ",STDR
7055 RADD=1.9: IF STDR=.1 THEN RADD=.2
7060 INPUT "Trial CURRENT (amps) to Start with ? ",CURI
7070 V0=CURI*(STDR+RADD)*1.2: V0$=STR$(V0)
7075 CURI$=STR$(CURI)
7080 S$="V"+V0$+"I"+CURI$+"W1X"
7090 PRINT#2,"OUTPUT";PADDR$;S$
7095 PRINT#2,"OUTPUT";PADDR$;"F1X"
7100 FOR J=1 TO 14000: NEXT J ' 2.5sec wait before read
7110 PRINT#2,"ENTER";PADDR$

```



```

7120 INPUT#3,VPS,CPS          ' read pwr supp output v,i
7122 IOCTL#2,"BREAK"
7125 PRINT#2,"OUTPUT";PADDR$;"FOX"
7130 RCIRC=VPS/CPS
7140 PRINT"Meas'd circuit V, I = ",VPS,CPS;:PRINT" ==> R= ",RCIRC
7150 INPUT" Do you wish to step up V 10% per step? < Y for yes > ",YESTP$
7160 IF YESTP$="Y" THEN GOTO 7170 ELSE GOTO 7330
7170 PRINT"          V(volts)      I(amps)      R(ohms) <ENTER to continue> "
7180 V0=VPS; C0=CPS
7190 V1=1.1*V0; C1=1.2*C0
7195 V1=.000001*INT(1000000#*V1+.5); C1=.000001*INT(1000000#*C1+.5)
7200 V1$=STR$(V1); C1$=STR$(C1)
7210 SP$=";V"+V1$+"I"+C1$+"W3X"
7220 'SN$=";V"+V1$+"I"+C1$+"W1X" 'neg not used here
7230 PRINT#2,"OUTPUT";PADDR$;SP$
7240 PRINT#2,"OUTPUT";PADDR$;"FIX"
7250 FOR J=1 TO 14000: NEXT J ' 2.5sec wait before read
7260 PRINT#2,"ENTER";PADDR$
7270 INPUT#3,VPS,CPS          ' read pwr supp output v,i
7272 IOCTL#2,"BREAK"
7280 PRINT#2,"OUTPUT";PADDR$;"FOX"
7290 RCIRC=VPS/CPS
7300 PRINT,VPS,CPS,RCIRC;: INPUT" ",YESTP$
7310 IF YESTP$="Y" THEN GOTO 7320 ELSE GOTO 7330
7320 GOTO 7180 'Loop back for another step-up of V
7330 IF MODE$="L" THEN INPUT "REINSTALL the 1 kOhm resistor and press RTN",DUM$
7340 RETURN
7350 '
7500 ' *** Find Control Params for Curr (K-228) ***
7505 IF MODE$="L" GOTO 7580
7507 ' HIGH Current Output Range ...
7510 VP=1.05*XC*RCIRC 'set voltage limit 5% over min for curr & resis
7530 CP$=STR$(XC); CN$=STR$(-XC)
7540 VP$=STR$(VP); VN$=STR$(-VP)
7550 SPOS$=";V"+VP$+"I"+CP$+"W1X"
7560 SNEG$=";V"+VN$+"I"+CN$+"W1X"
7570 RETURN
7580 ' LOW Current Output Range ...
7590 VP=XC*(1000+RCIRC) 'Ohms Law
7600 IF VP>10 THEN VP=10 'limit to 10 Volts
7610 CLIM=1.1*XC 'set current limit 10% over expected output
7620 IF CLIM<.001 THEN CLIM=.001
7630 IF CLIM>.01 THEN CLIM=.01
7635 CP$=STR$(CLIM); CN$=STR$(-CLIM)
7640 GOTO 7540
7650 '
8000 ' ***** EMERGENCY CURRENT SHUTDOWN *****
8010 PRINT#2,"OUTPUT";PADDR$;"FOX" 'turn off current
8020 BEEP: BEEP: BEEP
8030 LOCATE 25,1: INPUT"EMERGENCY CURRENT SHUTDOWN! Press <RTN> to continue or enter <Q> to stop ==>";R$
8040 IF R$="Q" THEN EMSS="Q": RETURN 8080
8050 IF R$="q" THEN EMSS="Q": RETURN 8080
8060 PRINT#2,"OUTPUT";PADDR$;"FIX" 'resume with current
8065 GOSUB 4090 'restore message at bottom of screen
8070 GOTO 6620
8080 RETURN 346 'to scan finished
8100 BEEP: BEEP: BEEP
8105 LOCATE 25,1: PRINT "
8110 LOCATE 25,1: INPUT"EXCESSIVE HEATING DETECTED! Enter a new heat limit (mW) or 0 to stop ==>";HLIMIT
8120 IF HLIMIT<=0 THEN RETURN 346 'to scan finished
8130 GOSUB 4090 'restore message at bottom
8140 GOTO 1790
8150 '
9000 ' *** LAKESHORE TEMPERATURE CONTROLLER PARAMETERS ***
9010 PRINT#2,"REMOTE";TADDR$
9020 PRINT#2,"OUTPUT";TADDR$;"FOKF1AKF2A0" 'Display Units
9030 IF T>=45 THEN PRINT#2,"OUTPUT";TADDR$;"R5115D0.0W0" 'Control Settings

```



```

9035 IF T<45 AND T>=19 THEN PRINT#2,"OUTPUT";TADDR$;"R4I10D0.5W0" 'Med. heat
9037 IF T<19 THEN PRINT#2,"OUTPUT";TADDR$;"R3I10D1.0W0" 'Low heat
9040 IF T>=130 THEN PRINT#2,"OUTPUT";TADDR$;"P10" 'Gain Setting = 10
9050 IF T>=65 AND T<130 THEN PRINT#2,"OUTPUT";TADDR$;"P6.0" 'Gain = 6
9060 IF T>=25 AND T<65 THEN PRINT#2,"OUTPUT";TADDR$;"P3.0" 'Gain = 3
9070 IF T<25 THEN PRINT#2,"OUTPUT";TADDR$;"P0.5" 'Gain = 0.5
9080 TC=T+SQR(ABS(T)/300)*TCDEL 'Calculate the Set Point
9083 IF ABS(T)>40 THEN TC=TC+.00897*ABS(T)+1.309 'CGR Correction Factor
9086 IF ABS(T)<=40 THEN TC=TC+.0417*ABS(T) 'CGR Correction Factor
9090 IF TC<TC1 THEN TC=TC1 'Minimum Set Point Allowed
9100 IF TC>TC2 THEN TC=TC2 'Maximum Set Point Allowed
9110 TC$=";"S"+STR$(INT(10*TC)/10)
9120 PRINT#2,"OUTPUT";TADDR$;TC$ 'Set Point Temperature
9130 RETURN
9999 END

```

Appendix C. I-V Acquisition Program

```

10 DEFINT I-N
20 '
30 ' *** IVT.BAS ***
40 '*** KEITHLEY 570 SYSTEM ***
50 '*** PERSONAL488 DATA ACQUISITION ***
100 ' X-VOLTAGE (J) IS STEPPED, AS CONTROLLED BY K-228 Power Supply
105 ' Program operates digital Pwr Supp in Curr-limited mode with 10% spare V
106 ' K-228 mini step is 1/1000 of any Full Range V: 1, 10; I: 0.1, 1, 10
107 ' There is provision (Menu step 13) for manual search for -Ic
110 ' ACQUIRED X1, X2 AND Y DATA UPON SPECIFIED Y-VOLTAGE CRITERION.
120 ' DATA STORED TO ASCII FILE. PLOTS AUXILIARY DATA FILE FOR COMPARISON
130 ' COMMAND P0 SENT TO Y-DVM (FOR K-181 TURNS OFF DIGITAL FILTERING)
132 ' MANUAL INITIATION OF I,V SETS. X1 data assumed to be Temperature
133 ' CALC Std Dev OF V-DATA FROM V-AVG, AND SAVE (unlike previous RMS Dev)
134 ' WITHOUT (CURR=0) PAUSE AFTER EA READ; (no JP function)
135 ' Uses both + & - currents (like previous DA-IVQT.. programs)
136 ' *** MINIMUM SWITCHING Version: Stays in OPERATE mode until Scan Finished
137 '   ic: Reduces curr to low ON value at end of ea set of nfil readings,
138 '   but does not go to Standby mode until end of whole Scan series.
140 'TWO RANGES: Now has a low current output mode (MODE$="L") allowing
145 '   outputs between 1 uA and 10 mA unavailable in the previous
150 '   version. This is achieved by use of a 1 kOhm Std. resistor
155 '   and utilization of the voltage limit mode of the K-228.
160 '
200 '*** MAIN PROGRAM ***
210 '
220 GOSUB 400 '--- SET DEFAULT PARAMETER VALUES ---
225 GOSUB 4150 '--- READ IN FILE OF SETUP AND GRAPHICS PARAMETERS ---
230 GOSUB 700 '--- SIGN-ON & HARDWARE SETTINGS MENU ---
240 GOSUB 1000 '--- SETUP PARAMETERS MENU ---
245 GOSUB 4500 '--- STORE SETUP AND GRAPHICS PARAMS TO FILE ---
250 GOSUB 1600 '--- DATA ACQUISITION INITIALIZATION ---
255 FOR XC=XMINC TO XMAXC STEP DELX'---STEP SCAN X-PARAMETER
258 GOSUB 7500 ' Get Pwr Supp control params SPOS$, SNEG$ from XC, RCIRC
260 GOSUB 1750 '--- TAKE ONE FILTERED DATUM-THERMAL EMF ---
270 ' GOSUB 3550 '--- CHECK FOR KEYBOARD INTERRUPT ---
300 GOSUB 3750 '--- CALC. TEMP. FROM THERM. CALIBRATION ---
301 IF IDATFLG=1 THEN IDATFLG=0: GOTO 310
302 ' GOSUB 6200 '--- Test TEMP. for designated interval---
310 GOSUB 2000 '--- PRINT DATA TO DISK ---
320 GOSUB 2700 '--- PLOT OR PRINT DATA TO SCREEN ---
330 GOSUB 3550 '--- CHECK FOR KEYBOARD INTERRUPT ---
332 IF VY>=DELY GOTO 340: PRINT " Exceeding Y-Limit !" 'End Scan - Exceed Y-Lim
335 NEXT XC '--- LOOP BACK FOR MORE DATA ---
340 GOSUB 7600 '--- set K228 to "best zero" off

```



```

346 BEEP: LOCATE 24,16: PRINT** SCAN FINISHED **;
347 GOSUB 3550 '--- CHECK FOR KEYBOARD INTERRUPT ---
348 GOTO 347
349 GOTO 240
350 '
360 '*** END MAIN PROGRAM ***
370 '
380 '
400 '*** DEFINE DEFAULT PARAMETERS ***
410 CLS: KEY OFF: KEY 1,"LIST 200-360"+CHR$(13)
420 DEFINT I-N
425 JD=30 'JD=1400 for .25sec delay after curr-switching
428 HLIMIT=20 'allowed safety limit for sample heating (mW)
430 DIM X(500),Y(500),Z(500),Q(500),YD(20),H(500) 'DIM DATA
440 DIM V(500),T(500) 'ARRAY FOR THERM. CALIBRATION TABLE(e.g. DIODE V,T)
445 DIM XG(500),YG(500),ZG(500),QG(500) 'ARRAY OF COMPARISON DATA FOR GRAPHICS
450 'ON ERROR GOTO 5400 '---ERROR TRAPPING
455 RCIRC = 2 'circuit resistance w/o std resistor
460 RESTORE 470
470 DATA 10,1,1,1000000,0,0,1,1,1
480 READ CUR,SCALEX,SCALEXC,SCALEY,DELX,DELY,G0%,G1%,NFILT 'Default Params
490 DATA "<INACTIVE>","<ACTIVE>"
500 READ INACT$,ACT$: GSET$=INACT$: GCSET$=INACT$
504 '--- GPIB BUS ADDRESSES & METER PARAMS
505 K$="KEITHLEY 181/199/197" '--- GPIB BUS ADDRESSES & METER PARAMS
506 KP$="Keithley 228 Power Supply"
507 DATA "26","14","11",5,5,1,"L"
508 READ XADDR$,YADDR$,PADDR$,NXM,NYM,NPM,MODE$
509 MX$=K$: MY$=K$: MP$=KP$
510 '
520 'GRAPHICS DEFAULT PARAMETERS
530 RESTORE 550
540 READ XMIN,XMAX,YMIN,YMAX
550 DATA 0,1,0,100,0
560 READ XS,Y1$,Y2$,T$
570 RESTORE 590
580 READ XS,Y1$,Y2$,T$
590 DATA "I (Amps)","V","(uVolts)","IV Curve"
600 RESTORE 620
610 READ DXPIX,DYPIX,XPIX0,YPIX0 'AXIS CONTANTS IN PIXELS
620 DATA 550,300,80,15
630 RETURN 'TO MAIN PROGRAM
640 '
650 '
700 '*** SIGN-ON HARDWARE SETTINGS MESSAGE ***
710 CLS: PRINT CHR$(7)
720 PRINT:PRINT " *** HARDWARE SETTINGS ***"
730 PRINT " 1: X-INPUT: GPIB Address: ";XADDR$; " Meter ID: ";MX$
740 PRINT " 2: Y-INPUT: GPIB Address: ";YADDR$; " Meter ID: ";MY$
747 PRINT " 3: P-INPUT: GPIB Address: ";PADDR$; " Pwr Supp ID: ";MP$
750 PRINT:PRINT
752 PRINT " Meter Setup: X channel #1 <===> Thermometer Voltage Signal"
754 PRINT " X channel #2 <===> Sample Current Std. Resistor"
755 PRINT " X channel #3 <===> Sample Heat Dissipation Signal"
756 PRINT " Y voltmeter <===> Sample Voltage"
758 PRINT
760 INPUT"ENTER SELECTION # (<C/R> TO CONTINUE): ",ICODE
770 ON ICODE GOTO 790,810,840
780 RETURN 'TO MAIN PROGRAM
790 INPUT"ENTER NEW GPIB ADDRESS FOR X-INPUT: ",XADDR
791 GOSUB 850 '--- METER ID CHOICES FOR READING STRING MASKING
792 INPUT"ENTER X-INPUT Meter ID CODE (DEFAULT = PREVIOUS): ",NMT
794 IF NMT < > 0 THEN NM=NMT ELSE 800
796 GOSUB 900: MX$=M$: NXM=NMSK '--- ASSIGN METER ID NAME & MASKING DATA
800 XADDR$=STR$(XADDR): GOTO 720
810 INPUT"ENTER NEW GPIB ADDRESS FOR Y-INPUT: ",YADDR
811 GOSUB 850 '--- METER ID CHOICES

```



```

812 INPUT "ENTER Y-INPUT Meter ID CODE (DEFAULT = PREVIOUS): ",NMT
814 IF NMT < > 0 THEN NM=NMT ELSE 820
816 GOSUB 900: MY$=M$: NYM=NMSK '--- ASSIGN METER ID NAME & MASKING DATA
820 YADDR$=STR$(YADDR): GOTO 720
840 INPUT "ENTER NEW GPIB ADDRESS FOR P-INPUT: ",PADDR
841 GOSUB 850 '--- METER ID CHOICES
842 INPUT "ENTER P-INPUT Meter ID CODE (DEFAULT = PREVIOUS): ",NMT
843 IF NMT < > 0 THEN NM=NMT ELSE 848
844 GOSUB 900: MP$=M$: NPM=NMSK '--- ASSIGN METER ID NAME & MASKING DATA
848 PADDR$=STR$(PADDR): GOTO 720
849 '
850 ' *** ASSIGN STRING MASKING PARAMS FOR METERS ***
854 PRINT "**** Meter ID Codes ****"
855 PRINT " 1: KEITHLEY 181,199,197"
856 PRINT " 2: FLUKE 8840A"
857 PRINT " 3: Keithley 228 Pwr Supp"
860 RETURN
870 '
880 '
890 '
900 '*** ASSIGN METER ID NAME ***
910 ON NM GOTO 930,940,950
920 PRINT CHR$(7): PRINT "< < WRONG METER ID > > ": RETURN 230
930 M$="KEITHLEY 181/199/197": NMSK=5: RETURN
940 M$="FLUKE 8840A": NMSK=1: RETURN
950 M$="KEITHLEY 228 Pwr Supp": NMSK=1: RETURN
960 '
1000 SCREEN 0: CLS
1010 GOSUB 5500 '--- INCREMENT EXTENSION ON DATA FILENAME
1020 PRINT: PRINT " *** SET-UP PARAMETERS for DA-IVT *** "
1025 IF MODE$="L" THEN PRINT " WARNING : INSTALL 1 kOhm Std. Resistor at K-228 Output !!!":BEEP
1030 PRINT " 1: FILENAME OF SETUP AND GRAPHICS PARAMETERS TO USE: ";PUFL$
1040 PRINT " 2: FILENAME OF SETUP AND GRAPHICS PARAMETERS TO SAVE TO: ";PSFL$
1050 PRINT " 3: X2-VOLTAGE SCALE FACTOR (Signal/Meas V or I/STD ohms): ";SCALEX
1060 PRINT " 4: X2-SIGNAL RANGE/STEP SIZE (Amps): ";XMINC;"to";XMAXC;" / ";DELX
1070 PRINT " 5: Y-VOLTAGE SCALE FACTOR (Signal/Meas V): ";SCALEY
1075 PRINT " 6: Y-SIGNAL LIMIT: ";DELY
1090 PRINT " 7: DATA FILENAME: ";DNM$
1095 IF DNM$="" GOTO 1110
1100 PRINT " TITLE: ";TITLE$
1110 PRINT " 8: THERM. CAL. TABLE FILENAME (for X1-signal conversion): ";THNM$
1112 IF THNM$="" GOTO 1120
1115 PRINT " TITLE: ";THTTL$
1120 PRINT " 9: TEMPERATURE INTERVAL BETWEEN DATA: ";DELT
1125 PRINT "10: NO. OF SAMPLES IN DIGITAL FILTERING: ";NFILT
1130 PRINT "11: SCREEN GRAPHICS PARAMETERS SETUP: ";GSET$
1135 PRINT "12: EXIT THE PROGRAM
1137 PRINT "13: Test circuit Resistance, or Sample Ic. Present Rcirc= ";RCIRC
1140 PRINT "14: Ic Operating Range (H, > 1mA; L, < 10mA): ";MODE$
1145 PRINT "15: Maximum Heating Allowed (mW): ";HLIMIT
1147 PRINT
1150 INPUT "> ENTER SELECTION # (< C/R > TO EXECUTE): ",ICODE
1160 ON ICODE GOTO 1400,1430,1290,1310,1180,1200,1220,1350,1460,1380,1330,1335 ,1480,1491,1325
1170 RETURN 'TO MAIN PROGRAM
1180 INPUT " ENTER Y-VOLTAGE SCALE FACTOR (Signal/Vmeas): ",SCALEY
1190 GOTO 1020
1200 INPUT " ENTER Y-SIGNAL LIMIT: ",DELY
1210 GOTO 1020
1220 INPUT " INPUT DATA FILENAME (EXT .DT6 WILL BE ADDED IF NOT ENTERED): ",DNM$
1230 IF DNM$="" THEN 1280
1240 PRINT " ENTER 80 CHARACTER DATA SET TITLE(DEFAULT=PREVIOUS): ":INPUT"DUM$
1250 IF DUM$="" THEN 1270
1260 TITLE$=DUM$
1270 FOR J=1 TO LEN(DNM$): IF MID$(DNM$,J,1) < > "." THEN NEXT J ELSE 1280
1272 DNM$=DNM$+" .DT6"
1280 GOTO 1020
1290 INPUT " ENTER X-VOLTAGE SCALE FACTOR (Signal/Vmeas): ",SCALEX

```

```

1300 GOTO 1020
1310 INPUT* ENTER X-SIGNAL RANGE & STEP SIZE(XMIN,XMAX,STEP(abs Amps)): ",XMINC,XMAXC,DELX
1315 ' INPUT* ENTER X-SIGNAL BACKSTEP (FRACTION OF CURRENT X): ",XOFFC
1320 GOTO 1020
1325 INPUT* ENTER MAXIMUM HEATING ALLOWED (mW): ",HLIMIT
1326 GOTO 1020
1330 GOSUB 2250 'Define Graphics Parameters
1332 GOTO 1020
1335 GOSUB 4500: END '--- STORE PARAMS TO FILE AND EXIT
1340 GOTO 1020
1350 INPUT* ENTER THERMOM. CALIB. TABLE FILENAME(EXT .CAL WILL BE ADDED): ",THNM$
1360 IF THNM$="" THEN 1370 ELSE THNM$=THNM$+".CAL"
1365 GOSUB 3900 '--- READ IN THERM. CALIB. DATA ---
1366 INPUT* ENTER VOLTAGE SCALE FACTOR (signal/voltage): ",SCALEZ
1370 GOTO 1020
1380 INPUT* ENTER NO. SAMPLES IN DIGITAL FILTERING: ",NFILT
1390 GOTO 1020
1400 INPUT " ENTER FILENAME FOR SETUP PARAMS. TO USE(EXT .PAR WILL BE ADDED): ",PUFL$
1410 IF PUFL$="" THEN 1420 ELSE PUFL$=PUFL$+".PAR"
1420 GOSUB 4150: GOTO 230 '---READ IN SETUP AND GRAPHICS PARAMS
1430 INPUT " ENTER FILENAME FOR SETUP PARAMS TO SAVE TO (.PAR WILL BE ADDED): ",PSFL$
1440 IF PSFL$="" THEN 1450 ELSE PSFL$=PSFL$+".PAR"
1450 GOTO 1020
1460 INPUT " ENTER TEMPERATURE INTERVAL BETWEEN DATA: ";DELT
1470 GOTO 1020
1480 GOSUB 7000 'Check out circuit resistance
1490 GOTO 1020
1491 INPUT " ENTER OPERATING RANGE (H, >1mA; L, <10mA): ",MODE$
1492 IF MODE$="H" THEN GOSUB 1800: GOTO 1020
1493 IF MODE$="L" THEN GOSUB 1810: GOTO 1020
1494 PRINT "Error" : BEEP : GOTO 1491
1495 '
1496 '
1500 '*** OPEN DATA FILE ***
1510 IF DNM$="" THEN 1550
1520 OPEN "O",#1,DNM$
1530 PRINT #1, TITLE$
1540 PRINT #1," I(A) uVolts T(K) Std Dev(V) Heating(mW)"
1550 RETURN
1560 '
1570 '
1600 ' *** INITIALIZATION FOR DATA ACQU. ***
1605 CLOSE '--- Close any open files
1610 GOSUB 4050 '---PRINT MESSAGE AT SCREEN BOTTOM
1620 I=0 'INITIALIZE DATA ARRAY INDEX
1626 XOFFV=2047 '---COUNTS FOR ZERO CURRENT THERMAL
1630 GOSUB 4850 '--- ESTABLISH COMMUNICATION W/PERSONAL488
1640 GOSUB 4950 '--- SIGNON MESSAGE
1650 GOSUB 5050 '---ASSIGN REMOTE MODE ADDRESSES
1657 'GOSUB 5700 '--- INITIALIZE FOR ANALOG OUTPUT xx not used here
1660 FLG$="L" 'INITIALIZE FOR DATA SCREEN PRINTOUT
1680 GOSUB 1500 '--- OPEN DATA FILE
1687 PRINT#2,"output";XADDR$;"N2X" 'Channel#2 for Isam std-R
1690 IVXFLG=0 '--- FLAG FOR FIRST TIME THRU
1700 PRINT "****Beginning Data Acquisition ****"
1706 PRINT " # I(A) V Std Dev(V) T(K) Heating(mW)"
1710 RETURN 'TO MAIN PROGRAM
1720 '
1730 '
1750 ' *** TAKE DATA SAMPLE ***
1760 '--- GPIB INPUT ---
1770 GOSUB 6400 '--- FIND AVG OF NFILT GPIB READINGS
1780 VX=ABS(SUMX*SCALEX): VY=ABS(SUMY*SCALEY): VZ=ABS(SUMZ*SCALEZ)
1785 IF HEAT>HLIMIT GOTO 8100 'Excessive heating detected
1790 RETURN 'TO MAIN PROGRAM
1800 SOUND 880, 15
1802 INPUT " REMOVE 1 kOhm Std. Resistor then press RTN",DUM$

```



```

1805 RETURN
1810 SOUND 880, 15
1815 INPUT "INSTALL 1 kOhm Std. Resistor then press RTN",DUM$
1820 RETURN
1830 '
1840 '
2000 ' *** PRINT VALUES ON DISK ***
2010 I=I+1: X(I)=VX: Y(I)=VY: Q(I)=QY: H(I)=HEAT 'INCREMENT INDEX
2020 IF THNMS="" THEN Z(I)=VZ: GOTO 2040
2030 Z(I)=T
2040 IF DNM$="" THEN 2060
2050 PRINT #1,X(I);Y(I);Z(I);Q(I);H(I)
2060 RETURN 'TO MAIN PROGRAM
2070 '
2080 '
2100 ' *** TEST TO REDEFINE GLOBAL GAIN ***
2110 IF VTST>=5 THEN G%=1: GOTO 2150
2120 IF VTST>=2 THEN G%=2: GOTO 2150
2130 IF VTST>=1 THEN G%=5: GOTO 2150
2140 G%=10
2150 RETURN
2160 IF VTST$="VX" THEN GT%=G%: GOSUB 1790: RETURN 'CHANGE TO NEW X-GAIN
2170 GS%=G%: GOSUB 1790 'CHANGE TO NEW Y-GAIN
2180 RETURN
2190 '
2200 '
2250 ' *** GRAPHICS PARAMETERS ***
2260 GSET$=ACT$ 'SCREEN GRAPHICS ACTIVE
2270 PRINT: PRINT: PRINT" *** SCREEN GRAPHICS PARAMETERS ***
2280 PRINT" 1: I-axis Imin, Imax: ",XMIN,XMAX
2290 PRINT" 2: V-axis Vmin, Vmax: ",YMIN,YMAX
2300 PRINT" 3: I-axis label: ",X$
2310 PRINT" 4: V-axis label: ",Y1$,Y2$
2320 PRINT" 5: Graph Title: ",T$
2325 PRINT" 6: COMPARISON DATA SET FILENAME: ",GCOMFL$
2326 PRINT" TITLE: ",GTTL$
2327 PRINT" 7: VIEW COMPARISON DATA SET: ",GCSET$
2330 PRINT
2340 INPUT"> ENTER SELECTION # (<C/R> TO MAIN MENU): ",ICODE
2350 ON ICODE GOTO 2370,2390,2410,2430,2470,2481,2483
2360 GOTO 2490
2370 INPUT" ENTER I-axis Imin, Imax: ",XMIN,XMAX
2380 GOTO 2270
2390 INPUT" ENTER V-axis Vmin, Vmax: ",YMIN,YMAX
2400 GOTO 2270
2410 INPUT" ENTER I-axis label: ",X$
2420 GOTO 2270
2430 INPUT" ENTER V-axis label: ",Y$
2440 FOR J=1 TO LEN(Y$): IF MID$(Y$,J,1)<>"(" THEN NEXT J
2450 Y1$=LEFT$(Y$,J-1): J=LEN(Y$)-J+1: Y2$=RIGHT$(Y$,J)
2460 GOTO 2270
2470 INPUT" ENTER Graph Title: ",T$
2480 GOTO 2270
2481 INPUT" ENTER DATA SET FILENAME: ",GCOMFL$
2482 GOSUB 5800: GOTO 2270 'READ IN DATA SET FROM FILE
2483 INPUT" VIEW PLOT OF DATA SET (Y=YES)?: ",ANS$
2484 IF ANS$="Y" OR ANS$="y" THEN GCSET$=ACT$ ELSE GCSET$=INACT$:GOTO 2270
2485 GOSUB 2490 'DEFINE GRAPH AXES RANGES
2486 GOSUB 5900 'PLOT DATA SET
2487 GOSUB 4111 'PRINT MESSAGE AT SCREEN BOTTOM
2488 IF INKEY$="" THEN 2488 ELSE SCREEN 0: GOTO 2270
2489 '
2490 XRNG=XMAX-XMIN: YRNG=YMAX-YMIN
2500 XMIN$=STR$(XMIN): XMAX$=STR$(XMAX)
2510 YMIN$=STR$(YMIN): YMAX$=STR$(YMAX)
2520 GOSUB 2610: GOSUB 2660 'DEFINE FUNCTION TO CALC COORD IN PIXELS
2530 RETURN

```

```

2540 '
2550 '
2600 '*** FN TO CALCULATE Y IN SCREEN PIXELS ***
2610 DEF FNYPIX(YVAR,YMIN,YRNG,DYPIX,YPIX0)=-(YVAR-YMIN)*DYPIX/YRNG+YPIX0+DYPIX
2620 RETURN
2630 '
2640 '
2650 '*** FN TO CALCULATE X IN SCREEN PIXELS ***
2660 DEF FNXPIX(XVAR,XMIN,XRNG,DXPIX,XPIX0)=(XVAR-XMIN)*DXPIX/XRNG+XPIX0
2670 RETURN
2680 '
2690 '
2700 ' *** PLOT OR PRINT DATA ***
2710 IF INK$ < > "L" THEN IF INK$ < > "I" THEN 2740
2720 IF FLG$="L" THEN 2780
2730 FLG$="L": GOSUB 3050: GOSUB 4050: RETURN 'LIST DATA TO CURRENT I
2740 IF GSET$=INACT$ THEN 2780
2750 IF INK$ < > "P" THEN IF INK$ < > "p" THEN 2780
2760 IF FLG$="P" THEN 2800
2770 FLG$="P": GOSUB 2900: GOSUB 4050: RETURN 'PLOT DATA TO CURRENT I
2780 IF FLG$ < > "L" THEN GOTO 2790
2781 PRINT USING " ### ";I;
2782 PRINT USING " +##.##### ";X(I);
2783 PRINT USING " +#.#####^ ^ ^ ";Y(I),Q(I);
2784 PRINT USING " ###.#####":Z(I),H(I)
2785 RETURN 'TO MAIN PROGRAM
2790 IF GSET$=INACT$ THEN 2840
2800 XP=FNXPPIX(X(I),XMIN,XRNG,DXPIX,XPIX0)
2805 IF XP>10000 THEN 2840
2810 YP=FNYPIX(Y(I),YMIN,YRNG,DYPIX,YPIX0)
2815 IF ABS(YP)>10000 THEN 2840
2820 PSET (XP,YP) 'PLOTS POINT
2830 IF THNM$="" GOTO 2840
2833 LOCATE 1,67: PRINT "T= " INT(I) " K ";
2836 LOCATE 24,1
2840 RETURN 'TO MAIN PROGRAM
2850 '
2860 '
2900 ' *** REFRESH PLOT OF DATA UP TO CURRENT POINT ***
2910 CLS: GOSUB 3150: GOSUB 3300 'DRAW AND LABEL AXES
2920 FOR J=1 TO I
2930 XP=FNXPPIX(X(J),XMIN,XRNG,DXPIX,XPIX0)
2935 IF ABS(XP)>10000 THEN 2970 '--- PT OUT OF RANGE
2940 YP=FNYPIX(Y(J),YMIN,YRNG,DYPIX,YPIX0)
2945 IF ABS(YP)>10000 THEN 2970
2950 'CIRCLE (XP,YP),3
2960 PSET (XP,YP)
2970 NEXT J
2975 IF GCOMFL$="" THEN RETURN
2976 IF GCSET$=ACT$ THEN GOSUB 5920 ' PLOT COMPARISON DATA
2980 RETURN
3000 '
3010 '
3050 '*** PRINT DATA ON SCREEN ***
3060 SCREEN 0: CLS: LOCATE 23,1,0
3066 PRINT " # I(A) V Std Dev(V) T(K) Heating(mW)"
3070 J1=1-20: IF J1<0 THEN J1=1
3080 FOR J=J1 TO I
3091 PRINT USING " ### ";J;
3092 PRINT USING " +##.##### ";X(J);
3093 PRINT USING " +#.#####^ ^ ^ ";Y(J),Q(J);
3094 PRINT USING " ###.#####":Z(J),H(J)
3100 NEXT J
3110 RETURN
3120 '
3130 '
3150 '*** SUB TO DRAW GRAPH AXES ***

```



```

3160 SCREEN 9 'HI RES GRAPHICS SCREEN
3170 CLS
3180 PSET (80,15)
3190 DWN=300: RGT=550: TICKU=30: TICKR=55: ZERO=0
3200 FOR J=1 TO 10: DRAW"D=TICKU;NM+550,0;":NEXT J '---LEFT VERT AXIS
3210 FOR J=1 TO 10: DRAW"R=TICKR;NM+0,-300;":NEXT J '---BOTTOM HORIZ AXIS
3220 DRAW"U=DWN;L=RGT;"
3230 RETURN
3240 '
3250 '
3300 '*** SUB TO LABEL AXES ***
3310 IF LEN(X$)>60 THEN X$=LEFT$(X$,60) 'TRUNCATE IF TOO LONG
3320 XAX=44-.5*LEN(X$)
3330 LOCATE 24,XAX: PRINT X$;
3340 IF LEN(Y1$)>9 THEN Y1$=LEFT$(Y1$,9) 'TRUNCATE IF TOO LONG
3350 TAX=5-.5*LEN(Y1$)
3360 LOCATE 12,TAX: PRINT Y1$;
3370 IF LEN(Y2$)>9 THEN Y2$=LEFT$(Y2$,9)
3380 TAX=5-.5*LEN(Y2$)
3390 LOCATE 13,TAX: PRINT Y2$;
3400 IF LEN(T$)>70 THEN T$=LEFT$(T$,70) 'TRUNCATE IF TOO LONG
3410 TAX=44-.5*LEN(T$)
3420 LOCATE 1,TAX: PRINT T$;
3430 LOCATE 24,12-LEN(XMIN$): PRINT XMIN$;
3440 IF XMAX$="" THEN 3460
3450 LOCATE 24,81-LEN(XMAX$): PRINT XMAX$;
3460 LOCATE 23,10-LEN(YMIN$): PRINT YMIN$;
3470 LOCATE 2,10-LEN(YMAX$): PRINT YMAX$;
3480 RETURN
3490 '
3500 '
3550 ' *** SUB TO CHECK KEYBOARD STATUS ***
3560 IN$=INKEY$
3570 IF IN$="" THEN RETURN
3575 IF IN$=CHR$(13) THEN 255 '---INITIATE ANOTHER SET OF READINGS
3580 IF IN$=CHR$(13) THEN IDATFLG=1: GOTO 3710 'MANUAL DATA STORAGE
3590 INK$=IN$
3600 IF INK$<>"Q" AND INK$<>"q" THEN 3680
3610 IF DNMS="" THEN 3630 'DATA FILENAME
3620 CLOSE #1: GOSUB 6000 '---REWRITE DATA TO FILE IN STD FORMAT
3630 SCREEN 0: INPUT "ANOTHER DATA SET (Y=YES)?":ANS2$
3640 IF ANS2$="y" OR ANS2$="Y" THEN 3670
3650 ON ERROR GOTO 0 'DISABLE ERROR TRAPPING
3660 CLS: END
3670 CLOSE: RETURN 240 'TO MAIN PROGRAM AT MENU
3680 IF INK$<>"P" THEN IF INK$<>"p" THEN RETURN
3690 IF INK$<>"I" THEN IF INK$<>"L" THEN RETURN
3700 RETURN 320 'TO MAIN PROGRAM AT PLT OR PRNT DATA
3710 RETURN 260 'TO MAIN PROGRAM AT TAKE ONE DATUM
3720 '
3730 '
3750 '*** SUB TO INTERPOLATE TEMPERATURES FROM DIODE T,V TABLE ***
3760 IF THNM$="" THEN RETURN 'TO MAIN PROGRAM
3770 VZC=VZ
3780 NLO=1: NHI=NDATA 'LOW AND HI INDICES OF TABLE DATA
3790 N=(NHI+NLO)/2 'INTEGER DIVIDE 'TABLE INDEX TO BE COMPARED TO DATUM
3800 IF VZ<V(N) THEN NHI=N: GOTO 3820
3810 NLO=N
3820 IF NHI<>NLO+1 THEN GOTO 3790
3830 T=T(NHI)+(VZ-V(NHI))*(T(NHI)-T(NLO))/(V(NHI)-V(NLO))
3840 RETURN
3850 '
3860 '
3900 '*** SUB TO READ IN THERM. CALIB DATA ***
3910 IF THNM$="" THEN RETURN
3930 THNMT$=THNM$
3940 PRINT"*** Reading in therm. calibration table ***"

```

```

3950 OPEN "1",#1,THNMS
3952 INPUT#1, THTTLS '---TITLE OF DATA SET
3960 INPUT #1,NDATA
3970 FOR J=1 TO NDATA
3980 INPUT #1,V(J),T(J)
3990 NEXT J
4000 CLOSE #1
4010 RETURN
4020 '
4030 '
4050 '*** PRINT MESSAGE AT BOTTOM OF SCREEN ***
4060 IF GSET$=ACT$ THEN 4090
4070 CLS: LOCATE 25,1: PRINT"PRESS: <C/R> STORE PT. <Q> QUIT";
4080 LOCATE 1,1: GOTO 4110
4090 LOCATE 25,1: PRINT"PRESS: <C/R> STORE PT. <Q> QUIT <P> PLOT RESTORE <L> LIST";
4100 LOCATE 24,1
4110 RETURN
4111 LOCATE 25,1: PRINT" PRESS <C/R> TO CONTINUE";
4112 LOCATE 24,1
4113 RETURN
4120 '
4130 '
4150 '*** READ IN SETUP AND GRAPHICS PARAMETERS ***
4160 IF PUFL$="" THEN RETURN
4170 OPEN "1",#1, PUFL$
4180 PRINT"*** RETRIEVING PARAMETERS FROM: ";PUFL$;" ***"
4190 '---SETUP PARAMETERS
4195 INPUT #1,PSFL$
4200 INPUT #1,SCALEX
4205 INPUT #1,RCIRC
4207 INPUT #1,XMINC,XMAXC,DELX
4210 INPUT #1,XOFFC
4220 INPUT #1,SCALEY
4230 INPUT #1,DELY
4240 INPUT #1,DNMS
4250 INPUT #1,TITLE$
4260 DUM$=TITLE$
4270 INPUT #1,THNMS
4272 INPUT #1,SCALEZ
4275 INPUT #1,DELT
4280 INPUT #1,NFILT
4290 INPUT #1,GSET$
4300 '---GRAPHICS PARAMETERS
4310 INPUT #1,XMIN,XMAX
4320 INPUT #1,YMIN,YMAX
4330 INPUT #1,X$
4340 INPUT #1,Y1$
4350 INPUT #1,Y2$
4360 INPUT #1,T$
4370 '---GPIB & METER PARAMS
4380 INPUT#1,XADDR$
4390 INPUT#1,YADDR$
4397 INPUT#1,PADDR$
4400 INPUT#1,MX$
4410 INPUT#1,MY$
4417 INPUT#1,MP$
4420 INPUT#1,NXM,NYM,NPM
4422 '--- COMPARISON GRAPHICS DATA FILE INFO
4424 INPUT#1,GCOMPL$ 'DATA FILENAME
4426 INPUT#1,GSET$ 'FLAG FOR GRAPHICS COMPARISON
4430 CLOSE #1
4435 GOSUB 3900 '---READ IN THERM CALIB. DATA
4440 IF GSET$=ACT$ THEN GOSUB 5800: GOSUB 2490 '---READ IN COMP DATA SET
4450 RETURN
4460 '
4470 '
4500 '*** SAVE SETUP AND GRAPHICS PARAMETERS TO FILE ***

```



```

4510 IF PSFL$="" THEN RETURN
4520 OPEN "O",#1, PSFL$
4530 PRINT"*** STORING PARAMETERS TO: ";PSFL$;" ***"
4540 '---SETUP PARAMETERS
4545 PRINT#1,PSFL$
4550 PRINT#1,SCALEX
4555 PRINT#1,RCIRC
4557 PRINT#1,XMINC,XMAXC,DELX
4560 PRINT#1,XOFFC
4570 PRINT#1,SCALEY
4580 PRINT#1,DELY
4590 PRINT#1,DNM$
4600 PRINT#1,TITLE$
4610 PRINT#1,THNM$
4612 PRINT#1,SCALEZ
4615 PRINT#1,DELT
4620 PRINT#1,NFILT
4630 PRINT#1,GSET$
4640 '---GRAPHICS PARAMETERS
4650 PRINT#1,XMIN,XMAX
4660 PRINT#1,YMIN,YMAX
4670 PRINT#1,X$
4680 PRINT#1,Y1$
4690 PRINT#1,Y2$
4700 PRINT#1,T$
4710 '---GPIB & METER PARAMS
4720 PRINT#1,XADDR$
4730 PRINT#1,YADDR$
4737 PRINT#1,PADDR$
4740 PRINT#1,MX$
4750 PRINT#1,MY$
4757 PRINT#1,MP$
4760 PRINT#1,NXM,NYM,NPM
4762 '---COMPARISON GRAPHICS DATA FILE INFO
4764 PRINT#1,GCOMPL$ 'FILENAME OF COMPARISON DATA SET
4766 PRINT#1,GCSET$ 'FLAG FOR ACTIVE GRAPICS COMPARISON
4770 CLOSE #1
4780 RETURN
4790 '
4800 '
4850 ' *** Establish communications with Personal488 ***
4860 OPEN "\DEV\IEEEOUT" FOR OUTPUT AS #2
4870 'Reset Personal488
4880 IOCTL#2,"BREAK"
4885 PRINT#2,"RESET"
4890 'Open file to read responses from Personal488
4900 OPEN "\DEV\IEEEIN" FOR INPUT AS #3
4904 'Enable SEQUENCE error detection by Personal488
4905 PRINT#2,"FILL ERROR"
4906 PRINT#2,"TIME OUT 10"
4910 RETURN
4920 '
4930 '
4950 ' *** Read the signon and revision message ***
4960 PRINT#2,"HELLO"
4970 INPUT#3,A$
4980 PRINT A$
4990 RETURN
5000 '
5010 '
5050 '*** Put the METERS into REMOTE ***
5060 PRINT#2,"REMOTE";YADDR$
5070 PRINT#2,"REMOTE";XADDR$
5075 PRINT#2,"REMOTE";PADDR$      'K-228 Pwr Supp
5080 'RETURN
5090 'R0: Auto range      X: Execute
5100 PRINT#2,"OUTPUT";XADDR$;"R0P0X"

```

```

5110 PRINT#2,"OUTPUT";YADDR$;"POT1X" 'K-181: P0=FILT OFF,T1=FRESH BUF @ TALK
5117 PRINT#2,"OUTPUT";PADDR$;"C0A0K0G5X" 'K0=await finish; G5=v,i val read
5120 RETURN
5130 '
5140 '
5150 '
5340 '
5350 '*** PRINTOUT MESSAGE FOR BAD READING ***
5360 PRINT CHR$(7);: IF FLG$="L" OR FLO$="I" THEN PRINT ">>>BAD READING<<<";R$
5370 RETURN
5380 '
5390 '
5400 '*** ERROR TRAPPING ***
5410 PRINT CHR$(7); '---BELL TO INDICATE ERROR
5415 IF ERR<>53 THEN PRINT ERR: END '---STOP AFTER ERROR
5420 'IF ERR<>53 THEN RESUME 260 '---TRY TO TAKE MORE DATA
5425 PRINT">>>BAD FILENAME<<": FOR J=1 TO 1000: NEXT J: RESUME 240
5440 '
5450 '
5500 ' *** INCREMENT EXTENSION ON DATA FILENAME ***
5510 PRINT CHR$(7)
5520 IF DNMS="" THEN RETURN
5530 FOR J=1 TO LEN(DNMS): IF MID$(DNMS,J,1)<> "." THEN NEXT J
5540 J1=LEN(DNMS)-J+1
5550 EXT$=RIGHT$(DNMS,J1): DNMS=LEFT$(DNMS,J-1)
5560 IEXT=VAL(RIGHT$(EXT$,1)): IEXT=IEXT+1
5570 IEXT$=RIGHT$(STR$(IEXT),1)
5580 EXT$=LEFT$(EXT$,3)+IEXT$
5590 DNMS=DNMS+EXT$
5600 RETURN
5610 '
5620 '
5700 '*** ANALOG OUTPUT INITIALIZATION ***
5705 '---SLOT 3, CHANNEL 1
5710 'CALL IONAME("ANOUT1",3,1)
5720 RETURN
5730 '
5740 '
5800 '*** READ IN DATA SET FOR GRAPHICS COMPARISION ***
5805 PRINT"*** RETRIEVING COMPARISON DATA SET *****"
5810 IF GCOMPL$="" THEN RETURN
5820 OPEN"1",#1, GCOMPL$
5822 INPUT#1, GTTL$ '---TITLE OF FILE DATA
5830 INPUT#1, NDATG
5833 INPUT#1, XG(1),YG(1),ZG(1),QG(1),DUMMY
5835 XMX=XG(1): XMN=XG(1): YMX=YG(1): YMN=YG(1)
5840 FOR J=2 TO NDATG
5850 INPUT#1, XG(J),YG(J),ZG(J),QG(J),DUMMY
5855 IF XG(J)>XMX THEN XMX=XG(J): GOTO 5857
5856 IF XG(J)<XMN THEN XMN=XG(J)
5857 IF YG(J)>YMX THEN YMX=YG(J): GOTO 5860
5858 IF YG(J)<YMN THEN YMN=YG(J)
5860 NEXT J
5870 CLOSE #1
5875 PRINT" XMIN: ";XMN,"XMAX: ";XMX
5876 PRINT" YMIN: ";YMN,"YMAX: ";YMX
5880 RETURN
5890 '
5900 ' *** PLOT OF COMPARISON DATA ***
5910 CLS: GOSUB 3150: GOSUB 3300 'DRAW AND LABEL AXES
5920 FOR J=1 TO NDATG
5930 XP=FNXP(XG(J),XMN,XRNG,DXPIX,XPIX0)
5935 IF ABS(XP)>10000 THEN 5970 '--- PT OUT OF RANGE
5940 YP=FNYP(YG(J),YMN,YRNG,DYPIX,YPIX0)
5945 IF ABS(YP)>10000 THEN 5970
5950 CIRCLE (XP,YP),1
5960 'PSET (XP,YP)

```



```

5970 NEXT J
5980 RETURN
5990 '
6000 '*** REWRITE DATA TO FILE ***
6010 IF DNM$="" THEN RETURN
6020 OPEN"O",#1, DNM$
6030 PRINT"*** STORING DATA ARRAY TO FILE ***"
6040 PRINT#1, TITLE$
6050 PRINT#1, I'—NO. OF DATA IN SET
6060 FOR J=1 TO I
6070 PRINT#1, X(J);Y(J);Z(J);Q(J);H(J)
6080 NEXT J
6090 CLOSE#1
6100 RETURN
6110 '
6200 '*** Test Temperature for designated interval ***
6205 IF THNM$="" THEN RETURN '—NO THERM CALIBRATION
6210 IF IVXFLG=0 THEN IVXFLG=1: TTMP=T: RETURN 'FIRST TIME THROUGH
6220 DELTT=T-TTMP
6230 IF ABS(DELTT)<=DELTT THEN RETURN 340 'LOOP BACK FOR MORE DATA
6250 TTMP=T: RETURN 'TO MAIN PROGRAM, STORE DATA
6260 '
6270 '
6400 ' *** Find the average of Navg readings ***
6410 SUMX=0: SUMY=0: SUMZ=0
6430 PRINT#2,"output";PADDR$;"R0X" 'auto-range
6440 PRINT#2,"output";PADDR$;SPOS$ 'v,i control string
6450 PRINT#2,"output";PADDR$;"F1X" 'turn on +curr
6455 FOR J= 1 TO NFILT
6460 FOR J1=1 TO JD: NEXT J1 ' ~.25 sec delay for JD=1400
6465 PRINT#2,"OUTPUT";XADDR$;"R0N2X" 'X channel #2
6470 PRINT#2,"ENTER";XADDR$
6480 INPUT#3,RX$: VALX=VAL(MID$(RX$,NXM))
6490 IF ABS(VALX)>100 THEN GOSUB 5350: GOTO 6410 '---START OVER -- BAD READING
6500 PRINT#2,"OUTPUT";YADDR$;"P0X" 'K-181: P0=FILTER OFF
6510 PRINT#2,"ENTER";YADDR$
6520 INPUT#3,RX$: VALY=VAL(MID$(RX$,NYM))
6530 PRINT#2,"output";PADDR$;"V-.001I-.0001W1X"
6540 PRINT#2,"output";PADDR$;SNEG$ 'v,i control string for NEG curr
6560 FOR J1=1 TO JD: NEXT J1 ' ~.25 sec delay for JD=1400
6570 PRINT#2,"OUTPUT";YADDR$;"P0X" 'K-181: P0=FILTER OFF
6580 PRINT#2,"ENTER";YADDR$
6590 INPUT#3,RX$: VALY=.5*(VALY-VAL(MID$(RX$,NYM))) ' Avg norm & rev emf's
6600 SUMY=SUMY+VALY: YD(J)=VALY
6605 PRINT#2,"OUTPUT";XADDR$;"R0N2X" 'X channel #2
6610 PRINT#2,"ENTER";XADDR$
6620 INPUT#3,RX$: VALX=.5*(VALX-VAL(MID$(RX$,NXM)))
6630 SUMX=SUMX+VALX
6650 'single read of temperature signal while Sample Curr ON
6655 PRINT#2,"OUTPUT";XADDR$;"R0N1X" 'X channel #1
6660 PRINT#2,"ENTER";XADDR$
6670 INPUT#3,RZ$: VALZ=VAL(MID$(RZ$,NXM))
6675 PRINT#2,"output";PADDR$;"V-.001I-.0001W1X"
6677 PRINT#2,"output";PADDR$;SPOS$ 'v,i control string for POS curr
6680 SUMZ=SUMZ+VALZ
6690 NEXT J
6692 PRINT#2,"OUTPUT";XADDR$;"R0N3X" 'channel #3: heat dissipation
6693 FOR J1=1 TO JD : NEXT J1 ' ~.25 sec delay
6694 PRINT#2,"ENTER";XADDR$
6695 INPUT#3,RM$: HEAT=ABS(1000*XC*VAL(MID$(RM$,NXM))) 'total mW heating
6696 PRINT#2,"OUTPUT";XADDR$;"R0N1X" 'exit SUB in channel #1
6697 S0$="V-.0001.0000W1X"
6698 PRINT#2,"OUTPUT";PADDR$;S0$ 'set curr down to lowest
6700 SUMX=SUMX/NFILT: SUMY=SUMY/NFILT: SUMZ=SUMZ/NFILT
6710 SUMDEV=0 'now calc Std Dev of YD from SUMY
6720 FOR J=1 TO NFILT
6730 SUMDEV=SUMDEV+(SUMY-YD(J))^2

```

```

6740 NEXT J
6745 NDEV=NFILT-1: IF NDEV=0 THEN NDEV=1
6750 QY=SQR(SUMDEV/NDEV)  "Quality of Y": now defined as Std Dev(Y)
6760 'Hold off current for cooling pause (JP defined by keybd input)
6770 FOR J1=1 TO JP: NEXT J1  'Pause ~ 1sec/5600 of JP
6780 RETURN
6790 '
6830 '
6840 '
7000 *** MEASURE CIRCUIT RESISTANCE (HIGH CURRENT MODE) ***
7002 IF MODE$="L" THEN INPUT "REMOVE 1 kOhm resistor then press RTN",DUM$
7005 CLOSE  'close any open files
7010 GOSUB 4850 '— establish communication with Personal488
7020 GOSUB 5050 '— put instruments in REMOTE mode & give addresses
7030 '— for K-228: K0=await instruc complete, G5=readout:v,i
7040 PRINT#2,"OUTPUT";PADDR$;"R0X" 'R0=auto-range
7045 PRINT#2,"OUTPUT";XADDR$;"R0N3X" 'display contact heating
7050 INPUT "What is EST RESISTANCE of circuit (ohms) ? ",STDR
7055 RADD=1.9: IF STDR=.1 THEN RADD=.2
7060 INPUT "Trial CURRENT (amps) to Start with ? ",CUR1
7070 V0=CUR1*(STDR+RADD)*1.2: V0$=STR$(V0)
7075 CUR1$=STR$(CUR1)
7080 S$="V"+V0$+"I"+CUR1$+"W1X"
7090 PRINT#2,"OUTPUT";PADDR$;S$
7095 PRINT#2,"OUTPUT";PADDR$;"F1X"
7100 FOR J=1 TO 14000: NEXT J  ' 2.5 sec wait before read
7110 PRINT#2,"ENTER";PADDR$
7120 INPUT#3,VPS,CPS  ' read pwr supp output v,i
7122 IOCTL#2,"BREAK"
7125 PRINT#2,"OUTPUT";PADDR$;"FOX"
7130 RCIRC=VPS/CPS
7140 PRINT "Meas'd circuit V, I = ",VPS,CPS; :PRINT " ==> R= ",RCIRC
7150 INPUT "Do you wish to step up V 10% per step? < Y for yes > ",YESTP$
7160 IF YE$TP$="Y" THEN GOTO 7170 ELSE GOTO 7330
7170 PRINT "      V(volts)      I(amps)      R(ohms) < ENTER to continue > "
7180 V0=VPS: C0=CPS
7190 V1=1.1*V0: C1=1.2*C0
7200 V1$=STR$(V1): C1$=STR$(C1)
7210 SP$="V"+V1$+"I"+C1$+"W3X"
7220 'SN$="V"+V1$+"I"+C1$+"W1X"  'neg not used here
7230 PRINT#2,"OUTPUT";PADDR$;SP$
7240 PRINT#2,"OUTPUT";PADDR$;"F1X"
7250 FOR J=1 TO 14000: NEXT J  ' 2.5 sec wait before read
7260 PRINT#2,"ENTER";PADDR$
7270 INPUT#3,VPS,CPS  ' read pwr supp output v,i
7272 IOCTL#2,"BREAK"
7280 PRINT#2,"OUTPUT";PADDR$;"FOX"
7290 RCIRC=VPS/CPS
7300 PRINT,VPS,CPS,RCIRC;: INPUT " ",YESTP$
7310 IF YE$TP$="Y" THEN GOTO 7320 ELSE GOTO 7330
7320 GOTO 7180  'Loop back for another step-up of V
7330 IF MODE$="L" THEN INPUT "REINSTALL the 1 kOhm resistor then press RTN",DUM$
7340 RETURN
7350 '
7500 ' *** Find Control Params for Curr (K-228) ***
7505 IF MODE$="L" GOTO 7580
7507 'HIGH Current Output Range ...
7510 VP=1.05*XC*RCIRC  'set voltage limit 5% over min for curr & reals
7530 CP$=STR$(XC): CPN$=STR$(-XC)
7540 VP$=STR$(VP): VPN$=STR$(-VP)
7550 SPOS$="V"+VP$+"I"+CP$+"W1X"
7560 SNEG$="V"+VPN$+"I"+CPN$+"W1X"
7570 RETURN
7580 'LOW Current Output Range ...
7590 VP=XC*(1000+RCIRC)  'Ohms Law
7600 IF VP>10 THEN VP=10  'Limit to 10 Volts
7610 CLIM=1.1*XC  'Set current limit 10% over expected output

```



```

7620 IF CLIM < .001 THEN CLIM = .001
7630 IF CLIM > .01 THEN CLIM = .01
7635 CP$ = STR$(CLIM) : CPN$ = STR$(-CLIM)
7640 GOTO 7540
7650 '
8000 ' ***** EMERGENCY CURRENT SHUTDOWN *****
8100 BEEP: BEEP: BEEP
8105 LOCATE 25,1: PRINT "
8110 LOCATE 25,1: INPUT "EXCESSIVE HEATING DETECTED ! Enter a new heat limit (mW) or 0 to stop == > ";HLIMIT
8120 IF HLIMIT < = 0 THEN RETURN 346 'to scan finished
8130 GOSUB 4090 'restore message at bottom
8140 GOTO 1790
8150 '
9999 END

```

Appendix D. X-Y Plotter Emulator

```

10 DEFINT I-N
20 '
30 ' *** DRIFT.BAS ***
40 '*** KEITHLEY 570 SYSTEM ***
50 '*** Y-VOLTAGE VS X-VOLTAGE -- PERSONAL488 DATA ACQUISITION ***
100 ' DATA SAMPLED AFTER SPECIFIED X- & Y-ABS-VALUE-INTERVALS HAVE PASSED
110 ' OUTPUTS X AND Y DATA TO AN ASCII FILE
120 ' SPECIFIED BY THE USER. PLOTS AUXILIARY DATA FILE FOR COMPARISON
130 ' COMMAND P0 SENT TO Y-DVM (FOR K-181 TURNS OFF DIGITAL FILTERING)
140 '
200 '*** MAIN PROGRAM ***
210 '
220 GOSUB 400 '--- SET DEFAULT PARAMETER VALUES ---
225 GOSUB 4150 '--- READ IN FILE OF SETUP AND GRAPHICS PARAMETERS ---
230 GOSUB 700 '--- SIGN-ON & HARDWARE SETTINGS MENU ---
240 GOSUB 1000 '--- SETUP PARAMETERS MENU ---
245 GOSUB 4500 '--- STORE SETUP AND GRAPHICS PARAMS TO FILE ---
250 GOSUB 1600 '--- DATA ACQUISITION INITIALIZATION ---
260 GOSUB 1750 '--- TAKE ONE DATUM SAMPLE ---
270 GOSUB 3550 '--- CHECK FOR KEYBOARD INTERRUPT ---
280 GOSUB 1850 '--- TEST DATA FOR OUTPUT ---
290 GOSUB 3550 '--- CHECK FOR KEYBOARD INTERRUPT ---
300 GOSUB 3750 '--- CALC. TEMP. FROM THERM. CALIBRATION ---
310 GOSUB 2000 '--- PRINT DATA TO DISK ---
320 GOSUB 2700 '--- PLOT OR PRINT DATA TO SCREEN ---
330 GOSUB 3550 '--- CHECK FOR KEYBOARD INTERRUPT ---
340 GOTO 260 '--- LOOP BACK FOR MORE DATA ---
350 '
360 '*** END MAIN PROGRAM ***
370 '
380 '
400 '*** DEFINE DEFAULT PARAMETERS ***
410 CLS: KEY OFF: KEY 1,"LIST 200-400"+CHR$(13)
420 DEFINT I-N
430 DIM X(1000),Y(1000) 'DIM DATA FOR GRAPHICS REFRESH
440 DIM V(1000),T(1000) 'ARRAY FOR THERM. CALIBRATION TABLE(e.g. DIODE V,T)
445 DIM XG(1000),YG(1000) 'ARRAY OF COMPARISON DATA FOR GRAPHICS
450 ON ERROR GOTO 5400 '---ERROR TRAPPING
460 RESTORE 470
470 DATA 10,1,1,0,0,1,1,1
480 READ CUR,SCALEX,SCALEY,DEL,DELY,G0%,G1%,NFILT 'Default Params
490 DATA "<INACTIVE>","<ACTIVE>"
500 READ INACT$,ACT$: GSET$=INACT$: GCSET$=INACT$
504 '--- GPIB BUS ADDRESSES & METER PARAMS
505 DATA " 26"," 14","KEITHLEY 181/199/197","KEITHLEY 181/199/197",5,5
506 READ XADDR$,YADDR$,MX$,MY$,NXM,NYM

```

```

510 '
520 'GRAPHICS DEFAULT PARAMETERS
530 RESTORE 550
540 READ XMIN,XMAX,YMIN,YMAX
550 DATA 0,300,0,50,0
560 READ X$,Y1$,Y2$,T$
570 RESTORE 590
580 READ X$,Y1$,Y2$,T$
590 DATA "X-AXIS(UNITS)","Y-AXIS","(UNITS)","TITLE OF X VS Y GRAPH"
600 RESTORE 620
610 READ DXPIX,DYPIX,XPIX0,YPIX0 'AXIS CONTANTS IN PIXELS
620 DATA 550,300,80,15
630 RETURN 'TO MAIN PROGRAM
640 '
650 '
700 '*** SIGN-ON HARDWARE SETTINGS MESSAGE ***
710 CLS: PRINT CHR$(7)
720 PRINT:PRINT " *** HARDWARE SETTINGS ***"
730 PRINT " 1: X-INPUT: GPIB Address: ";XADDR$;" Meter ID: ";MX$
740 PRINT " 2: Y-INPUT: GPIB Address: ";YADDR$;" Meter ID: ";MY$
750 PRINT
760 INPUT"ENTER SELECTION # (<C/R> TO CONTINUE): ";ICODE
770 ON ICODE GOTO 790,810
780 RETURN 'TO MAIN PROGRAM
790 INPUT"ENTER NEW GPIB ADDRESS FOR X-INPUT: ";XADDR
791 GOSUB 850 '— METER ID CHOICES FOR READING STRING MASKING
792 INPUT"ENTER X-INPUT Meter ID CODE (DEFAULT = PREVIOUS): ";NMT
794 IF NMT < > 0 THEN NM=NMT ELSE 800
796 GOSUB 900: MX$=M$: NXM=NMSK '— ASSIGN METER ID NAME & MASKING DATA
800 XADDR$=STR$(XADDR): GOTO 720
810 INPUT"ENTER NEW GPIB ADDRESS FOR Y-INPUT: ";YADDR
811 GOSUB 850 '— METER ID CHOICES
812 INPUT"ENTER Y-INPUT Meter ID CODE (DEFAULT = PREVIOUS): ";NMT
814 IF NMT < > 0 THEN NM=NMT ELSE 820
816 GOSUB 900: MY$=M$: NYM=NMSK '— ASSIGN METER ID NAME & MASKING DATA
820 YADDR$=STR$(YADDR): GOTO 720
830 '
840 '
850 ' *** ASSIGN STRING MASKING PARAMS FOR METERS ***
854 PRINT "**** Meter ID Codes ****"
855 PRINT" 1: KEITHLEY 181,197
856 PRINT" 2: FLUKE 8840A
860 RETURN
870 '
880 '
890 '
900 '*** ASSIGN METER ID NAME ***
910 ON NM GOTO 930,940
920 PRINT CHR$(7): PRINT "< < <WRONG METER ID> > ": RETURN 230
930 M$="KEITHLEY 181/197": NMSK=5: RETURN
940 M$="FLUKE 8840A": NMSK=1: RETURN
950 '
960 '
1000 SCREEN 0: CLS
1010 GOSUB 5500 '— INCREMENT EXTENSION ON DATA FILENAME
1020 PRINT:PRINT:PRINT " *** SET-UP PARAMETERS *** "
1030 PRINT " 1: FILENAME OF SETUP AND GRAPHICS PARAMETERS TO USE: ";PUFL$
1040 PRINT " 2: FILENAME OF SETUP AND GRAPHICS PARAMETERS TO SAVE TO: ";PSFL$
1050 PRINT " 3: X-VOLTAGE SCALE FACTOR (Signal/Mcas V): ";SCALEX
1060 PRINT " 4: X-SIGNAL STEP SIZE: ";DEL
1070 PRINT " 5: Y-VOLTAGE SCALE FACTOR (Signal/Mcas V): ";SCALEY
1080 PRINT " 6: Y-SIGNAL STEP SIZE: ";DELY
1090 PRINT " 7: DATA FILENAME: ";DNM$
1100 PRINT " TITLE: ";TTITLE$
1110 PRINT " 8: THERMOM. CAL. TABLE FILENAME (for X-signal conversion): ";THNMS
1115 PRINT " TITLE: ";THTTL$
1120 PRINT " 9: NO. OF SAMPLES IN DIGITAL FILTERING: ";NFILT

```



```

1130 PRINT "10: SCREEN GRAPHICS PARAMETERS SETUP: ";GSET$
1135 PRINT "11: EXIT PROGRAM"
1140 PRINT
1150 INPUT "> ENTER SELECTION # (< C/R> TO EXECUTE): ";ICODE
1160 ON ICODE GOTO 1400,1430,1290,1310,1180,1200,1220,1350,1380,1330,1335
1170 RETURN 'TO MAIN PROGRAM
1180 INPUT " ENTER Y-VOLTAGE SCALE FACTOR (Signal/Vmeas): ";SCALEY
1190 GOTO 1020
1200 INPUT " ENTER Y-SIGNAL STEP SIZE: ";DELY
1210 GOTO 1020
1220 INPUT " INPUT DATA FILENAME (EXT .DTa WILL BE ADDED IF NOT ENTERED): ";DNM$
1230 IF DNM$="" THEN 1280
1240 PRINT" ENTER 80 CHARACTER DATA SET TITLE(DEFAULT=PREVIOUS): ";INPUT";DUM$
1250 IF DUM$="" THEN 1270
1260 TITLE$=DUM$
1270 FOR J=1 TO LEN(DNM$): IF MID$(DNM$,J,1) < ">," THEN NEXT J ELSE 1280
1272 DNM$=DNM$+" ".DT0"
1280 GOTO 1020
1290 INPUT" ENTER X-VOLTAGE SCALE FACTOR (Signal/Vmeas): ";SCALEX
1300 GOTO 1020
1310 INPUT" ENTER X-SIGNAL STEP SIZE: ";DEL
1320 GOTO 1020
1330 GOSUB 2250 'Define Graphics Parameters
1332 GOTO 1020
1335 GOSUB 4500: END '— STORE PARAMS TO FILE AND EXIT
1340 GOTO 1020
1350 INPUT" ENTER THERMOM. CALIB. TABLE FILENAME(EXT .CAL WILL BE ADDED): ";THNM$
1360 IF THNM$="" THEN 1370 ELSE THNM$=THNM$+".CAL"
1365 GOSUB 3900 '— READ IN THERM. CALIB. DATA ---
1370 GOTO 1020
1380 INPUT" ENTER NO. SAMPLES IN DIGITAL FILTERING: ";NFILT
1390 GOTO 1020
1400 INPUT " ENTER FILENAME FOR SETUP PARAMS. TO USE(EXT .PAR WILL BE ADDED): ";PUFL$
1410 IF PUFL$="" THEN 1420 ELSE PUFL$=PUFL$+".PAR"
1420 GOSUB 4150: GOTO 230 '—READ IN SETUP AND GRAPHICS PARAMS
1430 INPUT " ENTER FILENAME FOR SETUP PARAMS TO SAVE TO (.PAR WILL BE ADDED): ";PSFL$
1440 IF PSFL$="" THEN 1450 ELSE PSFL$=PSFL$+".PAR"
1450 GOTO 1020
1460 '
1500 '*** OPEN DATA FILE ***
1510 IF DNM$="" THEN 1550
1520 OPEN "O",#1,DNM$
1530 PRINT #1, TITLE$
1540 PRINT #1," X-signal   Y-signal"
1550 RETURN
1560 '
1570 '
1600 ' *** INITIALIZATION FOR DATA ACQU. ***
1610 GOSUB 4050 '—PRINT MESSAGE AT SCREEN BOTTOM
1620 I=0 'INITIALIZE DATA ARRAY INDEX
1630 GOSUB 4850 '— ESTABLISH COMMUNICATION W/PERSONAL488
1640 GOSUB 4950 '— SIGNON MESSAGE
1650 GOSUB 5050 '—ASSIGN REMOTE MODE ADDRESSES
1660 FLG$="L" 'INITIALIZE FOR DATA SCREEN PRINTOUT
1680 GOSUB 1500 '— OPEN DATA FILE
1690 IVXFLG=0 '— FLAG FOR FIRST TIME THRU
1700 PRINT "****Beginning Data Acquisition ****"
1710 RETURN 'TO MAIN PROGRAM
1720 '
1730 '
1750 ' *** TAKE DATA SAMPLE ***
1760 '--- GPIB INPUT ---
1770 GOSUB 5200 '--- FIND AVG OF NFILT GPIB READINGS
1780 VX=SUMX*SCALEX: VY=SUMY*SCALEY
1790 RETURN 'TO MAIN PROGRAM
1800 '
1810 '

```

```

1850 '*** DATA TEST FOR OUTPUT ***
1860 IF IVXFLG=0 THEN IVXFLG=1: VXT=VX: VYT=VY: RETURN 'FIRST TIME THROUGH
1870 DELVX=VX-VXT: DELVY=VY-VYT
1880 IF IDATFLG=0 THEN 1920
1890 IF INK$ < > "P" AND INK$ < > "p" THEN PRINT "MANUAL STORE"
1900 PRINT CHR$(7); '— BELL TO INDICATE MANUAL DATA STORAGE
1910 IDATFLG=0: GOTO 1970 'MANUAL DATA STORAGE
1920 IF DEL=0 THEN 1970
1930 IF DELY=0 THEN 1970
1940 IF ABS(DELVY) > =DELY THEN 1970 'STORE DATA
1950 IF ABS(DELVX) > =DEL THEN 1970 ELSE RETURN 260 'TAKE MORE DATA
1970 VXT=VX: VYT=VY: RETURN 'TO MAIN PROGRAM
1980 '
1990 '
2000 ' *** PRINT VALUES ON DISK ***
2010 I=I+1: Y(I)=VY 'INCREMENT INDEX
2020 IF THNM$="" THEN X(I)=VX: GOTO 2040
2030 X(I)=T
2040 IF DNM$="" THEN 2060
2050 PRINT #1,X(I),Y(I)
2060 RETURN 'TO MAIN PROGRAM
2070 '
2080 '
2100 ' *** TEST TO REDEFINE GLOBAL GAIN ***
2110 IF VTST > =5 THEN G%=1: GOTO 2150
2120 IF VTST > =2 THEN G%=2: GOTO 2150
2130 IF VTST > =1 THEN G%=5: GOTO 2150
2140 G%=10
2150 RETURN
2160 IF VTST$="VX" THEN GT%=G%: GOSUB 1790: RETURN 'CHANGE TO NEW X-GAIN
2170 GS%=G%: GOSUB 1790 'CHANGE TO NEW Y-GAIN
2180 RETURN
2190 '
2200 '
2250 ' *** GRAPHICS PARAMETERS ***
2260 GSET$=ACT$ 'SCREEN GRAPHICS ACTIVE
2270 PRINT: PRINT: PRINT: '*** SCREEN GRAPHICS PARAMETERS ***
2280 PRINT* 1: X-axis Xmin, Xmax: ",XMIN,XMAX
2290 PRINT* 2: Y-axis YMIN, YMAX: ",YMIN,YMAX
2300 PRINT* 3: X-axis label: ",X$
2310 PRINT* 4: Y-axis label: ",Y1$,Y2$
2320 PRINT* 5: Graph Title: ",T$
2325 PRINT* 6: COMPARISON DATA SET FILENAME: ",GCOMPL$
2326 PRINT* TITLE: ",GTTL$
2327 PRINT* 7: VIEW COMPARISON DATA SET: ",GCSET$
2330 PRINT
2340 INPUT* "> ENTER SELECTION # (<C/R> TO MAIN MENU): ",ICODE
2350 ON ICODE GOTO 2370,2390,2410,2430,2470,2481,2483
2360 GOTO 2490
2370 INPUT* ENTER X-axis Xmin, Xmax: ",XMIN,XMAX
2380 GOTO 2270
2390 INPUT* ENTER Y-axis Ymin, Ymax: ",YMIN,YMAX
2400 GOTO 2270
2410 INPUT* ENTER X-axis label: ",X$
2420 GOTO 2270
2430 INPUT* ENTER Y-axis label: ",Y$
2440 FOR J=1 TO LEN(Y$): IF MID$(Y$,J,1) < > "(" THEN NEXT J
2450 Y1$=LEFT$(Y$,J-1): J=LEN(Y$)-J+1: Y2$=RIGHT$(Y$,J)
2460 GOTO 2270
2470 INPUT* ENTER Graph Title: ",T$
2480 GOTO 2270
2481 INPUT* ENTER DATA SET FILENAME: ",GCOMPL$
2482 GOSUB 5800: GOTO 2270 'READ IN DATA SET FROM FILE
2483 INPUT* VIEW PLOT OF DATA SET (Y=YES)?: ",ANS$
2484 IF ANS$="Y" OR ANS$="y" THEN GCSET$=ACT$ ELSE GCSET$=INACT$: GOTO 2270
2485 GOSUB 2490 'DEFINE GRAPH AXES RANGES
2486 GOSUB 5900 'PLOT DATA SET

```



```

2487 GOSUB 4111 'PRINT MESSAGE AT SCREEN BOTTOM
2488 IF INKEY$="" THEN 2488 ELSE SCREEN 0: GOTO 2270
2489 '
2490 XRNG=XMAX-XMIN: YRNG=YMAX-YMIN
2500 XMIN$=STR$(XMIN): XMAX$=STR$(XMAX)
2510 YMIN$=STR$(YMIN): YMAX$=STR$(YMAX)
2520 GOSUB 2610: GOSUB 2660 'DEFINE FUNCTION TO CALC COORD IN PIXELS
2530 RETURN
2540 '
2550 '
2600 '*** FN TO CALCULATE Y IN SCREEN PIXELS ***
2610 DEF FNYPIX(YVAR,YMIN,YRNG,DYPIX,YPIX0)=-(YVAR-YMIN)*DYPIX/YRNG+YPIX0+DYPIX
2620 RETURN
2630 '
2640 '
2650 '*** FN TO CALCULATE X IN SCREEN PIXELS ***
2660 DEF FNXPIX(XVAR,XMIN,XRNG,DXPIX,XPIX0)=(XVAR-XMIN)*DXPIX/XRNG+XPIX0
2670 RETURN
2680 '
2690 '
2700 ' *** PLOT OR PRINT DATA ***
2710 IF INK$ < > "L" THEN IF INK$ < > "I" THEN 2740
2720 IF FLG$="L" THEN 2780
2730 FLG$="L": GOSUB 3050: GOSUB 4050: RETURN 'LIST DATA TO CURRENT I
2740 IF GSET$=INACT$ THEN 2780
2750 IF INK$ < > "P" THEN IF INK$ < > "p" THEN 2780
2760 IF FLG$="P" THEN 2800
2770 FLG$="P": GOSUB 2900: GOSUB 4050: RETURN 'PLOT DATA TO CURRENT I
2780 IF FLG$="L" THEN PRINT I,X(I),Y(I): RETURN 'TO MAIN PROGRAM
2790 IF GSET$=INACT$ THEN 2840
2800 XP=FNXPPIX(X(I),XMIN,XRNG,DXPIX,XPIX0)
2805 IF ABS(XP)>10000 THEN 2840 '—OUT OF RANGE
2810 YP=FNYPIX(Y(I),YMIN,YRNG,DYPIX,YPIX0)
2815 IF ABS(YP)>10000 THEN 2840
2820 PSET (XP,YP) 'PLOTS POINT
2830 'CIRCLE (XP,YP),3 'PLOTS CIRCLE
2840 RETURN 'TO MAIN PROGRAM
2850 '
2860 '
2900 ' *** REFRESH PLOT OF DATA UP TO CURRENT POINT ***
2910 CLS: GOSUB 3150: GOSUB 3300 'DRAW AND LABEL AXES
2920 FOR J=1 TO I
2930 XP=FNXPPIX(X(J),XMIN,XRNG,DXPIX,XPIX0)
2935 IF ABS(XP)>10000 THEN 2970 '—OUT OF RANGE
2940 YP=FNYPIX(Y(J),YMIN,YRNG,DYPIX,YPIX0)
2945 IF ABS(YP)>10000 THEN 2970
2950 'CIRCLE (XP,YP),3
2960 PSET (XP,YP)
2970 NEXT J
2975 IF GCOMFL$="" THEN RETURN
2976 IF GCSET$=ACT$ THEN GOSUB 5920 ' PLOT COMPARISON DATA
2980 RETURN
3000 '
3010 '
3050 '*** PRINT DATA ON SCREEN ***
3060 SCREEN 0: CLS
3070 J1=1-20: IF J1<0 THEN J1=1
3080 FOR J=J1 TO I
3090 PRINT J,X(J),Y(J)
3100 NEXT J
3110 RETURN
3120 '
3130 '
3150 '*** SUB TO DRAW GRAPH AXES ***
3160 SCREEN 9 'HI RES GRAPHICS SCREEN
3170 CLS
3180 PSET (80,15)

```

```

3190 DWN=300: RGT=550: TICKU=30: TICKR=55: ZERO=0
3200 FOR J=1 TO 10: DRAW"D=TICKU;NM+550,0;": NEXT J '---LEFT VERT AXIS
3210 FOR J=1 TO 10: DRAW"R=TICKR;NM+0,-300;": NEXT J '---BOTTOM HORIZ AXIS
3220 DRAW"U=DWN;L=RGT;"
3230 RETURN
3240 '
3250 '
3300 '*** SUB TO LABEL AXES ***
3310 IF LEN(X$)>60 THEN X$=LEFT$(X$,60) 'TRUNCATE IF TOO LONG
3320 XAX=44-.5*LEN(X$)
3330 LOCATE 24,XAX: PRINT X$;
3340 IF LEN(Y1$)>9 THEN Y1$=LEFT$(Y1$,9) 'TRUNCATE IF TOO LONG
3350 TAX=5-.5*LEN(Y1$)
3360 LOCATE 12,TAX: PRINT Y1$;
3370 IF LEN(Y2$)>9 THEN Y2$=LEFT$(Y2$,9)
3380 TAX=5-.5*LEN(Y2$)
3390 LOCATE 13,TAX: PRINT Y2$;
3400 IF LEN(T$)>70 THEN T$=LEFT$(T$,70) 'TRUNCATE IF TOO LONG
3410 TAX=44-.5*LEN(T$)
3420 LOCATE 1,TAX: PRINT T$;
3430 LOCATE 24,12-LEN(XMIN$): PRINT XMIN$;
3440 IF XMAX$="" THEN 3460
3450 LOCATE 24,81-LEN(XMAX$): PRINT XMAX$;
3460 LOCATE 23,10-LEN(YMIN$): PRINT YMIN$;
3470 LOCATE 2,10-LEN(YMAX$): PRINT YMAX$;
3480 RETURN
3490 '
3500 '
3550 ' *** SUB TO CHECK KEYBOARD STATUS ***
3560 IN$=INKEY$
3570 IF IN$="" THEN RETURN
3580 IF IN$=CHR$(13) THEN IDATFLG=1: GOTO 3710 'MANUAL DATA STORAGE
3590 INK$=IN$
3600 IF INK$<>"Q" AND INK$<>"q" THEN 3680
3610 IF DNMS="" THEN 3630 'DATA FILENAME
3620 CLOSE #1: GOSUB 6000 '---REWRITE DATA TO FILE IN STD FORMAT
3630 SCREEN 0: INPUT "ANOTHER DATA SET? (Y/N):",ANS2$
3640 IF ANS2$="y" OR ANS2$="Y" THEN 3670
3650 ON ERROR GOTO 0 'DISABLE ERROR TRAPPING
3660 CLS: END
3670 CLOSE: RETURN 240 'TO MAIN PROGRAM AT MENU
3680 IF INK$<>"P" THEN IF INK$<>"p" THEN RETURN
3690 IF INK$<>"I" THEN IF INK$<>"L" THEN RETURN
3700 RETURN 320 'TO MAIN PROGRAM AT PLT OR PRNT DATA
3710 RETURN 260 'TO MAIN PROGRAM AT TAKE ONE DATUM
3720 '
3730 '
3750 '*** SUB TO INTERPOLATE TEMPERATURES FROM DIODE T,V TABLE ***
3760 IF THNMS="" THEN RETURN 'TO MAIN PROGRAM
3770 VXC=VX
3780 NLO=1: NHI=NDATA 'LOW AND HI INDICES OF TABLE DATA
3790 N=(NHI+NLO)/2 'INTEGER DIVIDE 'TABLE INDEX TO BE COMPARED TO DATUM
3800 IF VX<V(N) THEN NHI=N: GOTO 3820
3810 NLO=N
3820 IF NHI<>NLO+1 THEN GOTO 3790
3830 T=T(NHI)+(VX-V(NHI))*(T(NHI)-T(NLO))/(V(NHI)-V(NLO))
3840 RETURN
3850 '
3860 '
3900 '*** SUB TO READ IN THERM. CALIB DATA ***
3910 IF THNMS="" THEN RETURN
3920 IF THNMT$=THNMS THEN RETURN 'no need to read data again
3930 THNMT$=THNMS
3940 PRINT"*** Reading in therm. calibration table ***"
3950 OPEN "I",#1,THNMS
3952 INPUT#1, THTTLS '---TITLE OF DATA SET
3960 INPUT #1,NDATA

```



```

3970 FOR J=1 TO NDATA
3980 INPUT #1,V(J),T(J)
3990 NEXT J
4000 CLOSE #1
4010 RETURN
4020 '
4030 '
4050 '*** PRINT MESSAGE AT BOTTOM OF SCREEN ***
4060 IF GSET$=ACT$ THEN 4090
4070 CLS: LOCATE 25,1: PRINT"PRESS: <C/R> STORE PT. <Q> QUIT";
4080 LOCATE 1,1: GOTO 4110
4090 LOCATE 25,1: PRINT"PRESS: <C/R> STORE PT. <Q> QUIT <P> PLOT RESTORE <L> LIST";
4100 LOCATE 24,1
4110 RETURN
4111 LOCATE 25,1: PRINT" PRESS <C/R> TO CONTINUE";
4112 LOCATE 24,1
4113 RETURN
4120 '
4130 '
4150 '*** READ IN SETUP AND GRAPHICS PARAMETERS ***
4160 IF PUFL$="" THEN RETURN
4170 OPEN "I",#1, PUFL$
4180 PRINT"*** RETRIEVING PARAMETERS FROM: ";PUFL$;" ***"
4190 '---SETUP PARAMETERS
4195 INPUT#1,PSFL$
4200 INPUT #1,SCALEX
4210 INPUT #1,DEL
4220 INPUT #1,SCALEY
4230 INPUT #1,DELY
4240 INPUT #1,DNMS
4250 INPUT #1,TITLE$
4260 DUM$=TITLE$
4270 INPUT #1,THNM$
4280 INPUT #1,NFILT
4290 INPUT #1,GSET$
4300 '---GRAPHICS PARAMETERS
4310 INPUT #1,XMIN,XMAX
4320 INPUT #1,YMIN,YMAX
4330 INPUT #1,X$
4340 INPUT #1,Y1$
4350 INPUT #1,Y2$
4360 INPUT #1,T$
4370 '---GPIB & METER PARAMS
4380 INPUT#1,XADDR$
4390 INPUT#1,YADDR$
4400 INPUT#1,MX$
4410 INPUT#1,MY$
4420 INPUT#1,NXM,NYM
4422 '--- COMPARISON GRAPHICS DATA FILE INFO
4424 INPUT#1,GCOMFL$ 'DATA FILENAME
4426 INPUT#1,GCSET$ 'FLAG FOR GRAPHICS COMPARISON
4430 CLOSE #1
4440 IF GSET$=ACT$ THEN GOSUB 5800: GOSUB 2490 '---READ IN COMP DATA SET
4445 GOSUB 3900 '---READ IN THERM CALIB. DATA
4450 RETURN
4460 '
4470 '
4500 '*** SAVE SETUP AND GRAPHICS PARAMETERS TO FILE ***
4510 IF PSFL$="" THEN RETURN
4520 OPEN "O",#1, PSFL$
4530 PRINT"*** STORING PARAMETERS TO: ";PSFL$;" ***"
4540 '---SETUP PARAMETERS
4545 PRINT#1,PSFL$
4550 PRINT#1,SCALEX
4560 PRINT#1,DEL
4570 PRINT#1,SCALEY
4580 PRINT#1,DELY

```

```

4590 PRINT#1,DNMS
4600 PRINT#1,TITLE$
4610 PRINT#1,THNM$
4620 PRINT#1,NFILT
4630 PRINT#1,GSET$
4640 '---GRAPHICS PARAMETERS
4650 PRINT#1,XMIN,XMAX
4660 PRINT#1,YMIN,YMAX
4670 PRINT#1,X$
4680 PRINT#1,Y1$
4690 PRINT#1,Y2$
4700 PRINT#1,T$
4710 '---GPIB & METER PARAMS
4720 PRINT#1,XADDR$
4730 PRINT#1,YADDR$
4740 PRINT#1,MX$
4750 PRINT#1,MY$
4760 PRINT#1,NXM,NYM
4762 '---COMPARISON GRAPHICS DATA FILE INFO
4764 PRINT#1,GCOMPL$ 'FILENAME OF COMPARISON DATA SET
4766 PRINT#1,GCSSET$ 'FLAG FOR ACTIVE GRAPICS COMPARISON
4770 CLOSE #1
4780 RETURN
4790 '
4800 '
4850 ' *** Establish communications with Personal488 ***
4860 OPEN "DEV\IEEEOUT" FOR OUTPUT AS #2
4870 'Reset Personal488
4880 IOCTL#2,"BREAK"
4885 PRINT#2,"RESET"
4890 'Open file to read responses from Personal488
4900 OPEN "DEV\IEEEIN" FOR INPUT AS #3
4904 'Enable SEQUENCE error detection by Personal488
4905 PRINT#2,"FILL ERROR"
4906 PRINT#2,"TIME OUT 15"
4910 RETURN
4920 '
4930 '
4950 ' *** Read the signon and revision message ***
4960 PRINT#2,"HELLO"
4970 INPUT#3,A$
4980 PRINT A$
4990 RETURN
5000 '
5010 '
5050 '*** Put the 197's into REMOTE ***
5060 PRINT#2,"REMOTE";YADDR$
5070 PRINT#2,"REMOTE";XADDR$
5080 RETURN
5090 'R0: Auto range   X: Execute   P0: Disable filter
5100 PRINT#2,"OUTPUT";XADDR$;"R0X"
5110 PRINT#2,"OUTPUT";YADDR$;"P0T1X"
5120 RETURN
5130 '
5140 '
5150 '
5200 ' *** Find the average of Navg readings ***
5210 SUMX=0: SUMY=0
5220 FOR J= 1 TO NFILT
5225 PRINT#2,"OUTPUT";XADDR$;"R0X"
5230 PRINT#2,"ENTER";XADDR$
5240 INPUT#3,R$: VALX=VAL(MID$(R$,NXM))
5250 IF ABS(VALX)>100 THEN GOSUB 5350: GOTO 5210 '---START OVER -- BAD READING
5260 SUMX=SUMX+VALX
5265 PRINT#2,"OUTPUT";YADDR$;"P0X" '---Uses front panel range
5270 PRINT#2,"ENTER";YADDR$
5280 INPUT#3,R$: VALY=VAL(MID$(R$,NYM))

```



```

5290 IF ABS(VALY) > 100 THEN GOSUB 5350: GOTO 5210 '---START OVER
5300 SUMY = SUMY + VALY
5310 NEXT J
5320 SUMX = SUMX/NFILT: SUMY = SUMY/NFILT
5330 RETURN
5340 '
5350 '*** PRINTOUT MESSAGE FOR BAD READING ***
5360 PRINT CHR$(7); IF FLG$="L" OR FLG$="I" THEN PRINT ">>> BAD READING<<<";R$
5370 RETURN
5380 '
5390 '
5400 '*** ERROR TRAPPING ***
5410 PRINT CHR$(7); '---BELL TO INDICATE ERROR
5420 IF ERR < > 53 THEN RESUME 260 '---TRY TO TAKE MORE DATA
5425 PRINT">>> BAD FILENAME<<<"; FOR J=1 TO 1000: NEXT J: RESUME 240
5440 '
5450 '
5500 ' *** INCREMENT EXTENSION ON DATA FILENAME ***
5510 PRINT CHR$(7)
5520 IF DNMS="" THEN RETURN
5530 FOR J=1 TO LEN(DNMS): IF MID$(DNMS,J,1) < > "." THEN NEXT J
5540 J1=LEN(DNMS)-J+1
5550 EXT$=RIGHT$(DNMS,J1): DNMS=LEFT$(DNMS,J-1)
5560 IEXT=VAL(RIGHT$(EXT$,1)): IEXT=IEXT+1
5570 IEXT$=RIGHT$(STR$(IEXT),1)
5580 EXT$=LEFT$(EXT$,3)+IEXT$
5590 DNMS=DNMS+EXT$
5600 RETURN
5610 '
5620 '
5800 '*** READ IN DATA SET FOR GRAPHICS COMPARISON ***
5805 PRINT"*** RETRIEVING COMPARISON DATA SET *****"
5810 IF GCOMFL$="" THEN RETURN
5820 OPEN"1",#1,GCOMFL$
5822 INPUT#1, GTTL$ '---TITLE OF FILE DATA
5830 INPUT#1, NDATG
5835 XMX=XG(1): XMN=XG(1): YMX=YG(1): YMN=YG(1)
5840 FOR J=1 TO NDATG
5850 INPUT#1, XG(J),YG(J)
5855 IF XG(J) > XMX THEN XMX=XG(J): GOTO 5857
5856 IF XG(J) < XMN THEN XMN=XG(J)
5857 IF YG(J) > YMX THEN YMX=YG(J): GOTO 5860
5858 IF YG(J) < YMN THEN YMN=YG(J)
5860 NEXT J
5870 CLOSE #1
5875 PRINT" XMIN: ";XMN,"XMAX: ";XMX
5876 PRINT" YMIN: ";YMN,"YMAX: ";YMX
5880 RETURN
5890 '
5900 ' *** PLOT OF COMPARISON DATA ***
5910 CLS: GOSUB 3150: GOSUB 3300 'DRAW AND LABEL AXES
5920 FOR J=1 TO NDATG
5930 XP=FNXP(XG(J),XMN,XRNG,DXPIX,XPIX0)
5935 IF ABS(XP) > 10000 THEN 5970 '---OUT OF RANGE
5940 YP=FNYP(YG(J),YMN,YRNG,DYPIX,YPIX0)
5945 IF ABS(YP) > 10000 THEN 5970
5950 CIRCLE (XP,YP),1
5960 PSET (XP,YP)
5970 NEXT J
5980 RETURN
5990 '
6000 '*** REWRITE DATA TO FILE ***
6010 IF DNMS="" THEN RETURN
6020 OPEN"O",#1,DNMS
6030 PRINT"*** STORING DATA ARRAY TO FILE *****"
6040 PRINT#1,TITLE$
6050 PRINT#1,1 '---NO. OF DATA IN SET

```

```

6060 FOR J=1 TO 1
6070 PRINT#1, X(J),Y(J)
6080 NEXT J
6090 CLOSE#1
6100 RETURN
6110 '
10000 PRINT#2,"OUTPUT";YADDR$;"RSX"
10010 PRINT#2,"ENTER 20"
10020 INPUT #3,RS
10030 PRINT RS
10040 RETURN

```

Appendix E. Monte Carlo Computational Information

In the Monte Carlo simulations, the percolation paths were allowed 64 degrees of freedom at each increment along each current path. This is preferable over the choice of only four directions used in many percolation theories published elsewhere,^{1,2} since the Hall effect, unlike most other transport properties, is highly sensitive to the current direction. However, since the high- T_c materials are best described as quasi-two dimensional superconductors, the current paths were confined to remain within a two dimensional conduction plane. Similarly, the current paths were also constrained to remain within a conduction bridge of fixed width. While maintaining these constraints, increments of fixed spatial distances were made at each step along the percolation path. Thus, instead of defining a matrix of resistivities as modelled by others,¹ the simulations here required predefined T_c distributions in terms of the two spatial coordinates (x_i, y_i). A total of 60 Gaussian T_c distributions were constructed, ranging from purely homogeneous to moderately inhomogeneous ($\Delta T_c \leq 6K$), while maintaining as much randomness between the various distributions as possible. Moreover, in each simulation ten equally spaced current paths were started well ahead of the Hall measurement region to allow ample opportunity for the current

paths to converge towards the regions of least resistance. Immediately upon the reaching the Hall terminals, the integration of R_H (described in detail in the main text) was initiated. A total of $\sim 10^6$ increments were allowed for each path while in the Hall measurement region in order to obtain reasonable convergence.

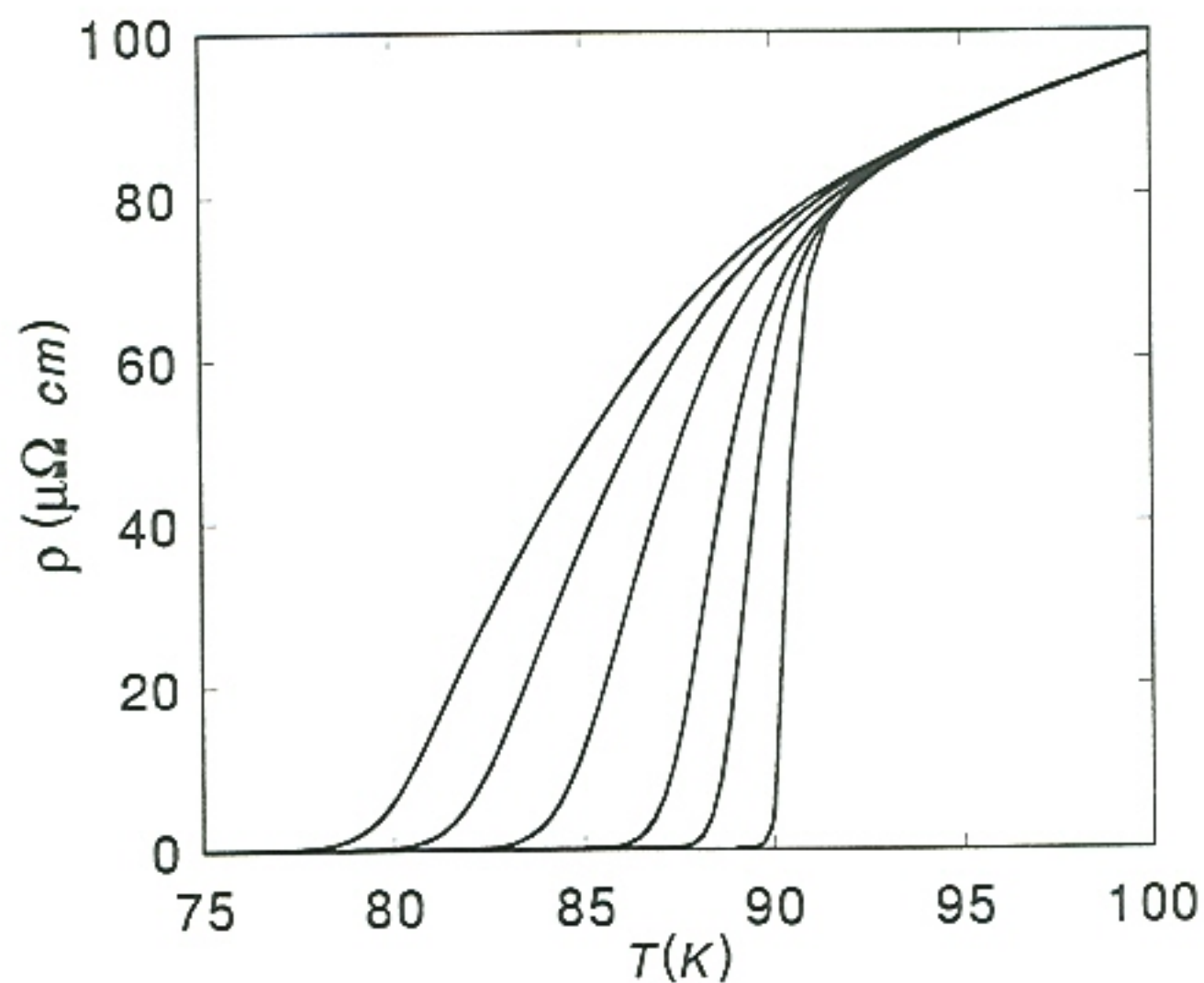
To a good approximation, the path of least resistance will be obtained if the current is required to move in the local direction of least resistance at each increment. In accomplishing this, an "effort" value ϵ_j was assigned to each of the 64 possible directions where

$$\epsilon_j = \begin{cases} \infty, & \text{if } \theta_j = 180^\circ \\ [2 - \cos(\theta_j)] \sum_i \frac{\rho[r_i, T + (\langle T_c \rangle - T_{ci})_j, H]}{r_i^{N-1}}, & \text{otherwise.} \end{cases} \quad (94)$$

Here $\theta = 0^\circ$ is defined as the preferred forward direction. Since a complete reversal of the current direction is unphysical, ϵ_j is set to infinity whenever $\theta = 180^\circ$ or the current path reaches the edge of the defined bridge. The multiplicative term comes from the fact that a measured voltage is proportional to the spatial length of the measurement, i.e., $V \propto I \int \rho d\ell$. The summation term represents discrete radial scans, e.g., $r_{i+1} = r_i + C$, proportional to the "local" resistivities that originate from the spatial coordinate (x_i, y_i) through a distance of roughly one bridge width. The step size C is taken small enough to allow good convergence of the final results and depends on the spatial coarseness of the particular T_c distribution. The "local" resistivities $\rho[(x_i, y_i), T, H]$ are obtained from a compiled table of in-field resistive transitions [Figure 43] taken on a coevaporated epitaxial thin film. For simplicity, the

effect of the "local" T_c is approximated by a simple temperature shift of the representative resistive transitions. This is reasonable provided the T_c distribution is on the order of only a few Kelvins. In Equation (94), $\langle T_c \rangle$ is the mean T_c of the distribution and T_{ci} is the T_c at a radius r_i from the point (x_i, y_i) . Finally, the "scanned" resistivities are divided by weight factors proportional to the surface area defined at each radius r_i from the point (x_i, y_i) . These weight factors, e.g., r_i^{N-1} , depend on the effective dimensionality N , where in thin films, the dimensionality is set equal to two ($N=2$). Therefore, the unique numerical procedure described above provides a simple means of determining the apparent Hall coefficients in a variety of moderately inhomogeneous systems.

Figure 43



In-field resistive transitions obtained from a highly crystalline, coevaporated, epitaxial thin film of $\text{YBa}_2\text{Cu}_3\text{O}_7$. These transitions were utilized in the Monte Carlo simulations of the Hall effect transitions. "Local" resistivities were approximated by shifting these transitions up or down in temperature in order to represent the "local" deviations of the transition temperatures from the mean transition temperature.

VITA

He earned the Doctor of Philosophy degree in December of 1992. In addition, he has authored or coauthored eight journal publications. Finally, he expects to obtain a total of 12 journal publications as a result of this dissertation.

The author is a member of Sigma Xi, the American Physical Society, Sigma Pi Sigma, Pi Mu Epsilon, and the Planetary Society. The author is also an honorary member of the Oak Ridge Isochronous Observation Network.